SERTOLI CELL MICROTUBULES: THEIR POLARITY AND BINDING TO SPERMATID-ASSOCIATED ECTOPLASMIC SPECIALIZATIONS

by

DARLENE MARIE REDENBACH

B.S.R., The University of British Columbia, 1982
M.Sc., The University of British Columbia, 1986

A THESIS SUBMITTED IN PARTIAL FULFULLMENT OF
THE REQUIREMENTS FOR THE DEGREE OF
DOCTOR OF PHILOSOPHY
in
THE FACULTY OF GRADUATE STUDIES
(Department of Anatomy)

We accept this thesis as conforming
to the required standard

THE UNIVERSITY OF BRITISH COLUMBIA
April, 1992

© Darlene Marie Redenbach, 1992

In presenting this thesis in partial fulfilment of the requirements for an advanced degree at the University of British Columbia, I agree that the Library shall make it freely available for reference and study. I further agree that permission for extensive copying of this thesis for scholarly purposes may be granted by the head of my department or by his or her representatives. It is understood that copying or publication of this thesis for financial gain shall not be allowed without my written permission.

Department of Anatomy

The University of British Columbia
Vancouver, Canada

Date March 24/92

ABSTRACT

During spermatogenesis, spermatogenic cells are moved through the blood testis barrier from the basal to the apical compartment, where they become oriented parallel to the long axis of the Sertoli cell, and situated within Sertoli cell crypts. They are moved again toward the base of the epithelium, before being translocated across the epithelium for release into the tubule lumen. Crypts are lined with unique actin containing submembrane structures called ectoplasmic specializations (ESs) that form part of the Sertoli cell-spermatid junction. ESs consist of the Sertoli cell membrane, a fenestrated cistern of smooth endoplasmic reticulum, and a highly ordered intervening array of actin filaments. ESs are thought to participate in establishing junctional domains at Sertoli cell-spermatid adhesion junctions, which serve to anchor the developing spermatids within the Sertoli cell crypts. Sertoli cell microtubules occur adjacent to the endoplasmic reticulum of the ES (ESER), oriented parallel to the long axis of the cell, and to the direction of spermatid translocation. Other investigators have described linkages between the ESER and adjacent microtubules. Sertoli cell microtubules have been suggested to aid in orientation and positioning of spermatogenic cells, within the seminiferous epithelium. It is proposed that this may be achieved by a microtubule-based transport mechanism known to be involved in establishing and maintaining organelle positioning in other cells. As part of a study to test the hypothesis that spermatid translocation is a microtubule-based event, the polarity of Sertoli cell microtubules was determined. The potential for binding between spermatid-ESs and microtubules was assayed, and the binding characterized, using a selection of conditions known to alter organelle-microtubule interaction in other systems. The results of this study indicate that Sertoli cell microtubules are orientated with their minus-end directed toward the apical surface of the cell and that microtubules bind to spermatid-ES complexes, are releasable in the presence of nucleotides, and share binding properties with known mechanoenzymes. These results are consistent with the hypothesis that spermatids are moved through the seminiferous epithelium by a microtubule-based transport mechanism.

TABLE OF CONTENTS

ABSTRACT ii
TABLE OF CONTENTS iii
LIST OF TABLES x
LIST OF FIGURES xi
ABBREVIATIONS xiii
ACKNOWLEDGEMENTS xiv

CHAPTER 1: INTRODUCTION 1
OVERVIEW 2
BACKGROUND 6
TESTIS 6
    Cellular organization of the testis 6
    Function of the testis 6
    Terminology of spermatogenesis 14
    Positional changes during spermatogenesis 14
SPERMATIDS 16
    Overview of spermiogenesis 16
    Morphological changes during spermiogenesis 16
    Positional changes of spermatids during spermiogenesis 20
    Regulation of spermatogenic cell development 23
SERTOLI CELLS 24
    General morphology 24
    Membrane bounded organelles 25
        Mitochondria 28
        Exocytotic and Endocytotic compartments 28
        Golgi apparatus 29
        Endoplasmic reticulum 29
    Cytoskeleton 32
        Microfilaments 32
        Intermediate filaments 33
        Microtubules 34
    Ectoplasmic specializations 34
        Organization 37
        Relationship with cytoskeleton 38
        Linkages 39
        ESER 39

Stage specific changes 40
Functions 41
Regulation 42
Changing events in Sertoli cells during spermatogenesis 43
SERTOLI-GERM CELL RELATIONS 44
Processes 44
Lateral processes 44
Apical processes 45
Penetrating processes 45
Tubulobulbar processes 46
Junctions 47
Blood testis barrier 47
Sertoli cell-Spermatid junction 48
MICROTUBULES 49
Introductory statement 49
Microtubule structure and kinetics 50
Microtubule organizing centers (MTOCs) 51
Microtubule structures 53
Tubulin isoforms 53
Post-translational modification of tubulin 53
Microtubule associated proteins (MAPs) 54
Microtubule polarity 56
Microtubule based intracellular transport 57
Mechanoenzymes 61
Kinesin 62
molecular structure 63
biochemical properties 63
sensitivity to inhibitors 64
rate and direction of transport 64
other properties 65
Cytoplasmic dynein 65
molecular structure 66
biochemical properties 66
sensitivity to inhibitors 66
rate and direction of transport 67
other properties 67
Other putative microtubule based motors for organelle transport 67
visiken 67

        10 S sea urchin egg motor 68
        Reticulomyxa motor 68
        C. elegans motor 68
        Kar 3 and ncd non claret disjunctional gene product....................69
      Organelle-microtubule binding proteins 69
        170 kD protein from Hela cells....................69
    The mechanochemical cycles of kinesin and cytoplasmic dynein....................70
    Mechanoenzyme inhibitors and how they work 73
      EHNA....................74
      NEM: 74
      Vanadate....................74
      AMPPNP 77
    Binding Assays....................77
    The organelle-microtubule binding complex 79
      Where is the motor located?....................80
      How are motors kept available for bidirectional transport?....................81
      Are the motors alone sufficient for transport?....................82
      How are motors regulated?....................83
    Microtubule-dependent organelle positioning....................84
    Cellular organization (microtubules in cells in general) 87
MICROTUBULES IN SERTOLI CELLS....................90
    Distribution 90
    Sertoli cell MTOC 93
    Tubulin post translational modifications in Sertoli cells 94
    Stage dependent changes in Sertoli cell microtubule distribution....................94
    Sertoli cell MAPs....................96
    Relationship of microtubules to other organelles in Sertoli cells....................97
    Function of Sertoli cell microtubules....................97
      Sertoli cell shape 98
      Organelle positioning and translocation during spermatogenesis 100
    Influence of Sertoli cell microtubules on the head shape of spermatogenic cells 101
    Microtubule perturbation....................102
DEVELOPMENT OF THE HYPOTHESIS 104
HYPOTHESIS STATEMENT....................108
PREDICTIONS....................108
EXPERIMENTAL OUTLINE 109
    Microtubule polarity study....................109

Microtubule-spermatid-ES binding study 109

CHAPTER 2: MICROTUBULE POLARITY 111
INTRODUCTION 112
DETERMINATION OF MICROTUBULE POLARITY: THE APPROACH 112
DETERMINATION OF MICROTUBULE POLARITY: THE STRATEGY 113
MATERIALS AND METHODS 115
MATERIALS 115
Animals 115
Chemicals and supplies 115
Buffers 115
METHODS 116
Preparation of purified tubulin 116
Hook decoration 117
Electron microscopy 122
Negative stain electron microscopy 125
Video enhanced differential interference contrast microscopy 125
RESULTS 127
MICROTUBULE POLARITY 127
Effects of lysis decoration buffer 127
Sampling for montage 136
Scoring criteria 136
Microtubule polarity: observations 141
Microtubule polarity: counts 141
DISCUSSION 151
MICROTUBULE POLARITY IN SERTOLI CELLS 151
SUMMARY 153

CHAPTER 3: BINDING ASSAY 158
INTRODUCTION 158
BINDING ASSAY CRITERIA: COMPONENTS 158
Spermatid-ES 158
Labelled microtubules 163
BINDING ASSAY: ESTABLISHING THE CRITERIA 163
Development of the binding assay 163
Establishing that counts represented microtubules 164
CHARACTERISTICS OF BINDING 164
Reversal of binding. 164

Experiments to characterize ^3MT_X and spermatid-ESs binding 164
LOCALIZATION OF LABEL 165
Morphological support for results of binding assay 165
CALCIUM AS A PROPOSED REGULATOR 167
MATERIALS AND METHODS 168
MATERIALS 168
Animals 168
Chemicals and reagents 168
General 168
Buffers 168
Primary antibodies 169
Secondary antibodies 169
Binding assay treatment reagents 169
METHODS 170
General 170
Protein determinations 170
SDS-PAGE gels 170
Isolation of ^3MTx - spermatid-ES binding assay components 170
Tubulin purification for binding assay 170
Preparation of ^3HGTP labelled, taxol stabilized microtubules (^3MT_X)172
Length measurement of ^3HGTP labelled, taxol stabilized, microtubules (^3MT_X) 172
Spermatid-ES isolation 173
Binding assay: preparation 176
Sample preparation for binding assay 176
Gradient preparation for binding assay 176
Binding assay: methods 179
Running the binding assays 179
Binding assays: experimental design 179
Design of binding assay experiments (general) 179
Experiments for which total sample added to gradients was not 150 μl180
Direct effect of treatments on microtubules 180
Design of matched experiments 181
Design of [MT] experiment 181
Topical binding assay 185
Preparation of treatment materials used in binding assays 185
Isolation of rat testis crude supernatant for cytoplasmic dynein enriched MAP preparation 185

Isolation of cytoplasmic dynein enriched MAP preparation from testis crude supernatant 186
Sertoli Cell enriched isolation from 21 day old rats 187
Preparation of cytosol: Sertoli cell enriched preparation from 21 day rat testis 188
Data collection for binding assays 188
Data analysis 189
Immunohistochemistry 189
Immunofluoresence: sample preparation and microscopy (5A6: antitubulin) 189
Rhodamine phalloidin staining 190
Preparation of normal mouse IgG: control for 5A6 anti-tubulin antibody 190
Autoradiography of binding assay 191
Autoradiography: methods 191
Electron Microscopy 192
Routine electron microscopy 192
Methods for calcium study 193
RESULTS 196
COMPONENTS OF THE BINDING ASSAY 196
Spermatid-ESs 196
Ectoplasmic specialization endoplasmic reticulum: ESER 202
Endogenous microtubules remain attached during warm isolation 202
Microtubule isolation and measurement 213
Labelling exogenous microtubules 213
Incorporation of label and stability of microtubules over time 216
Microtubule stability: effect of agents for characterization of microtubule binding 216
BINDING ASSAY: ESTABLISHING THE CRITERIA 216
Buffer conditions 217
Spermatid-ES enrichment by gradients 218
Controls: "same spin controls" in every spin 224
Sampling 224
BINDING ASSAY: RESULTS 231
Microtubules bind to spermatid-ESs 231
Label entering the gradient with spermatid-ESs is primarily from microtubules 231
There is a time course to 3MTx - spermatid-ES binding 232

Nucleotides reverse 3MTx - spermatid-ES binding 233
The effect of ATP depletion on $^{3}MT_{X}$-spermatid-ES binding 245
Microtubule concentration has a nonlinear effect on binding 245
$^{3}MT_{X}$ - spermatid-ES binding is dynamic 249
Characterization of $^{3}MT_{X}$ - spermatid-Es binding..254
LOCALIZATION OF LABEL TO SPERMATID HEADS 258
Labelled microtubules are localized to the spermatid-ES...................................258
Actin and tubulin dual staining of amorphous clusters 266
Pursuit of a proposed regulation of events around the spermatid-ES 271
DISCUSSION...280
COMPONENTS OF THE BINDING ASSAY 280
Spermatid-ESs..280
THE BINDING ASSAY MEASURES MICROTUBULE- SPERMATID-ES BINDING 282
Effects of the sucrose gradient...282
Counts represent microtubule binding..282
Binding time course 283
Effects of added nucleotide..284
Competition by unlabelled microtubules 285
CHARACTERIZATION OF BINDING...285
LOCALIZATION OF $^{3}MT_{X}$-SPERMATID-ES BINDING..286
Label associates with spermatid heads...286
Localization to amorphous clusters 287
ANTIMONY PRECIPITATION EVIDENCE OF CALCIUM IN ESER IS INCONCLUSIVE.............287

CHAPTER 4: DISCUSSION..289
INTRODUCTORY REMARKS...290
MICROTUBULE POLARITY IN SERTOLI CELLS...290
$^{3}MT_{X}$-SPERMATID-ES BINDING 297
BIBLIOGRAPHY 308

LIST OF TABLES

CHAPTER 2

Table II-I Classification of microtubules according to hook decoration: cold/warm incubation 142
Table II-II Percent of microtubules with clockwise, counterclockwise and ambiguous hook decoration: cold/warm incubation. 143
Table II-III Classification of microtubules according to hook decoration: exogenous tubulin/warm incubation 148
Table II-IV Percent of microtubules with clockwise, counterclockwise and ambiguous hook decoration: exogenous tubulin/warm incubation 148

CHAPTER 3

Table III-I Sample data from binding assay..229
Table III-II Non-microtubule component of binding: summary...............................235
Table III-III Effect of the addition of excess cold label: 5X cold taxol stabilized microtubules on ^3MT_X-spermatid-ES binding 252
Table III-IV Effect of the non-microtubule component of 5X cold taxol stabilized microtubule sample on ^3MT_X-spermatid-ES binding ..252
Table III-V Characterization of ^3MT_X-spermatid-ES binding 257

LIST OF FIGURES

CHAPTER 1

Fig. 1-1: Organization of the testis. 8
Fig. 1-2: Stages of the seminiferous epithelium........ 11
Fig. 1-3 Sertoli cell Regulation. 13
Fig. 1-4: Spermiogenesis. 18
Fig. 1-5 Spermatid translocation in the seminiferous epithelium. 22
Fig. 1-6: Sertoli cell fine features........ 27
Fig. 1-7: Ectoplasmic specializations. 37
Fig. 1-8: Mechanoenzyme cycles. 72
Fig. 1-9: Mechanoenzyme inhibitors. 76
Fig. 1-10: Continuous organelle circulatory system: radial model. 89
Fig. 1-11: Microtubule distribution in Sertoli cells........ 92
Fig. 1-12: Microtubule-based spermatid translocation model........ 107

CHAPTER 2

Fig. 2-1: Evidence of purity and polymerization capability of bovine brain tubulin 119
Fig. 2-2: Microtubule decoration: sampling methods for EM sections. 124
Fig. 2-3: Verification of spermatid tail axoneme orientation........ 129
Fig. 2-4: Rat seminiferous epithelium: highly extracted following incubation in lysis/decoration buffer 131
Fig. 2-5: Low power view of an area of seminiferous epithelium that has been incubated in lysis decoration buffer. 133
Fig. 2-6: Rat seminiferous epithelium moderately extracted in lysis/decoration buffer 135
Fig. 2-7: Rat seminiferous epithelium only slightly extracted in lysis/decoration buffer 138
Fig. 2-8: Montage of rat seminiferous epithelium incubated in lysis decoration buffer 140
Fig. 2-9: Montage of rat seminiferous epithelium incubated in warm lysis/decoration buffer 147
Fig. 2-10: Hook decoration of seminiferous epithelium, incubated immediately at 35°C. 150
Fig. 2-11: Summary diagram of microtubule polarity results. 156

CHAPTER 3

Fig. 3-1: Isolation of spermatids from seminiferous epithelium with intact ESs. 160
Fig. 3-2: Transillumination methods of seminiferous cycle staging. 162
Fig. 3-3: Spermatid-ES isolation........ 175
Fig. 3-4: Binding assay: methods........ 178
Fig. 3-5: Microtubule concentration experiment: strategy........ 183
Fig. 3-6: Appearance of spermaid-ES isolate. 198
Fig. 3-7: Actin staining associated with the heads of isolated spermatids: Spermatid ESs. 201
Fig. 3-8: ESER remains attached to spermatid head following spermatid-ES isolation. 205
Fig. 3-9: Tubulin staining pattern on spermatid-ESs under warm or cold conditions. 207
Fig. 3-10: Control figure for 5A6 antibody staining for tubulin (1). 209
Fig. 3-11: Control figure for 5A6 antibody staining for tubulin (2). 212
Fig. 3-12: Length and fine structure of taxol stabilized microtubules used for 215

MT_X-spermatid-ESs
Fig. 3-13: Testing for microtubule migration using sucrose gradients in MT_X-spermatid-ESs binding assays. 220
Fig. 3-14: Establishing spin criteria for binding assay: SDS page gels. 222
Fig. 3-15: Establishing centrifugation conditions for binding assay using ^3MT_X counts. 223
Fig. 3-16: Centrifugation of crude spermatid-ES isolate on a discontinuous 30-45-60% sucrose gradient results in enrichment of spermatid-ESs. 226
Fig. 3-17: Binding assay method: short sample experiment 228
Fig. 3-18: Results sample binding assay 230
Fig. 3-19: Non-microtubule component of binding. 234
Fig. 3-20: Time course for ^3MT_X-spermatid-ES binding: overlay plots 237
Fig. 3-21: Time course for ^3MT_X-spermatid-ES binding: collapsed data 239
Fig. 3-22: Effect of 10 mM MgATP on ^3MT_X-spermatid-ES binding. 241
Fig. 3-23: Reduction in tubulin staining on ^3MT_X-spermatid-ES binding after treatment with 10 mM MgATP. 243
Fig. 3-24: Comparison of effects of MgATP and GTP on ^3MT_X-spermatid-ES binding 244
Fig. 3-25: ATP depletion effect on ^3MT_X-spermatid-ES binding. 246
Fig. 3-26: Effect of varying spermatid-ES concentration on ^3MT_X-spermatid-ES binding. .248
Fig. 3-27: Effect of varying microtubule concentration on ^3MT_X-spermatid-ES binding. 250
Fig. 3-28: ^3MT_X-Spermatid-ES binding expressed as a function of microtubule concentration. 251
Fig. 3-29: Characterization of ^3MT_X-spermatid-ES binding: matched experiments. 256
Fig. 3-30: Localization of label in ^3MT_X-spermatid-ES binding from pre-gradient autoradiography samples. 261
Fig. 3-31: DIC and bright field micrograph pairs to show localization of label in ^3MT_X-spermatid-ES binding from post-gradient autoradiography samples. ...263
Fig. 3-32: DIC and bright field micrograph pairs to show localization of label in ^3MT_X- spermatid-ES binding in the presence of 10mM MgATP from post-gradient autoradiography samples 265
Fig. 3-33: Actin staining of amorphous clusters, like those seen in the autoradiography slides, show that spermatid heads are present in the clusters. 268
Fig. 3-34: ^3MT_X-spermatid-ESs stain for both actin and tubulin 270
Fig. 3-35: Localization of calcium in seminiferous epithelium (Method 1) 275
Fig. 3-36: Localization of calcium in seminiferous epithelium (Method 2) 277
Fig. 3-37: Localization of calcium in seminiferous epithelium (Method 4) 279

CHAPTER 4

Fig. 4-1: Summary diagram of microtubule-based spermatid translocation model 305
Fig. 4-2: Summary diagram of microtubule-spermatid-ES binding 307

ABBREVIATIONS

5A6	monoclonal antibody to alpha tubulin
ADP	adenosine diphosphate
AMPPNP	adenylimidodiphosphate: nonhydrolyzable analogue of ATP
ATP	adenosin triphosphate
DIC	differential interference contrast microscopy
EHNA	erythro-9-[3(2hydroxynonyl)] adenine analogue of adenosine
EM	electron microscopy
ER	endoplasmic reticulum
ES	ectoplasmic specialization
ESER	endoplasmic reticulum of ectoplasmic specialization
FSH	follicle stimulating hormone
GTP	guanosine triphosphate
LH	leutenizing hormone
LM	light microscopy
MAPs	microtubule associated proteins
${}^3MT_X$	microtubules labelled with tritium GTP (^{3}), and stabilized with taxol
${}^3MT_X$-spermatid-ES	spermatid-ESs complexes with bound microtubules
MT	microtubule
NEM	N-ethylmaleimide, sulfhydryl alkylating agent
Pi	inorganic phosphate
spermatid-ES	spermatids, isolated with intact ectoplasmic specializations
TuJ1	monoclonal antibody to beta tubulin

ACKNOWLEDGEMENTS

First, I would like to thank my husband, Jak and my children, Karoline, Katharine and Jason, for their patience and understanding during the pursuit of this goal. Without their love, and encouragement this would not have been possible.

A dept of gratitude is owed to the members of my supervisory committee: Drs. Wayne Vogl, Nelly Auersperg, Bruce Crawford, Harold Kasinsky, and Kim Boekelheide, for their guidance, friendship, and support through this study. In addition, the many hours spent in sharing their experience and their equipment, and in reading this thesis are gratefully acknowledged.

I would especially like to thank my mentor, Dr. A. Wayne Vogl, for his support, and to acknowledge his enthusiasm and dedication to the pursuit of science, that has instilled in me an appreciation for the process of science. His pursuit of excellence in science and teaching provides an inspiration to all his students and colleagues.

I would like to thank Dr. C. Slonecker, the faculty, staff and students in the Anatomy department at UBC, in particular David Pfeiffer, for their friendship, fruitful discussions and many good times.

I am very grateful to Dr. Kim Boekelheide and the members of his lab, in the department of Pathology and Laboratory Medicine at Brown University, that were so generous with their friendship, and expertise during the completion of this study.

Appreciation is due, Franke Crymble and Jak Redenbach for excellent art work.

CHAPTER 1

INTRODUCTION

OVERVIEW

Sertoli cells have been described as nurse or nurturing cells for developing male germ cells. They make up the columnar cells of the seminiferous epithelium across which developing germ cells must be translocated before they can be released into the tubule lumen. The dependence of germ cells on Sertoli cells, implied by the intimate relationship between these two cell types, has long been assumed and continuing investigation supports that conclusion. A great deal of work has been done to describe the events of spermatogenesis and elucidate the underlying mechanisms, yet precisely what role the Sertoli cell plays and how it may serve to nurture the developing germ cell is not entirely understood.

Sertoli cell-germ cell relations are highly complex and constantly undergoing elaborate changes, including the formation of a variety of Sertoli-Sertoli and Sertoli-germ cell junctions during spermatogenesis (Nicander, 1967; Gilula et al., 1976; Gravis, 1979; Dym and Fawcett, 1970; Russell et al., 1983b; Russell and Peterson, 1985; Russell, 1977a, 1980; Grove and Vogl, 1989). Unique actin containing structures called ectoplasmic specializations (ESs) form within Sertoli cells, adjacent to regions of attachment to spermatids, lining the Sertoli cell crypts that hold developing spermatids (Brökelmann, 1963; Flickinger and Fawcett, 1967; Nicander, 1967; Russell, 1977a; Vogl, 1989; Vogl et al., 1991a,b). ESs are thought to assist in establishing membrane domains for the adhesion junction and have been proposed to play a role in the orientating and positioning of spermatids (Vogl, 1989; Grove and Vogl, 1989; Grove et al., 1990; Vogl et al., 1991a).

ESs consist of an hexagonal array of actin filaments sandwiched between the Sertoli cell plasma membrane and a fenestrated cistern of endoplasmic reticulum (for reviews see Vogl, 1989; Vogl, et al., 1991a). Bundles of Sertoli cell microtubules occur adjacent to the endoplasmic reticulum of the ES (ESER) (Fawcett, 1975; Russell, 1977c; Vogl, 1988, 1989; Amlani and Vogl, 1988; Vogl, et al., 1991a). The microtubules surround elongating spermatids and are oriented parallel to the long axis of the Sertoli cell and to the direction of spermatid translocation (Fawcett, 1975; Vogl, 1988, 1989; Amlani and Vogl, 1988, Neely and Boekelheide, 1988; Hermo et al., 1991; Redenbach and Vogl, 1991). Significantly, ESs occur during the orientation and translocation of spermatids and are dismantled just prior to the release of late spermatids into the tubule lumen (Russell, 1977b,c, 1984). The microtubules have both a temporal and structural relationship to ESs, suggesting a coordinated function.

The close association of microtubules with ESER is reminiscent of other systems in which membrane bound organelles, observed adjacent to microtubules, can be demonstrated to translocate along microtubule tracks. Much attention has been focused on microtubule based transport in axons (Smith, 1972; Lasek and Brady, 1985; see Okabe and Hirokawa, 1989; Sheetz et al., 1989) and, more recently, in a number of other cell types (Allen et al., 1981b; Koonce and Schliwa, 1985; Hayden et al., 1983; McNiven et al., 1984; Steuer et al., 1990; see Kelly, 1990b; Kreis, 1990; Schroer and Sheetz, 1991a). It is becoming increasingly apparent that microtubule-based transport is fundamental to a surprising number of housekeeping functions in cells generally (Terasaki, et al., 1984; van der Sluijs et al., 1990; Duden et al., 1990; see Kelly, 1990b; Kreis, 1990; Schroer and Sheetz, 1991a), in addition to being the underlying mechanism of many highly specialized events (Steuer et al., 1990; Troutt and Burnside, 1988a; Vallee et al., 1989b). Microtubule associated proteins, and in particular mechanoenzymes or 'motors', are thought to mediate microtubule dependent events, and are currently under intense investigation (Vallee et al., 1989a,b; Schroer et al., 1989; Balch; Vale, 1990; Schroer and Sheetz, 1991a; Schroer and Sheetz, 1989; Sloboda and Gilbert, 1989; Kelly, 1990a;. There is recent evidence that other microtubule binding proteins may also function to position organelles (Rickard and Kreis, 1990, 1991; Scheel and Kreis, 1991a,b).

A system for translocating spermatogenic cells, in general, through the seminiferous epithelium has the following requirements: 1) developing spermatogenic cells must be translocated from the base to the apex of the seminiferous epithelium, without breaking the seal that maintains the exclusive basal and apical environments; 2) provision must be made for the temporal and spatial economy to simultaneously accommodate more than one stage of maturation of spermatogenic cells within the apical environment; 3) spermatids must complete their differentiation and yet be released only when they are precisely ready; 4) a mechanism is required for orientation and movement of spermatids situated within Sertoli cell crypts.

A number of occurrences in Sertoli cells address these requirements. Compartmentalization is established by the blood testis barrier (Dym and Fawcett, 1970), a tight junction formed between lateral processes of Sertoli cells that serves to separate the apical and basal environments. The translocating spermatogenic cells are shuttled toward the tubule lumen by the formation of Sertoli cell lateral processes that segregate the germ cells from subsequent generations of translocating cells (Russell, 1977b; Weber et al., 1983). Spermatids are retained in apical crypts of Sertoli cells by an adhesive junction, the ectoplasmic specialization, which is progressively dismantled prior to spermatid release. As spermatids undergo differentiation, they are precisely oriented and positioned, being returned within their crypts toward the base of the Sertoli cell, then translocated to the tubule lumen for release. One factor that remains to be explained is the mechanism by which spermatids are oriented and positioned in the seminiferous epithelium.

The means of providing spermatid orientation and positioning may lie in a novel application of an ubiquitous mechanism: microtubule-based transport. A potential interaction between the ER of ESs (ESER) and adjacent bundles of microtubules, oriented in the direction of germ cell translocation, is the basis of the microtubule-based spermatid translocation model proposed in this study. The model is consistent with what is known of Sertoli cell morphology and of microtubule-based transport. A microtubule-based motility model for orientation, positioning, and translocation of spermatids, is feasible whether these events are viewed as passive on the part of the spermatid, or reciprocally regulated between spermatids and Sertoli cells. Because spermatids do not appear to move independently, the model satisfies the conditions of a highly active roll for Sertoli cells while not excluding a feedback role for spermatids. Most importantly, it accommodates what is known of the morphology of Sertoli cells; in particular, at their interface with developing germ cells. It is supported by analogy to known systems of intracellular transport; however, it introduces what may be a unique example of intracellular transport, the regulation of an extracellular event.

This thesis is presented in four parts. Chapter 1 provides the background information for the study as a whole, the development of the hypothesis, and the approach used to test the hypothesis. Chapter 2 describes the Sertoli cell microtubule polarity portion of the study and Chapter 3 the assay developed to examine the potential binding of microtubules to spermatid-ESs, each with introduction, methods, results, and discussion sections pertaining to that portion of the study. Chapter 4 provides a discussion of the significance of the findings from chapters 2 and 3 and their relevance to the proposed hypothesis.

The introduction, in this chapter, begins with a description of the events of spermatogenesis and the morphological features of spermatids and Sertoli cells that will be encountered in this study. These introductory sections are followed by a detailed description of microtubules and their function in microtubule-based transport, generally. What is currently known about microtubules in Sertoli cells is then reviewed and a model developed for their proposed function in microtubule-based spermatid translocation. Finally, the rationale and approach to testing this model is presented.

BACKGROUND

TESTIS

Cellular organization of the testis

The mammalian testis consists of closely packed seminiferous tubules and intervening interstitial tissue enclosed in a connective tissue capsule. Seminiferous tubules are comprised of fluid filled tubes lined by seminiferous epithelium and ensheathed by a squamous sheet of myoid cells. Fig. 1-1 shows the cellular organization of the testis and the seminiferous epithelium, in the rat. Unless otherwise indicated, descriptions apply to the animal model used in this study, rat testis. The seminiferous epithelium is a modified columnar epithelium consisting of two cell types, a sessile, non-proliferating population of 'nurse cells', or Sertoli cells, and a highly proliferative population of spermatogenic cells, undergoing complex morphological and positional changes (Sertoli, 1865; Leblond and Clermont, 1952a,b; Perey et al., 1961; Russell, 1977c; Vogl et al., 1983a; Vogl et al., 1991a,b). The interstitial compartment is comprised of clusters of steroidogenic Leydig cells in addition to vascular and lymphatic tissue. The structural compartmentalization of the testis, into seminiferous tubules and interstitial tissue, reflects its functional duality.

Function of the testis

The mature mammalian testis participates in both exocrine and endocrine activities. Its primary exocrine function, spermatogenesis, involves the production and release of spermatozoa under the nurturing influence of Sertoli cells. Its endocrine function, steroidogenesis, is carried out primarily in the interstitial compartment by Leydig cells.

Spermatogenesis has been described in detail in a number of species (Brökelmann, 1963; Leblond and Clermont, 1952a,b; Clermont, 1972; Perey et al., 1961; Russell et al., 1990). In rat, full maturation takes approximately 52 days

Figure 1-1: Organization of the testis: This light micrograph shows a cross-section of rat testis with a number of seminiferous tubules and the interstitial tissue. The seminiferous tubules are composed of a modified columnar epithelium (seminiferous epithelium) which includes Sertoli cells and intervening spermatogenic cells. Sertoli cells extend from the base to the tubule lumen identified by highly infolded nuclei with prominent nucleoli, situated at the base of the epithelium. Spermatogenic cells are situated between the Sertoli cells and include spermatagonia that lie along the base of the epithelium, spermatocytes, identified by large round nuclei found midway between the base and the lumen of the epithelium, and spermatids, recognized by their darkly staining nuclei. Elongate spermatids are found deep within the epithelium from stages II to VI, being deepest at stage V, and extend into the tubule lumen by stage VIII. They can be identified by their elongate nuclei during these stages. Released spermatozoa are seen in the tubule lumen. Surrounding the seminiferous tubule are myoid cells. The interstitial compartment is made up of vascular elements, and clusters of round Leydig cells. Seminiferous tubules at different stages of development are included in this field. (Micrograph courtesy of W. Vogl.)

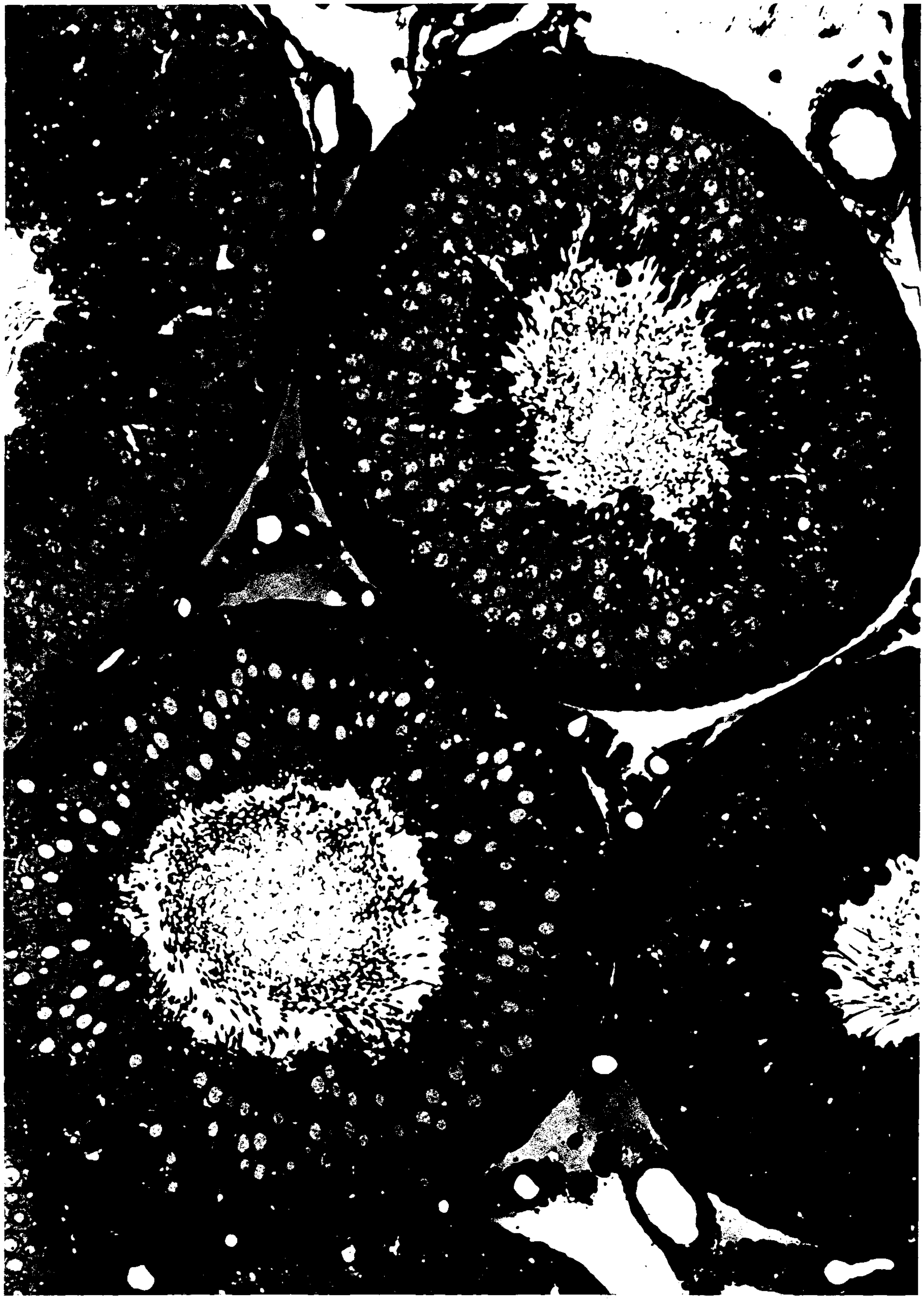

(Clermont, 1972). Before one generation of spermatogenic cells have completed spermatogenesis, the subsequent generation begins, resulting in a highly coordinated stacking of spermatogenic cells from four to five generations. The time between the initiation of one generation of spermatogenesis to the initiation of the next is one 'cycle' of the seminiferous epithelium, requires about 13 days (Clermont, 1972) and produces specific 'cell associations' (Leblond and Clermont 1952a). These 'cell associations' arise from precisely coordinated morphological and positional changes in spermatogenic cells as they progress together through the seminiferous epithelium. Their invariable coexistence has been used to distinguish the 14 'stages' of spermatogenesis, conventionally used to identify events in spermatogenesis. Fig. 1-2 shows the cycle of the seminiferous epithelium the the cell associations that occur at each stage (adapted from Perey et al., 1961).

Sertoli cells undergo morphological and physiological, stage dependent, changes in order to provide the changing milieu required to nurture spermatogenic cells at different stages of development. Presumably, all spermatogenic cells in a given cell association thrive in a similar environment.

The endocrine function of the testis is steroidogenesis, mainly the province of Leydig cells (see Means et al., 1980; Purvis and Hansson, 1981). Fig. 1-3 shows the fundamental feedback mechanisms by which steroidogenic functions of the testis are regulated (adapted from Purvis and Hansson, 1981). The pituitary releases two trophic hormones that influence testicular function: follicle stimulating hormone (FSH) and luteinizing hormone (LH). Stimulated by LH, Leydig cells synthesize and secrete testosterone which concentrates to very high levels in the seminiferous epithelium. FSH, through the second messenger system and LH, directly influence protein synthesis, secretion, and enzyme activity in Sertoli cells which in turn regulate spermatogenesis. Sertoli cells secrete tubule fluid and a number of proteins including: androgen binding protein, that binds testosterone to keep local levels high, inhibin, to regulate FSH levels, plasminogen activator, which is involved in the cycle of tissue resorption, and a number

Figure 1-2: Stages of the seminiferous epithelium: This chart shows 14 cell associations, in vertical columns (roman numerals) that invariably coexist in the seminiferous epithelium of the rat. The 14 cell associations occur consecutively in the order shown here, making up the 14 stages of the cycle of the seminiferous epithelium in the rat, as described by Leblond and Clermont (1952a). Four and one half cycles are required to complete spermatogenesis; however, after one cycle, the next generation of spermatogenic cells are initiated resulting in the accumulation of five generations of germ cells in the epithelium by the time the mature germ cells are released. 'A' indicates type A spermatogonia, 'In', intermediate spermatogonia, and 'B', type B spermatogonia. Primary spermatocytes are indicated as 'Pl' (preleptotene), 'L' (leptotene), 'Z' (zygotene), 'P' (pachytene), 'Di' (diplotene) and secondary spermtocytes 'II'. The 19 steps of spermiogenesis occur from stage I through stage XIV of the 4th cycle and are completed by stage VIII of the fifth cycle. (This chart is modified from Perey et al., 1961. Details shown in the developing spermatids are adapted from Clermont and Rambourg 1978; Russell et al.,1990).

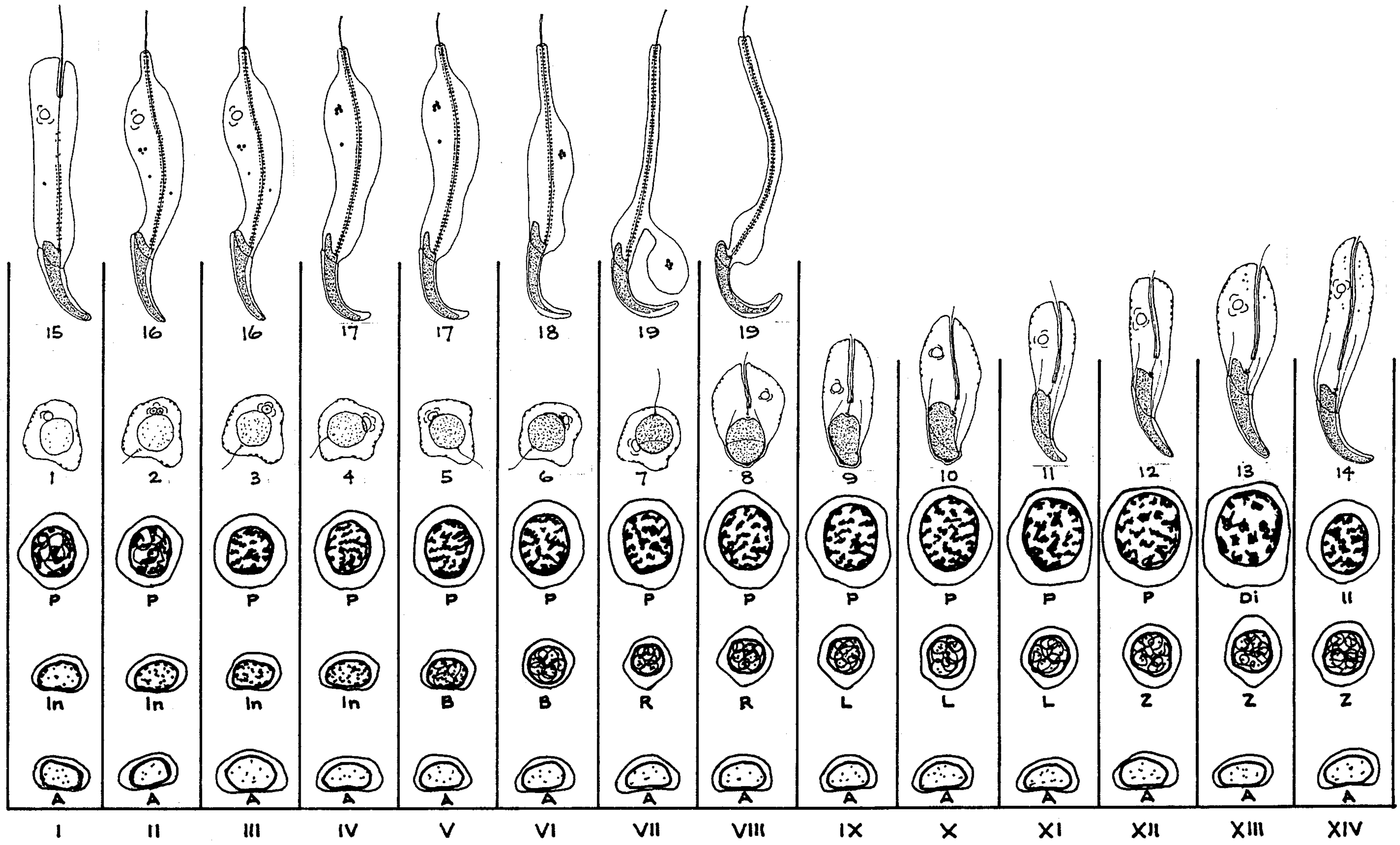
15 16 16 17 17 18 19 19
1 2 3 4 5 6 7 8 9 10 11 12 13 14
P P P P P P P P P P P P Di II
In In In In B B R R L L L Z Z Z
A A A A A A A A A A A A A A
I II III IV V VI VII VIII IX X XI XII XIII XIV

Figure 1-3: Sertoli cell regulation: This diagram gives an overview of the hormonal regulation of the testis. The stimulatory effects of the steroid hormone: testosterone (from Leydig cells) and the protein hormone: follicle stimulating hormone (from the pituitary gland) activate protein synthesis, protein secretion, and enzyme activity. The effects of follicle stimulating hormone are activated through a second messenger system and are proposed to be modulated, in part, by calcium sequestration and release by the ER (adapted from Purvis and Hansson, 1981).

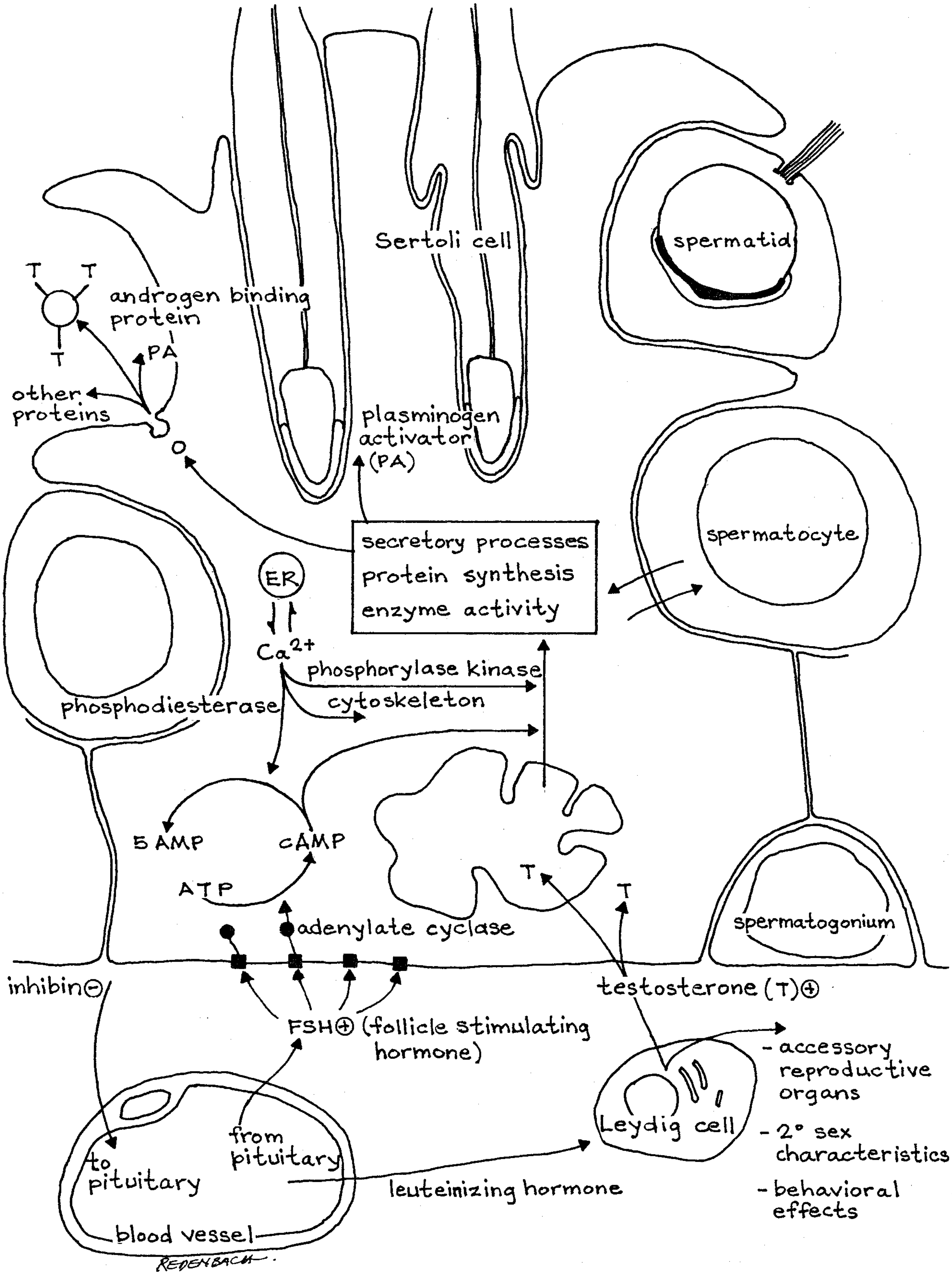
Sertoli cell
spermatid
T
T
T
androgen binding protein
PA
other proteins
plasminogen activator (PA)
secretory processes
protein synthesis
enzyme activity
spermatocyte
ER
Ca^{2+}
phosphorylase kinase
cytoskeleton
phosphodiesterase
5 AMP
cAMP
ATP
T
T
adenylate cyclase
spermatogonium
inhibin⊖
testosterone (T)⊕
FSH⊕ (follicle stimulating hormone)
- accessory reproductive organs
- 2° sex characteristics
- behavioral effects
Leydig cell
from pituitary
to pituitary
leuteinizing hormone
blood vessel
REDENBACH

of other proteins. Of particular interest here is the second messenger cascade, initiated by FSH, that triggers the many functions under calcium/calmodulin modulation, including proposed cytoskeleton regulation. The response of Sertoli and Leydig cells to trophic hormone involves inter-organ, intercellular and even intracellular feedback mechanisms that modulate the response (Purvis and Hansson, 1981). The complete picture is infinitely complex and includes paracrine regulatory events by which spermatogenic cells are thought to influence Sertoli cell activities, both of which are only partially understood (Saez et al., 1985).

Terminology of spermatogenesis

A complex terminology has evolved to distinguish the spermatogenic cell types and their maturation. Spermatogenesis can be subdivided into three stages, spermatocytogenesis (proliferative phase), meiosis, and spermatid differentiation (spermiogenesis). *'Spermatogonia'* include stem cells and early mitotic spermatogenic cells. Cells undergoing the first and second meiotic divisions are '*primary and secondary spermatocytes*' respectively. At the completion of meiosis, they become *'spermatids'* that undergo morphological differentiation and are released as *'spermatozoa'* from the epithelium. *'Spermatogenesis'* is the complete process of transformation of spermatogonia into spermatozoa. *'Spermatocytogenesis'* is the process by which spermatogonia become spermatocytes and includes a number of mitotic divisions. *"Meiosis"* is the formation of haploid spermatids from spermatocytes. *'Spermiogenesis'* is the differentiation of spermatids which culminates at *'spermiation'*, the release of mature germ cells into the tubule lumen, at which point they are referred to as *'spermatozoa"*(see Leblond and Clermont, 1952a).

Positional changes during spermatogenesis

During spermatocytogenesis, spermatogonia reside on the basal lamina of the seminiferous epithelium between Sertoli cells. They undergo mitosis, after which they assume one of two fates, to remain as stem cells, or become committed to development and begin their migration toward the tubule lumen. The committed spermatogonia carry out a number of incomplete mitotic divisions, thereafter remaining linked with their clones by intercellular bridges, first described by Von Ebner (see Perey et al., 1961; Gondos, 1984). They then begin the next phase of spermatogenesis, meiosis.

The area between Sertoli cells, in which spermatogenic cells migrate, is divided into apical (or adluminal) and basal compartments by a very tight occluding junction, the blood-testis barrier, (Dym and Fawcett, 1970). The barrier is formed between neighbouring Sertoli cells, separating the environment of the the basal compartment, accessible to blood borne substances, from that of the adluminal compartment, accessible only to Sertoli cell lumenal secretions.

During the second phase, meiosis, primary spermatocytes synchronously begin the first of two meiotic divisions as they pass from the basal compartment through the blood testis barrier, to the adlumenal compartment. This is achieved, partly, by the extension of Sertoli cell lateral processes between the basal lamina and the migrating cell, to re-establish the tight junction of the blood testis barrier, thereby separating migrating spermatocytes from the basal compartment. Once the seal is complete, the barrier above the spermatocyte is disassembled and the spermatocyte occupies the adluminal compartment (Clermont, 1972). During the pachytene stage of the first meiotic division, chromosome crossover occurs; spermatocytes are rendered immunologically different. Having been isolated from their vascular supply, they are dependent on the Sertoli cell for nourishment and protection from immunological attack. After pre-leptotene spermatocytes arrive in the adluminal compartment, they complete the first meiotic division and then, as secondary spermatocytes, undergo a rapid second meiotic division to become early, or round haploid spermatids, ending the meiotic stage.

During the third stage, spermiogenesis, spermatids undergo differentiation, become oriented to the long axis of Sertoli cells, and are moved from their lateral position between Sertoli cells to become embedded in apical crypts within individual

Sertoli cells. During their encasement in the crypts, spermatids are brought deeper within the Sertoli cell, then returned to the apical region of the Sertoli cell, and released into the tubule lumen. The reason for this return to a basal position is not known. There is no evidence to suggest germ cells play an active role in their positioning or translocation.

After spermiation, spermatozoa become motile and continue to undergo subtle changes as they complete their journey through the male reproductive tract.

SPERMATIDS

The steps of spermiogenesis

Based on morphological changes in differentiating spermatids, spermiogenesis has been divided into 19 'steps' (not to be confused with stages) (Leblond and Clermont, 1952a,b; Clermont, 1972; for detailed account of staging criteria, see Russell et al., 1990). The occurrence of these 19 steps is shown in Fig. 1-2. The morphological changes that occur during the 19 spermatid steps (Arabic numerals) are illustrated in Fig. 1-4.

During spermiogenesis, two types of changes occur in spermatogenic cells, morphological and positional.

Morphological changes in spermatids during spermiogenesis

The 19 steps of spermiogenesis, are grouped into four phases: Golgi phase, cap phase, acrosome phase, and maturation phase (Leblond and Clermont, 1952; for details see Russell, et al. 1990) (Figure 1-4). The Golgi phase (stages I to III) begins the differentiation of round spermatids and is characterized by initiation of the the future axoneme from the distal centriole and the formation of an acrosome granule from the Golgi. During the cap phase (stages IV to VII), a head cap grows out of the acrosomal granule and spreads over the surface of the nucleus describing a 140° arc by the end of

Figure 1-4: Spermiogenesis: This diagram shows the 19 recognizable steps of spermiogenesis that occur in four phases (LeBlond and Clermont, 1952a): Golgi phase, cap phase, acrosomal phase, and maturation phase. See text for details of morphological features of the 19 stages. (G) Golgi, (AV) acrosomal vesical, (N) nucleus, (T) tail, (C) cap, (M) manchette, (A) acrosome, (VF) ventral fin, (DF) dorsal fin, (MIT) mitochondria, (RB) residual body. (The diagram is adapted from Leblond and Clermont, 1952a; Clermont and Rambourg, 1978; Russell et al., 1990).

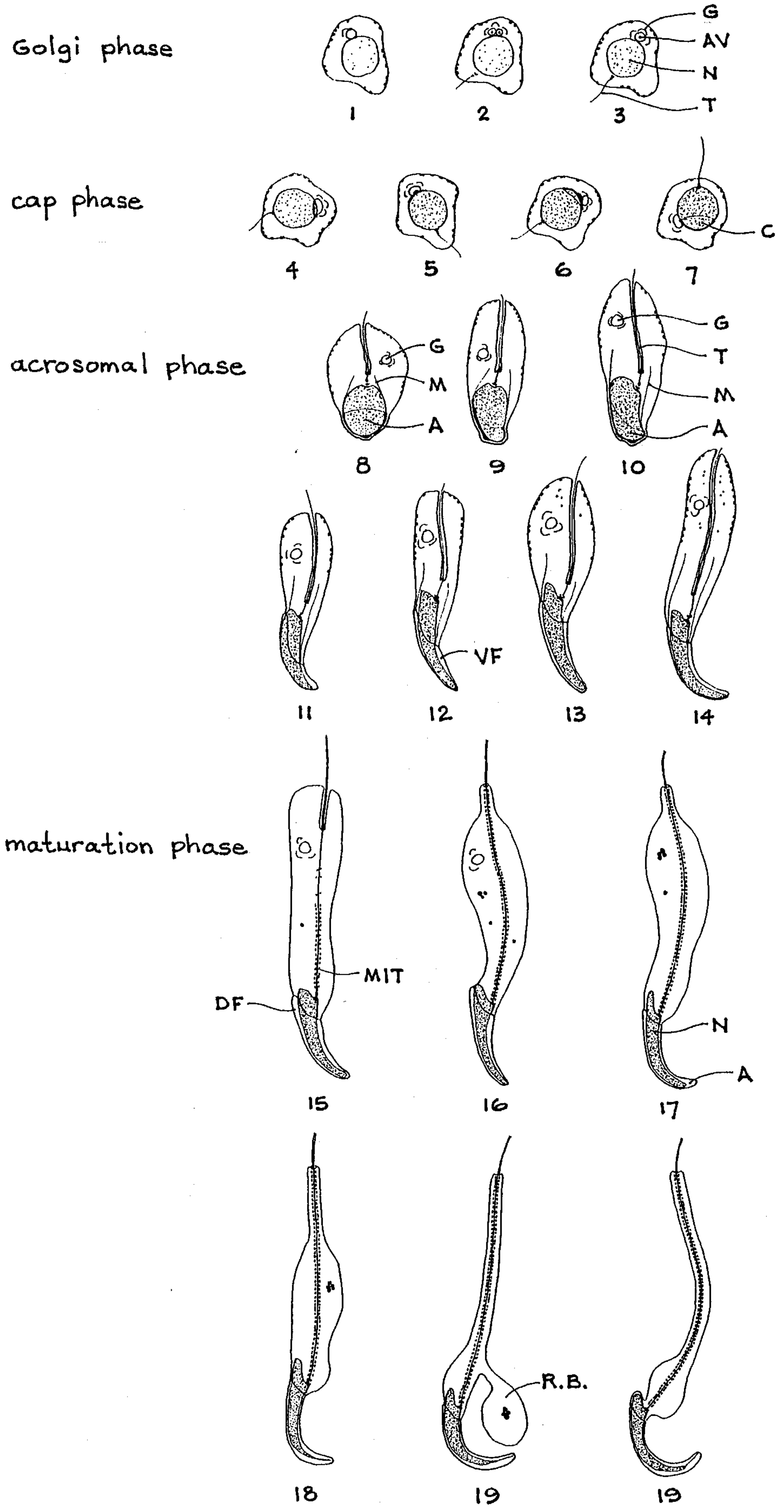
Golgi phase
G
AV
N
T
1
2
3
cap phase
C
4
5
6
7
acrosomal phase
G
M
A
G
T
M
A
8
9
10
VF
11
12
13
14
maturation phase
MIT
DF
N
A
15
16
17
R.B.
18
19
19

stage VII (Russell et al., 1990); meanwhile, the paired centrioles move closer to the nucleus, with the proximal one becoming attached to the nucleus and the distal one associated with the developing axoneme, the future tail. The next phase sees the beginning of spermatid elongation. At the onset of the acrosome phase (stages VIII to XIV), the acrosome becomes oriented toward the base of the epithelium and the cytoplasm toward the tubule lumen, with the acrosomal cap diametrically opposed to the developing tail. The caudal migration of spermatid cytoplasm results in an anterior displacement of the acrosome capped nucleus until it abuts against its rostral plasma membrane immediately adjacent to the neighbouring Sertoli cell. A sheath of microtubules, the manchette, begins to assemble from a point midway along the nucleus extending caudally over the developing tail. After the beginning of manchette development in step 8 (Cole, 1988; Russell, 1990), the nucleus begins condensation and elongation. By the end of the acrosome phase, the acrosome extends well over the nucleus with a space between the acrosome and nucleus ventrally, becoming pointed at the apical end. The nucleus reaches its maximum length at step 14, shortening slightly thereafter. By stage XIV, a ridge forms on the dorsal aspect of the acrosome. The caudal displacement of spermatid cytoplasm continues to be maneuvered into an isolated lobe of residual cytoplasm, approaching the manchette which is beginning to dismantle. At the end of stage XIV, a new generation of spermatids begin spermiogenesis. The maturation phase begins at step XV and sees the brief appearance of a dorsal fin on the acrosome. This marks the beginning of the assembly of the middle piece. At step 17, the acrosome moves forward and cytoplasm accumulates in the concave side of the head. During step 18, the cytoplasm becomes segregated into a residual body which is retained by the Sertoli cell at spermiation. The nucleus and acrosome become increasingly curved during steps 18 and 19. Stages I to XIV coincide with steps 1-14. Step 15 coincides with stage I, step 16 with stages II and III, step 17 with stages IV and V, step 18 with stage VI, and step 19 with stage VII, followed by release of the free spermatozoa after stage VIII.

Spermatogenic cells form elaborate, specialized, microtubule structures, only some of whose functions are readily apparent. Microtubules form mitotic and meiotic spindles that act as scaffolds for chromosome movement during cell division. In addition, an elaborate and extensively cross linked sheath of microtubules, the manchette, extends posteriorly over the caudal portion of elongating spermatids, surrounding the developing axoneme (Rattner and Brinkley, 1972; Cole et al., 1988). The function of manchettes remains controversial. Flagellar axonemes form the basis of the structurally complex spermatid tail that transduces microtubule-microtubule interaction into sperm motility. Arms, that extend from the microtubule doublets that form the outer cytoskeleton of the axoneme, are the basis of its kinetic properties. The arms are an axonemal form of the mechanoenzyme, dynein. Studies on the mechanochemical properties of axonemal dynein, and their role in sperm motility have provided a basis for the characterization of cytoplasmic mechanoenzymes (Tash, 1989). Isolated and demembranated axonemes have been used to study microtubule based motility (Paschal and Vallee, 1987) and have been used as a source of stable microtubules in studies of microtubule dynamics (Borisy and Bergen, 1982).

Positional changes of spermatids during spermiogenesis

Differentiating spermatids (step 8) become oriented perpendicular to the base of the epithelium in stage VIII. At this time, they are moved from the lateral compartment and become situated within a crypt of an individual Sertoli cell (Russell, et al., 1983a). Within Sertoli cell crypts, spermatids become oriented to the long axis of the Sertoli cell (stage VIII step 8) (Figs 1-2 and 1-5). The crypt deepens, carrying the spermatid once more toward the base of the Sertoli cell, passing spermatogenic cells of subsequent generations that are being moved toward the lumen. The basal migration occurs between stages II and VII with elongating spermatids reaching their most basal position during stages IV - V (see Clermont, 1972). These events are illustrated in Fig 1-5 (adapted from Clermont, 1972; Clermont and Rambourg, 1978 and Leblond and

Figure 1-5: Spermatid translocation in the seminiferous epithelium: This diagram depicts the stages of the seminiferous epithelium during which spermatids are moved from an apical, to a basal position, deep within Sertoli cell crypts and returned to the lumen for release. In each figure a Sertoli cell can be recognized by its infolded nucleus (S). Numbers indicate the steps of spermiogenesis for spermatids during these stages. Other cell types include spermatogonia (A)type A, (In) intermediate; (B) type B, (InM) intermediate in mitosis, (BM) type B in mitosis, and spermatocytes (Pl) preleptotene and (P) pachytene. Arabic numbers indicate the steps of spermiogenesis of spermatids during these stages. The spermatids reach their deepest position during stage V. Stages of spermatogenic cells are as indicated in Figure 1-2. (Adapted from: Clermont, 1972; Clermont and Ramborg, 1978; and Russell et al., 1990).

Stage I

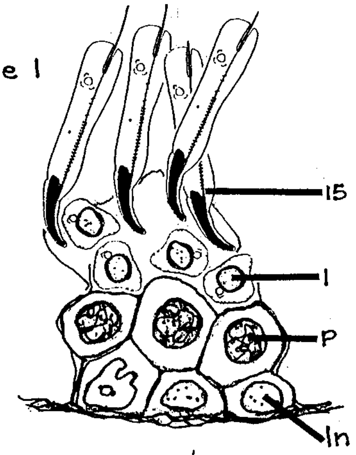

Stage II

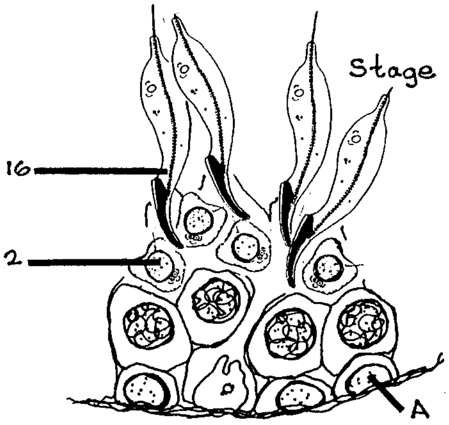

Stage III

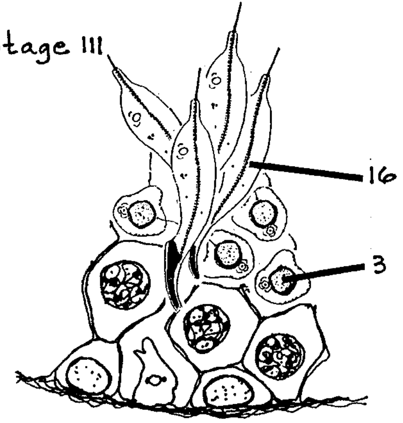

Stage IV

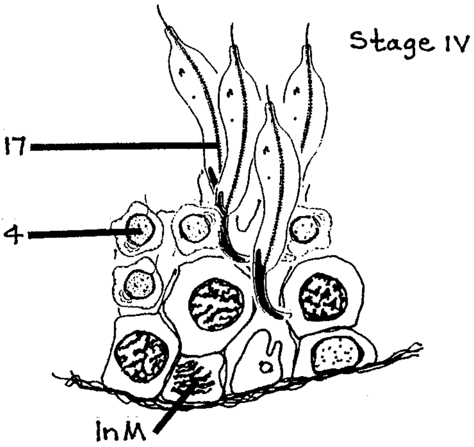

Stage V

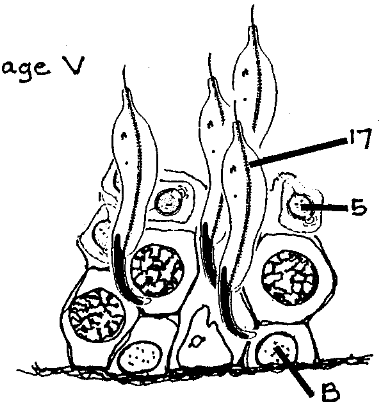

Stage VI

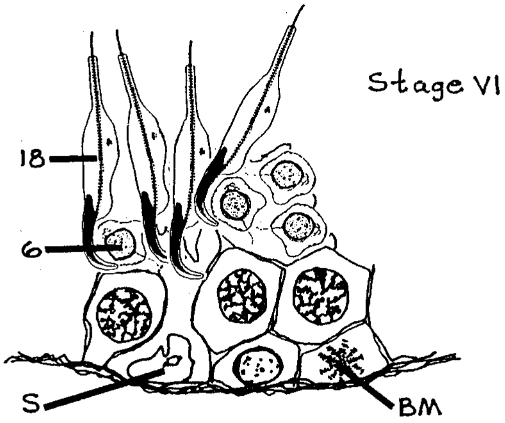

Stage VII

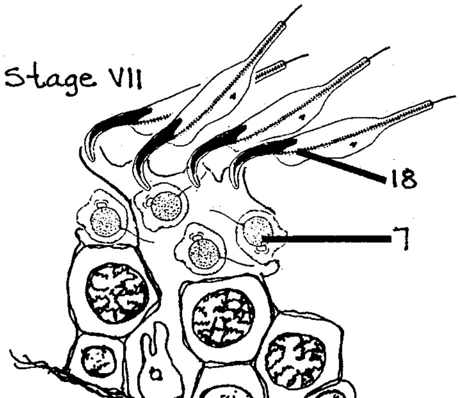

Stage VIII

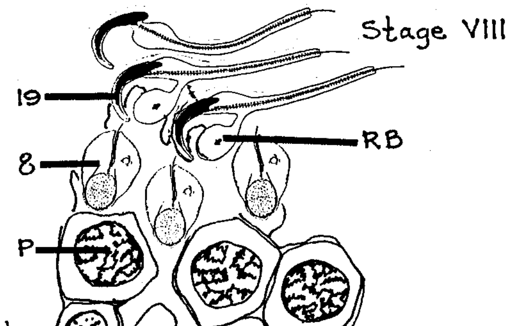

Clermont, 1952a), showing the relative positions of spermatogenic cells during the basal and subsequent apical spermatid migration.

A consequence of the positional changes of spermatogenic cells, that establish specific cell associations, is the segregation of spermatid residual cytoplasm (Russell, 1984). As the spermatid is moved toward the base of the epithelium, the residual cytoplasm becomes segregated from the elongating spermatid and anchored by processes extending from the Sertoli cell. As the spermatid returns to the tubule lumen, the spermatid nucleus is attached to the residual cytoplasm by a slender stalk. During spermiation, the residual cytoplasm is retained by the Sertoli cell and undergoes partial autolysis and then phagocytosis by the Sertoli cell (Russell, 1984).

Very little is known about the mechanisms that bring about these positional changes; however, in the absence of any evidence of inherent motility in the spermatogenic cells, they are thought to be mediated by Sertoli cells. During the initial migration toward the lumen the combined formation of Sertoli cell processes and the addition of subsequent generations of spermatogenic cells may explain the lumenal migration of spermatocytes. It has been suggested that unique actin containing structures, ectoplasmic specializations, lining Sertoli cell crypts during the orientation and translocation of spermatids, may participate in these positional changes (Fawcett, 1975; Vogl et al., 1983a; Russell, 1977c; Vogl, 1989).

Regulation of spermatogenic cell development

Little is known about how the development of spermatogenic cells is programmed or regulated. There are bridges between spermatids of the same stage, making possible a syncytial development of clones (Gondos, 1964). What was initially thought to be a wave of development passing along the tubule, suggesting a time line of morphogenesis, is no longer considered to result from the transmission of a wave like signal (Perey et al., 1961). Their stage-dependent changes in synthesis, secretion, and morphology imply that Sertoli cells play a very important role in the nourishment, and protection, as well as translocation and positioning of spermatogenic cells.

SERTOLI CELLS

One of the first features to be described in Sertoli cells, was their intimate relationship with spermatogenic cells (Sertoli, 1865), prompting the suggestion that they may play a role in the formation of spermatozoa. The responsibility of Sertoli cells for the nurturing of spermatogenic cells begins very early in development. Embryonic Sertoli cells arise from an undifferentiated blastema, not from the branching of a pre-existing epithelium as is frequently thought, are present before Leydig cells, and play a central role in the differentiation of the testis (Magre and Jost, 1991). In fetal testis, Sertoli cells carry out an endocrine function, secreting a Mullerian inhibiting substance, preventing spermatogenesis. Later, with the establishment of a basal tight junctions and cell polarity, they assume an exocrine role, the production of spermatozoa.

Mature Sertoli cells are non-proliferative, but exhibit stage specific physiological and morphological variation. Not only are germ cell associations constant with each other, but each cell association corresponds to specific Sertoli cell events. Although the causal relationships of most of these events is not known, it is the coordination of events in Sertoli cells with stages of spermatogenesis, that has led to the assertion that Sertoli cells largely regulate the events of spermatogenesis. However, the influence is not all one way, with paracrine effects of germ cells on Sertoli cells also known to occur (Saez, 1985; Kerr, 1988).

General morphology

Sertoli cells are essentially columnar cells that are continually being modified in correlation with changes in neighbouring spermatogenic cells. The fine structure of Sertoli cells has been studied extensively (Fawcett, 1975; Ritzen et al., 1981; Russell et al., 1983a; Plöen and Ritzen; 1984; Tindall et al, 1985; Kerr, 1988) and reflects their morphological and physiological support of spermatogenic cells. Fig. 1-6 is a diagramatic representation of the fine structural features found in Sertoli cells.

Sertoli cells extend from the base to the lumen of the seminiferous tubule. For purposes of discussion, the cell can be divided into three regions: the infranuclear or basal region, the nuclear region, and the supranuclear or apical region. The basal region is a narrow band between the nucleus and the base of the cell, with the nuclear region also situated deep within the cell. The apical region includes the extensive area above the nucleus that forms the body or stalk of the cell and a variety of highly pleomorphic processes. The most elaborate changes in volume, shape, and placement of organelles, occur in the apical region of the cell, corresponding to changes occuring in spermatogenic cells (Kerr, 1988); yet it is the most highly organized region, with most organelles oriented to the long axis of the cell. The cell volume is greatest from stage XIII to XIV and lowest at stage VIII, with most changes occurring in the apical portion of the cell (Kerr, 1988).

Sertoli cells can be easily discerned from adjacent spermatogonia by their highly infolded euchromatic nucleus, containing two perikaryosomes and a nucleolus, suggestive of synthetic activity. Centrioles have been described in a supranuclear position (Nagano, 1966).

Membrane bounded organelles

The presence of a large Golgi apparatus (Rambourg et al., 1979), lipid droplets, and elaborate accumulations of SER, argues for steroid synthesis in Sertoli cells, particularly in such species as ground squirrel (Vogl, 1983a). However, the role of Sertoli cells in steroidogenesis is still not clear.

Figure. 1-6: Sertoli cell fine features: This diagram illustrates the fine features of Sertoli cells. The figure is not intended to represent any specific stage of spermatogenesis. Shown are spermatogenic cells surrounded by Sertoli cell processes. Note that in the apical portion of the cell, microtubules and membranous organelles are oriented parallel to the long axis of the cell; whereas, in the basal portion they are more randomly distributed. Bundles of microtubules pass adjacent to the ESER of apical ESs. Spermatids are situated in Sertoli cell crypts that are lined by apical ESs. The blood testis barrier is closely associated with the basal ES. (SER) smooth endoplasmic reticulum, (IFs) intermediate filaments, (RER) rough endoplasmic reticulum, (mit) mitochondria, (ECM) extra cellular matrix, and (ES) ectoplasmic specialization.

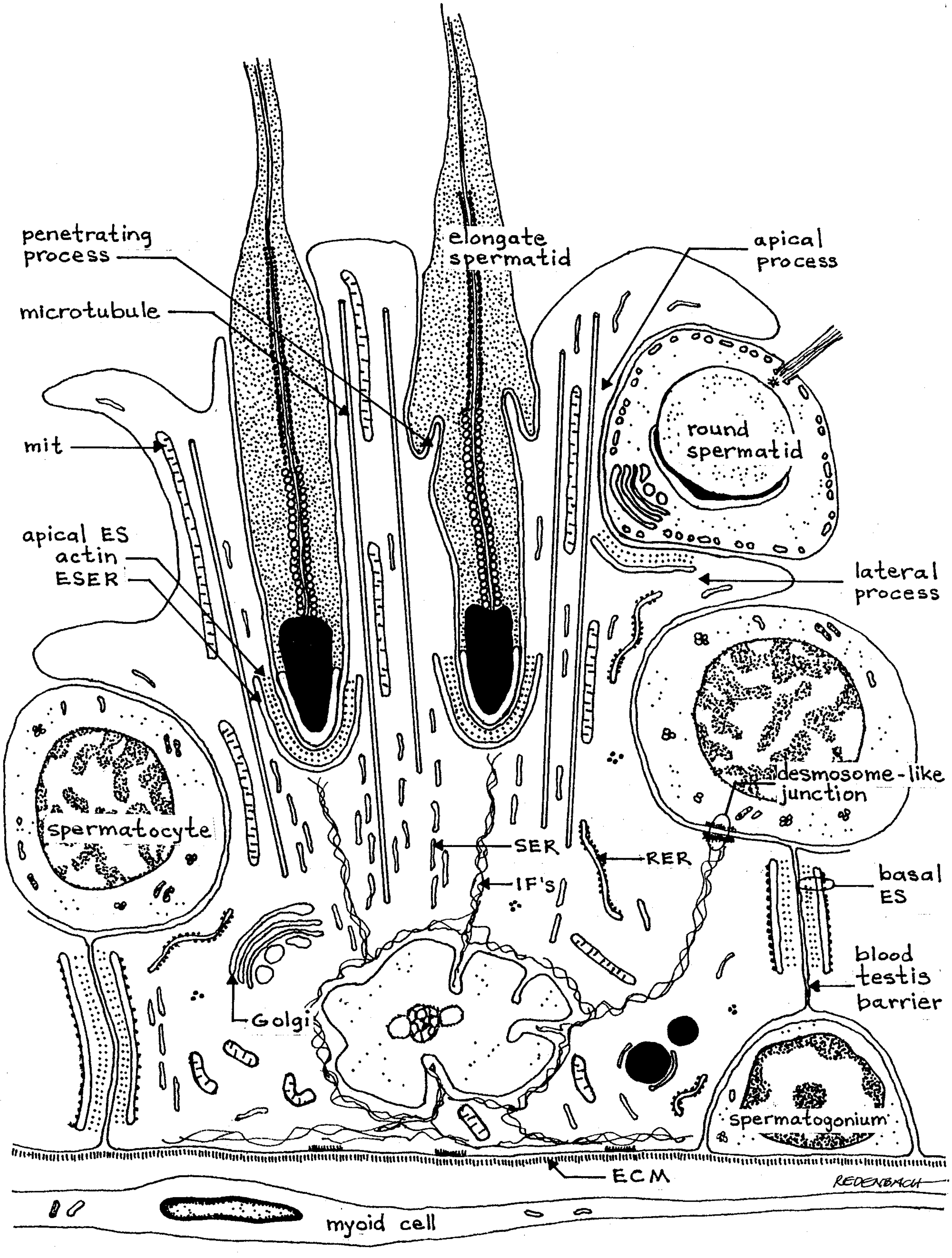
penetrating process
elongate spermatid
apical process
microtubule
round spermatid
mit
apical ES
actin
ESER
lateral process
spermatocyte
desmosome-like junction
SER
RER
IF's
basal ES
blood testis barrier
Golgi
spermatogonium
ECM
REDENBACH
myoid cell

Mitochondria

Basally, mitochondria are small and haphazardly organized, while apically they are numerous, elongated, and oriented parallel to the long axis of the cell, closely packed between the abundant microtubules (Fawcett, 1975).

Exocytotic and Endocytotic compartments

Sertoli cells synthesize and secrete a wide range of proteins (Ritzen et al., 1981 Kerr, 1988) including inhibin, androgen binding protein and plasminogen activator. Fawcett (1975) describes a paucity of vacuoles or membrane bound granules that would support the extensive export of a secretory product.

Morales and coworkers, (1986) describe an apical fluid phase endocytosis at all stages of spermatogenesis in which endocytotic vesicles fuse to become endosomes and transform into acid phosphatase-positive secondary lysosomes. Exclusively during stages VII through IX the endosomes fuse with phagocytosed residual bodies. Lysosomes increase in number from stages X though XIV, decreasing from stages I to II, and remaining low from IV to VIII. This period also reflects a rapid turnover rate. In addition to elimination of their own end products of metabolism, Sertoli cells play a role in the reduction and phagocytosis of spermatid residual cytoplasm. However, much of the residual cytoplasm is thought to undergo autolysis before it is phagocytosed by the Sertoli cell. The increase in lysosomes coincides with the elimination of spermatid residual cytoplasm. Ueno and Mori (1990) describe an earlier wave of primary then secondary lysosomes, in a basal location, between stages IV to VI prior to the increase reported by Morales et al (1986). The explanation for this increase remains speculative.

Golgi apparatus

The Golgi apparatus in Sertoli cells is well developed and found primarily in the basal portion of the cell (Fawcett, 1975; Rambourg et al., 1979). It consists of saccular regions, showing classical cis and trans regions, interconnected into one continuous organelle (Rambourg et al, 1979), with an unusual relationship to ER elements situated at trans but not cis regions.

The Golgi shows a biphasic, stage dependent change in volume, maximum at stage VIII and XIII to XIV and minimum at stage VII and IX-XI (Ueno and Mori, 1990). This change in volume is accompanied by a repositioning from the usual basal location of the Golgi to a more apical location, as described by Rambourg and coworkers in a 3D model of Golgi in stage V-VIII Sertoli cells (Rambourg et al., 1979). The authors suggest that this may be in response to an increased need for glycoproteins with changes in lysosome and plasma membrane in these regions apically, and that it is dependent on the presence of late spermatids (Ueno et al, 1991). In that positioning of the Golgi is microtubule dependent (see Kreis, 1990), with the Golgi being maintained at the microtubule minus-end in rat and mouse pituitary and monkey kidney immortalized cells (Skoufias et al., 1990), microtubules could be expected to play a role in the stage dependent relocation of the Golgi in Sertoli cells.

Endoplasmic reticulum

In Sertoli cells, rough endoplasmic reticulum and free ribosomes, located mainly at the base of the cell, are not prominent features (Nagano, 1966; Fawcett, 1975). The volume of RER is greatest at the time of spermatid release and lowest in stage XIII (Ueno and Mori, 1990; Kerr, 1988).

Sertoli cell SER demonstrates species and stage dependent variation, both in volume and distribution (Nagano, 1966; Fawcett, 1975; Vogl, et al., 1983a; Pudney, 1986; Clermont et al., 1980). Its greatest volume (three times the minimum volume) occuring at stages XIII-XIV and minimum at stages VII to VIII are reciprocal to the changes in RER (Kerr, 1988).

In the rat, abundant SER predominates in the apical region, particularly in association with round spermatids (Fawcett, 1975; Rambourg et al., 1979). During stage VI, while the spermatid is still deeply recessed in the epithelium, flattened cisterns of SER surround the head of the elongate spermatid while other SER profiles extend throughout the apical cytoplasm, oriented with the long axis of the cell. Early in stage VII, as the spermatid is being moved toward the lumen, bundles of microtubules are interspersed between the layers of SER. During stage VII, the residual cytoplasm moves basally, the nucleus becomes more curved, and tubulobulbar processes extend from the concave surface of the head. Becoming more fenestrated, the cisternae of SER give way to tubular forms, except at ES sites. The tubular forms of the ER enter the apical process from the apical stalk, extend along the dorsal surface as well as span the ventral curvature of the spermatid, anastomosing with the SER that cups the bulbous portions of the tubulobulbar processes, as they cross from the tip to the base of the nucleus (Clermont et al., 1980). The flattened cisternae of the ESER are disassembled along with the actin filaments, followed by disintegration of the tubular complexes and its SER system, leaving only the microtubules as spermiation proceeds.

In the ground squirrel, a large volume of SER is transported through the body of the Sertoli cell and into the apical stalk where it accumulates in cytoplasm surrounding the late spermatid. (Vogl et al., 1983a). The function of this dense layer of SER is not known. In this species, colchicine perturbation of microtubules results in the failure of the SER to be transported to the apical position, suggesting a role for microtubules in the SER positioning (Vogl, et al., 1983b).

Much of what has been learned about the functions of SER is derived from specialized systems such as steroidogenesis in the SER of endocrine cells, calcium sequestration in sarcoplasmic reticulum of striated muscle and metabolism of toxic substances in the SER in liver. Steroidogenesis, a common function of SER, is considered limited in Sertoli cells.

Intracellular calcium plays a role in a wide range of cell events and as would be expected, is unevenly distributed in the cytoplasm. In a 1984 review of calcium in cells, Somlyo pointed out, "Unfortunately for biologists, living systems often evolve to use different structures and mechanisms to solve the same problems (photoreceptors and contractile regulation are but two examples), and grand unifying schemes with fundamental principles applicable to 'all cells' are rare. In the regulation of cell calcium by the ER in all nucleated cells, we may have a rare example." (Somlyo, 1984). Currently, with such ubiquitous processes as microtubule-based transport and membrane targeting by coat proteins being described, a unifying scheme such as calcium sequestration by the SER, as described by Somlyo (1984), seems even more plausible. Calcium probes such as equorin used in Chironomus salivary glands (Rose and Lowenstein, 1975), indicate that selective calcium sequestration by SER is able to maintain heterogeneous microenvironments of calcium concentration within single cells. This permits local control of cell functions in which calcium acts as the second messenger. Calcium is a known regulator of the cytoskeleton and its chelation has been shown to mimic FSH induced shape changes in cultured Sertoli cells (see Dedman et al., 1979). In addition, the binding of microtubule associated proteins to tubulin is regulated by phosphorylation of microtubule associated proteins modulated by calcium calmodulin and cAMP dependent kinases (Bershadsky and Vasileiv, 1988c). Franchini and Camatini (1985b) report the presence of calcium in the ESER in guinea pig Sertoli cells, using a pyroantimonate precipitation technique. The data shown are not convincing and are inconsistent with the results of Kierszenbaum and coworkers (1971) in mouse Sertoli cells. The possibility that local calcium levels could be maintained by the ESER to regulate the cytoskeletal associated events around ESs bears further study.

The constant and elaborate, stage dependent, changes in membranous organelles that occur in Sertoli cells, most of which are microtubule dependent in cells generally

(See Schroer and Sheetz, 1991a), indicate a crucial role for microtubules in organelle positioning in Sertoli cells. The parallel orientation of many organelles and microtubules may reflect this association.

Cytoskeleton

In keeping with their role of providing morphological support for spermatogenic cells, in addition to their many intracellular functions, Sertoli cells possess an elaborate cytoskeleton of actin filaments, intermediate filaments, and microtubules (Amlani and Vogl, 1988; Vogl, 1988; 1989; Vogl et al., 1992). Except where they are part of stabilized structures, actin filaments and microtubules are highly dynamic polymers, undergoing constant assembly/disassembly in equilibrium with their respective soluble cytosolic pools. They both participate in structural and motility functions. In contrast, intermediate filaments are thought to be mainly architectural in function and less dynamic. The stability of each of these cytoskeletal elements as well as their association with each other, with membrane bounded organelles, and the Sertoli cell membrane is modified by the presence of a vast array of cytoskeleton associated proteins.

microfilaments

Microfilaments (filamentous actin) are assembled from monomers of globular actin (g-actin) polarized with a slow growing and a fast growing end, identified with myosin decoration as the barbed and pointed end respectively. They occur throughout the Sertoli cell, particularly in regions of the plasma membrane, as well as in areas of specialized function such as at ES sites, junctional sites, and tubulobulbar complexes (Franke, et al., 1978; Vogl et al., 1986; see for review Vogl, 1989; Vogl et al., 1992).

Microfilaments, identified by their 6 nm diameter size and ability to bind phallotoxins, are particularly prominent at ES sites where they form a highly ordered and stable hexagonal array between a cistern of endoplasmic reticulum and the Sertoli cell membrane (for review, Vogl, 1989). Fine strands between actin filaments suggest that they may be highly crosslinked to each other and to their adjacent membranes. Actin filaments at ES sites are very stable, being resistant to mechanical perturbation and the effects of cytochalasin, an actin disrupting agent (Russell et al., 1988).

intermediate filaments

In immature Sertoli cells, intermediate filaments are of vimentin, and to a lesser extent cytokeratin, types. Only the vimentin intermediate filaments are present in healthy Sertoli cells of the mature rat (Franke, et al., 1979; Amlani and Vogl, 1988; Hall et al., 1991). Intermediate filaments, identified ultrastructurally as 12nm filaments, are particularly prominent at the base of the cell and among infoldings of, and surrounding, the nucleus (Fawcett, 1975; Franke et al., 1979; Plöen and Ritzen, 1984; Brökelmann, 1963) giving the impression of a halo (Fawcett, 1975) that excludes other organelles from the nuclear region. From the nucleus they extend to desmosome-like junctions formed with translocating germ cells (Amlani and Vogl, 1988). Intermediate filaments appear to form a stabilizing scaffold between the nucleus and intercellular junctional sites, possibly adding stability to the epithelium and serving to position the nucleus at the base of the cell (Franke, et al., 1979). The stabilizing scaffold extends to intermediate filaments that form a network at the base of the cell in close association with hemidesmosome-like junctions between Sertoli cells and the extracellular matrix. Small bundles of 8-12 intermediate filaments reach from the nucleus into the apical portion of the cell, extending along the dorsal surface of elongating spermatids through a defect in the ESER to approach the cell membrane (Amlani and Vogl, 1988; Vogl, 1989; Vogl et al., 1991). The distribution of intermediate filaments changes with spermatogenesis, particularly in those associated with ESs. They are most prominent when spermatids are at their deepest location (Stage V), diminishing thereafter (Amlani and Vogl, 1988). It is proposed that these bundles may serve an anchoring function at Sertoli cell crypts.

microtubules

It was not long after the first discovery of microtubules that they were described in the cells of the seminiferous epithelium (Christensen, 1965; Fawcett, 1975). The seminiferous epithelium is a showcase of microtubule architecture, with many highly specialized microtubule structures in developing germ cells (Wolosewick and DeMay, 1982; Cherry and Hsu, 1984; Hermo et al., 1991) and cytoplasmic microtubules in Sertoli cells (Christensen, 1965; Fawcett, 1975; Amlani and Vogl, 1988; Vogl et al., 1983a; Vogl, 1988, 1989; Hermo et al., 1991). In contrast to the complexity of microtubule structures found in germ cells, the conspicuous feature of cytoplasmic microtubules in Sertoli cells is their abundance. They are most prominent in the supranuclear portion of the cell in which they are oriented parallel to one another and to the long axis of the Sertoli cell. As they extend into the apical processes, microtubules surround ESs that line Sertoli cell crypts and conform to stage dependent morphological and positional changes that occur in developing spermatids.

In that Sertoli cell microtubules are a prime focus of this study, they will be discussed later in greater detail following a description of the molecular, kinetic, and functional properties of microtubules in cells generally.

Ectoplasmic specializations

Unique actin containing structures called 'ectoplasmic specializations' (ESs) (Russell, 1977c) form within Sertoli cells in two locations: apically, they occur adjacent to regions of spermatid attachment to Sertoli cells; basally, they are present at the blood testis barrier (Brökelmann, 1963; Flickinger and Fawcett, 1967; Nicander, 1967; Dym and Fawcett, 1970; Russell, 1977c; for review see Vogl, 1989; 1991a,b). ESs are found on both sides of Sertoli-Sertoli cell junctions, but only on the Sertoli cell side of Sertoli-spermatid junctions (Romrell and Ross, 1979). Ribosomes are a constant feature of the outer face of the ESER at basal junctions but rarely occur on the apical ESER. Close association with intermediate filaments and microtubules are only a feature at apical ESs. The location of basal and apical ESs is indicated diagrammatically in Fig. 1-6 and their fine structure in Fig. 1-7.

Organization

ESs form adjacent to early spermatids becoming aligned with the rostral surface of the spermatid as the acrosome and nucleus migrate to the plasma membrane during step 8. At this point, orientation of the spermatid occurs. Failure of acrosome formation following injection with anti-cancer drug procarbazine indicates that acrosome-ES association is required for early spermatids to become aligned within the epithelium and enter Sertoli cell crypts (Russell, et al., 1983a).

As elongation ensues, ESs line the Sertoli cell crypts in areas adjacent to the acrosome. Although it is generally considered that ESs occur only adjacent to spermatid heads, Weber and coworkers, in a morphometric study of stage V rat Sertoli cell, describe ESs that extend as far as the midpiece of step 17 spermatids (Weber, et al., 1983). ESs are more concentrated over the dorsal than the concave ventral surface in step 17 spermatids (Weber, et al., 1983).

For purposes of correlating structure and function, Vogl and coworkers, (1991a) divide ESs into four major domains: 1) extracellular, 2) integral membrane (plasma membrane), 3) ectoplasmic, and 4) endoplasmic reticulum domains.

The extracellular domain spans the intercellular space and would contain the extracellular regions of adhesion molecules that would be present in the second domain, the integral membrane domain. In an attempt to identify adhesion molecules that may provide intercellular adhesion at ES sites, Pfeiffer and coworkers (Pfeiffer et al., 1991) were able to demonstrate a Beta 1 integrin subunit at apical and basal sites which could potentially occupy these first two domains. They were unable to detect E cadherin, N Cam or A Cam at these same sites (Pfeiffer et al., 1991). The third domain, the ectoplasmic domain, can be subdivided into three zones, encompassing the middle zone of

Figure 1-7: Ectoplasmic specializations: These micrographs show the ultrastructural features of apical ectoplasmic specializations in the rat (a,b) and squirrel (b,c) testis. Microtubules (arrowheads) can be seen in close association with the endoplasmic reticulum of ectoplasmic specializations or ESER (long fine arrows) in each case. Actin filaments (asterisks) are situated between the ESER and the Sertoli cell membrane (thick short arrow). Note the fine linkages that can be seen between the ESER and microtubules (short thin arrow). Bars: a-c = 250 μm, d= 100 μm.

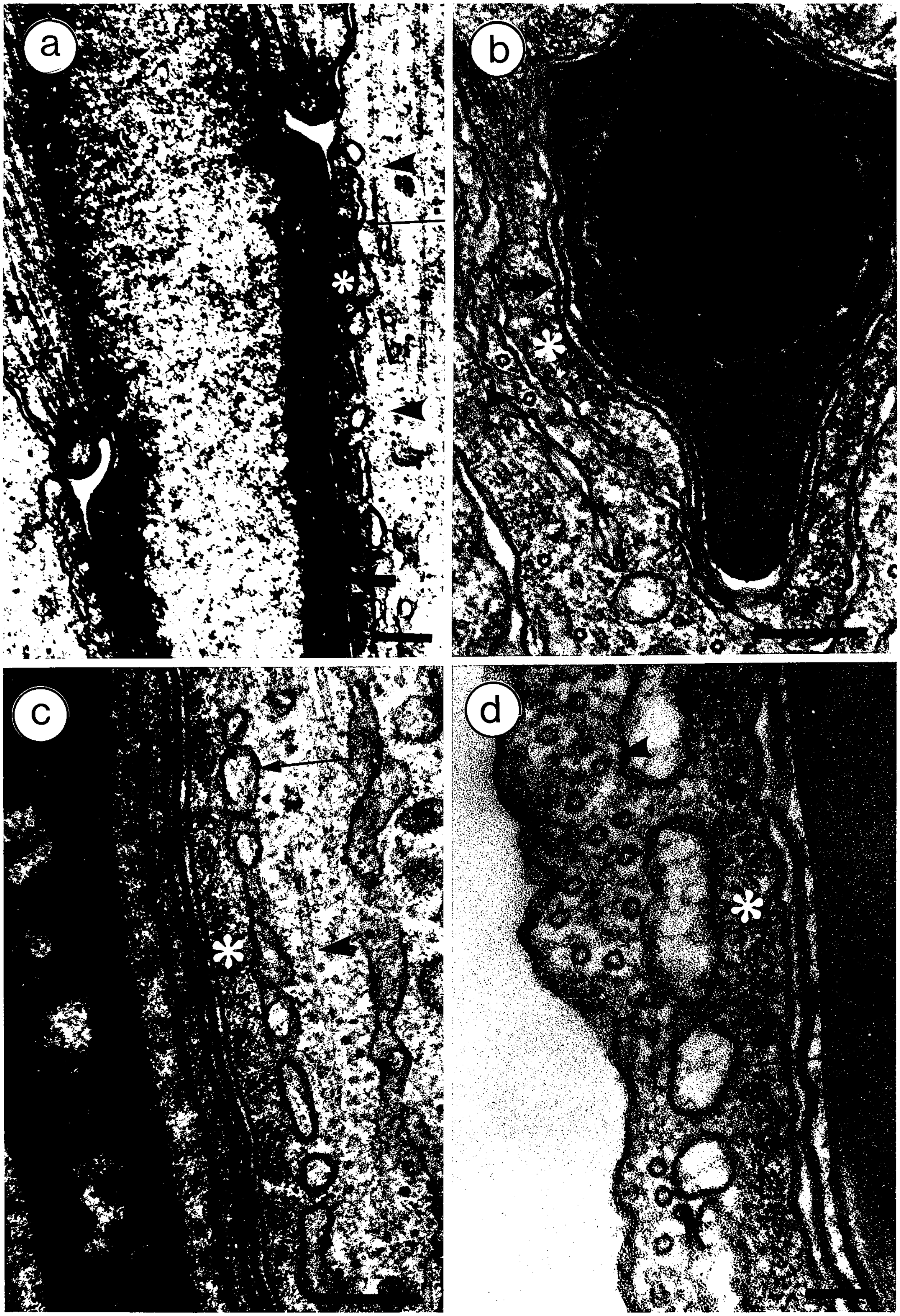
a
b
c
d
*
*
*
*

actin filaments and flanking zones of actin membrane attachment. The zones of attachment of actin to the plasmalemma is a likely location of vinculin, shown to be present at ESs sites (Grove and Vogl, 1989; Grove et al., 1989; Pfeiffer and Vogl, 1991). The actin zone contains an orderly array of actin filaments with an inter-filament spacing approximately 10 nm apart which appear to be crosslinked by fine strands, among which the actin binding proteins fimbrin (Grove and Vogl, 1989) and alpha actinin (Russell and Goh, 1988), present at ES sites, may occur. Very little information is available about the fourth domain, the endoplasmic reticulum domain. There is some evidence that the ESER may be continuous with the ER of the rest of the cell (Clermont et al., 1980), but whether its function is that of general ER, or if the ESER has specialized functions requires further study. Calcium has been reported in the ESER (Franchi and Camatini, 1985b) but due to the insensitivity of calcium localization technique used corroborative data are needed. In view of the increasing number of enzymes and coating protein markers available for ER and Golgi, this information may be available soon.

A provisional fifth domain, the cytoplasmic domain, is described. While not yet determined to be a part of the ES, microtubules occur in close association with the cytoplasmic face of ESs. At apical ESs, microtubules come in contact with the ESER, reminiscent of other systems in which microtubules are associated with membrane bound organelles and involved in microtubule based transport. It remains to be shown whether the fifth zone is a functional component of ESs.

Relationship with cytoskeleton

Intermediate filaments extend from the nucleus to ESs, reach along the dorsal surface of the spermatid, and pass through a gap in the ESER to reach the junctional membrane. Bundles of microtubules pass adjacent to ESs and are oriented parallel to the path of spermatid translocation. The close association of ESs with cytoskeletal elements suggests a role in positioning of spermatids at apical sites.

Linkages

Fine cross-linking strands have been described between actin filaments and from them to the adjacent membranes (Franke et al., 1978; Russell, 1977c). At ESs, actin filaments are firmly attached to the Sertoli cell membrane and to the cytoplasmic face of the ER component (Russell, 1977c) such that during very vigorous isolation of Sertoli cell organelles, ribbons of ESs are seen with both the Sertoli cell and ER membranes still attached (unpublished observations). The microfilaments and ER are tightly bound to the junctional site and remain attached when the cell is perturbed mechanically (Franke et al. 1978; Masri et al., 1987; Vogl and Soucy, 1985 Vogl et al., 1985a; 1986.) or with collagenase. However, they can be dissociated from the adjacent membrane by treatment with trypsin (Romrell and Ross, 1979; Masri et al., 1987; Vogl et al, 1986), resulting in the loss of the intense actin positive staining with NBD phallacidin, typical of ESs (Masri et al., 1987). Filament-filament or filament-membrane proteins alpha actinin (Franke, 1978) and fimbrin (Grove and Vogl, 1986b) are present but myosin is not (Vogl and Soucy, 1985). The cross-linking of actin filaments and their adjacent membranes contributes to the structural continuity to the spermatid to ESER linkage.

Strands, occasionally seen extending between the ESER and microtubules (Fig. 1-7), were first described by Russell (1977c). The nature of these linkages is not known nor is it known whether they are discrete structures.

ESER

The ESER is thought to arise from the ER of the Sertoli cell (Clermont et al., 1980) which extends into the apical cytoplasm and surrounds developing spermatids. The stage dependent changes in the ER that associates with the ESER have been described earlier. The ESER is seen as a flattened fenestrated cistern of ES that lies adjacent to the actin component of ESs from their first appearance adjacent to early spermatids. The function of the ESER is not known. Franchi and Camatini (1985b) have reported the presence of calcium in the ESER, using calcium precipitating agents, but the evidence is weak and requires confirmation. It is not known whether the ESER forms a functional unit with any of the membranous organelles that make up the secretory, Golgi, or endosomal compartments.

Stage specific changes

Although it is not known what specifies their formation, the current view holds that ES complexes arise from precursors in a cytosolic pool with basal ESs forming independently from apical ESs, rather than being cycled between apical and basal sites as an intact structure as had been proposed earlier by Russell (1984). Basal ESs form at approximately 16 to 19 days in the rat, coinciding with with the establishment of the blood testis barrier (Gilula et al., 1976) and the beginning of spermatogenesis. They are dismantled and reassembled with the shuttling of spermatocytes into the adluminal compartment, with little change in their overall pattern.

At apical sites, ESs show stage specific changes in their organization (Vogl and Soucy, 1985, Vogl et al, 1985). The appearance of apical ESs has been reported as early as the mid pachytene spermatocytes in the mouse (Ross and Dobler, 1975; Ross, 1976), although Weber and coworkers (Weber, 1983) indicate that few ESs are associated with spermatocytes, in the rat. They are present by the time spermatids begin differentiation and persist until step 18, just before spermiation (Russell, 1977c, 1984). Stage dependent reorganization of the actin filament pattern, of ESs, during spermatogenesis, has been described in squirrel (Vogl and Soucy, 1985; Pfeiffer and Vogl, 1991; Vogl et al., 1991a) and rat (Vogl et al., 1985b) and corresponds with species specific shaping of the spermatid head. Timing of ES disassembly shows species variation, being before (opossum and bandicoot), slightly before or during (guinea pig, chinchilla, stallion, bull, sheep, pig, dog, cat, rabbit, and rat) or after (mouse) disengagement of spermatozoa (see Russell, 1984). In rat, as ESs are gradually being dismantled, during stage VII, as a consecutive series of tubulobulbar complexes form and resorb, immediately prior to spermiation at stage VIII.

Functions

The numerous roles that have been suggested for the ES include: stabilization of the junctional membrane (Suarez-Quain and Dym 1984), intercellular attachment (Brökelmann, 1963; Nicander, 1967; Ross, 1976), cell communication (Flickinger and Fawcett, 1967), anchoring of the spermatid (Fawcett, 1975), regulation of surface contour and positioning of the crypt (Russell, 1977c), enzymatic digestion (Tindall et al, 1985), regulation of spermatogenesis (Saez et al., 1985), or secretion of steroids (Pudney, 1986), among which two functions seem most likely (Vogl, 1989): participation in establishment of adhesion domains at sites of the intercellular attachment and positioning of germ cells within the seminiferous epithelium (for reviews see Vogl, 1989; Vogl, et al., 1991a,b). Rather than being mutually exclusive, these roles are complementary.

The adhesion hypothesis is supported by a number of findings. The intimate association of ESs with sites of spermatid-Sertoli cell and Sertoli-Sertoli cell attachment suggests that the ESs play a role in their regulation. The naturally occuring breakdown in adhesion accompanies the resorption of ESs during the remodelling of the blood testis barrier and at spermiation (Vogl et al., 1983a). The pharmacological disruption of actin filaments with cytochalasin D (Russell, et al., 1988) leads to loss of adhesion at basal sites and release of spermatids. Evidence that ES actin filaments are of uniform polarity, demonstrated by S1 decoration in ground squirrel (Vogl et al., 1986) and rat (Masri et al., 1987), that myosin is not present in mammalian ESs, and that filaments do not contract defines a non-contractile role for ESs (Vogl and Soucy, 1985; Vogl et al., 1983 a). There is biochemical and immunological evidence that vinculin, typically present at adhesion junctions, is present at ES sites (Grove and Vogl, 1989; Grove et al., 1990; Pfeiffer and Vogl, 1991). Finally, when spermatids are mechanically removed from the seminiferous epithelium, the linkage between spermatids, the Sertoli cell membrane, and ESs remains intact (Romrell and Ross, 1979; Vogl et al., 1985; Masari et al., 1987; Grove and Vogl, 1989), indicating an adhesive continuity between ES and spermatid-Sertoli cell junctions. Taken together, these data suggest that ESs are part of actin-associated intercellular adhesion junctions (Vogl et al., 1986; Grove and Vogl, 1989; Vogl, 1989) which remain present throughout spermiogenesis and serve to anchor spermatids within Sertoli cell crypts.

Based on their presence at sites of spermatid-Sertoli cell attachment and close association with elements of the Sertoli cell cytoskeleton, they have also been suggested to participate in orienting and positioning spermatids within the epithelium.

Regulation

Very little is known about the regulation of ESs. There is some evidence that there may be an indirect calcium effect on ESs by a calcium-calmodulin pathway. Treatment of seminiferous tubules with trifluoroperazine, a calmodulin inhibitor, results in disorganization of actin filaments and displacement of ER (Franchi and Camatini, 1985a). Using a pyroantimonate method to localize calcium in guinea pig testis, these authors report the presence of calcium at ES sites (Franchi and Camatini, 1985b). Intratesticular injections of high doses of dibutyryl cyclic AMP results in retention of spermatozoa past their normal release at stage VIII through stages VIII, IX and X, accompanied by retained fluid in the subacrosomal space and surrounding the middle piece of the unreleased spermatozoa, and a failure of the dismantling of ESs and formation of tubulobulbar process (Gravis, 1980). The author concludes that the effect of dibutyryl cyclic AMP is to delay the dismantling of ESs and the consequential formation of tubulobulbar processes, producing persistent adhesion of the spermatids and retention of cytoplasmic fluid respectively. The mechanism behind these events is not known.

Changing physiological events in Sertoli cells during spermatogenesis

Morphological and positional changes that occur in spermatogenic cells have been described above. These events occur in a changing milieu established primarily by the Sertoli cell. The stage dependent changes in Sertoli cell organelles have been described and indicate that the physiological activities of Sertoli cells and the environment they establish, in the adluminal compartment and tubule lumen, change with spermatogenesis.

Using a 'transillumination' technique, similar to that introduced by Perey and coworkers (1961), Parvenin and Ruokonen (1982) have developed an approach to studying the physiological events of the spermatogenic cycle, devised to relate the external morphology of isolated seminiferous tubules with the conventional staging according to Leblond and Clermont (1952). Lengths of seminiferous tubules are dissected free from the interstitial tissue, and staged along their length, after which segments of the tubule are used to identify stage specific activities of the seminiferous epithelium. This allows for stage specific sampling of the seminiferous tubule for studies in which material from selected stages is required. The markers for determining stages of the seminiferous epithelium in dissected individual tubules are described in Chapter 3 Methods.

Stimulated by FSH and LH, Sertoli cells secrete a wide range of testis specific proteins, many of which are stage dependent (for review, Griswold, 1988). Kangasneimi and coworkers (1990), using transillumination techniques, (1990) have shown that FSH stimulated cAMP production is elevated between stages II and VI and suggested that this may correlate with the transport of spermatids deep within the epithelium. Mali et al (1985) found the LH stimulation of testosterone is highest at the onset of meiosis, a time when the rate of RNA transcription is greatest (stages VII-X1) and spermiation has just occurred. Levels of plasminogen activator, a protease thought to be involved with tissue reconstruction, are highest just before spermiation (stages VII and VIII), coinciding with reorganization of the blood testis barrier.

SERTOLI-GERM CELL RELATIONS

Processes

Of particular importance to the events of spermatogenesis are the elaborate cell processes and complex cytoskeleton of the Sertoli cell. Because of the translocation of germ cells through the epithelium, intimate Sertoli-Sertoli and Sertoli cell-germ cell relationships exist (Weber, et al., 1983). Specialized structures are formed in both cell types that serve to modify the Sertoli cell-germ cell relationship (Russell, 1980). The Sertoli cells interface with each other and with developing germ cells by extending a number of cytoplasmic processes. These structures include the lateral, apical, and penetrating processes of Sertoli cells and tubulobulbar processes of spermatids (Russell, 1980).

lateral processes

The Sertoli cell extends lateral processes which interlock with each other and enshroud the developing germ cells. The seminiferous epithelium is divided into basal and apical compartments by tight junctions, circumscribing the base of the Sertoli cells (Dym and Fawcett, 1980). This provides for separate apical and basal environments as well as an immunological barrier for germ cells having completed meiosis. Sertoli cells are involved in the ushering of spermatocytes from the basal to the apical compartment by both surrounding, and therefore isolating, translocating germ cells. As the germ cell is moved upward (a seemingly passive process) new lateral processes form behind the translocating germ cell then only after the new barrier is formed is the barrier above the germ cell dismantled, ensuring that there is not any communication between the two compartments (Russell, 1977a).

Apical processes

Apical processes extend from a microtubule rich stalk and support developing spermatids (Russell et al., 1983b; Weber et al., 1983, Vogl et al, 1983a). After spermatids are returned from their basal migration in Sertoli cell crypts, they become extended into the lumen on the apical stalk, held by apical processes. This is particularly evident in the 'simple' seminiferous epithelium of the squirrel where spermatids are extended into the tubule lumen on apical processes, extending from thin apical stalks (Vogl et al., 1983a,b). The elaborately convoluted surface of the apical portion of Sertoli cells contrasts sharply with other epithelial cells which typically possess microvilli and apically placed tight junctions.

Penetrating processes

Penetrating processes, from the Sertoli cell, invaginate into germ cell cytoplasm during its segregation from the rest of the spermatid (Nicander, 1967; Morales and Clermont, 1982; Vogl et al, 1985b). The presence of coated pits, in both the Sertoli cell penetrating processes and adjacent germ cells, suggests there is an exchange between the two cells (Vogl et. al., 1985b). Organelle content is variable, frequently including coated vesicles and pits. Penetrating processes have been suggested to aid in relocation and possible anchoring of residual cytoplasm, to be retained at spermiation, and to participate in intercellular exchange.

Vogl et al., (1983a, 1985a) have shown that, in squirrel testis, penetrating processes initially do not contain microtubules, but as the residual cytoplasm is extended into the tubule lumen, microtubules become abundant in these processes, suggesting that microtubules may participate in the maintenance of the shape of these processes and participate in the movement or removal of residual cytoplasm from the lumen to within the epithelium, following spermatid elongation.

Tubulobulbar processes

Tubulobulbar complexes form apically as cytoplasmic evaginations from the ventral surface of elongate spermatids, or basally from evaginations of Sertoli cells, coupled to invaginations of the adjacent Sertoli cell cytoplasm (Russell and Clermont, 1976; Russell, 1979a,b, 1984). They include a long slender penetrating process, the reciprocal Sertoli cell membrane, and its associated underlying structures. Tubulobulbar processes terminate in a bulbous swelling which may or may not have a further short tubular process. Surrounding the tubular portion, is a network of actin filaments (Vogl et al., 1985b; Vogl, 1989); capping the bulbar portion, is a cistern of endoplasmic reticulum (Russell and Clermont, 1976; Russell, 1979a). The endoplasmic reticulum is continuous with general ER (Russell, 1984). The tubulobulbar complex terminates in a coated pit. Basally, they occur in discontinuities of ESs and apically, occur at sites where ESs are being dismantled (Russell, 1979a; Clermont et al., 1980).

Apically, a series of these process form and disintegrate just before spermiation (mid stage VII to stage VIII) (Russell, 1979a). Their extent is species specific, being prominent in rat spermatids (Russell and Clermont, 1976; Russell, 1979a,b), less so in opossum, vole, guinea-pig, mouse, hamster, rabbit, dog, monkey and human (Russell and Malone, 1981), but seldom seen in the squirrel (Vogl 1989). Their function is unknown, but a correlation of their appearance apically at stage VII (Russell, 1979a) with a loss of cellular volume from spermatids suggests a function of fluid regulation (Russell, 1979c). As apical tubulobulbar processes persist until just prior to the loss of Sertoli-germ cell contact (stage VIII), an anchoring function is also possible (Russell and Clermont, 1976). Basally, they appear between stages II to V (Russell, 1979b), and are resorbed during the apical movement of spermatocytes through the blood-testis barrier late in stage VII (Russell, 1977a, 1979b). It is interesting that they occur at times when ESs are being modified and may be involved in the elimination of junctional membrane domains (see Vogl, 1989 for discussion).

Junctions

Junctional sites associated with the specialized intercellular relations of the seminiferous epithelium change during spermatogenesis. There are a variety of junctions which occur at the Sertoli-Sertoli cell and Sertoli-germ cell interface (Brökelmann, 1963). A tight junctional complex forms between lateral processes at the base of Sertoli cells, forming the blood testis barrier and is closely associated with, but distinct from, the adhesive junctions that occur at basal ES sites. At early germ cell-Sertoli cell contacts, desmosome-like junctions and gap junctions are encountered (Nagano, 1966; Russell, 1977a,c, Russell and Peterson, 1985). These junctions decrease in number until the second meiotic division of the germ cell is complete. Finally unique adhesive junctions (apical ESs) form between spermatids and Sertoli cells.

Blood testis barrier

Unlike many other epithelia, the tight junction of the seminiferous epithelium forms at the base of adjacent epithelial cells. Staining for filamentous actin at basal ES sites provides a close approximation of the pattern of tight junctions of the blood-testis barrier with which basal ESs are closely associated. The actin staining of basal ESs indicates an interconnecting honeycomb shaped junctional network, when epithelial sheets are viewed enface (Vogl et al, 1985a; Vogl, 1989), marking the ring like seal of the blood-testis barrier. The tight junction separates the basal and adluminal compartments (Dym and Fawcett, 1970) establishing the unusually tight blood testis barrier, evidenced by its impermeability to lanthanum (Dym and Fawcett, 1970) and the large number of parallel sealing strands seen on freeze fracture replicas (Gilula et. al., 1976). The formation of the junction, indicated by the appearance of actin filaments between days 16 and 22 in the rat (Russell et al., 1989) and the exclusion of lanthanum, coincides with the beginning of spermatogenesis and is required for the directional secretion of tubule fluid. An adhesion junction occurs in close associations with the tight junction, resulting in a close association of ESs with this junctional complex.

The blood testis barrier is thought to provide two functions: 1) the creation of a separate adluminal environment suitable for the nourishment of developing germ cells, and 2) immunological protection for post pachytene spermatocytes (Dym and Fawcett, 1970)

Sertoli cell-Spermatid junction

Sertoli cell-spermatid junctions are unique adhesion junctions, formed between spermatids and Sertoli cells, and possessing subsurface specializations, ESs, on the Sertoli cell side of the junction. Details of this junction have been included in previous discussions but a number of points should be summarized. These junctions occur in areas of contact between spermatids and Sertoli cells. That they are adhesion junctions is shown by the retention of the Sertoli cell membrane and ESs, at these sites, during mechanical removal of spermatids from the epithelium. They do not prevent the passage of such molecules as lanthanum and are therefore not tight junctions. It is thought that their adhesive function serves to anchor spermatids in Sertoli cell crypts in which they are moved to the base of Sertoli cells, before being translocated to the tubule lumen. It is through these junctions and their subsurface specializations that microtubules may exert their influence on positioning and translocation of spermatids. Loss of adhesiveness at these junctions, which occurs at spermiation, coincides with the dismantling of ESs.

MICROTUBULES

Introductory statement

Although the activities of microtubule based transport were observed as long ago as 1879, when microscopist, Joseph Leidy, described movement of small granules on invisible microtubule tracks in the freshwater foraminer, Gromia, it is not until recently that the fundamental and ubiquitous involvement of microtubules in cell activities has begun to be appreciated. The microtubule story has been closely tied to advances in microscopy. Leidy was unable to see the tracks that supported particle movement because microtubules, just 25nm in diameter, are well below the limit of resolution of 200 nm (Inoué 1986) in the light microscope.

Taking advantage of the improved resolution of electron microscopy, tubular fibrils were first identified by Grassier in 1965, Faure, et al., in 1958, and Roth in 1958, in axonemes of cilia and flagella, and Porter in 1954 in plants (see Gibbons 1988). These structures, were christened "microtubules" by Slautterback (1963), and first reviewed extensively by Porter in 1966. While electron microscopy soon revealed the ubiquitous occurrence of microtubules, it was the work of Allen and coworkers (Allen et al., 1981c,1982, Hayden et al. 1983) who, using computer assisted, video enhanced differential interference contrast microscopy (Allen et al. 1981a; Inoue, 1981), and extruded axoplasm of the squid giant axon (Brady et al., 1982, 1985; Vale et al., 1985c), brought to life the dynamic nature of microtubules. Immunocytochemical staining, viewed with fluorescence microscopy, proved to be an invaluable tool for studying microtubule associated events (Horio and Hotani, 1986; Sammak and Borisy, 1988). These techniques, coupled with the purification and characterization of the major microtubule protein, tubulin (see Mandelkow and Mandelkow, 1989b), and its copurifying proteins, microtubule associated proteins or MAPs (see Olmsted, 1986), made possible *in vivo* (Allen et al., 1982; Gilbert and Sloboda, 1984; Hayden et al., 1983) and *in vitro* (Vale et al., 1985b,d; Paschal et al., 1987; see Vale and Toyoshima, 1989) assays of microtubule-based transport. These studies have stimulated the isolation and characterization of a number of microtubule-associated ATPases, mainly falling into two families; kinesin (Vale et al.,1985a) and cytoplasmic dynein (Pratt, 1980; Paschal and Vallee, 1987), candidates for microtubule-based transport motors. More recently, other potential candidates for microtubule-organelle binding proteins (Rickard and Kreis, 1991; Van der Sluijs et al., 1990; Scheel and Kreis, 1991a,b) have been described. The extensive role of microtubules in organelle transport and positioning is rapidly being elucidated (see Schroer and Sheetz, 1991a).

Microtubule structure and kinetics

Microtubules can assemble from purified tubulin, but native microtubules are made of 'microtubule protein': that is, tubulin and its associated copurifying proteins, referred to as "microtubule associated proteins or MAPs" (Borisy et al., 1974; Williams and Detrich, 1979; Timasheff and Grisham, 1980; Vallee; 1982; McKeithan and Rosenbaum, 1989; Mandelkow and Mandelkow, 1989a,b).

Tubulin exists as a dimer comprised of alpha and beta tubulin monomers, total molecular weight 100 kD, sharing up to 60% homology. The tubulin dimer has one exchangeable and one nonexchangeable GTP binding site. Above a critical concentration, tubulin dimers assemble into microtubules, catalyzed by GTP binding at the exchangeable site (Timasheff and Grisham, 1980; Shelanski et al., 1973 for reviews see McKeitham and Rosenbaum, 1989; Mandelkow and Mandelkow, 1989a). Tubulin dimers assemble, head to tail, into protofilaments which in turn form lateral associations at a 10^{o} offset, resulting in a tubule format with a spiral orientation of neighbouring dimers (see Mandlekow and Mandlekow, 1989 a,b). Native microtubules approximately 25 nm in diameter are generally comprised of 13 protofilaments, but higher or lower numbers occur. The heterogeneity of dimers confers a structural and kinetic polarity on microtubules, giving them a slow growing minus-end and a fast growing plus-end (Allen and Borisy, 1974). Tubulin dimer exchange occurs exclusively at the ends of the polymer (Margolis, 1982; Rothwell et al., 1985). *In vivo*, cytoplasmic microtubules are in dynamic equilibrium with a cytosolic pool, which in turn regulates tubulin mRNA levels (Bershadsky, 1988).

Microtubule protein can be isolated by exposure of crude cell extracts to a series of temperature-dependent microtubule assembly/disassembly cycles (Borisy et al., 1974; Williams and Lee, 1982; Lee, 1982). Typically, microtubules are assembled at 37°C, pelleted by centrifugation and depolymerized at 0°C. Tubulin is then separated from the copurifying proteins (MAPS) by ion exchange chromatography (see Timasheff and Grisham 1980; Vallee, 1986b). Alternatively, capitalizing on the stabilization of microtubules at all temperatures by taxol, the microtubule protein is polymerized in the presence of taxol (Vallee, 1982, 1986a) and MAPs removed by high salt buffer, after which soluble MAPs and MAP free microtubules are separated by centrifugation.

Taxol promotes tubulin polymerization by lowering the critical concentration of tubulin required for assembly and strengthening inter-tubulin bonding (Wilson et al 1985), producing short stable microtubules (Schiff et al., 1979). Taxol binding, at a site distinct from the exchangeable GTP catalytic site (Horowitz, 1986), can proceed in the absence of GTP (Shelanski, 1970) and is able to stabilize microtubules against depolymerization conditions (Schiff et al., 1979; Horowitz et al., 1981,86; Wilson et al, 1985). These conditions include cold temperatures, $Ca^{+2,}$ buffer dilution, and depolymerizing agents such as nocodozole, vinblastine, and colchicine (Timasheff and Grisham, 1980 Shelanski, et al., 1979, Na and Timasheff, 1982, Dedmann et al. 1971).

Microtubule Organizing Centers (MTOC)

In many cells, microtubules radiate from a centrally located centrosome that consists of electron dense pericentrosomal material, and variably, a pair of centrioles. Centrosomes are the preferred site for microtubule assembly *in vivo* (Soltys and

Borisy, 1985) and nucleate microtubules *in vitro* (Mitchison and Kirschner, 1984; Kuriyama, 1984, Bergen and Borisy, 1980), determining their length, number, direction of growth, polarity, and protofilament number (Kuriyama, 1984; Bornens et al., 1987; Brinkley et al., 1981; Mitchison and Kirschner, 1984; Soltys and Borisy, 1985; Evans et al., 1985). These centrally located structures were initially considered the organizers of the cytoskeleton (Tilney ,1971), but a more dynamic scheme is now recognized in which MTOCs are able to assume different forms and cellular positions (Brinkley, 1985), the obvious example being cell division.

With the polarization of cells during mouse blastocyst formation, centrioles change position and microtubules ultimately become oriented with the long axis of the cell (Houliston et al., 1987; Fleming and Johnson, 1988). Similarly, the establishment of polarity in MDCK cells as they reach confluence, is accompanied by separation of centrioles, dispersion of the pericentrosomal material, realignment of microtubules, and increased microtubule stability (Bacallao et al., 1989; Bré et al., 1990), as evidenced by reduced tubulin incorporation and increased microtubule half-life (Pepperkok et al.,, 1990). These changes do not occur in fibroblasts, grown to confluence (Pepperkok et al., 1990; Bacallao et al., 1989).

Structures known to act as MTOCs include basal bodies, kinectochores, and centrosomes, of which only kinetochores nucleate microtubules at their plus-end (Brinkley et al., 1985). Not all microtubules are nucleated at centrosomes or identifiable MTOCs (Fleming and Johnson, 1988). Particularly graphic examples of this are the reorganization of microtubule polarity and direction of pigment transport that occurs in amputated segments of melanophore arms (McNiven et al, 1984; McNiven, and Porter, 1986) and chicken sensory neurites (Baas et al., 1987) and the reorganization of microtubule polarity that accompanies dendrite differentiation (Baas et al., 1988, 1989), indicating a potential for local regulation of microtubule polarity. Recently, it has been shown that gamma tubulin, a component of pericentrosomal material, nucleates microtubule assembly *in vitro*. Moreover, gamma tubulin antibodies block microtubule assembly *in vivo* (Zheng et al., 1991; Stearns et al., 1991; Joshi et al., 1991), and may be a candidate for nucleation at other sites.

Microtubule structures

We do not have to look any farther than the testis to find a variety of microtubule structures such as mitotic and meiotic spindles, axonemes, manchettes, and cytoplasmic microtubules, all functionally distinct. The question rises: how are these structural and functional microtubule differences determined? There are at least three levels at which structural and functional diversity of microtubules may be specified; genetic expression of tubulin isoforms, post translational modification, or regulation by associated proteins.

Tubulin isoforms

While there are multiple gene families encoding both alpha and beta tubulin, more than one gene will encode a single isoform or a single gene may encode multiple isoforms (Vilasante et al., 1986; McKeith and Rosenbaum, 1989). Furthermore, multiple isoforms can coexist in a single microtubule, or single isoforms occur in a broad range of microtubule structures in the same cell (Greer and Rosenbaum, 1989). Isoforms can be substituted for one another (Hoyle and Raff, 1990) and *in vitro*, diverse isoforms can assemble indiscriminately. In a recent review summarizing the available evidence for genetic determination of tubulin function, Bulinski and Gundersen (1991) conclude that, while the possibility of isoform specific microtubule functions cannot be excluded, the existence of multigene families of tubulin is not likely to be a significant determinant of microtubule structure or function (Greer and Rosenbaum, 1989).

Post-translational modification of tubulin

Post-translational tubulin modification, is a rapid and reversible means of producing covalently diverse tubulins and has been examined in a variety of tubulin containing structures (for reviews see McKietham and Rosenbaum, 1984; Bulinski and Gundersen, 1991: Greer and Rosenbaum, 1989). Known modifications include: phosphorylation, acetylation, and detyrosination. In comparative studies of tubulin modification and microtubule stability, using structural models of retinoblastoma cells (Schulze et al., 1987) and testis (Hermo et al., 1991) and morphogenetic models of fibroblast orientation, neurite outgrowth, and myogenesis (Bulinski and Gundersen, 1991), support has been found for a correlation between microtubule stability and the presence of detyrosinated and acetylated forms of tubulin. The simple assumption is that detyrosination and acetylation confer stability on tubulin. Accumulating evidence suggests that the correlation may be circumstantial; that detyrosination and acetylation are modifications that may occur on "older" microtubules, explaining the correlation with stability. Furthermore, the correlation between the stability/instability of microtubules and known categories of post-translation modification is not complete (Schultz et al., 1987; McBeath and Fujiwara, 1989). Idriss and coworkers (1991) have shown that kinetic indicators of dynamic instability are not changed by microtubule detyrosination. The current consensus is that these modifications are coincidental: not being a consequence, nor a cause of stability Schulze et al., 1987; Greer and Rosenbaum, 1989; Bulinski and Gundersen, 1991; Idriss et al., 1991). Functional diversity, only circumstantially related to post-translational modifications, may be primarily modulated by the presence of MAPs and other regulatory proteins.

Microtubule associated proteins (MAPs)

A number of proteins copurify with tubulin, for which Sloboda coined the term "microtubule associated proteins" or MAPs, classified generally according to their size determined on SDSPAGE gels (Vallee and Bloom, 1984; Paschal et al, 1987; for reviews see Olmsted, 1986; Sloboda and Gilbert, 1989; Wiche, 1989; Vallee, 1990b). Many MAPs are cAMP or calcium/calmodulin protein kinase stimulated phosphoproteins that, in turn, stimulate microtubule assembly (Wiche, 1989). MAPs have been divided into: two high molecular weight classes, MAP 1 and MAP 2; a second heterogenous group (~200kDa) that figures predominantly in non neuronal sources, including MAP 3 and MAP4; and a group of smaller MAPS, that includes Kinesin (110-130kDa) and tau (52-55 kDa) (Wiche, 1989).

Further characterization has now identified at least five subgroups of the high molecular weight (HMW) MAPs: MAPS 1A,1B,1C, and MAPS 2A and 2B. In neuronal tissue MAP 2, like tau, is heat stable distinguishing it from MAP 1. MAP properties, the basis of their terminology, vary considerably depending on the source and conditions of isolation, leading to some confusion. For example, a number of different MAPs have been designated MAP 1C (Wiche, 1989), including a low affinity mechanoenzyme whose yield is potentiated by isolation on microtubules that have been assembled with taxol in the absence of any triphosphate nucleotides (Paschal et al., 1987). This MAP has been identified as cytoplasmic dynein (Paschal et al., 1987), an ATPase and potential retrograde motor for organelle transport (Paschal and Vallee, 1987). Although not strictly 'MAPs', additional proteins are found to copurify with tubulin under special conditions, including the mechanoenzyme, kinesin. In a broad sense, 'microtubule binding proteins' would include all proteins that can bind to microtubules including: tubulin copurifying MAPs; transiently associating mechanoenzymes; and more stably binding microtubule binding proteins.

MAPs share a number of functions in addition to promotion of microtubule assembly. They mediate interactions between microtubules and with organelles, including other cytoskeletal elements (Gyoeva and Gelfand, 1991). These associations range from the dynamic interactions of mechanoenzymes to stable interactions produced by crosslinking or spacing mechanisms (Heins, et al., 1991) and can be translated into a wide variety of cellular functions.

Microtubule polarity

The asymmetry of tubulin dimers confers a physiological (Allen and Borisy, 1974; Summer and Kirschner, 1979; Bergen and Borisy, 1980; Mandelkow and Mandelkow, 1989a) and structural (Allen and Borisy, 1974; Mitchison and Kirschner, 1984; Horio and Hotani, 1986) polarity on microtubules, resulting in different assembly rates at the fast growing (plus) and slow growing (minus) ends (Borisy, 1978). Two morphological techniques have been devised to determine microtubule polarity *in vivo* : microtubule decoration with purified dynein (Haimo, 1982), or hook formations with purified tubulin (Heidemann and McIntosh, 1980; Heidemann and Euteneuer, 1982; McIntosh and Euteneuer, 1984; Heidemann, 1991). Incubation of microtubules in tubulin containing hook promoting buffer induces curved protofilament sheets to assemble along microtubules with a consistent handedness that gives the appearance of hooks, when viewed in cross section, indicating the pole from which the decorated microtubules are being viewed (Heidemann and McIntosh, 1980). This method correctly identifies over 90% of microtubules of known polarity, the remaining less than 10% being of the 'wrong' polarity. The occasional decoration of a single microtubule with hooks of both clockwise and counterclockwise handedness supports the assumption that those of opposite polarity are "wrong" in 5-10% of cases. When viewed from the plus-end, hooks form in a clockwise direction. Using the tubulin hook technique, cytoplasmic microtubules have been found to be unipolar with their plus-ends directed toward the periphery of the cell in axons (Burton and Paige, 1981; Heidemann et al, 1981; Baas et al., 1988), melanophores (McNiven et al., 1984; Euteneuer and McIntosh, 1981; Heidemann et al., 1981) chromatophores, (McNiven and Porter, 1986), neurites (Baas et al., 1987), photoreceptors (Troutt and Burnside, 1988a), *Reticulomyxa* (Euteneuer et al., 1989) and ciliary axonemes in a number of cells (Heidemann and McIntosh, 1980; Euteneuer and McIntosh, 1981). The single example of nonuniform polarity occurs when unipolar microtubules in developing neuronal cells become bipolar, coincidental with the onset of dendrite specific morphology (Baas et al., 1988, 1989; Black and Baas, 1989; Burton, 1988). Recently, examples have been found in which the minus-ends of microtubules are directed toward the periphery of the cell, including teleost retinal pigment epithelial cells (Troutt and Burnside, 1988b) insect ovarioles (Stebbings and Hunt, 1983) and *Drosophila* wing epidermal cells (Mogensen et al., 1989).

Cytoplasmic microtubules are highly dynamic and subject to changes in polarity under physiological conditions such as establishment of cell polarity (Houliston et al., 1987; Bacallao et al., 1989; Bré et al., 1990; Pepperkok et al., 1990) and dendrite formation (Baas et al., 1988, 1989), and experimental conditions, such as amputation of cell segments (McNiven et al, 1984; McNiven and Porter, 1986; Baas et al., 1987).

Microtubule polarity has important functional implications in cells, most notably in those which depend on important asymmetrical microtubule-based transport activities, such as the orthograde transport of neurosecretory products and retrograde transport of degradation products that occurs in axons. The more subtle activities, involved in organelle transport and positioning, also depend on vectorial microtubule transport (see Schroer and Sheetz, 1991a).

Microtubule based intracellular transport

Although intracellular motility was first described as long ago as 1879, almost a century passed before scientists began to elucidate the mechanisms of intracellular motility. While morphologists, reported microtubules in an increasing number of structures and cell types, physiologists studied the transport of radiolabelled substances, as well as vesicles, along axons (Smith, 1972). However, not until differential interference contrast microscopy was combined with video and computer image enhancement (Allen, at. al., 1981a,1982; Inoué, 1986, Schnapp, 1986), was it possible to visualize the participating organelles of intracellular motility, many as small as 25 nm, in real time, bringing the two fields together (Allen et al., 1981c, 1985; Brady et al., 1982; Lasek and Brady, 1985; Schnapp et al., 1985).

Much interest initially centered around two model systems of intracellular motility, pigment granule dispersal and aggregation, and axonal transport (for reviews see Vale, 1987; Sloboda and Gilbert, 1989). The aggregation and dispersion of pigment granules were proposed to occur on a dynamic scaffold, the microtrabecular lattice (Ellisman and Porter, 1980). Current evidence, such as the sensitivity of chromatophore distribution to vanadate (Ogawa, 1987), supports a mechanoenzyme driven microtubule-based transport mechanism.

Axonal transport, has been studied extensively since the first radiolabelling evidence of its existence. By ligating individual crab axons, Smith (1972) showed that organelles accumulate at both sides of the ligature, indicating that axonal transport is bidirectional. The organelles undergoing anterograde and retrograde transport were found to differ. With the development of Allen's video enhanced contrast differential interference contrast (AVECDIC) microscopy, Allen and coworkers (1981a,c; 1982) began following the events of axonal transport in the squid giant axon (Allen et al., 1981c, 1982). Brady and coworkers (1982) found that axoplasm extruded from the squid giant axon retains its transport activity, arguing against any involvement of the axonal membrane in axonal transport. In diluted extruded axoplasm, vesicles move bidirectionally along filaments (Brady, et. al., 1982; Allen et. al., 1985; Vale et al, 1985c); stirring of the axoplasm causes disordered transport. Vesicles were observed to transport bidirectionally on single transport filaments (Allen et al., 1983; Schnapp et al., 1985; Koonce and Schliwa, 1985). The diameter of the transport filaments was distorted because of the light diffracting effect of differential interference contrast microscopy which causes structures smaller that 200nm to appear uniformly as 200 nm. For this reason, the size of the transport filament, could not be measured accurately from the AVECDIC images (Inoué,1986). Immunofluoresence and video enhanced microscopy followed by slam freezing and rotary shadow electron microscopy on the same area of axoplasm, verified that the transport filaments are single microtubules (Schnapp et. al., 1985; Koonce and Schliwa, 1985). Allen and coworkers

(1985) used taxol to stabilize axonal microtubules, showing that treadmilling is not the mechanism of microtubule-based transport in axons.

To study microtubule based transport, Vale and coworkers (Vale et. al., 1985a-d) devised an elegantly simple *in vitro assay* in which isolated axoplasmic vesicles, in the presence of a high speed supernatant (S2) from axoplasm were added to MAP-free microtubules that had been adhered to glass slides. They found that: 1) in the presence of S2, axoplasmic vesicles transported along microtubules, 2) polystyrene beads, in the presence of S2 (or preincubated in S2), transport along microtubules; and 3) glass slides that had been coated with S2, (even if the slide had been rinsed with a buffer that does not support transport), supported the movement of microtubules. In the presence of S2, vesicle transport was shown to be sensitive to heat, trypsin, AMPPNP (non hydrolyzable analogue to ATP), 100μM vanadate, but not 20μM vanadate (phosphate analogue), or NEM (sulphydryl alkylating agent). Unlike their behavior in vivo, all axoplasmic vesicles were found to transport at the same rate (1.63 μm/sec) (Vale et al., 1985b,d), independent of vesicle size. Furthermore, in all these studies the transported vesicle (or surface) moved toward the plus-end of the microtubule. These findings indicate that: a 'motor' is present in the S2 high speed supernatant, the motor is able to bind microtubules, and the motor is able to bind vesicles (or form or a nonspecific binding to beads or glass) at its non microtubule end. Although the non microtubule end of the 'motor' binds nonspecifically to the glass or polystyrene beads, its binding to vesicles is highly specific.

In similar experiments using a crude axoplasm supernatant (S1), they found transport to be bidirectional and vesicles passed one another on the same microtubule without interference (Vale, et. al., 1985d). The S1 supernatant supported both minus-end and plus- end directed transport and was inhibited by NEM and by a lower concentration of vanadate (20μM) than was S2 supported transport (Vale et al, 1985d). This indicated the presence of a minus-end directed motor in the crude S1 supernatant, that had not been present in the S2 preparation. Taking advantage of the finding that vesicle transport in axons can be immobilized by the addition of the nonhydrolyzable analogue of ATP, AMPPNP (Lasek and Brady, 1985; Brady et al., 1985), Vale and coworkers isolated a plus-end directed motor, kinesin, from squid axoplasm (Vale et al., 1985a,b). Subsequently, the retrograde transport factor has been found to be a cytoplasmic form of the mechanoenzyme dynein that powers intermicrotubule transport in axonemes (Pratt, 1980; Paschal et al., 1987; Paschal and Vallee, 1987), now called 'cytoplasmic dynein'.

Gilbert and Sloboda (1984) injected rhodamine labelled vesicles into freshly extruded axoplasm, confirming that, *in vivo*, vesicles are transported in both directions, but do not reverse during their journey. Vesicles are able to move on purified microtubules, indicating that the motor resides on the vesicle. Moreover, by predigestion of vesicle surface proteins with triton, they showed that vesicle surface proteins are required for transport.

In vivo, organelles transport along axonal microtubules at a variety of rates varying over a 100 fold range (Pratt, 1989a) depending on load, rate limiting step, and phosphorylation state of the enzyme, and the presence of other governors (Pratt, 1989a). Vale, (Vale at. al., 1985ac) showed that transport rates varied in intact axoplasm but in extruded, diluted axoplasm and *in vitro* assays, vesicles travelled at the same rate of 2.2μm/second (Vale et al., 1985c), irrespective of size (Vale , 1987; Okabe and Hirokawa, 1989). It may be that mechanoenzymes have an inherent rate of transport which, *in vivo*, is differentially impeded by the viscous drag imposed by the cytoplasm.

In axons, vesicles transport along microtubules in both directions, transferring from one microtubule to another, passing one another without interference, and seldom changing direction. As they transfer from one microtubule to another they temporarily travel on two filaments at once. These observations have led to the conclusion that vesicles may have multiple motor binding sites (Vale et al, 1985c).

Axoplasm preparations remain viable for hours, even after two-fold dilution with buffer, (Lasek and Brady, 1985; Allen et al, 1985; Cohn et al., 1987) but, with time, vesicle transport slows. Addition of MgATP restores transport, indicating transport is MgATP dependent (Allen et al., 1985).

The terms 'anterograde' and 'retrograde' transport were initially used to distinguish the direction of microtubule-based transport in axons but with new models being studied, the terms are misleading; they imply that all microtubules are oriented with their plus end directed toward the cell periphery and they don't apply to cell free systems. The terms minus-end and plus-end directed motors indicate the direction of transport on microtubules and are more accurate.

An earlier hypothesis proposed that microtubule polarity was the sole determinant of the direction of microtubule based transport, like a one way street. This has been challenged by the fact that, with the notable exception of dendrites in neurons (Burton, 1988, Baas et al., 1988), cytoplasmic microtubules are unipolar tracks (Burton and Paige, 1981; Heidemann et al, 1981; Stebbings and Hunt, 1983; Euteneuer et al., 1989; Troutt and Burnside, 1988a,b; Baas et al, 1989; Bacallao et al., 1989; Black and Baas, 1998; Mogensen et al., 1998; Redenbach and Vogl, 1991). Using flagellar microtubules as tracks, Gilbert and coworkers (1985) showed that axoplasmic vesicle transport occurs bidirectionally on the unipolar microtubules. The *in vitro* assays of Vale and coworkers (Vale et al, 1985a-d) clearly showed that the polarity of microtubules does dictate the direction of transport, for given motors. This left unanswered: 1) how does bidirectional transport occur on single microtubules; 2) how is the direction of transport determined for a given vesicle and; 3) at what level is this decision regulated?

Mechanoenzymes

The issue of direction of transport was partially addressed with the discovery of the two families of microtubule associated mechanoenzymes, kinesin (Vale et al, 1985a,b,d; Brady, 1985) and cytoplasmic dynein (Paschal and Vallee, 1987). A great deal of evidence supports the proposal that kinesin and cytoplasmic dynein are the plus-end and minus-end directed motors respectively (Vale et al., 1985a,d; Paschal et al., 1987; Vale, 1987, 1990). However, the elegant simplicity of this story may be short lived, in light of a number of exceptions reported recently (Malik and Vale, 1990; Vale, 1990; Walker et al., 1990; Hirokawa et al, 1990; McDonald et al., 1990; Schliwa et al., 1991). The characterization of the mechanoenzyme families, by their molecular structure, biochemical properties, sensitivity to inhibitors, and rate and direction of transport provides criteria for their family members and a basis for comparison of those that may belong to other groups. Many of the properties of these putative motor families have been derived from microtubule binding, ATPase activity and motility assays which, while good predictors of one another, are not the same (Vallee, et al., 1989b). The mechanoenzyme activity of these motors is stimulated by microtubules. The effect of organelle binding is not known. The properties of mechanoenzymes vary considerably, depending on their source (Hollenbeck, 1989a,b), experimental conditions, and purity (Wagner et al., 1989). Purified systems can also be expected to differ substantially from *in vivo* systems. These differences in method of characterization have important implications for this study. Bearing this in mind, an attempt is made here to generalize the properties representative of each family, acquired under a variety of test conditions.

Kinesin:

Kinesin, was the first microtubule-based mechanoenzyme to be identified (Vale et al., 1985a,d; Brady, 1985; for reviews see Pratt 1989a; McIntosh and Porter, 1989; Vale, 1987; Bloom et al., 1989). It has been isolated from a number of species including squid (Vale et al., 1985a,b), chicken (Brady, 1985), cow (Kutznetsov and Gelfand, 1986), sea urchin egg (Scholey et al., 1988), and pig (Amos, 1987). The basis of kinesin isolation is its tight binding to microtubules in the presence of

AMPPNP, or ATP depletion (Cohn et al., 1989; Amos, 1987), and exclusive GTP dependent release from microtubules (Paschal et al., 1987a). In addition, general members of the kinesin family are distinguished from cytoplasmic dyneins by their: support of plus-end directed organelle transport, response to GTP, and relative insensitivity to the pharmacological agents vanadate, NEM, and EHNA. The kinesin family of mechanoenzymes share the following characteristics.

molecular structure:

Combined biochemical and ultrastructural data indicate that kinesin is a tetramer with a molecular weight of 350kD (Vale et al., 1985b) composed of two globular heavy chains (90-135 kD (Vale et al, 1985d) joined by a bent stalk, that terminates in a feathered end comprised of 2 light chains (55-80 kD) (McIntosh and Porter, 1989; Vale et al., 1985d). It has a sedimentation coefficient of 9.5 S. The ATPase activity resides in the heavy chains (Yang et al., 1989 Hirokawa et al., 1989), which is thought to be the microtubule binding site (Amos, 1987; Gilbert and Sloboda, 1986), while the feathered end, is the organelle binding site (Yang et al, 1989; see Sheetz, 1989). Although usually seen in a bent formation (Amos, 1987; Hirokawa et al., 1989), the molecule extends to 80 nm in length (Hisanga et al., 1989; Hirokawa et al., 1989) bent to 32nm (Hirokawa et al., 1989).

biochemical properties:

Kinesin has a low ATPase activity (Brady, 1985; Kutznetsov and Gelfand, 1986), that is stimulated by microtubules or Ca^{2+} (Cohn et al., 1987). It forms rigor complexes with microtubules in the presence of the nonhydrolyzable analogues of ATP, which are releasable with ATP and GTP (Lasek and Brady, 1985; Vale et al, 1985a; Porter et al., 1987).

sensitivity to inhibitors:

A number of inhibitors modify both the ATPase activity and transport capability of kinesin, although not always to the same extent (for reviews see Penningroth, 1989; Vale, 1990; Vallee et al., 1989; Wagner et al., 1989). Kinesin differs from cytoplasmic dynein in its generally low sensitivity to NEM (Vale et al, 1985a; Lye, 1989) and insensitivity to vanadate dependent photocleavage (Porter et al., 1987; Scholey et al., 1988). Although kinesin is relatively insensitive to vanadate at concentrations lower than 25 μM, both ATPase activity and motility are reduced by 100 μM vanadate (Lasek and Brady, 1985; Vale et al., 1985d; Porter et al, 1987). However, inhibitions at lower concentrations have been reported (Wagner et al., 1989). Porter and coworkers (1987) found that kinesin based motility declined in the presence of 3-5 mM NEM, but, unlike with other inhibitors, the effect is caused by failure to bind, rather than formation of rigor complexes. In contrast, kinesin ATPase activity is markedly reduced and transport activity suspended by quantities as low as 5μM AMPPNP (Okaba and Hirokawa, 1989), or by the ATP depleting agents apyrase or hexokinase and glucose

rate and direction of transport:

Kinesin's plus-end directed organelle transport activity (Vale et al, 1985a,cd; Brady, 1985; Porter et al., 1987ab, Scholey et al., 1988) is dependent, in a dose dependent manner, on MgATP (as low as 10 μM)(Porter et al., 1987) and GTP (above 1 mM) (Vale,et al., 1985c) at an *in vitro* rate of 0.6μm/sec (Vale et al, 1985c; Porter et al, 1987a). Low concentrations of ATP slow the rate of transport and the number of organelles participating. Kinesin's transport properties diminish with increased purity (Schroer et al., 1989; Schroer and Sheetz, 1991b), supporting the growing view that accessory proteins are required for transport activity.

other properties:

Although kinesin can be isolated in both organelle and microtubule fractions, 60-80% is found in the cytosolic fractions (Hollenbeck, 1989a; Vale et al., 1985; Sheetz, 1987, 1989). However, even without the use of AMPPNP or ATP depletion, low quantities of kinesin can be released from microtubules (Porter et al., 1987). Furthermore, it has been identified immunocytochemically with organelles, *in vivo*, and in isolated vesicle fractions (Brady and Pfister, 1991; Pfister et al., 1989b).

Cytoplasmic dynein

The isolation of cytoplasmic dynein was much more elusive, although its presence was anticipated, by analogy to axonemal dynein, even before the discovery of kinesin (Pratt, 1980). Its presence was suspected as the minus-end motor in the crude axoplasm supernatant S1 (Vale et al., 1985d). It has been identified as the high molecular weight MAP, MAP1C (Paschal et al, 1987; Paschal and Vallee, 1987; Gibbons, 1988), but the term cytoplasmic dynein is in current use, based on is close resemblance to axonemal dynein (Pratt, 1989a; Gilbert and Sloboda, 1986 Paschal and Vallee, 1987,1988 Paschal et al., 1987). It has been isolated in a wide variety of cells including, bovine brain (Paschal et al., 1987), amoeba (Euteneuer et al., 1989a), nematode (Lye et al., 1987), rat liver (Collins and Vallee, 1989), rat testis (Collins and Vallee, 1989; Neely and Boekelheide, 1988), squid optic lobe (Schnapp and Reese, 1989), and chick brain (Hollenbeck, 1989a). Like kinesin, cytoplasmic dynein supports organelle transport and can bind nonspecifically to glass at the non-microtubule end. The basis of its isolation is its binding to microtubules in the absence of ATP, selective retention during a GTP release step (to remove any bound kinesin), and then release by ATP. Although there is considerable yield of cytoplasmic dynein using this method of isolation, the majority of cytoplasmic dynein is thought to be associated with membrane bound organelles.

molecular structure:

Cytoplasmic dynein is a 140 kD mechanoenzyme consisting of two identical globular heads, (Stebbings, 1988; Neely et al., 1989), that comprise the heavy chains and one or more intermediate and light chains (Vallee, et al., 1989a) sedimenting at 20S. The ATPase activity resides on the heavy chains (Vallee et al., 1989a; see Pratt, 1989a), considered to be the microtubule binding end, with variable intermediate (68-72 kD) and light chains (50-55kD) (Neely and Boekelheide, 1988; Collins and Vallee, 1989), thought to make up the stalk and small globular organelle binding end (for review see Schroer and Sheetz, 1991a).

biochemical properties:

Cytoplasmic dynein has a weak ATPase activity (Paschal et al., 1987) which is stimulated markedly by microtubules in a dose dependent manner (Shpetner et al., 1988). Although dynein hydrolyzes other nucleotides, the rigor complexes it forms with microtubules are releasable only by MgATP (Paschal et al., 1987; Paschal and Vallee, 1987) but some forms of cytoplasmic dynein (sea urchin egg dynein) are less discriminating in their nucleotide dependence than others (Pratt, 1986b). Unlike kinesin, but like myosin, it does not form rigor complexes with nonhydrolyzable analogues to ATP. Its increased binding to microtubules with ATP depletion varies with the source of cytoplasmic dynein (Lye, 1989).

sensitivity to inhibitors:

Cytoplasmic dynein is distinguishable from kinesin by its sensitivity to NEM, at concentrations greater than 1 mM (Shpetner et al., 1988)(being reported as low as 100μM) (Okawa and Hirokawa, 1989; Lye, 1989; Paschal et al., 1988; Paschal and Vallee, 1987), vanadate, at concentration as low as 10 μM increasing to 100μM (Shpetner et al., 1988), EHNA, at 1-5 mM, although mainly at high ionic strength (Okaba and Hirokawa, 1989; Pratt, 1989a; Shpetner et al., 1988), and vanadate dependent photocleavage (Lye, 1989; Neely and Boekelheide, 1988). ATP depletion decreases transport (Vale et al, 1985b).

rate and direction of transport:

Cytoplasmic dynein supports minus-end directed microtubule based transport (Paschal and Vallee, 1987; Schroer et al., 1988a,b) at a rate of 2.0 µm/sec (Porter et al., 1987).

other properties:

Based on immunocytochemical staining and negative staining, dynein is thought to reside mainly on organelles but is also present in solution (Pratt, 1989a) and can be isolated on microtubules.

Other putative microtubule-based motors for organelle transport

Interpreting the characteristics of kinesin and cytoplasmic dynein broadly, most isolated motors or proposed motors fit into the two families. However, some decidedly do not. In some cases, it is not known whether these represent a unique family of motors, or if the experimental conditions have produced the contradictions. The failure of highly purified kinesin to support transport is but one example. They are described here to illustrate the potential for other motor families, as well as the differences that may lead to a better understanding of the underlying mechanisms of organelle transport.

visiken

Gilbert and Sloboda (1986, 1989) have isolated a microtubule associated protein: 'vesiken', present in both vesicle and microtubule fractions, that cross reacts with MAP2 antibodies. Although transport has not been demonstrated directly, anti-vesiken antibodies label vesicles and can block vesicle transport. Unlike dynein, vesiken does not photocleave in the presence of vanadate.

10 S sea urchin egg motor

Collins and Vallee (1986) have isolated a 10 S sea urchin egg motor with the following properties: microtubule stimulated ATPase activity, hydrolyzes ATP and GTP and is unaffected by vanadate. However, it remains bound in the presence of ATP

Reticulomyxa motor

Koonce and coworkers (Koonce et al., 1985, 1986; Koonce and Schliwa 1985a; Euteneuer et al., 1988b, 1989a,c) report a 20-23S putative motor from *reticulomyxa* that shares many properties with cytoplasmic dynein. It is insensitive to AMPPNP. ATP depletion increases binding which is released with ATP but not GTP. The motor is subject to vanadate dependent photocleavage and sensitive to 100 μM vanadate, EHNA and millimolar concentrations of NEM. Intriguingly, it supports bidirectional transport, which reverses readily and can be reversed by phosphorylation.

The pharmacological agents inhibit both directions of transport in the same manner, suggesting that the bidirectional transport is not an artifact of isolation (Porter and Johnson, 1989).

C. elegans motor

Lye and colleagues (1987) have isolated a 400 kD putative motor from *C. elegans*, that resembles both kinesin and cytoplasmic dynein. It was initially reported to have ATPase activity that is sensitive to vanadate (5 μM), 1 mM NEM, 5 mM AMPPNP, subject to vanadate dependent photocleavage, and does not release from microtubules with GTP. However, it was found to support plus-end directed microtubule-based transport. Subsequent studies showed it to be minus-end directed, illustrating the characterization problems that occur with different experimental conditions.

A similar danger lies in extrapolating untested parameters from the generalization of a group of tested effects (Malik and Vale, 1990), as the next example illustrates.

Kar 3 and ncd non claret disjunctional gene product

Using a genetic approach, a putative motor has been encoded from Drosophila non claret disjunctional gene from *Drosophila*. It has properties similar to kinesin with AMPPNP binding, and has a 40-45% homology with kinesin heavy chain (McDonald et al., 1990; McDonald and Goldstein, 1990; Walker et al, 1990; see Vale and Goldstein, 1990), suggesting that it belongs to the kinesin family, and it was presumed it would be a plus-end directed motor. However, it is a minus-end directed motor. Its homology with kinesin is only in the heavy chain (motor) component. The ATPase site is on the opposite terminus from that of kinesin.

Organelle-microtubule binding proteins

It is safe to say that all microtubule-based mechanoenzymes are microtubule binding proteins. Not all support organelle-microtubule binding; some, for example axonemal dynein, support inter-microtubule transport. Of those proteins that do link organelles to microtubules, not all are mechanoenzymes. The term organelle-microtubule binding proteins may best describe these proteins.

170 kD protein from Hela cells

There is some evidence that not all the proteins for which microtubule binding is affected by nucleotides are motors, but may represent another class of proteins that function to anchor, rather than transport, organelles. Why then do they require ATP? The nucleotide dependence may reflect regulation of microtubule binding by phosphorylation as that described in the 170 kD protein reported by Rickard and Kreis (1990, 1991; Rickard and Kreis, 1990), rather than the use of nucleotides for transport. The 170 kD protein is released from microtubules with ATP,*in vivo* but not *in vitro.* The presence of ATP prevents binding, due to a change in the phosphorylation state of 170 kD protein. These authors propose that the ATP dependence is in an enzyme mediating binding between endocytic vesicles and microtubules (Scheel and Kreis, 1991b), resulting in release of 170 kD from microtubules with ATP and GTP, in the presence of cytosolic factors. 170 kD protein is unaffected by AMPPNP, immunolocalizes with microtubule pathways *in vivo* becoming dispersed with microtubule disruption. This protein is reminiscent of the 173 kD protein in testis (Neely and Boekelheide, 1988), that is releasable with ATP and GTP. The exact nucleotide interaction remains to be clarified. Proteins such as this one, that are releasable with both ATP and GTP may have missed detection in other systems because they would not be recovered during kinesin isolation, because they are not AMPPNP responsive, and would have been lost in a dynein preparation because they would not survive the early GTP step to release kinesin.

The mechanochemical cycles of kinesin and cytoplasmic dynein

In order to explain some of the effects of pharmacological properties on the ATPase activity and motor capabilities of these motors, it is useful to understand their mechanochemical cycles. Although these cycles are not fully elucidated some information is available.

The mechanochemical cycles of microtubule-kinesin (M·K) and microtubule-dynein (M·D) cycle can be compared to the well studied actin-myosin cycle (A·M). The cycles of these three mechanoenzymes share three properties: 1) the formation of enzyme-cytoskeletal complexes in the absence of ATP, 2) dissociation of the complex with the addition of ATP (complexed to Mg), 3) activation of enzyme ATPase activity in the presence of the cytoskeletal cofactor (Scholey et al., 1988).

In the actomyosin cycle (see Fig.1-8), ATP has two functions. It provides energy for the power stroke and reduces affinity of the linking partners. The well studied

Figure 1-8: Mechanoenzyme cycles: This figure is an abbreviated version of the events of the mechanochemical cycles of the interaction of myosin with actin, dynein with microtubules (upper figure), and kinesin with microtubules (lower figure). In the upper figure, using the well studied actomyosin cycle as the example, the cycle begins with myosin bound to actin (AM), ATP then binds to AM (AM·ATP) reducing the affinity of myosin for actin and resulting in release of myosin-ATP from actin (M·ATP). ATP is then hydrolyzed to ADP and inorganic phosphate (ADP · Pi) and Pi is released to yield myosin ADP (M·ADP). The ADP is released (AM). The kinesin-microtubule mechanochemical cycle is similar except that the microtubule is not released until after the release of inorganic phosphate. In the actin-myosin cycle the rate limiting step is phosphate release. In the kinesin-microtubule cycle, the rate limiting step is ADP release. The difference between the two cycles is reflected in the fact that actin and myosin (dynein and microtubules) are released before hydrolysis, but kinesin and microtubule release follows hydrolysis. This is the basis for their different response to non hydrolyzable analogues of ATP.

Actin · Myosin and Microtubule · dynein pathways

$$\begin{tikzcd}
AM \arrow[r, phantom, "\rightleftharpoons"] \arrow[d, phantom, "\upharpoonleft\downharpoonright"] & AM \cdot ATP \arrow[r, phantom, "\rightleftharpoons"] & M \cdot ATP \arrow[d, phantom, "\upharpoonleft\downharpoonright"] \\
AM \cdot ADP & M \cdot ADP \arrow[l, phantom, "\leftrightharpoons"] & M \cdot ADP \cdot Pi \arrow[l, phantom, "\leftrightharpoons"]
\end{tikzcd}$$

Microtubule · Kinesin pathway

$$\begin{tikzcd}
MK \arrow[r, phantom, "\rightleftharpoons"] \arrow[d, phantom, "\upharpoonleft\downharpoonright"] & MK \cdot ATP \arrow[r, phantom, "\rightleftharpoons"] & MK \cdot ATP \arrow[d, phantom, "\upharpoonleft\downharpoonright"] \\
K \cdot ADP & MK \cdot ADP \arrow[l, phantom, "\leftrightharpoons"] & MK \cdot ADP \cdot Pi \arrow[l, phantom, "\leftrightharpoons"]
\end{tikzcd}$$

actomyosin system provides a model. ATP binds to the rigor complex, actomyosin, producing dissociation to actin and myosin, the ATP is hydrolyzed producing an activated myosin·ADP·Pi complex with increased affinity for actin. As a result of the higher affinity, actin binds to myosin and the phosphate (Pi) is released, providing energy for the power stroke. This cycle would appear to be the same for cytoplasmic dynein as well. The following evidence indicates that the situation is different for kinesin. As a nonhydrolyzable analogue of ATP, APMPNP stabilizes the transient intermediates that occur just before hydrolysis (Lasek and Brady, 1985) at a point which, in the myosin or dynein cycles dissociation has already occurred, yet in the kinesin cycle dissociation has not occurred. This indicates that, unlike the case of myosin and dynein, dissociation follows not precedes hydrolysis, for kinesin (Lasek and Brady, 1985; Vale, 1987). The rate limiting steps are different for the two enzymes with that of kinesin being ADP release, and dynein being phosphate release (Pi). For kinesin, it is the fast release of Pi and the very slow release of ADP that results in dissociation occuring after hydrolysis (Chilcote and Johnson, 1989; Hackney, 1988, Hackney et al., 1989). The result is that AMPPNP, by blocking hydrolysis, blocks release of the rigor complexes, in kinesin only. Myosin and dynein have a low affinity for AMPPNP, and in these two motors, AMPPNP is less effective in dissociating rigor complexes than ATP (Chilcote and Johnson, 1989), although slow dissociation occurs. If AMPPNP is added to rigor complexes formed by dynein (or myosin), the binding may be reduced by the slow activity of AMPPNP, acting as a slow substitute for ATP. The effects of AMPPNP for both kinesin and dynein are small compared with ATP, and high concentrations of ATP negate these effects. Now it may be useful to look more closely at the inhibitors of these events.

Mechanoenzyme inhibitors and how they work

Penningroth (1989) points out that characterization of mechanoenzyme properties in the presence of selected inhibitors is most reliable in a well defined system, such as axonemal dynein based transport, where the only ATPase activity is expressed as inter-microtubule sliding. The complexities of organelle transport, even in fairly well defined systems, presents some problems of interpretation of mechanoenzyme behavior. The composition of the motor complex is unknown, as is the presence of activators that may be present in the cytoplasm. Bearing that in mind, the inhibitors EHNA, Vanadate, NEM, and AMPPNP are frequently used to characterize putative motors and their properties (See Fig. 1-9 for the molecular structures of EHNA, vanadate, and AMPPNP).

EHNA: (erythro-9(3-(2-Hydroxynonyl) adenine is a structural analogue of adenosine. It binds at a site that is separate from the catalytic site, inhibits dynein ATPase activity in a dose dependent manner, is reversible with ATP, is effective below 0.2 mM ATP, gives a mixed response to dynein, and generally behaves similarly to reduction in ATP. It is more inhibitory on motility mediated by dynein than kinesin (Vale et al., 1985b)

NEM: (N-ethylmalemide) is a sulphydryl alkylating agent interfering with SH bonds, and is blocked by ATP, indicating its effect is near the catalytic site. As an inhibitor, it is not very specific in that it potentially affects any SH groups. It does however illustrate the interpretive difficulties that occur comparing ATPase activity, motility, and binding assays. Unlike ATP depletion, which would increase binding but reduce transport, NEM would reduce both, because it interferes with cytoplasmic dynein by preventing binding rather than by blocking hydrolysis and forming rigor complexes (Porter et al., 1987; Dabora and Sheetz, 1988a).

Vanadate: $V0_3$ is an analogue of phosphate. It forms by attaching to ADP, with hydrolysis of ATP needed for its formation. It binds near but not in the catalytic site; it does not compete directly with ATP; and its effects depend on ionic strength. It acts as a general phosphate poison. Therefore, if there is no turnover of binding, no change would be expected. Its effect may be dependent on the relationship between the timing of the rate limiting step and product release in the mechanochemical cycle.

Figure 1-9: Mechanoenzyme inhibitors: This figure indicates the molecular structure of analogue of ATP or its components used as inhibitors to characterize microtubule-spermatid-ES binding. The inhibitors are shown on the left and their counterparts on the right. EHNA is a structural analogue for adenosine; vanadate is an analogue for phosphate; and AMPPNP is a nonhydolyzable analogue for ATP.

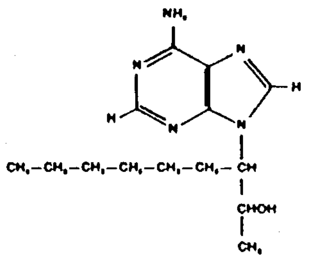

erythro-9-[3-(2-Hydroxynonyl)]Adenine (EHNA)

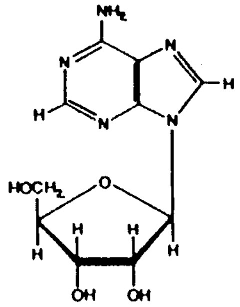

Adenosine

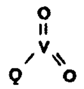

Vanadate

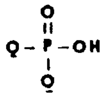

$O^{-}-\underset{\underset{\displaystyle O^{-}}{|}}{\overset{\overset{\displaystyle O}{\|}}{P}}-OH$

Phosphate

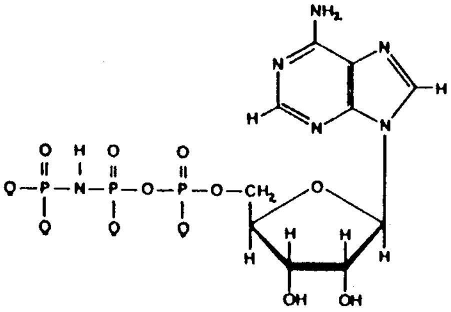

AMP-PNP

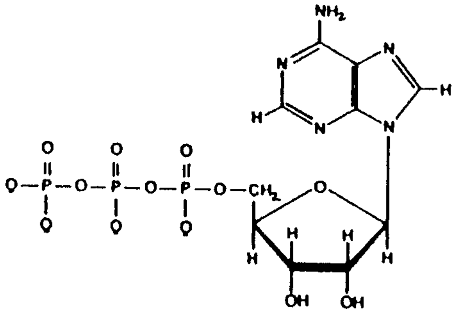

ATP

Alternatively it may be influencing the phosphorylation state of the enzyme or accessory proteins.

AMPPNP: (adenyl imidodiphosphate) is a non hydrolyzable analogue of ATP. It binds at the catalytic site inhibiting ATPase activity by blocking the hydrolysis step. This points to a potential difference in the mechanochemical pathway of dynein and myosin compared with kinesin. The formation of rigor complexes by AMPPNP implies that product release follows ATP hydrolysis (kinesin), whereas the absence of rigor complexes implies that product release is before hydrolysis (dynein and myosin), although it could conceivably reduce future binding potential in a cycling system as the hydrolysis step increases affinity for binding, at least in the case of actin and myosin.

Binding Assays

One of the criteria for classification of a protein as a microtubule dependent mechanoenzyme is evidence of participation in microtubule-based transport. This is assayed indirectly, in the form of microtubule-stimulated ATPase activity, in ATPase activity assays, or directly, in the observation microtubule-based transport, in motility assays. The formation of rigor complexes can be detected in motility assays, because, if binding occurs followed by the formation of rigor complexes, transport stops. However, transport also stops if binding does not occur. Therefore, lack of motility in motility assays could be manifested by both binding and non binding, in binding assays. For example when NEM prevents binding, it produces non-transport in motility assays and non binding, in binding assays. In contrast, ATP depletion produces rigor, also producing non-transport in motility assays but binding in binding assays. This example illustrates that binding assays are not synonymous with motility assays.

Binding assays have been used for a number of reasons. In a complex system, they provide a means to test a relationship between a given organelle and microtubules and they allow a known relationship to be characterized. One aspect of microtubule-based organelle transport that has had very little study is the events that occur at the organelle-motor site. Recently, there has been interest in possible activators for motors that are thought to operate at this site (Schroer et al., 1989; Schroer and Sheetz, 1991a,b; Brady and Pfister, 1991).

One of the first binding assays was used to test the binding of porcine pituitary secretory granules to microtubules, based on cosedimentation on a sucrose gradient (Sherline et al., 1977). The granules bind microtubules, but not tubulin, in the absence of ATP and are releasable with both ATP and GTP. Binding is mildly inhibited by AMPPNP. Using a morphological approach, Suprenant and Dentler (1982) demonstrated binding of anglefish pancreas secretory granules to microtubules. This interaction is releasable with ATP. Pratt (1986b) assembled vesicle-microtubule complexes in the presence of supernatant from sonicated axoplasm, producing rigor complexes that were releasable with ATP or AMPPNP. Polypeptides isolated from the vesicle-microtubule complexes showed ATPase activity and remained with the vesicles upon microtubule depolymerization. Only one of the polypepties extracted from the vesicle-microtubule complex required ATP to rebind. Rothwell and coworkers (1989) combined human neutrophil granules and taxol stabilized microtubules to observe binding that was increased with vanadate and decreased with NEM, AMPPNP, and ATP. Van der Sluijs and coworkers (1990) examined exocytotic vesicle-microtubule binding in the absence of ATP; nucleotide release did not occur at 1mM ATP or 1mM GTP. Exocytotic vesicle-microtubule binding was found to require cytosol. The binding was sensitive to heat, trypsin, or NEM treatment of the cytosol but not of the vesicles, suggesting that the activator was soluble. Scheel and Kreis (1991a,) used a new approach to test the binding of exocytic vesicle to microtubules. Microtubules were complexed to magnetic beads by immunoadsorption to provide an affinity matrix. Trypsin treatment of the vesicles blocked binding, as did heat, trypsin and NEM treatment of the cytosol. They were releasable with ATP and GTP but not affected by AMPPNP, ATPγS, GTPPNP, and ATPγS (all nonhydrolyzable nucleotide analogues).

In each case, described above, the binding assay established a relationship between the organelle and microtubules but further approaches were required to determine if the binding was mediated by a mechanoenzyme. For example, in an attempt to identify the protein binding exocytic vesicles to microtubules, Scheel and Kreis (1991b) immunodepleted the cytosol of 170 kD protein, kinesin, or cytoplasmic dynein, of which only the removal of 170 kD affected binding, as did salt treatment of the organelles. This indicates that, in this case, binding is not mediated by dynein or kinesin but requires a 170 kD protein. They found a time course to the binding, requiring 45 minutes to reach maximum binding. It will be remembered from a description of microtubule binding proteins, that a 170 kD protein binds to microtubules, and is releasable from microtubules when it is phosphorylated by a cytosolic factor. It is not thought to be a motor but whether it has a tethering role, or is involved in regulation of other motors is not known (Scheel and Kreis, 1991a,b).

This group of binding experiments illustrates the diverse properties that have been identified in binding assays between membranous organelles and microtubules. These binding assays serve to verify the relationship between microtubules and these organelles and characterize their interaction. It is clear that the microtubule-organelle binding properties determined in binding assays will not be the same as the ATPase activity or motility assays. Binding only tests part of the mechanochemical cycle and therefore does not distinguish between mechanoenzymes and non motor microtubule binding proteins. They may also be testing a different aspect of motor protein regulation. In most cases, cytosolic factors have been required for binding. This supports the growing consensus that accessory factors, either in the cytosol or on the protein complex, are required for microtubule-organelle interaction.

The organelle-microtubule binding complex

One issue, that has not been resolved in microtubule-based organelle transport, is: What constitutes the essential components for transport? It encompasses a number of problems. Firstly, what elements constitute the organelle-motor binding, that is, does the motor reside on the organelle and if so is there direct binding (Lacey and Haimo, 1992) or are integral membrane receptors required? Secondly, in the case of bidirectional transport, how does the motor for minus-end directed transport remain available during plus-end directed transport, as for example in axons? Thirdly, how is the direction of transport regulated, that is, how is the appropriate motor activated? Each question has implications for the other.

Where is the motor located?

Central to this issue is the question: does the motor reside on the vesicle, on the microtubule, or in the cytosol? The answers have been contradictory, which may result from the questionable assumption that immunolocalization *in vivo* and colocalization on isolated cell homogenate fractions are measuring the same thing (Brady and Pfister, 1991). Hollenbeck (1989) used an antiserum to kinesin, to determine the distribution of kinesin following sequential extraction with saponin, 1% triton and finally SDS, in cell fractions that contained cytoplasm, membrane bounded organelles and cytoskeleton. He reported that, in fibroblasts, 68% of kinesin is in soluble form, 32% in membrane or organelle associated form and none is present in cytoskeletal fraction. However, Pfister et. al. (1989a) used monoclonal antibodies to the 124 kD heavy chain and 64 kD light chain, showing that kinesin, in cultured cells, associates with membrane bounded organelles, but not Golgi or nuclear membrane and associates with microtubules, only in the presence of AMP-PNP. Cytoplasmic dynein has been shown to reside with membranous organelles (Pfarr et al., 1990; Steuer et al, 1990). Brady and Pfister (1991) address this contradiction of where the motor resides, by suggesting that organelle-microtubule binding is weak enough to cause release during isolation, or alternatively, that their concentration in the cytosolic pool is not sufficient to be detected by immunocytochemical means. A third possibility is that motors may change their state such that they are less 'visible' to antibodies in the soluble state.

Presumably much of the variability in the need for cytosolic factors in binding and transport assays may arise from conditions that mediate the organelle-motor or motor-microtubule interactions and or their activators.

In motility assays, three states are observed: vesicles transport along microtubules (motility); vesicles remain bound without transport (binding); or vesicles 'fall off' microtubules (dissociated). In keeping with the ATPase activity of mechanoenzymes being in the microtubule binding domains, it is assumed that much of the pharmacological inhibitors reflect activity at the motor-microtubule site, making this the most likely site for regulation. It is not known what causes vesicles to abandon their cycling and dissociate from microtubules, as opposed to forming rigor complexes and remaining bound, but immobile. Nor is it known how high their affinity is to microtubules during transport. The question is: where do they reside when transport stops?

How are motors kept available for bidirectional transport?

This problem is most clearly illustrated in axons, in which organelles travel long distances to the axon terminus and, in modified form, return to the cell body. Protein synthesis occurs only in the cell body; therefore, any motor travelling retrograde would have to be first carried to the terminus. Probably similar but less dramatic events occur in less polarized cells. If kinesin is in the soluble fraction in axons, how could it get to the terminus to be used for the return trip? In axons, anterorade and retrograde travelling organelles are different in size and can be distinguished from one another. Axons were ligated and colocalization of cytoplasmic dynein on retrograde and anterograde vesicles was examined with immunocytochemical probes. Cytoplasmic dynein was present on both classes of organelle (Hirokawa et al., 1990), while kinesin was much more abundant on the anterograde than the retrograde vesicles (Hirokawa et al., 1991). However, antibodies to kinesin inhibit both anterograde and retrograde transport (Brady et al., 1990). These data suggest that the retrograde motor cytoplasmic dynein is carried to the axon terminus in some inactive state ferried by kinesin, then transfers to the retrograde vesicle and returns with a limited amount of inactive kinesin to the cell body. The reason for kinesin's interference with bidirectional transport is not clear.

Are the motors alone sufficient for transport?

Very little is known about vesicle-motor interactions and how they are affected during isolation. Lacey and Haimo have shown that dynein binds directly to extracted synaptosomes (Lacey and Haimo, 1992). This binding is not ATP releasable, supporting the impression that ATP dependent regulation is probably not occuring at the organelle-motor site. In contrast, many motility assays fail if vesicles are salt extracted (Schroer et al., 1988a,b; Pratt, 1986), or treated with trypsin Gilbert and Sloboda, 1986). Covering the middle ground, Vale et al. (1985c; Schroer et al, 1988) found membranous organelles moved along purified microtubules in the absence of soluble factors, but were further stimulated by addition of high speed cytosol. The contradictions may lie in the purity of the components or differences between systems.

Kinesin and cytoplasmic dynein are both known to support microtubule based transport; however, Schroer and coworkers have shown that neither of these motors support transport when they are highly purified (Schroer et al., 1988a,b; Sheetz and Schroer 1989; Schnapp and Reese, 1989). Illustrative of this problem, is a study in which kinesin was removed from the crude axoplasmic supernatant S1, which previously had been shown to support bidirectional transport (Schroer et al., 1988a). The kinesin depleted supernatant was then added to vesicles that had been washed in high salt to reduce contamination by supernatant proteins. The result was a reduction in minus-end and plus-end organelle transport. When the removed kinesin was further purified on an affinity column and returned to the S1, anterograde transport was not fully restored, suggesting that something had been removed with the kinesin and had been lost during the affinity purification. This was verified in that, the elutant from the kinesin purification column was able to support some bidirectional transport. These findings could be explained by the existence of accessory proteins to mediate organelle binding having been removed with kinesin, or by the occurrence of active and inactive states of the enzyme and necessary regulators. Sheetz and coworkers (1989) have proposed that there is an 'organelle translocation complex' which may include: the motor(s), accessory protein(s), and an organelle (with a motor binding site). The recent finding of two potential activators (Schroer and Sheetz, 1991b) supports the proposal that highly purified motors are not sufficient for transport.

How are motors regulated?

Sheetz and coworkers (1989) have proposed two models to explain the availability of motors for directional transport. They reconcile the existence of a factor that is progressively removed during the purification of cytoplasmic dynein (Sheetz et al, 1989; Schroer et al., 1989) which they have termed an accessory factor, with active and inactive states of the motor. In the first model, the organelle has separate binding sites for the minus-end and plus-end motors. Organelle receptors are proposed to be active or inactive, resulting in an active complex dictating transport direction and and inactive complex carrying the inactive motor. The second model involves a single motor complex containing both motors, in which the motor complex has two conformations to activate either the minus-end or plus-end component of the motor complex. Regulation could occur by a number of methods including: phosphorylation, activation by 'activator' proteins (Schroer and Sheetz, 1991b), inactivation by selective proteolysis (Sheetz et al, 1989), or cooperative action between the two motors.

Schroer and Sheetz (1991b) point out that in the presence of highly purified motors, microtubules bind to and transport along glass slides, but do not transport vesicles. This indicates that the transport potential of mechanoenzymes can be inhibited by their binding to vesicles. Furthermore these workers isolated two activators that are capable of converting the tethered binding of vesicles to microtubules mediated by highly purified motors, to vesicle transport. They propose that these activators have been present in the mechanoenzyme preparations that have supported vesicle transport. This finding has important implications for both binding assays and motility assays. The difference between binding and non-binding in binding assays, or transport and non transport in motility assays, may lie not with the motor itself, but whether potential activators have been retained in the system used.

In that the direction of transport is not the only issue for mechanoenzymes, but organelle specificity as well, current interest in membrane sorting by capping proteins may reveal other mechanoenzyme regulation mechanisms. There may prove to be a relationship between activating proteins and capping proteins involved in organelle sorting.

Microtubule-dependent organelle positioning

Two basic cell functions have been linked with microtubule-based transport: organization and distribution of organelles (Schroer et al, 1988, 1989; Schnapp and Reese, 1989; Pfister et al, 1989b), which includes the formation of endoplasmic reticulum networks (Lee et al, 1989; Teraskai et al, 1984; Vale and Hotani, 1988); and events of mitosis and meiosis (Mitchison, 1986).

Studies of microtubule-based transport have been extended to a multitude of cell types, leading to the realization that it is the underlying mechanism for a vast number of fundamental cell functions. It will soon be easier to list the cell events that are not microtubule dependent than those that are (see Schroer and Sheetz, 1991a for review).

In order to integrate the many cellular functions in which they participate, organelles are transported along, or positioned in, specific locations in the cell. Positioning involves two states transport to and maintenance at the destination, that is, motility or binding.

Many of the processes in the cell, that involve membranous organelles, are microtubule dependent and require the movement of organelles along pathways both morphological and physiological (for review Bershadsky and Vasiliev, 1988). Essentially, they are being either transported or anchored. These two processes may even be combined, as in the shaping and elongating of membrane profiles in ER, lysosomes and possibly even elongation of mitochondria involve anchoring in some areas while moving in another. They may involve the same mechanisms, although different proteins, or the same proteins with different instructions.

A number of methods have been used to establish the microtubule dependency of organelle positioning: the effects of microtubule perturbation, colocalization of the organelle with microtubules, or by direct observation with video enhanced microscopy. Fig. 1-10 illustrates the many organelle pathways that are microtubule dependent. In general, the pathways that require organelles either cover relatively long distances, or there is a short life span of the components, requiring efficiency in both cases (for reviews see Duden et al., 1990; Kreis, 1990; Kelly, 1990a,b; Schroer and Sheetz, 1991a; Bomsel et al., 1990). Many pathways spanning short distances such as, between Golgi stacks, membrane to early endosome, late secretory granules to membrane, or from ER to cis Golgi, do not require microtubules.

In the secretory pathway, formation and maintenance of ER networks is microtubule dependent (Terasaki et al., 1984; Lee and Chen, 1988); it collapses with microtubule disruption (Terasaki et al., 1984) and can be formed *in vitro* by a kinesin dependent process (Vale and Hotani, 1988; Dabora and Sheetz, 1988b). Although the pathway from ER to Golgi is not microtubule dependent, the salvage compartment, in which vesicles are returned from trans Golgi to ER to retain ER specific proteins, requires microtubules (Achler et al, 1989; van Zeijl and Matlan, 1990). In polarized cells, the targeting of proteins to the basolateral surface is by bulk flow, but to apical surfaces is microtubule dependent. This was illustrated in a particularly interesting study in which microtubule disruption caused the failure of targeting of apical proteins in the brush border of intestinal epithelial cells (Achler et al, 1989). Profiles of brush border structures, complete with microvilli and actin components, were seen to mistarget to basolateral surfaces, or assemble within the cytoplasm. Glycosylation of of mistargeted apical membrane proteins indicates that the mistargeting occurs after they pass through the Golgi (van Zeijl and Matlin, 1990). Exocytotic vesicles have been shown to bind to microtubules by a protein that is thought to be involved in anchoring rather than transport (Scheel and Kreis, 1991a,b).

Placement of the Golgi is microtubule dependent, in that disruption of microtubules causes dispersal of the Golgi, although its internal structure remains intact and the Golgi is still able to function (Bacallao et al., 1989; Ho et al., 1989; see Kreis 1990 for review). Removal of the disrupting agent causes microtubule dependent transport of Golgi to the microtubule minus-end in some cell types (see Duden et al., 1990). In the endocytotic pathway, the movement of early endosomes is microtubule independent, but their transport to and fusion with late endosomes or lysosomes requires microtubules (Bomsel et al., 1990), as does lysosome elongation (see Duden et al., 1990).

It would seem, with the positioning of most organelles and their transport during cell activities, that there must be an overall coordination in what Heuser (1989) has called the "continuous intracellular circulatory system". Alan and Vale (1991), have described a cell cycle dependent regulatory factor that serves to activate microtubule based organelle positioning. Using extracts from metaphase and interphase cells, they showed that organelles from both cell types could participate in microtubule-based transport and membrane fusion in the presence of interphase cell extracts, but not metaphase cell extracts. This indicates that these events are activated in interphase cells by a regulatory mechanism that is absent in metaphase cells.

Certainly, organelle positioning on microtubule tracks results in cell specific organelle patterns with some common underlying themes.

Cellular organization (microtubules in cells in general)

Until very recently, it was assumed that microtubules radiate from a perinuclear position, oriented with their minus-ends directed toward the cell surface. In this plan, the organelles would be placed by appropriate minus-end or plus-end directed motors to be positioned or transported, as required, along microtubule tracks (for reviews see Gibbons, 1988; Duden et al., 1990, Kelly, 1990a,b). Both kinesin and cytoplasmic dynein have been implicated in these events (for review, see Schroer and Sheetz, 1991a). However, Bacallao and coworkers (1989) have shown that during the polarization of MDCK cells, there is reorganization of cellular organelles and redistribution of microtubules. This results in separation of the paired centrioles, migration of centrosomal material to the apical region of the cell, from which microtubules emanate, with their minus-ends toward the cell surface and their plus-ends toward the nuclear region of the cell. Microtubules in the basal area are less organized. The junctional complex is reported to move upward toward the apical region. The Golgi is repositioned in a ribbon-like complex extending apically from the nucleus. The authors noted a striking similarity of the Golgi pattern of the polarized MDCK to the Golgi pattern of Sertoli cells, as described by Rambourg and coworkers (1979). This extensive reorganization, indicates that polarized epithelial cells may have a different continuous organelle circulatory system than the model shown in Fig. 1-10. Although there is little direct evidence, it is reasonable to assume that Sertoli cell microtubules participate in most of these housekeeping activities.

Schroer and Sheetz (1991a) have proposed three models of cellular organization to accommodate these observations. The first, the radial model accounts for the plan shown in Fig. 1-10), typical of what has been observed in many cell lines. The second, a linear model accounts for the overlapping microtubule plan that has been identified in axons. The third, addresses the findings of the MDCK cell organization (Bacallao et al., 1989) and is supported by findings of minus-end out orientation of the *Drosophila wing*

Figure 1-10: Continuous organelle circulatory system: radial model: This diagram indicates the classical radial model of microtubule and membranous organelle distribution and pathways that have been shown to be microtubule dependent (for review see Schroer and Sheetz, 1991a). The microtubule dependent pathways include: formation of ER networks; membrane recycling from the transition compartment; positioning of the Golgi apparatus; some secretory vesicle transport; movement of endosomes from the early to late endosome compartment; cycling to the trans Golgi network; transport of endosomes to lysosomes; and the shaping of lysosomes. Those pathways that are thought to be microtubule independent are movement of vesicles between Golgi stacks, movement of ER to Golgi, and the early events of endocytosis and late events of exocytosis. (Modified from Schroer and Sheetz, 1991a; Duden et al., 1990; Kreis, 1991; Kelly, 1991 a,b)

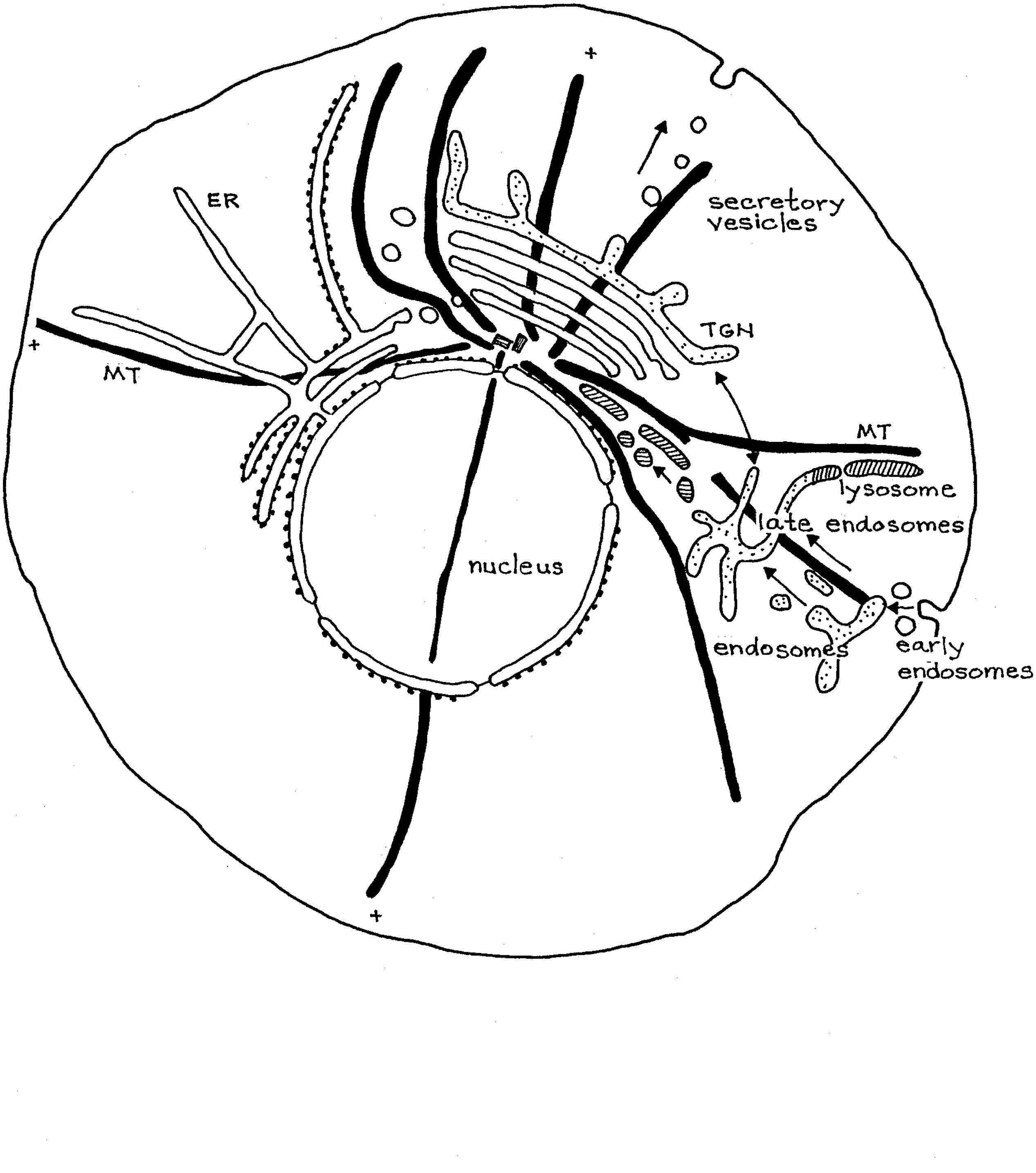
+
ER
+
MT
nucleus
+
+
secretory vesicles
TGN
MT
lysosome
late endosomes
endosomes
early endosomes

epidermal cell (Mogensen et al., 1989) and retinal pigment epithelial cell (Troutt and Burnside, 1988b), in which microtubule minus-ends are directed toward the cell periphery. The prospect of microtubule polarity being different in polarized epithelial cells, has prompted a numbers of reviewers to emphasize the importance of determining microtubule polarity in cells to the understanding of the events of organelle positioning, and the motors that carry it out (Boekelheide et al, 1989; Kelly, 1990a,b; Duden et al., 1990; Kreis, 1990).

MICROTUBULES IN SERTOLI CELLS

Distribution

The distribution of microtubules in Sertoli cells was first described by Christensen (1965) and later in greater detail by others (Fawcett, 1975; Vogl et al., 1983a,b; Vogl, 1988; Amlani and Vogl, 1988; Hermo et al., 1991). Sertoli cell microtubules have been reported to be abundant in the Sertoli cells of all mammalian species studied. Although mention is made of them in most accounts of Sertoli cell morphology, only a few studies have addressed their distribution in Sertoli cells (Vogl et al., 1983a,b; Vogl, 1988; Amlani and Vogl, 1988), tending instead to focus observations on germ cell microtubules (Wolosewick and deMay, 1982; Cherry and Hsu, 1984).

In Sertoli cells of both the squirrel and rat, microtubules are prominent in the body of the cell, extending from a supranuclear position into the apical stalk and apical processes that support late spermatids (Amlani and Vogl, 1988; Vogl, 1988). In Fig. 1-11, immunofluoresent staining with a polyclonal antibody to tubulin, shows the parallel orientation of microtubules in apical portions of rat seminiferous epithelium. In immunofluoresence studies, few microtubules have been described at the base of the cell (Vogl et al., 1983a,b, Amlani and Vogl, 1988 and Vogl, 1988) but they have been detected basally with antibodies to tyrosinated alpha tubulin (Hermo et al., 1991). There is ultrastructural evidence for a limited number of somewhat randomly organized microtubules in this location (Fawcett, 1975).

Figure 1-11: Microtubule distribution in Sertoli cells: These are paired phase contrast and immunofluoresence light micrographs of apical fragments of Sertoli cells, reacted with a polyclonal antibody to tubulin (gift of Kegi Fugiwara). Early spermatogenic cells (asterisk in phase image), are seen as dark areas in (b). Microtubules do not occupy the lateral processes that surround these early spermatogenic cells. Late spermatids can be identified by their dark nuclei and tails in the phase image in (a). The late spermatids in (a) correspond to the negative images in (b) indicating the deep placement of spermatids in Sertoli cell crypts. Positive staining Sertoli cell microtubules are seen in (b) oriented parallel to the long axis of the cell and surrounding the late spermatids. Tubulin containing axonemes in germ cells do not stain in this preparation. bar = 10 µm. (Micrograph courtesy of W. Vogl from Vogl et al., 1991b and 1992)

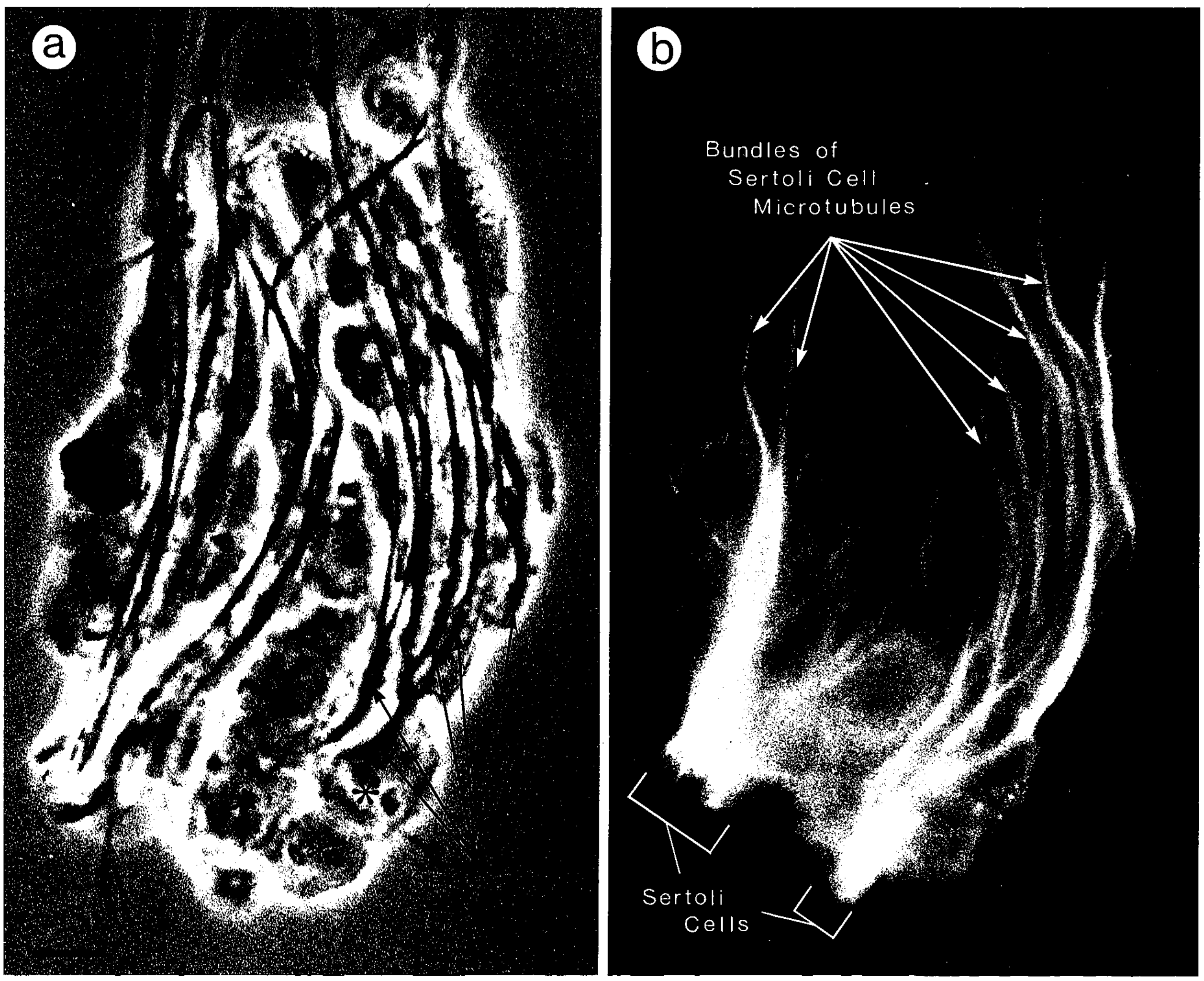
a
b
Bundles of Sertoli Cell Microtubules
Sertoli Cells

Microtubules do not extend into lateral processes that encircle meiotic spermatocytes. However, they are present in lateral processes surrounding late round spermatids, in squirrel (Amlani and Vogl, 1988), and early elongating spermatids, in rat (Vogl, 1988). As spermatids become oriented perpendicular to the base of the epithelium and become situated within Sertoli cell crypts, they become richly ensheathed by dense bundles of microtubules, continuous with those of the Sertoli cell stalk.

Thick bundles of microtubules extend into apical processes that support Sertoli cell crypts running parallel to the long axis, as well as the path of transport, of maturing spermatids. Subsequently, they become concentrated, adjacent to the acrosome, around translocating spermatids, and remain there until spermiation. The appearance of microtubules in Sertoli cell processes with their regular spacing and adjacent organelles has been compared to that in axons (Fawcett, 1975; Vogl et al., 1983a; Neely and Boekelheide, 1988). Microtubules course past the cistern of ESER as well as other membrane bounded organelles. Elongate mitochondria are prominent in areas rich in microtubules. Considering this distribution, Sertoli cell microtubules have opportunity, through ESs, to serve as tracks on which to translocate germ cells. Disruption of Sertoli cell microtubules following colchicine injections, resulted in basal accumulation of smooth ER and failure of elongate spermatids to be moved apically to the tubule lumen. This is consistent with apical translocation of ER and spermatids on microtubule tracks.

Sertoli cell MTOC

The site of microtubule organization, in Sertoli cells, has received virtually no attention. Paired centrioles have been observed in a supranuclear position (Nagano, 1966). However, Sertoli cell microtubules do not appear to radiate from this area, instead running parallel to the body of the cell (Amlani and Vogl, 1988; Vogl, 1988), typical of epithelial cells generally (Kelly et al., 1990a,b; Schroer and Sheetz, 1991a).

In MDCK cells, grown to confluence, microtubule organizing centers have been described to relocate, and microtubules reorganize, during the establishment of cell polarity (Bacallao et al., 1989; Bré et al, 1989). This may occur in Sertoli cells.

Tubulin post translational modifications in Sertoli cells

Immunocytochemical staining with antibodies to tyrosinated tubulin indicates a progressive increase in density of staining in the apical region, from the time that spermatids are deeply situated in Sertoli cell crypts to the time they reach their most apical position: stages II to VIII (Hermo et al., 1991), concentrated in apical processes surrounding step 15 to 19 spermatids. This finding is supported by observations of Vogl and coworkers (Vogl et al. 1983a,b; Amlani and Vogl, 1988; Vogl, 1988) which place the maximum density of microtubules in apical processes surrounding elongate spermatids beginning at stage V. Specific changes that occur in relation to differentiating spermatids are described below.

Stage dependent changes in Sertoli cell microtubule distribution

Information about stage dependent changes in Sertoli cell microtubules is primarily morphological. A number of changes in the distribution of Sertoli cell microtubules during spermatogenesis have been described, including their distribution in lateral, penetrating, and apical processes. Microtubules do not extend into the lateral processes that envelop spermatocytes and early spermatids (Vogl et al., 1983a; Vogl et al., 1988; Amlani and Vogl, 1988), being first observed in these processes as they surround elongating spermatids that are being reoriented to the base of the Sertoli cell. Microtubules are most abundant surrounding elongate spermatids as they become situated within Sertoli cell crypts (stage II to IV), descend deep within the epithelium (stage VI - stage V), and are subsequently moved toward the tubule lumen, supported by Sertoli cell apical processes (stage VII stage)(Vogl et al., 1983a; Vogl, 1988; Amlani and Vogl, 1988; Hermo et al., 1991). Microtubules pass adjacent to ESs and around the elongating spermatid, reaching into the most apical confines of the cell (Fig. 1-11). As microtubules extend into apical processes, the modifications they undergo to conform to the changing shape of germ cells are different from a simple accommodation to an object placed in a stream of microtubules. There is a species difference in this conformation immediately adjacent to spermatid heads (Vogl, 1988, Amlani and Vogl, 1988).

In both squirrel and rat, the microtubules remain faithful to the shape of the spermatid head, but take on a species specific distribution when apical processes extend late spermatids toward the epithelial lumen (Amlani and Vogl, 1988; Vogl, 1988). In squirrel, microtubules surround the saucer shaped spermatid head forming a C shape, lining the inner aspect of the rim of the lip of the acrosome. In immunofluoresence images of fixed and fragmented sections of apical Sertoli cells, in squirrel, these microtubules appear to have lost their continuity with the microtubules of the stalk (Vogl et al., 1983a; Amlani and Vogl, 1988). An accumulation of the elaborate network of SER adjacent to the concave surface of the squirrel spermatid head corresponds to the C shaped microtubule confirmation, suggesting a relationship between the two events.

The reorganization of microtubules adjacent to spermatid heads in the rat is similar, although less striking, forming a canoe shape that cradles the late spermatid, and concentrating particularly at the dorsal and ventral aspects of the head (Vogl, 1988). In rat, the microtubules surrounding spermatid heads appear to retain their continuity with those in the apical processes. These specific differences suggest more than a simple bypassing of spermatid heads but an intimate involvement in this relationship, possibly involving placement and orientation of the spermatid and the assembly of nearby ER (Clermont et al., 1980).

Although stage and species specific changes occur in the distribution of Sertoli cell microtubules during spermatogenesis; not a lot is known about the factors that induce this redistribution, or for that matter, the more subtle alterations that occur in microtubules themselves. The profile of post-translationaly modified tubulins in Sertoli cell microtubules, during different stages of spermatogenesis, indicates that stage dependent changes do not arise from the tubulin modifications presently known (Hermo et al., 1991) The functional capacity of microtubules is also modified by interactions with other molecules including ions, nucleotides, regulatory proteins, and MAPs.

Sertoli cell MAPs

Cytoplasmic dynein has been isolated in high quantities in testis (Neely and Boekelheide, 1988; Collins and Vallee, 1989) and in Sertoli cell enriched preparations (Neely and Boekelheide, 1988) In a profile of testis MAPs, Neely and Boekelheide describe HMW MAPs similar in electrophoretic properties to brain MAP, MAP1 and MAP 2, although they do not share immunoreactivity with brain MAPs MAP1A and MAP 2. They differ from brain MAPs in a reduced ability to promote microtubule polymerization and lack of heat stability. The MAP content changes with development with a prominent MAP, 'HMW-2', present at all time points. Furthermore, this MAP is present in Sertoli cell enriched and germ cell depleted (cryptorchid and 2,5-hexanedione treated) testis preparations, indicating a likely localization in Sertoli cells. HMW-2 (Neely and Boekelheide, 1988) is released from microtubules by MgATP and possesses microtubule stimulated ATPase activity, which, in turn, is inhibited by vanadate (75% at 5μM, 58% at 50μM), vanadate dependent photocleavage and EHNA (4mM but not 0.4mM). In addition, Neely and Boekelheide report the presence of a 173 kD protein, which is partially released with 5 mM GTP. In a MAP profile from 5, 10, 15, 24 day old and adult rat testis, a MAP of a slightly slower electrophoretic mobility than HMW2, 'HMW-3)' is first identified as a minor component at 24 days and is a major component in adult testis. It has not yet been established whether this MAP only occurs while late spermatids are present, or whether it is a variant of another MAP present earlier.

Relationship of microtubules to other organelles in Sertoli cells

The close packing and parallel alignment of Sertoli cell microtubules is reflected in the shape and orientation of nearby organelles. Numerous elongate mitochondria and long profiles of smooth endoplasmic reticulum conform, in alignment and shape, to microtubules in Sertoli cell apical processes. In contrast to the shape and orientation of these organelles in the apical portion of Sertoli cells, Fawcett (1975) describes mitochondria to be less elongate and randomly distributed in the base of Sertoli cells, as are microtubules. Microtubules occur in the vicinity of elaborate changes in ER distribution that occur in Sertoli cells of the rat (Clermont et al., 1980) and squirrel (Vogl et al., 1983a,b). While it is not known whether microtubules play a role in shaping these organelles in Sertoli cells, a role has been established for shaping of ER *in vitro* (Vale and Hotani, 1988; Dabora and Sheetz, 1988) and *in vivo* (Lee et al., 1989). Mitochondria have been shown to form links with microtubules (Hirokawa, 1982; Linden et al., 1989) and have been observed to travel along microtubule tracks in axons (Forman et al., 1983). It is not known whether Sertoli cell mitochondria and other organelles, observed in close relation to Sertoli cell microtubules, are undergoing transport or being maintained in that location.

Function of Sertoli cell microtubules

Most of the suggested functions of microtubules in Sertoli cells arise from analogy with microtubule functions that have been demonstrated in other systems (Vale and Hotani, 1988; Allen at al., 1981; Duden et al., 1990; Sheetz et al, 1986; Schnapp et al., 1986; Schliwa, 1984; van Zeijl and Matlin, 1990; van der Sluijs et al., 1990; Balch, 1989; Ho et al., 1989; Heuser, 1989; Achler et al, 1989; Burnside, 1989; Bomsel et al, 1990; for reviews see Schroer and Sheetz, 1991a; Duden et al, 1990; and Kelly, 1990a,b). Collectively, these and other studies have provided an extensive list of ongoing functions in interphase cells, which are generally agreed to be microtubule dependent, including: maintenance of cell shape, transport for late events in endocytosis and early events in exocytosis, recycling of membrane from cis Golgi to ER, targeting of apical membrane proteins, formation of ER network; Golgi assembly and placement; and lysosome shaping and distribution, all described earlier. Although most of these events apply to all cells, few have been demonstrated in Sertoli cells. Apart from microtubule disruption studies and their inherent problems, most evidence of microtubule function in Sertoli cells is morphological and somewhat speculative. The complexity of the seminiferous epithelium presents technical constraints for direct testing of Sertoli cell microtubule function. Functions that have been suggested for Sertoli cell microtubules include: maintenance of cell shape, shaping of the spermatid head, positioning and translocation of organelles, and translocation of residual cytoplasm and spermatids. The abundance of microtubules and MAPs in Sertoli cells argues for an important microtubule function, possibly one that is unique to Sertoli cells. Sertoli cells have been relegated the special function of nurturing and maintaining germ cells during spermatogenesis (Dym, 1977; Ritzen et al., 1981; Griswold, 1988). A special function for Sertoli cell microtubules may be directed toward that end.

Sertoli cell shape

One of the first functions attributed to microtubules was maintenance of cell shape (Porter, 1966). Extensive changes occur in Sertoli cell shape (Clermont et al., 1980; Dym,. 1977; Fawcett, 1975; Gravis, 1979; Morales and Clermont, 1982; Ross, 1976; Russell, 1980, 1984; Russell and Malone, 1980; Vogl, 1988; Vogl et al., 1983a,b, 1985a, Amlani and Vogl, 1988). They are directly related to spermatogenesis, and result from the accommodation of Sertoli cell processes to the changing shape and position of developing spermatids, and the selective retention of residual cytoplasm.

Sertoli cells lack the apical tight junctional complexes typical of many polarized epithelia. Unlike most other epithelia, Sertoli cells are highly convoluted, however they are tightly bound to apically placed germ cells. The extensive germ cell-Sertoli cell attachment and the interconnection between germs cells by intercellular bridges may serve to substantially stabilize much of the apical region of the epithelium. Reinforcement by microtubules may add to this stability. Microtubule bundles in Sertoli cells run parallel to one another maintaining an even spacing, forming what looks on electron micrographs to be a zone of exclusion around each microtubule. With fine linkages frequently seen between microtubules, the easy assumption is that a cross-linked scaffold exists. MAPs have been proposed as the source of linkages seen extending from microtubules and have been proposed to provide the zone of exclusion. How could Sertoli cell microtubules be cross-linked to reinforce cell shape and at the same time allow passage of organelles along microtubule tracks? The question of microtubule cross-linking has been addressed in a study testing the effect of a potential cross-linking MAP, MAP-2 in the presence of the mechanoenzyme, kinesin (Massow et al., 1989; Heins et al., 1991). MAP-2 is a larger molecule than kinesin. It was found that MAP-2, included in the incubation solution of kinesin on a glass substrate, acted as a spacer disabling kinesin's ability to transport microtubules. However, if MAP-2 was preincubated with the microtubules and not the substrate, glass bound kinesin was able to interact with microtubules, and induce transport, in spite of microtubule bound MAP-2 (Heins et al., 1991). It was deduced that MAP-2 may act as a spacer protein not by cross-linking microtubules but by repelling adjacent microtubules. Such a mechanism for the creation of a network of evenly spaced microtubules would address the problem of moving organelles through a cross-linked scaffold at the same time as providing the function of maintaining cell shape. Although there is no evidence for MAP-2 in Sertoli cell microtubules, a similar mechanism would provide for the movement of organelles including spermatid bound ESs through a field of microtubules without energy consumptive binding and release and without diminishing the role of microtubules in the maintenance of cell shape. Support for a role for Sertoli cell microtubules in the maintenance of cell shape comes from evidence that when Sertoli cell microtubules are disrupted with colchicine, Sertoli cells loose their columnar shape, or become unstable with the apical portion bulging into the lumen, in some cases sloughing a lining consisting of apical Sertoli cells and associated spermatids (Russell, et al., 1981; Vogl et al., 1983b).

Organelle positioning and translocation during spermatogenesis

The unvarying association of specific stages of developing germ cells with one another in the seminiferous cycle (Brökelmann, 1963; Perey, et al, 1961; Clermont, 1972) and stage dependence of cycling biochemical and morphological events in Sertoli cells indicate that the Sertoli cell milieu changes in a constant and regulated manner. Dynamic changes that occur in the positioning of such organelles as Golgi and endoplasmic reticulum are stage dependent (Clermont et al, 1980; Rambourg et al., 1979; Ueno et al, 1991) and therefore likely to be important to the overall program. In the face of constant change in cell shape, critical positioning of organelles is required to place components of the synthetic and secretory pathways in positions of optimum efficiency for the synthesis of proteins, targeting of membrane proteins, and delivery of secretory products to their destination. Considering the distances involved, leaving such positioning to diffusion would be inefficient.

Evidence for a role of Sertoli cell microtubules in the shaping and distribution of organelles is indirect. In the apical region of the cell, organelles are observed in close association with microtubules; they are oriented parallel to microtubules; and they assume elongate shapes consistent with elongation of membrane bounded organelles by the adjacent microtubules. Sertoli cell microtubules have been reported in areas of accumulated ER (Clermont et al, 1980; Vogl, et al., 1983a). The close temporal and spatial association of ER with microtubules next to the acrosome lip of late spermatid in squirrel, as well as the failure of that network of ER to accumulate apically following microtubule disruption (Vogl, 1983b), is consistent with a role for transporting and accumulating ER in that region (Vogl, 1983a; Amlani and Vogl, 1988). A role for Sertoli cell microtubules in the orientation and shaping of organelles can only be predicted by analogy to other systems, where positioning and shaping of organelles has been shown to be microtubule dependent (Lee et al., 1989; Vale and Hotani, 1988).

Influence of Sertoli cell microtubules on the head shape of spermatogenic cells

The role of microtubules, of either spermatid or Sertoli cell origin, in the shaping of spermatid heads has been the subject of a long-standing debate (Fawcett et al., 1971). Sertoli cell microtubules do not lie adjacent to spermatids, but are separated by ESs. It seems unlikely that microtubules could exert a force through these structures to modify the shape of the spermatid head. In addition, the orientation of Sertoli cell microtubules is not consistent with the head shape changes that occur. Evidence of Sertoli cell microtubules as contributors to shaping of spermatid head is indirect and comes mainly from perturbation of microtubules in hamsters (Rattner, 1970), mouse (Handel, 1979; Wolosewick and Bryan, 1977), rat (Aoki, 1980; Russell et al 1989), and squirrel (Vogl et al., 1983b). Of those that reported on the effects of Sertoli cell microtubule perturbation on head shape, Vogl et al. (1983b) and Handel (1979) found distortion in head shape while Russell et al. (1981) did not. However, the latter group questioned whether the apparently normal spermatid heads, observed in their study, had in fact been exposed to the agent before being sloughed into the tubule lumen. Considering the limitations of these studies, the evidence is scant. Aside from the perturbation studies, the only other observation addressing the question of microtubule involvement in the determination of head shape has been that of dense bands of Sertoli cell microtubules which conform intimately to the inner lip of the acrosome during shaping of spermatid head in the squirrel (Amlani and Vogl, 1988), and are not separated by ESs. These authors concede the possibility that this band of Sertoli cell microtubules may have some influence on formation of that portion of the acrosome. The suggestion that the spermatid nuclear shape is due to chromosome condensation (Fawcett,

1971) while attractive because of the wide range of species specific spermatid shapes that occur (Fawcett et al. 1971), has no experimental support.

Microtubule perturbation

A number of pharmacological agents including vinblastine, nocodozole, colchicine, and colcemid, disrupt microtubules, while taxol stabilizes microtubules. Investigators have enlisted these agents to disrupt or stabilize microtubules in attempts to explain the role of microtubules in cells. Studies of this type have always been viewed with caution because: with systemic treatment they produce profound morbidity in the animal; it is difficult to determine if the observed effects are primary effects due to loss of the microtubule scaffold, or secondary to the disruption of another microtubule dependent process; and these agents do not bind exclusively to microtubules. These cautions are increasingly germane with the blossoming list of cell events in which microtubules are implicated (Schroer and Sheetz, 1991a).

Viewed in that light, a number of investigators have used microtubule inhibiting agents to understand the function of microtubules in hamsters (Rattner, 1970), mouse (Handel, 1979; Wolosewick and Bryan, 1977), rat (Aoki, 1980; Russell et al 81,89), and squirrel (Vogl et al., 1983b) Sertoli cells. The agents used were microtubule depolymerizing drugs; colcemid (Wolosewick and Bryan, 1977; Rattner, 1970), colchicine (Handel, 1979; Wolosewick and Bryan; 1977; Russell et al.1981; Aoki, 1980; Vogl et al., 1983b); nocodozole (Aoki, 1980) and vinblastine (Wolosewick and Bryan, 1977; Russell et al., 1981). In most reports, differences between depolymerizing agents (or their doses) were essentially a matter of degree.

A common finding of microtubule disruption studies is the sloughing of apical portions of Sertoli cells and associated spermatids. This may result from a loss of reinforcement by microtubules in the Sertoli cell stalk. The remaining Sertoli cell takes on a cuboidal shape. Probably one of the most dramatic findings of microtubule disruption is that of the changes in squirrel Sertoli cell morphology during spermatogenesis. The extensive sloughing is not seen in the squirrel seminiferous epithelium treated with colchicine. In untreated squirrel testis, large caches of endoplasmic reticulum are produced at the base of Sertoli cells and delivered to the vicinity of the spermatid head as spermatids elongate, become aligned with the long axis of Sertoli cells and move toward the lumen (Vogl, 1983a). During this time, the residual cytoplasm that has been segregated from the rest of the spermatid, is extended into the tubule lumen. It is then drawn basally, possibly with the help of Sertoli cell penetrating processes, to be phagocytosed by Sertoli cells. Concurrent with spermiation, the mass of SER that is situated on the concave side of the spermatid head returns to its basal position. When squirrel Sertoli cell microtubules are disrupted with colchicine, the SER that has not ascended to the apex of the cell fails to do so (Vogl et al., 1983b). Equally, the SER that has ascended to that position does not return. The residual cytoplasm is not extended into the tubule lumen but remains at the apical surface of the Sertoli cell. These events suggest that intracellular transport of ER is unable to occur in the absence of microtubules. It also suggests that cell shape is not maintained, with residual cytoplasm no longer suspended into the tubule lumen.

Probably one of the most interesting changes that occurs with the disruption of Sertoli cell microtubules, is the failure of spermatids to be moved toward the lumen. In squirrel testis, treated with colchicine, elongate spermatids remain, in their crypts, in the basal portion of the Sertoli cell, failing to be translocated to the tubule lumen (Vogl et al., 1983b). Similarly, spermatids fail to be translocated to the tubule lumen in stage VI following intratesticular injections of taxol, in rat (Russell et al., 1989b). These findings support a proposed model in which spermatids are translocated across the epithelium by a mechanism of microtubule-based transport (Vogl, 1989; Vogl et al., 1983a, 1991a,b, 1992; Redenbach and Vogl, 1991; Redenbach et al, 1991).

DEVELOPMENT OF THE HYPOTHESIS

Sertoli cell microtubules are suspected to be involved with numerous motility related events, during spermatogenesis, such as redistribution of Sertoli cell organelles and translocation of spermatids in the seminiferous epithelium (Amlani and Vogl, 1988; Russell, 1977a,b; Fawcett, 1975, Vogl, 1989). The abundance of microtubules and MAPs in Sertoli cells lends credence to the notion that there may be a special role for microtubules in Sertoli cells, beyond the housekeeping functions of a secretory cell and the maintenance of cell shape. It is reasonable to assume that the abundant, highly organized and stage specific distribution of microtubules in Sertoli cells may signify that, in addition to supporting the many microtubule-dependent functions common to other cells, Sertoli cell microtubules participate in functions unique to Sertoli cells.

In rats, spermatids are translocated toward the apex of Sertoli cells, interrupted at least once by a basal excursion, before finally achieving the apical position from which they are released. ESs are junctional complexes that are part of an adhesion junction, assemble prior to the positioning of spermatids, and persist until immediately prior to spermatid release. ESs line Sertoli cell crypts in which spermatids are translocated (see Vogl, 1989). The ER of the ES (ESER) is linked to a highly ordered layer of actin filaments which is linked to the Sertoli cell plasma membrane. This membrane is in turn adherent to the spermatid. The ES-spermatid unit remains intact when spermatids are mechanically separated from Sertoli cells (Franke et al., 1978; Grove and Vogl, 1989; Romrell and Ross, 1979). Through this linkage, forces applied to ESs would be transmitted to spermatids. Parallel arrays of microtubules occur adjacent to the cytoplasmic face of the ESER. The structural components are present for a microtubule-based transport system to position and transport spermatogenic cells in the Sertoli cell cytoplasm. Spermatid positioning has long been attributed to Sertoli cells.

An hypothesis, proposed by Christensen (1965) and later by Fawcett (1975), held that the morphology of Sertoli cell microtubules implied an involvement in the movement of spermatids within the seminiferous epithelium. This notion was further extended by Russell (1977a), who suggested that spermatid translocation may be a microtubule-based transport event. Reasoning that if microtubules can bind to membrane bounded organelles, it follows that they may interact in the same way with the ESER to transport spermatids along microtubule tracks. The hypothesis has been further modified to include the movement of spermatids on microtubule tracks by mechanoenzymes (Vogl, 1989; Vogl et al, 1989; Redenbach and Vogl, 1991).

Fig. 1-12 is a proposed model of microtubule-based spermatid translocation model to explain movement of spermatids within the seminiferous epithelium. A spermatid is shown having been moved deep within a Sertoli cell crypt. Just deep to the Sertoli cell membrane, the crypt is lined by an ectoplasmic specializations consisting of actin filaments flanked on their cytoplasmic side by a cistern of endoplasmic reticulum (ESER). Microtubules occur adjacent to the ESER. Mechanoenzymes are illustrated as a bridge between the microtubules and ESER. In this model, it is proposed that mechanoenzymes may act as motors to move the spermatid-ES complexes along microtubule tracks toward the base of the epithelium and then back to the tubule lumen.

This model is supported by a number of pieces of evidence. First, microtubules are oriented parallel to the direction of spermatid translocation (Christensen, 1965; Fawcett, 1987; Vogl et al., 1983; Amlani and Vogl, 1988; Vogl, 1988). Second, microtubules occur adjacent to the ESER (for reviews see Vogl, 1988; Vogl et al., 1991a,b; 1992). Third, linkages have been reported between microtubules and the ESER (Russell, 1977b). Fourth, cytoplasmic dynein is present in high concentration in testis (Neely and Boekelheide, 1988; Collins and Vallee, 1989) and has been isolated from Sertoli cell enriched preparations (Neely and Boekelheide, 1988), suggesting an active role for microtubule based motility in Sertoli cells. Fifth, ESs remain attached to spermatids when the seminiferous epithelium is mechanically disrupted, indicating that

Figure. 1-12: Microtubule-based translocation model. This is a model to explain the movements of spermatids within the seminiferous epithelium. A spermatid is depicted as having been moved toward the base of the epithelium, deep within a Sertoli cell crypt (left), and then returned toward the lumen of the epithelium (right) for release. The crypt is lined by an ectoplasmic specialization (ES). The ER of the ES (ESER) is linked through the actin network to the Sertoli cell membrane, and across the adhesion junction to the spermatid. This linkage remains intact during mechanical disruption of the seminiferous epithelium Forces applied to the ESER could be transmitted through this linkage to the spermatid. Microtubules occur adjacent to the ESER. It is suggested that the ESER acts as a vehicle that is moved along microtubule tracks, resulting in movement of spermatids through the seminiferous epithelium. Mechanoenzymes are illustrated as a bridge between the microtubules and ESER. It is proposed that mechanoenzymes may act as motors to move the spermatid-ES complex along microtubule tracks, toward the lumen of the seminiferous epithelium. A requirement of this model is that microtubules are able to bind to the ESs.

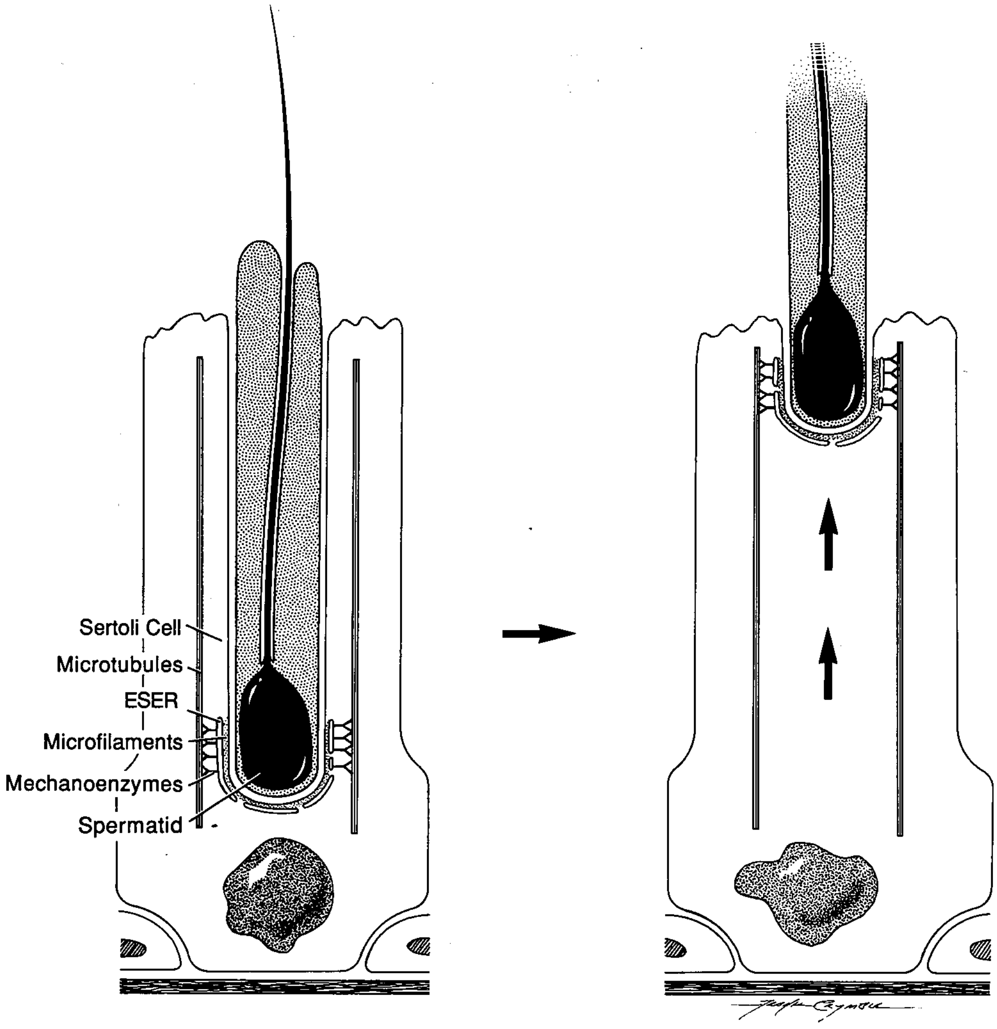
Sertoli Cell
Microtubules
ESER
Microfilaments
Mechanoenzymes
Spermatid

there is a tight linkage from the ESER, transmitted through the actin network of the ES to the Sertoli-spermatid junction, providing a means of directly linking events at the microtubule ESER interface with spermatids. The direction of this proposed transport would necessarily be a function of available mechanoenzymes and the polarity of Sertoli cell microtubules. Taken together, this evidence supports the notion that spermatid translocation is a microtubule based-event.

HYPOTHESIS STATEMENT

HYPOTHESIS:

Elongate spermatids are oriented and positioned in the seminiferous epithelium by means of a microtubule-based transport mechanism, through their attachment to ectoplasmic specializations, which serve as vehicles, being moved along Sertoli cell microtubule tracks, powered by Sertoli cell mechanoenzymes.

PREDICTIONS

1) If spermatids are oriented and positioned on microtubules, they should, through their linkage to ESs, be able to bind to microtubules.
2) If spermatid-ES binding is mediated by a mechanoenzyme or other dynamically regulated linking protein, the binding will share some characteristics with microtubule-organelle binding observed in other systems.

Sertoli cell microtubules share microtubule distribution with other polarized epithelial cells, in that they are oriented parallel with the long axis of the cell. As is the case in other cells, they are likely to be unipolar in orientation. Furthermore, they may share the minus-end out polarity that has been demonstrated in polarized MDCK cells. This would be consistent with the presence of an abundance of cytoplasmic dynein, a known minus-end directed mechanoenzyme. As part of the study to test the microtubule-based spermatid translocation hypothesis, the polarity of Sertoli cell microtubules was determined. This is the focus of **Chapter 2: Microtubule Polarity**.

Spermatid-ES-microtubule binding is required for microtubule-based spermatid translocation. The development of a binding assay to test for spermatid-ES-microtubule binding and its characterization are the focus of **Chapter 3: Binding Assay**.

EXPERIMENTAL OUTLINE

Microtubule polarity study

In this study, a morphological technique was used to determine the polarity of Sertoli cell microtubules, in which blocks of rat testis were treated with lysis decoration buffer, with and without exogenous tubulin, adapted from the method of Heidemann and McIntosh (1980; Heidemann, 1991). Polarity was assessed by determining the direction of hook formation on Sertoli cell microtubules, using montages constructed from photographs of thin sections through the seminiferous epithelium, parallel to the base of the epithelium. Microtubules are decorated with clockwise hooks when observed from their plus-ends to their minus-ends. Section orientation was verified by the direction of axonemal dynein arms in spermatid axonemes, being clockwise when viewed from the tip to the base of the axoneme.

Microtubule-spermatid-ES binding study

An *in vitro* assay was developed to test the potential for spermatids, through their attachment to Sertoli cell ESs, to bind to microtubules. Microtubules were assembled in the presence of [^{3}H] labelled GTP and taxol to provide radiolabelled, stable microtubules. Spermatid-ESs complexes were isolated, by a squash technique, from rat seminiferous tubules, and incubated with the labelled microtubules.

Binding was characterized using pharmacological agents and nucleotides that have been used to characterize microtubule binding in other systems.

The results of this study have implications for the Sertoli cell and its role in spermatogenesis and, in a broader sense, for cellular microtubules in general and their role in microtubule dependent organelle positioning. Furthermore, they imply that an intracellular activity, microtubule-based transport, can extend its influence to an extracellular event.

CHAPTER 2

MICROTUBULE POLARITY

INTRODUCTION

DETERMINATION OF MICROTUBULE POLARITY: THE APPROACH

To determine the polarity of microtubules in Sertoli cells, a morphological technique, introduced by Heidemann and McIntosh (1980), was adapted for use in testis. This technique involves the use of a lysis/decoration buffer to lyse cells and decorate endogenous microtubules, usually with the addition of exogenous tubulin. The buffer components, essential to induce the assembly of curved protofilament sheets on existing microtubules, are a high salt buffer, preferably 0.5 M PIPES, and DMSO. The addition of purified tubulin contributes to the soluble tubulin pool that provides tubulin substrate for hook assembly. A number of modifications of the original technique have been reported in the literature, usually invoked because of buffer penetration constraints, specific to the tissue being studied. The technique has been used successfully without exogenous tubulin in tissue with abundant microtubules (Troutt and Burnside, 1988a,b).

The technique is a valid measure of microtubule polarity (Heidemann and McIntosh, 1980). This was demonstrated by determining the direction of tubulin hooks on microtubules grown from basal bodies for which the polarity was known (Heidemann and McIntosh). The handedness of the hook formation identified microtubule polarity accurately in at least 90% of microtubules examined. This accuracy has been consistent in subsequent use of this method. The assumption was made that the remaining microtubules, decorated in an opposite direction to their known polarity, were decorated 'erroneously'. One alternate interpretation is that exogenous microtubules may have formed from exogenous tubulin, added with the decoration buffer. Because the microtubules of 'erroneous' polarity are generally oriented parallel to the others, the former explanation is preferred. In the literature, microtubule systems with a polarity of ≥ 90 % have been interpreted as "unipolar" (Troutt and Burnside, 1988a, b; Mogensen et al., 1989; Burton, 1988; Baas et al, 1987, 1988; McIntosh and

Euteneuer; McNiven et al., 1984; Euteneuer and McIntosh, 1981; Burton and Paige, 1981).

DETERMINATION OF MICROTUBULE POLARITY: THE STRATEGY

The degree of hook formation can be varied to some degree, by altering the buffer and incubation conditions, or by changing the concentration of tubulin added to the lysis decoration treatment (Heidemann and Euteneuer, 1982; Heidemann, 1990. However, in many tissues, the rate and depth of penetration of the treating buffer will vary, within, as well as between, samples. Preliminary experiments showed this to be true for testis. For this reason, a number of different buffer conditions, as well as tissue from two species, were used in this study to ensure that buffer conditions did not play a role in these observations. In view of the fact that the microtubules are abundant in Sertoli cells, the use of hook decoration buffer, without exogenous tubulin, was also employed.

The majority of Sertoli cell microtubules arise from a supranuclear location and course parallel to the long axis of the cell, extending into the apical stalk. Of particular interest in this study are microtubules found in the supranuclear portion of the Sertoli cell as well as in the vicinity of differentiating spermatids with associated ESs. Sections were taken from a supranuclear position, in areas which included spermatids. In this location, spermatid tails were frequently included in the section. Microtubules were parallel to each other in these areas.

Purified, polymerization competent, bovine brain tubulin was the source of exogenous tubulin for this study. There was a concern that microtubules would polymerize from the exogenous tubulin before gaining access to the cytoplasmic microtubules. For this reason, the concentration of exogenous tubulin was kept low; however, the assembly promoting nature of the buffer and the presence of endogenous tubulin could alter that threshold, particularly at higher temperatures. For this reason a range of temperature and incubation time combinations were tried, both with and without exogenous tubulin.

In these experiments, care was taken to follow the 'sidedness' of the sections, ensuring that the assumed direction from which the tissue was viewed was correct. Dynein arms on axoneme microtubules are always oriented in a clockwise direction, when viewed from their base to their tip (Bershadsky, 1988, chapter 2). The presence of spermatid tail axonemes was used to provide verification of the section orientation, in many sections.

Taken together, these experiments consistently give the same answer to the question: What is the polarity of Sertoli cell microtubules?

MATERIALS AND METHODS

MATERIALS

Animals

Testes from six adult, Sprague Dawley rats (200 to 275 gms) and one reproductively active ground squirrel (*Citellus. lateralis*) (244 gms) were used in the microtubule polarity study. The animals were maintained in the animal care facilities at the University of B.C. Beef brains were acquired from Intercontinental Packers, Vancouver, B. C.

Chemicals and supplies

Unless otherwise mentioned all chemicals used for the microtubule polarity studies were from Sigma Chemical Co. (Springfield Missouri). Taxol was the generous gift of Dr. Matthew Suffness, National Cancer Institute USA. Chemicals for electron microscopy were from JB EM and embedding media from Polysciences (Warrington PA.). SS34 rotor is from Sorvall. The other rotors are from Beckman.

Buffers

PEM: 100 mM PIPES, 1 mM $MgCl_2$, 1 mM EGTA, pH 6.9. PEM4M or PEM8M: PEM with 4M or 8M glycerol.

Lysis decoration buffer (0.5 M Pipes, 2.5% DMSO, 1mM EGTA, 1 mM $MgCl_2$, 1% triton X100, 0.02% SDS (optional), 0.5% deoxycholate, 1 mM GTP with or without exogenous tubulin). For detailed description of making lysis decoration buffer, (see Heidemann, et al., 1980). In experiments where tubulin was dialyzed in 2X PEM and then mixed 1:1 with the remaining components of lysis/decoration buffer, these components were 2X(0.4 M Pipes, 2.5% DMSO, 1% triton X100, 0.02% SDS (optional), 0.5% deoxycholate, 1 mM GTP).

METHODS

Preparation of purified tubulin:

Microtubule protein, for the microtubule decoration experiments, was prepared from two beef brains, using a temperature dependent assembly-disassembly protocol modified from that of Williams and Lee (1982). Two steer heads were obtained from Intercontinental Packers, packed in ice and transported to the lab. Brains were removed and dissected free of vascular and connective tissue (yield 700g brain). The tissue was placed in PEM4M buffer (70% of original volume), homogenized in an Oster blender for 50 seconds, and centrifuged at 23,500g for 5 minutes at 4°C in an SS34 rotor (14,000 rpm). The pellet was discarded. The supernatant was centrifuged at 39,000g for 30 minutes at 4°C in SS34 rotor. The supernatant was brought to 1mg/ml GTP, incubated at 37°C for 35 minutes then centrifuged at 35°C, at 39,000g for 30 minutes in the SS34 rotor (18,000 rpm). The supernatant was discarded. The pellet was resuspended in 15% of original homogenate volume in PEM4M, solubilized on ice for 30-40 minutes then centrifuged at 39,000g for 30 minutes at 4°C. The supernatant was again made 1 mg/ml GTP, incubated at 37°C for 30 min, and then centrifuged at 39,000g for 30 minutes at 35°C in an SS34 rotor. The pellet was resuspended on ice in 10% original volume in PEM without glycerol, solubilized for 30 minutes with homogenization, and cleared at 39,000g for 30 minutes at 4°C in SS34 rotor. The supernatant, containing 19 mg/ml protein (Biorad), was frozen and stored in liquid nitrogen (protein concentration 19 mg/ml).

Microtubule protein was thawed, as needed, cleared with a 39000g spin at 4°C for 20 minutes, cycled one more time through one warm, and then one cold step as described above, and purified by a phosphocellulose chromatography. A chromatography column was packed with activated P-11 (Whatman), equilibrated with PEM buffer (no glycerol) pH 6.9 and loaded with 2.5mls of microtubule protein. Purified tubulin was recovered from column fractions, monitored for tubulin content by A280, and dialyzed into PEM4M glycerol. It was stored in liquid nitrogen (final concentration 0.6 -0.7 mg/ml). Tubulin purity was verified by SDS PAGE gel electrophoresis (Fig 2-1: d) using a 7% gel, based on the method of Laemmli (1970).

Purified tubulin from the column did not appear to polymerize in a post column warm cycle; therefore, the polymerization competency of post column purified tubulin was checked (see below). A pellet of polymerized tubulin was not visible in warm cycled post column tubulin, at this concentration (0.6 to 0.7 mg/ml); therefore, verification of polymerization competency was sought using three methods: 1) negative staining of tubulin incubated on sea urchin axonemes isolated and demembranated according to the method of Stephens (1986a) (Fig. 2-1:b), 2) negative stain electron microscopy (Fig 2-1:c), and 3) video enhanced differential interference contrast microscopy (Fig 2-1:d) of purified tubulin in the presence of 20µM taxol at 37°C. Although self polymerization did not occur, taxol stabilization or sea urchin axoneme nucleation resulted in polymerization.

For microtubule decoration experiments, aliquots of purified tubulin were thawed immediately prior to use, concentrated to one half original volume in an ultrafree-PF filtration unit (Millipore), then dialyzed against 1000 volumes of 2X PEM buffer (100 mM PIPES, 1 mM EGTA and 1mM $MgCl_2$) buffer at 4°C for 2 hrs, and finally brought to predialysis volume. Dialyzed tubulin in 2X PEM was diluted 1:1 with 2X concentration of remaining components of lysis/decoration buffer, to give a final lysis/decoration buffer the same as that used for endogenous tubulin preparations described below, with final a tubulin concentration of 0.6 to 0.7 mg/ml. Protein concentration was determined after the method of Bradford (1976) using Biorad reagents.

Hook decoration

The method for microtubule decoration was modified after the procedure of Heidemann and McIntosh (Heidemann and McIntosh, 1980, Heidemann et al., 1980).

Figure 2-1. Evidence of purity and polymerization capability of purified bovine brain tubulin.

(a, b, c) Micrographs from the same image of taxol polymerized microtubules from the purified bovine brain tubulin used in microtubule polarity experiments. This is the appearance of the microtubules (a) viewed with DIC video-enhanced microscopy , (b) further contrast enhanced by computer, using expansion of assigned grey levels, and (c) 'cleaned' by computer subtraction of out of focus background image.

(d) SDS PAGE gel (7%) loaded with 3X cycled bovine brain microtubule protein (lane 1) before purification on phosphocellulose column, (lane 2) purified tubulin after MAPs were removed by chromatography, and (lane 3) molecular weight markers (ovalbumin 45kD, bovine plasma albumin 66kD, rabbit muscle phosphorylase b 97.4 kD, beta-galactosidase 116 kD, and rabbit muscle myosin 205 kD). (Direction of migration on gel is from top to bottom). Prominent bands of alpha and beta tubulin (>) are seen (approximately 55kD) (lanes 1 and 2) with minor bands of microtubule associated proteins in microtubule protein (lane 1) which were subsequently removed by chromatography (lane 2).

(e) Negative stain EM image of purified tubulin polymerized in the presence of 20μM taxol.

(f) Video enhanced, DIC image of purified tubulin polymerized in the presence of 20 μM taxol, from the same sample as in (e).

(g) Isolated and demembranated sea urchin sperm axonemes incubated with and without (inset: center) exogenous bovine brain tubulin to illustrate polymerization capability of purified tubulin is shown using negative stain EM. A high power view shows the microtubule protofilament detail of axoneme nucleated microtubule growth in area marked with an astrisk (inset upper right). This also marks the end of the axoneme that supported longer microtubule growth (plus-end).

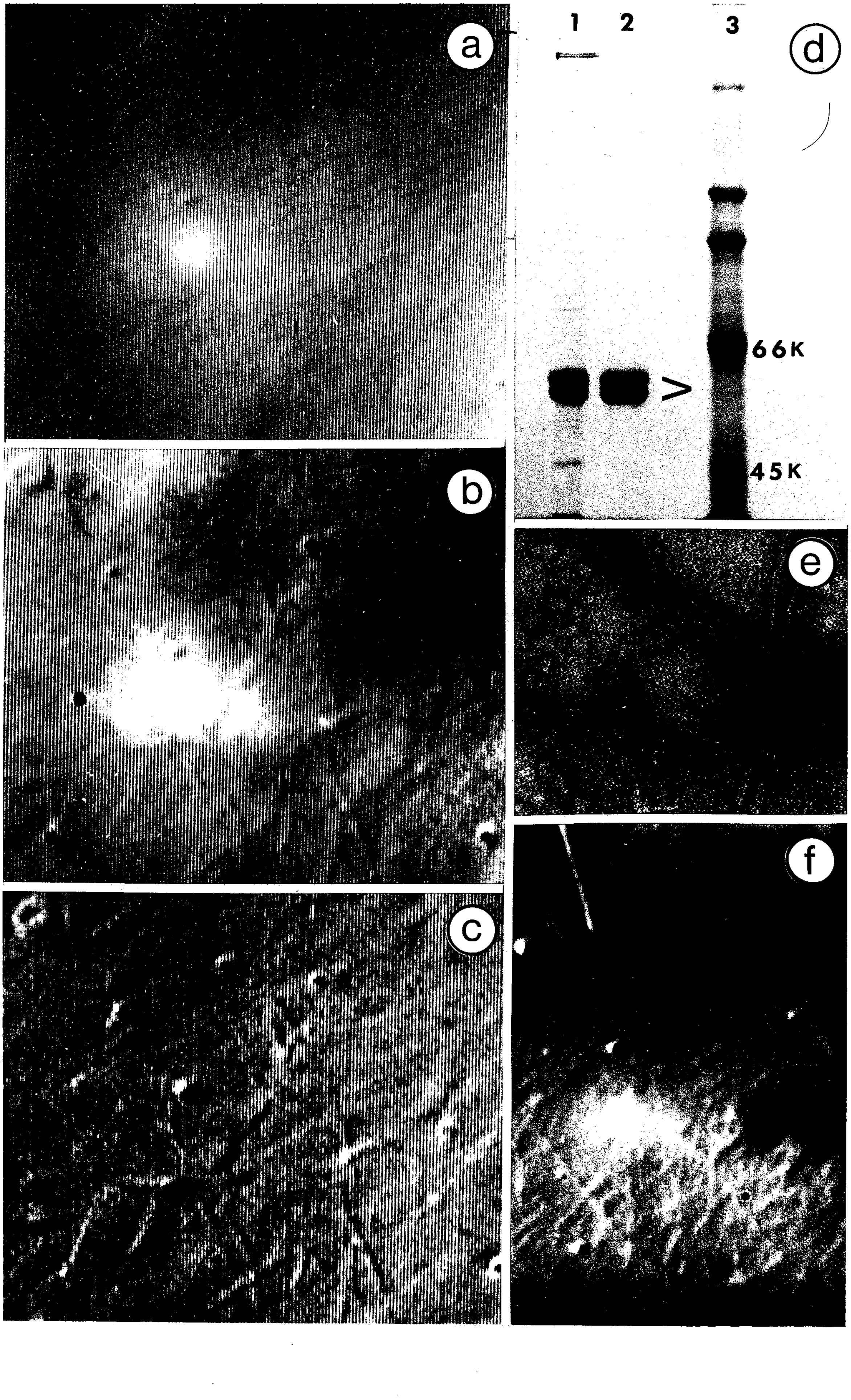
a
1
2
3
d
66K
>
45K
b
e
c
f

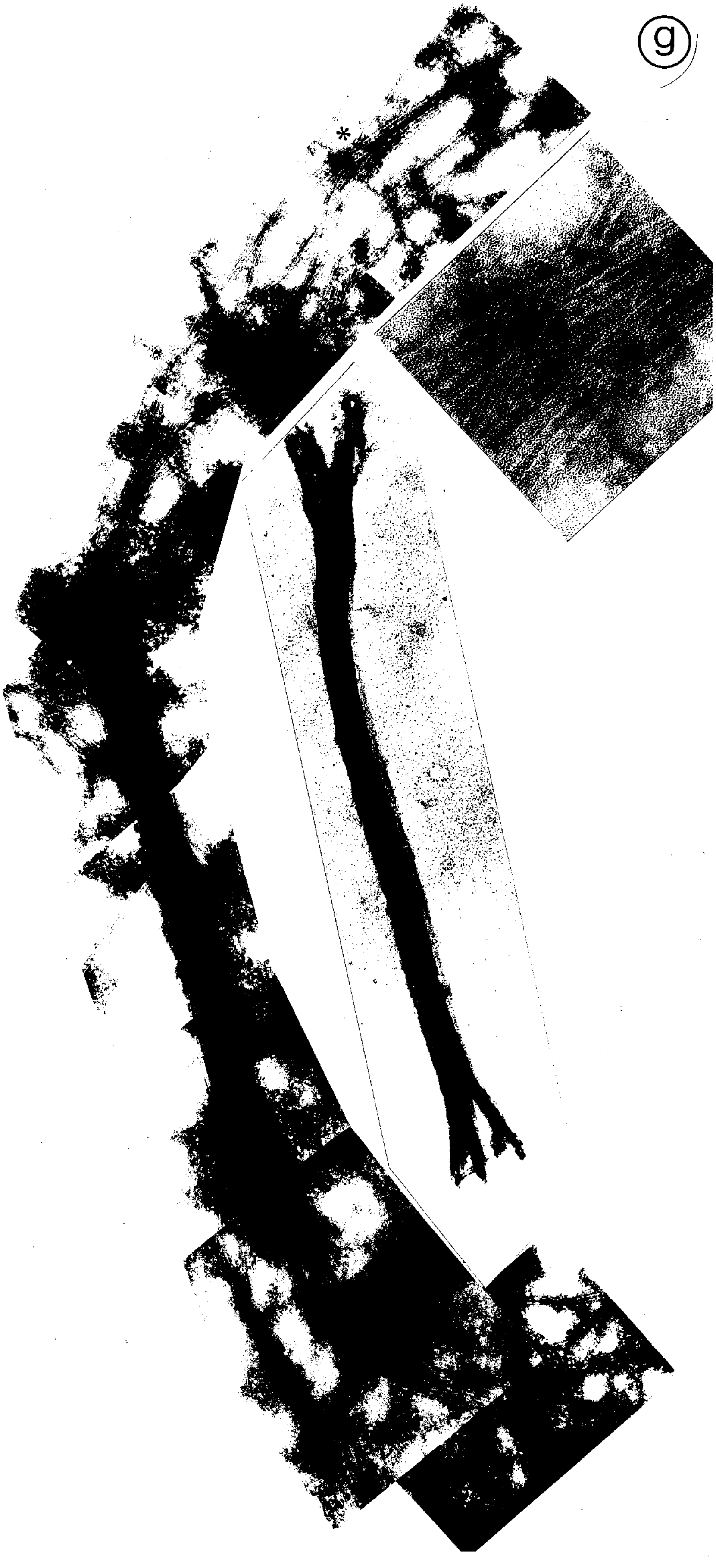
g
*

Animals were anesthetized with halothane and the testes removed, decapsulated, placed in lysis/decoration buffer (with or without exogenous tubulin), and quickly cut into 2 mm cubes. Samples were incubated in lysis/decoration buffer:

1) with exogenous tubulin, for 30 minutes on ice (4°C),10 minutes at 22°C and 15 minutes at 37°C, (rat testis): control 1a - without exogenous tubulin, for 30 minutes on ice, 10 minutes at 22°C and15 minutes at 37°C. or control 1b - without exogenous tubulin (and omitting the cold step) incubated for 40 minutes at 22°C and 15 minutes at 37°C (rat),

2) without exogenous tubulin for 10 minutes on ice, followed by 20 minutes at 33°C (rat and squirrel testis). control 2 - (omitting the cold step) - 30 minutes at 33°C (rat and squirrel testis). Number 2 gave the best results.

This technique has been used widely to examine microtubule polarity (Heidemann and McIntosh, 1980) with, and without, the addition of exogenous tubulin using a number of different incubation conditions, including warm and cold preincubation temperatures. The rationale here for using an initial cold step, was to permit the exogenous tubulin to penetrate the tissue in the depolymerized form, favoring its contribution to hook formation rather than self assembly. However, using these conditions, microtubules may depolymerize, resulting in the examination of an exclusively cold stable population, or depolymerize and repolymerize in a manner different to what was present before the incubation. To address this concern, regarding the effect of the cold step on endogenous microtubules, additional experiments were carried out in which purified tubulin was added without the initial cold incubation. In these experiments, tissue was excised from the animal and immediately incubated in lysis decoration buffer with exogenous tubulin for 15 minutes at 22°C followed by 15 minutes at 33°C. If self assembly occurred, it was anticipated that it would occur with random polarity. In the earlier experiments, controls had included the use of 33°C but in the absence of exogenous tubulin; therefore, they showed limited decoration, albeit consistent with experimental findings. In order to determine the effect of incubation entirely at 35°C with added tubulin, a further experiment was done in which the tissue was immediately incubated in lysis buffer at 35°C for 30 minutes with exogenous tubulin. To reduce self polymerization of exogenous tubulin before tubulin gained access to the cell, the tubulin in 2X PEM buffer was quickly warmed to 35°C in 2X PEM buffer and added to the remaining components of lysis decoration buffer at 35°C, immediately before tissue incubation.

Electron microscopy

All EM fixation and processing steps were carried out at room temperature. Tissue blocks were fixed for electron microscopy in 3% glutaraldehyde in PEM for 45 minutes, with or without 1.0% tannic acid, rinsed 3 times, and postfixed in buffered osmium tetroxide for 30 to 45 minutes. (Adequate fixation was also obtained using 2% glutaraldehyde for 30 minutes). Samples were rinsed 3 times in PEM and then stained "en bloc", in aqueous 1% uranyl acetate for 1 hr, dehydrated and embedded in Polybed 812 (Polysciences, Inc., Warrington, PA). Sections were cut and collected on 300 mesh copper grids. Sectioning strategy is illustrated in Fig. 2-2. Sections were stained with uranyl acetate and lead citrate for 8 minutes each, and viewed on a Phillips 300 transmission EM at 80kV.

In order to be certain of Sertoli cell orientation, the sampling strategy was as follows: Blocks were positioned so that the seminiferous tubule to be sectioned was oriented parallel to, and just deep to, the block face. (Fig. 2-2). They were trimmed with enantomeric shaped mezas to eliminate errors in section orientation from the block to final photographs. Seminiferous tubules were sampled serially from the base to the apex of the epithelium. A series of sections were cut, consisting of semi-thin sections for light microscopy, interspersed between thin sections for electron microscopy, proceeding from the base to the apex of the epithelium. Semi-thin sections were stained with toludine blue to establish the orientation and approximate tissue depth of the corresponding intervening thin EM sections. Areas for observation were selected from

Figure 2-2. Microtubule decoration: sampling method for EM sections. Strategy used to orientate the seminiferous tubule such that Sertoli cells could be sectioned perpendicular to their long axes. The morphology of the seminiferous tubule has been simplified to show a simple columnar epithelial tube of Sertoli cells each supporting a single spermatid, which in turn projects into the tubule lumen. As sectioning progresses toward the apical surface of Sertoli cells, the spermatid is included in the section. By selecting cells from a central strip of the section (shaded area), structures, which are orientated with their long axes parallel to that of the Sertoli cell, such as spermatid tails or microtubules, are viewed in cross section (depicted as circles in the section).

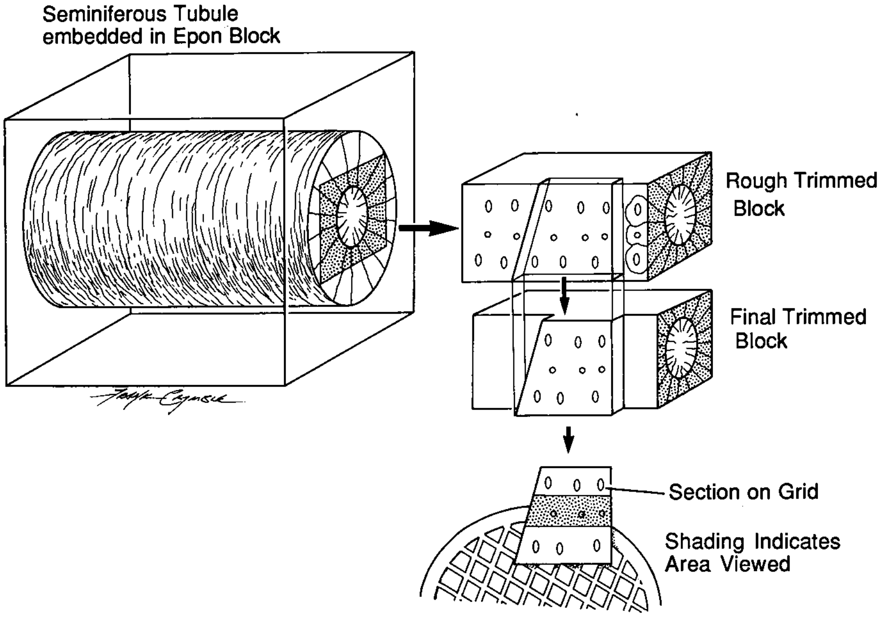
Seminiferous Tubule embedded in Epon Block
Rough Trimmed Block
Final Trimmed Block
Section on Grid
Shading Indicates Area Viewed

the central strip of the seminiferous tubule sections where the knife passed at right angles to the long axis of Sertoli cells.

To provide further verification of the tissue orientation, advantage was taken of the inherent polarity of sperm tail axonemes, which extend their distal ends into the lumen of the seminiferous tubule. When a spermatid axoneme is viewed from the base to the tip, its microtubules are being viewed looking toward their plus end (Heidemann and McIntosh, 1980). In this orientation, dynein arms extend from the A toward the B subfiber, and are thereby pointing in a clockwise direction. It was verified that, when observed from the base to the apex of the seminiferous epithelium, dynein arms of all spermatid axonemes extended in a clockwise direction providing an internal check on the orientation of the tissue, in most sections.

Negative stain electron microscopy

Droplets of axoneme nucleated or taxol stabilized microtubules from purified tubulin, were placed on copper grids, that had been coated with parlodian, coated with carbon, next dipped in acetone to remove parlodian, and finally glow discharged. Tissue was allowed to settle; then blotted gently. A few drops of aqueous 1% uranyl acetate were applied, rinsed carefully with 2 drops of distilled water, and allowed to dry. They were then visualized on a Phillips 300 at 60-80 kV.

Video enhanced differential interference microscopy

Tubulin polymerization capacity was checked with video enhanced differential interference contrast microscopy. Microtubules, polymerized from the purified tubulin with 20μM taxol, were placed in a tissue chamber as described by Schnapp (1980). Briefly, this consisted of placing sample within a partial circle of vacuum grease applied to a polylysine coated acid cleaned slide (or coverslip fixed to a specially tooled adaptor). #0 spacers were placed on either side of the grease, and all covered with #O coverslip. A drop of sample was applied with its meniscus rising just slightly above the level of the grease. The sides were sealed with Varlap (1:1:1 vaseline/lanolin/paraffin) leaving access at the front and back to exchange solutions. These techniques reduced the tendency of the sample to stream. Samples were observed, under oil, using a Zeiss Photomicroscope I, fitted with a 200/4 mercury light source, heat filters, and DIC optics. The image was captured by Dage video camera with manual gain and background grey level control. The camera was fitted with on Zeiss zoom attachment fitted with a 10X eyepiece, and the image displayed on a Sony monitor screen. Images were recorded on a Sony 3/4 inch video cassette recorder and photographed with a Pentax camera mounted on a tripod to allow greater than 1 second exposures to fuse the video image. (video microscopy: Allen et al., 1981a; Inoué, 1981,1986)

RESULTS

MICROTUBULE POLARITY

Effects of lysis decoration buffer

Sertoli cells were examined at a level where microtubules are associated with ESs surrounding spermatids in order to determine the polarity of microtubules in locations where they may be involved in orientation and translocation of germ cells. In most cases, this included the presence of sperm tails of more deeply placed spermatids.

Figure 2-3 shows an area of seminiferous epithelium that has been treated with lysis/decoration buffer and sectioned as shown in Fig. 2-2. A number of sperm tail axonemes are included in the section. This section is oriented such that axonemes are viewed looking toward the tubule lumen. Dynein arms, projecting from A subfibers, are oriented in a clockwise direction.

Figures 2-4 to 2-8 are electron micrographs from four different samples, incubated in cold then warm lysis decoration buffer, illustrating the consistency of the results in spite of the variability of tissue appearance encountered. The degree of membrane extraction, nuclear decondensation, and germ cell collapse that varied with depth and location of the seminiferous tubule within the tissue block can be seen.

In the seminiferous epithelium there are complex relationships between Sertoli cells and germ cells. In more highly extracted tissue, there was little to mark these elaborate cell boundaries (Fig. 2-4). It was found that, incubation in lysis/decoration buffer produced some decondensation of chromatin, as has been reported previously (Euteneuer and McIntosh, 1980), further reducing tissue boundary indicators (compare Figs. 2-4, and 2-6). However, in many areas, selective shrinkage of germ cells was observed (Figs. 2-7 to, 2-9) permitting observations to be limited exclusively to Sertoli cell microtubules, in those samples. In other samples, manchettes

Figure 2-3. Verification of spermatid tail axoneme orientation.

(a) An area of seminiferous epithelium, which has been incubated in lysis/decoration buffer, in which the axonemes of a number of spermatid tails can be seen in cross section. This section is viewed as though looking toward the distal end of the axoneme. The orientation of dynein arms extending from A subfibers is in a clockwise direction. Included in the section are a number of microtubules decorated with hooks oriented (thick arrow) in a clockwise direction.

(b) Micrograph showing greater detail of a spermatid axoneme indicated by an asterisk in (a). Note dynein arms (arrows) which project from A subfibers (arrowheads) are oriented in a clockwise direction.

bars: a = 1µm, b = 0.25µm.

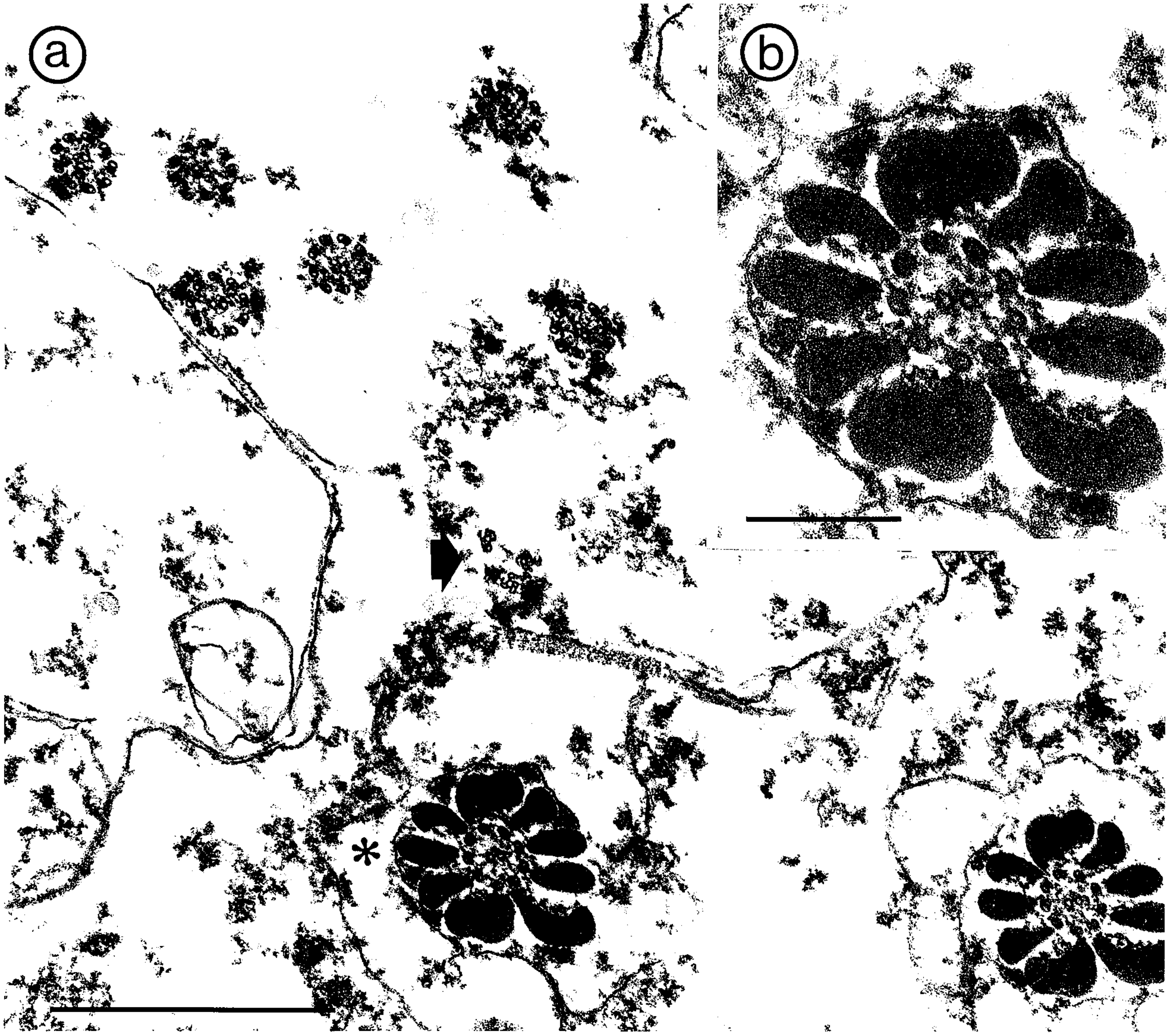
a
b
*

Figure 2-4. Rat seminiferous epithelium, highly extracted following incubation in lysis/decoration buffer.

(a) Section of seminiferous epithelium, oriented as though looking from the base toward the lumen of the epithelium. The spermatid nucleus has undergone decondensation and membranes are fragmented. Actin filaments of an ES are seen adjacent to the spermatid (arrows). Decorated microtubules can be seen with hooks oriented in a clockwise direction. Tangentially sectioned microtubules are seen in this section (arrowhead).

(b) Enlargement of decorated microtubule cluster and remnant of adjacent ES indicated in (a).

(c) Axoneme indicated in (a). Note A subfibers (arrowheads) and dynein arms (arrows) oriented in a clockwise direction.

(d) Hook-decorated microtubules indicated in (a).

bars: a = 1 µm, b = 0.1 µm.

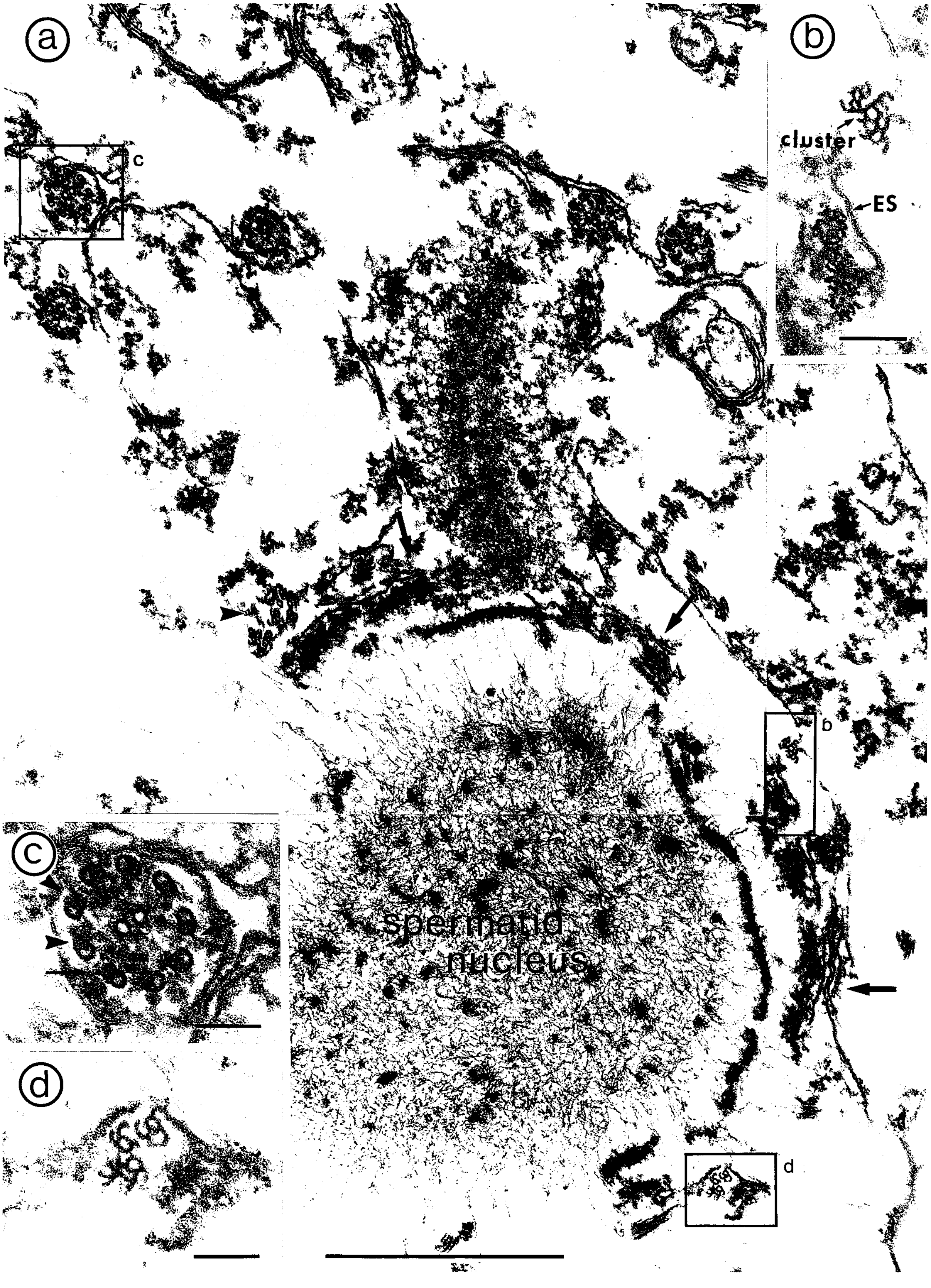
a
c
b
cluster
ES
b
c
spermatid
nucleus
d
d

Figure 2-5. Low power view of an area of seminiferous epithelium that has been incubated in lysis decoration buffer. Groups of decorated microtubules are seen between elongating spermatids (arrows). This is a typical view in which the orientation of microtubules (arrows) can be compared to the associated sperm tails (arrowhead). The area outlined with a dotted line, in this figure, is shown at higher magnification in following figure.

bar: = 1μm

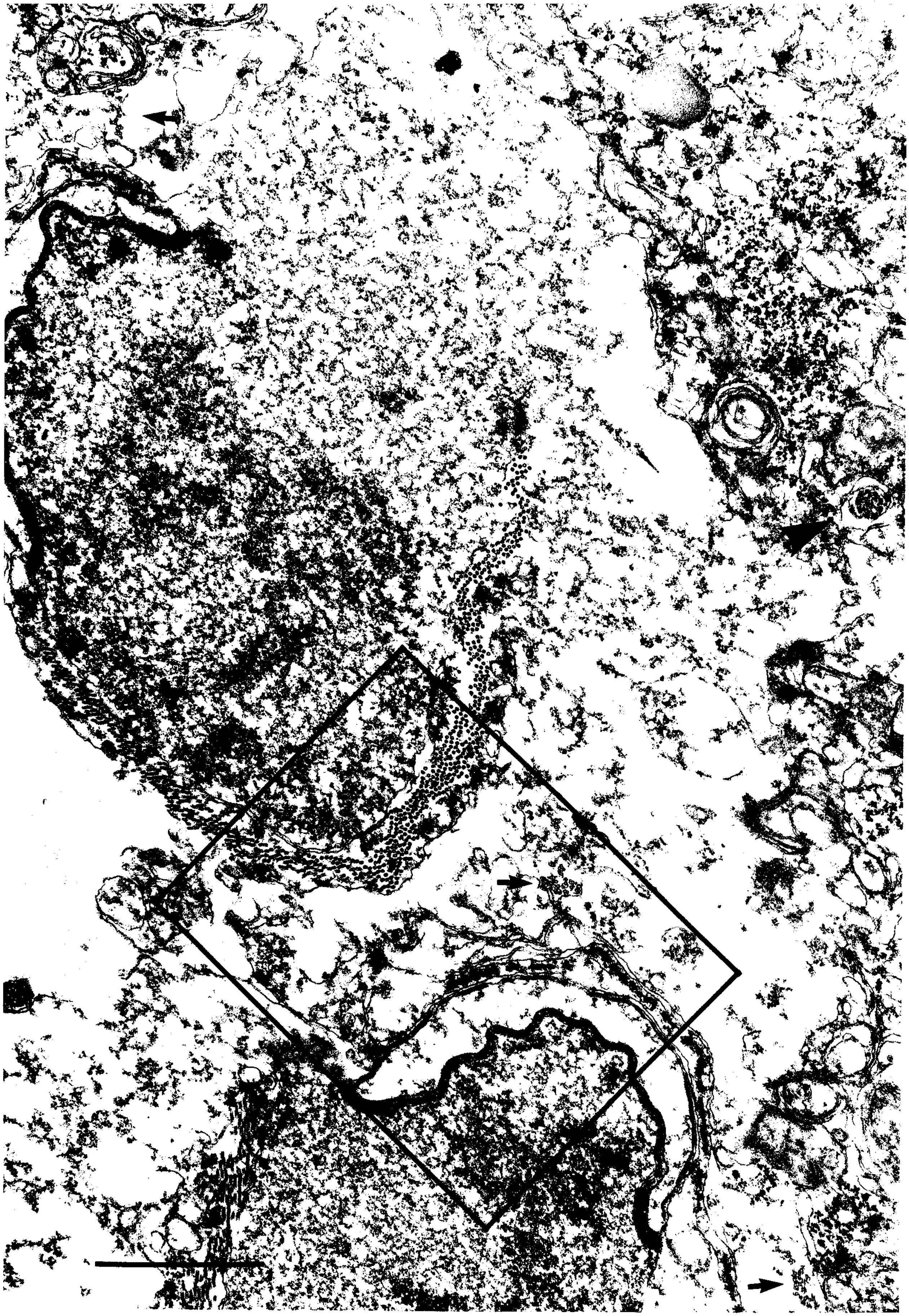

Figure 2-6. Rat seminiferous epithelium moderately extracted following incubation in lysis decoration buffer.

(b) Micrograph of Sertoli cell microtubule decoration. Membranes are disrupted, but more intact than those seen in Fig. 2-3. A spermatid nucleus and adjacent acrosome are indicated. An ES (arrows) and nearby decorated microtubules (arrowheads) can be seen. Manchette microtubules do not show hook formation. Sertoli cell microtubule hooks are oriented in a clockwise direction.

(a) Axoneme from the same section as shown above, showing clockwise orientation of dynein arms (arrows) in same field as clockwise decoration of Sertoli cell microtubules. bars: a = 1 µm, b = 0.25 µm.

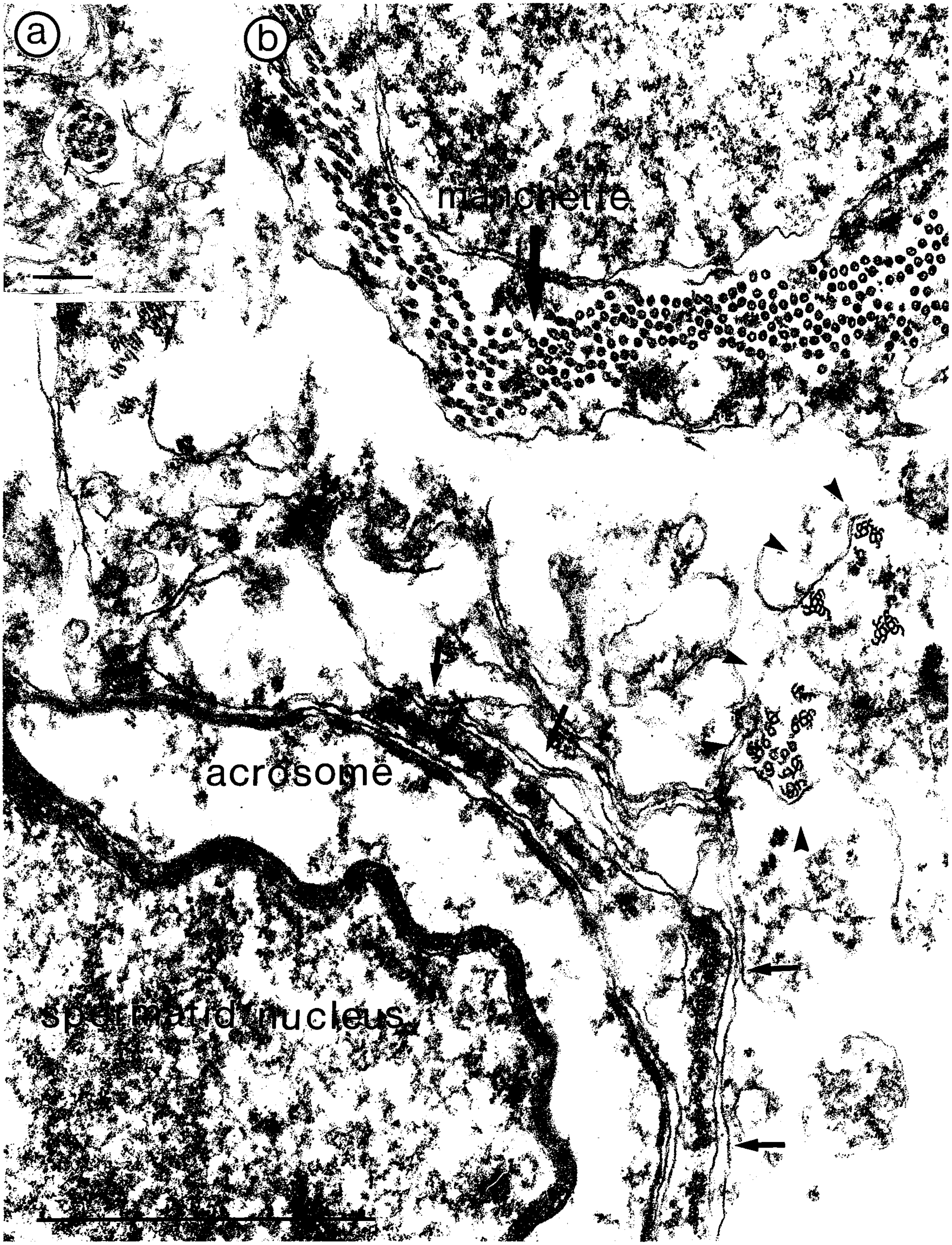
a
b
manchette
acrosome
spermatid nucleus

were easily distinguished from cytoplasmic microtubules, providing an additional boundary marker (Fig 2-5).

Decorated microtubules must be cut in precise cross section for hook formation to be clear. In all fields, some microtubules were found that were slightly tangential to the plane of the knife, appearing as short striated bundles (Fig 2-6). Although the tangential microtubules were decorated, as indicated by their striated appearance, they could not be scored for polarity. Because there was no pattern to the distribution of tangential microtubules, it is presumed that those that could be scored were representative of all those present.

Sampling for montages

Areas showing different degrees of extraction were chosen for sampling. To be certain that the results were representative of all microtubules in the area, large fields of epithelium were sampled. These were recorded by sampling either the entire area of a 300 mesh grid square or strips across an entire grid, photographing them at 18,800X on Agfa plate film. Montages 3, 4 and 5 are derived from this method of sampling. The 50 to 80 negatives for each field were printed at final magnification of approximately 50,000X. Resulting micrographs were then spliced together into working montages and scored with the aid of a hand held magnifying glass. Figure 2-8 is a reduction of montage 3. In addition, small montages were photographed and assembled from areas more enriched with microtubules (montages 1 and 2).

Scoring criteria

To determine the polarity of microtubules from each montage, microtubules were classified according to the following criteria. Microtubules were grouped into "clockwise", "counterclockwise" or "ambiguous" categories. These were further subdivided into "hook" or "cluster" groups. In all microtubules scored in the "hook" category, hooks arose from a single microtubule (first order hooks). Hooks on hooks were not counted, nor were closed hooks. In those few cases where first order hooks of

Figure 2-7. Rat seminiferous epithelium only slightly extracted following incubation in lysis/decoration buffer.

(a) Micrograph of seminiferous epithelium, orientated as though looking toward the epithelial lumen. In this sample, decondensation of the spermatid nucleus is minimal. Microtubule decoration of Sertoli cell microtubules is mostly with hooks orientated in a clockwise direction (small arrowheads). A microtubule with counter-clockwise orientation is indicated (arrow). ES is indicated with large arrowhead.

(b) An axoneme from the same section shows clockwise orientation of dynein arms.

bars: a= 1 µm, b = 0.25µm

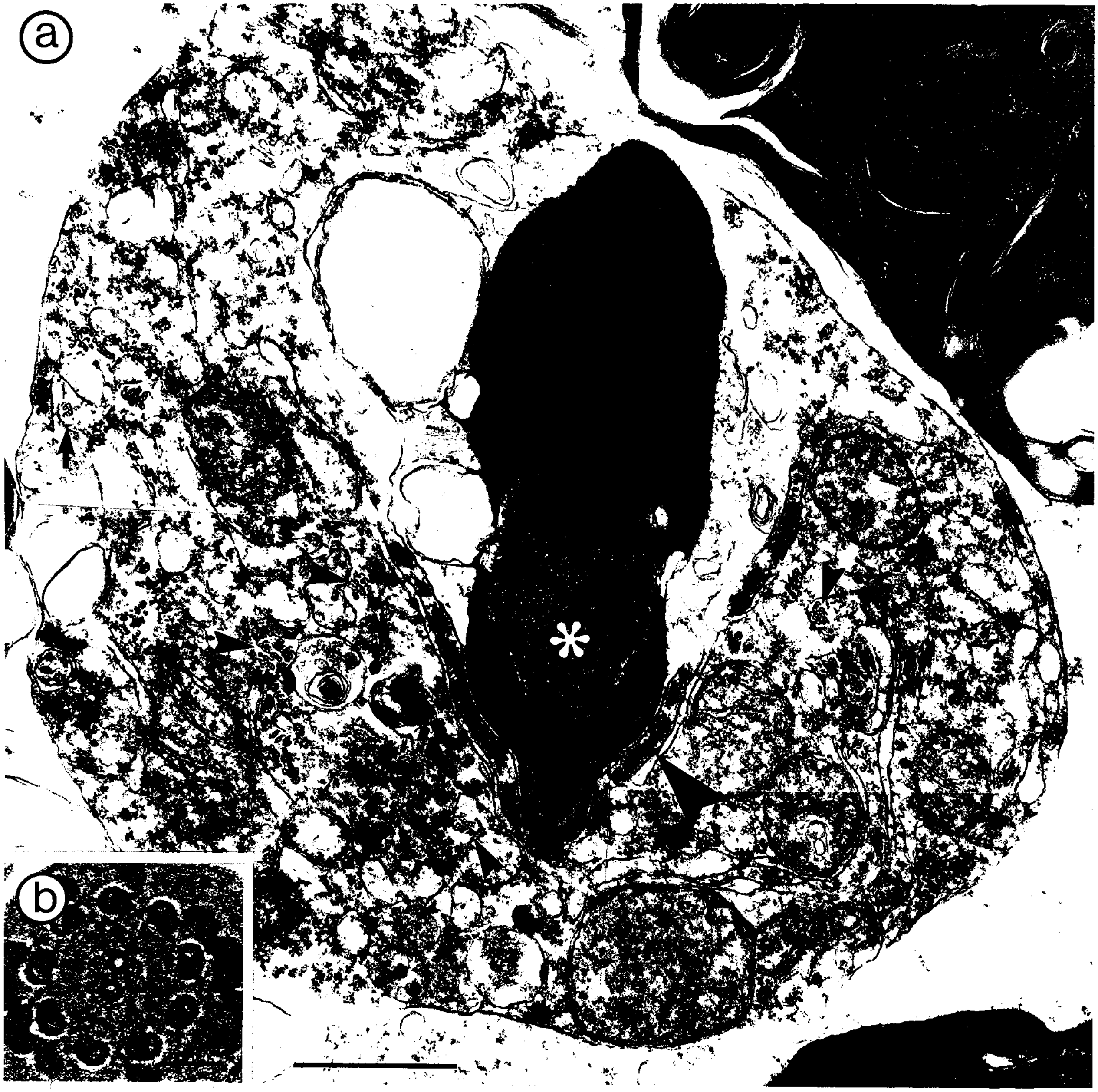
a
b
*

Fig. 2-8. Montage of rat seminiferous epithelium incubated in lysis/decoration buffer. Section of rat seminiferous epithelium, incubated in lysis/decoration buffer, viewed as though looking toward the tubule lumen.

(a) Reduced photograph of a working montage assembled from micrographs of an entire square of 300-mesh EM grid. Selective shrinkage of germ cells has occurred.

(b) An enlargement of the area indicated, showing microtubules oriented in a clockwise direction.

(c) Axoneme from the area indicated on the montage, also showing clockwise directed dynein arms.

(d) Axoneme from an adjacent grid square. The clockwise orientation of dynein arms can be seen (arrows).

bars: a = 10μm, b = 0.25 μm, c = 0.1μm.

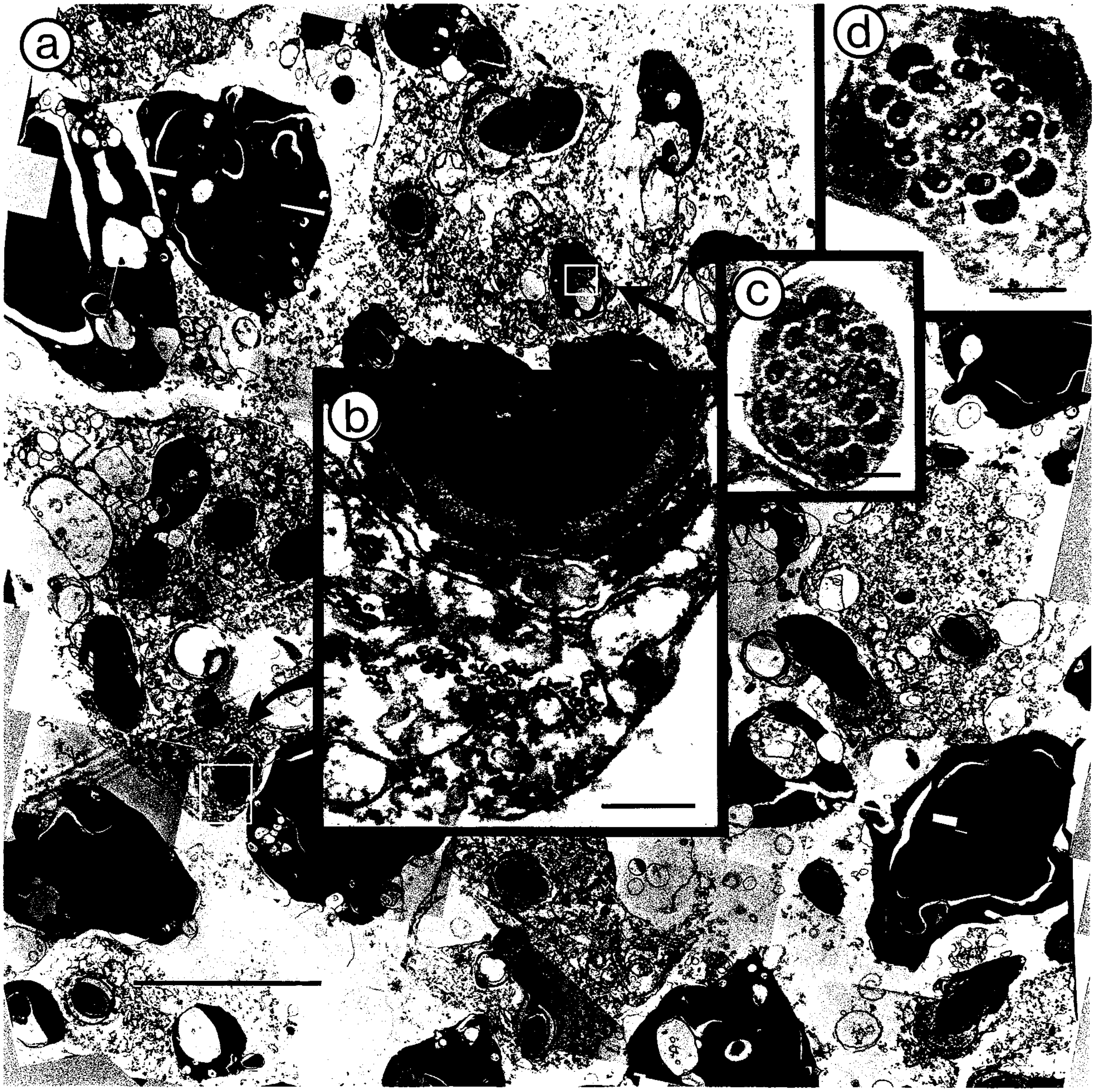
a
b
c
d

both orientations were present, microtubules were scored as "ambiguous". In order not to bias the scoring by excluding the heavily decorated microtubules, those with only second order hooks were assigned to a separate category of "clusters". In no case were more than 10% of the secondary hooks on clusters of a reverse orientation and therefore none were considered ambiguous.

Microtubule polarity: observations

In samples that included cold incubation (on ice), virtually all cytoplasmic microtubules were decorated. In contrast, the easily distinguishable manchette microtubules were rarely decorated and axonemes were never observed to be decorated with tubulin.

In samples with added tubulin, initially incubated on ice, microtubule decoration often consisted of elaborate clusters. In those without added tubulin, initially incubated on ice, decoration was less complex; however, the total number of microtubules was low. In samples not incubated on ice, without added tubulin, the total number of microtubules was higher, but the number that were decorated was low. In this group, although those that were decorated seldom possessed more than one hook, their orientation was the same as those with cold incubation. Under all incubation conditions, regardless of the microtubule density or complexity of hook formation (Fig. 4), the majority of decorated microtubules possessed hooks curving in the same direction, indicating uniform polarity. Similarly, variability in the extent and pattern of hook decoration has been reported in other studies (Heidemann et al., 1981).

Microtubule polarity: counts

Table II-I shows the scoring of microtubules in each montage assembled from rat seminiferous epithelium (montages 1-4). Ground squirrel Sertoli cells were also examined and decorated microtubule counts from a representative montage of seminiferous epithelium, from this animal, are included in Table II- I (montage 5).

Tab. II-I. Classification of microtubules according to hook decoration: cold/warm incubation.

Montage	Clockwise						Counterclockwise				Ambiguous
	Hooks					Clusters	Hooks			Clusters	Hooks
	1	2	3	4	5		1	2	3		
1	3	0	1	1	0	9	0	0	0	0	0
2	1	5	2	5	0	5	0	1	0	0	1
3	8	3	3	0	1	21	0	0	0	0	0
4	71	34	14	3	5	1	16	6	2	0	3
5	72	16	4	1	0	0	9	1	0	0	0

Orientation of decorated cytoplasmic microtubules in montages of seminiferous epithelium which was incubated in cold followed by warm lysis decoration buffer. Microtubules were viewed as though looking toward the apex of the Sertoli cell, scored for polarity, and classified according to the orientation and number of hooks formed. Values given indicate the number of microtubules decorated with clockwise, counterclockwise or ambiguous hook decoration. The maximum number of clockwise and counterclockwise open hooks that were observed to originate directly from a single microtubule, was 5 and 3 respectively, in these samples. Some microtubules were observed, in which no hooks arose directly from a single microtubule but formed an elaborate structure in which multiple open hooks of the same orientation arose from a microtubule bearing only closed hooks. These were scored as "clusters". Montages 1 to 4 are from rat, and montage 5 is from ground squirrel seminiferous epithelium.

Tab. II-II. Percent of microtubules with clockwise, counterclockwise and ambiguous hook decoration: cold/warm incubation.

	Clockwise		Counter clockwise		Ambiguous		Microtubules
Montage	Total	%	Total	%	Total	%	Total
1	14	100.0	0	0.0	0	0.0	14
2	18	90.0	1	5.0	1	5.0	20
3	36	100.0	0	0.0	0	0.0	36
4	128	83.0	24	15.0	3	2.0	155
Average		**93.3**		5.0		1.7	
5	93	90.3	10	9.7	0	0.0	103

The total and percent of microtubules decorated with hooks of clockwise, counterclockwise or ambiguous orientation for each montage scored in Table II-I. The average number of microtubules with hooks oriented in a clockwise direction for montages 1 to 4 is 93.3%. Counts from the ground squirrel epithelium are indicated in montage 5 for comparison.

Table II-II indicates the percentage of microtubules of each orientation, in each montage. These data indicate that between 83 and 100% of microtubules were oriented in the same direction, the average being 93.3%; that is, when viewed from the base to apex of the epithelium, an average of 93.3% of microtubules were oriented in a clockwise direction.

In addition, axonemes from the same field as these microtubules, show clockwise orientation of dynein arms. In order to pursue this point, axonemes were sought that were in clear cross section in, and surrounding, the area sampled for each montage and in many other samples observed. The orientation of dynein arms was found to be the same as hooks on surrounding cytoplasmic microtubules, in each case (see Figs 2-3 to - 2-8).

In the experiments in which exogenous tubulin was added without an initial incubation on ice, a similar variation in tissue appearance was noted. Using the same criteria as was used for in the cold incubation group (Tables II-II and II-II), four montages from the experiments using warm lysis/decoration buffer with added tubulin were scored for polarity (Tables II-III and II-IV). Microtubules were again found to be of uniform polarity and oriented with the minus-end directed toward the apex of the cell (Fig. 2-9).

Using this microtubule decoration technique, quantitative differences in the density of microtubules and the complexity of their decoration were seen. These differences depend on the area of sampling, incubation temperatures, and on the presence of exogenous compared with endogenous tubulin; however, in all cases, the qualitative findings do not vary. That is, most microtubule hooks are of the same orientation, indicating a uniform polarity. When cytoplasmic microtubules are observed from the base to the apical surface of the epithelium, hook decoration is in the clockwise direction, indicating that the minus ends of the cytoplasmic microtubules are directed toward the apex of the cell (Redenbach and Vogl, 1991). Additional experiments in which tissue was incubated directly in 35°C lysis decoration buffer, with exogenous tubulin, were found to have decorated microtubules in the extracellular space (Fig. 2-10), indicating that polymerization had occurred before tubulin was able to enter Sertoli cells. However, the microtubules were found to be oriented in a random manner, both outside and in some areas within the cell membrane (Fig 2-10). They could be distinguished from the highly ordered microtubules oriented parallel to one another and of uniform polarity. Furthermore, where the majority of microtubules were unipolar and oriented with the long axis of the cell, they were oriented, as had been found in all the other samples, with their minus-ends directed toward the apex of the cell. In view of the possible artifact of self polymerizing microtubules, no counts were made from this group.

Fig. 2-9. Montage of rat seminiferous epithelium incubated in warm lysis/decoration buffer.

(a) Micrograph of a portion of montage 9 (Tabs. II-III, -IV); rat seminiferous epithelium that was incubated in warm lysis/decoration buffer in the presence of exogenous tubulin. The field includes part of a lightly staining Sertoli cell which is flanked by darker staining germ cells (broad arrows). The tissue is viewed as though looking toward the apical surface of the cell. The clockwise orientation of hooks on cytoplasmic microtubules (long arrows) indicates that, in Sertoli cells, microtubules are oriented with their minus ends directed toward the apical surface of the cell.

(b) Higher magnification of decorated microtubules from tissue shown above.

bars: a = 0.5 μm, b = 0.1 μm.

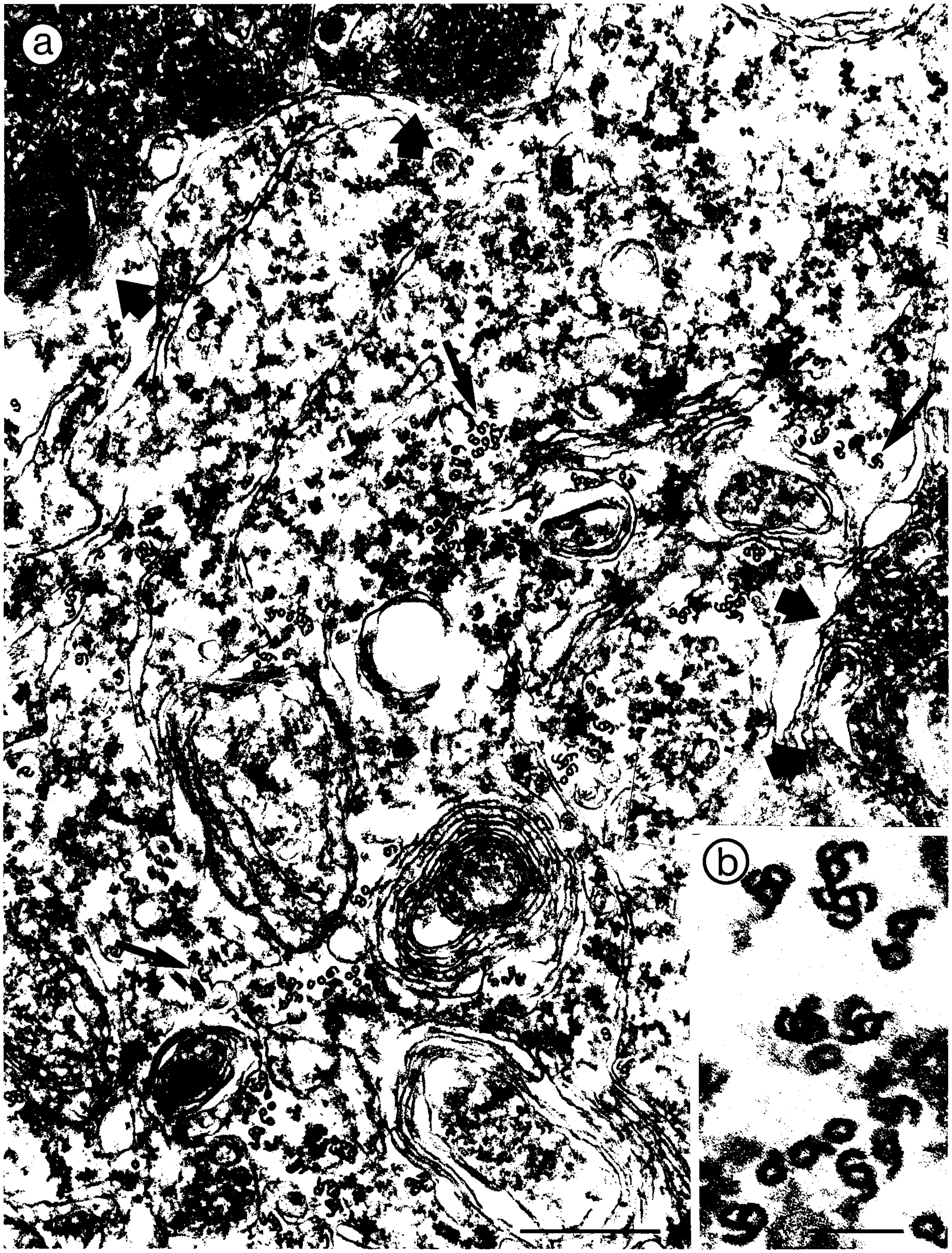
a
b

Tab. II-III. Classification of microtubules according to hook decoration: exogenous tubulin/warm incubation.

	Clockwise						Counterclockwise				Ambiguous
Montages	Hooks					Clusters	Hooks			Clusters	Hooks
	1	2	3	4	5		1	2	3		
6	25	13	10	0	1	0	0	2	0	0	0
7	9	7	1	0	1	0	0	0	0	0	0
8	11	15	5	3	0	0	0	0	0	0	0
9	17	9	9	2	0	1	2	0	0	0	0

Hook orientation of decorated cytoplasmic microtubules in montages of seminiferous epithelium which was incubated in warm lysis decoration buffer containing exogenous tubulin. As in Table II-I, microtubules are viewed as though looking toward the apex of the Sertoli cell, scored for polarity, and classified according to the orientation and number of hooks formed. These data are from montages from rat seminiferous epithelium.

Tab. II-IV. Percent of microtubules with clockwise, counterclockwise and ambiguous hook decoration: exogenous tubulin/warm incubation.

	Clockwise		Counter clockwise		Ambiguous		Microtubules
Montage	Total	%	Total	%	Total	%	Total
6	49	95.0	2	5.0	0	0	51
7	18	100.0	0	0	0	0	18
8	34	100.0	0	0	0	0	34
9	38	95.0	2	5.0	0	0	40
Average		97.5		2.5		0.0	

The total and percent of microtubules decorated with hooks of clockwise, counterclockwise or ambiguous orientation for each montage scored in Table II-III.

Figure 2-10: Microtubule decoration in seminiferous epithelium incubated immediately in lysis decoration buffer with exogenous tubulin at 35°C. Micrographs of seminiferous epithelium incubated at 35°C in lysis decoration buffer to which purified bovine brain tubulin was added immediately prior to incubation. There was evidence of polymerization and decoration of microtubules before entry to cells and of haphazard organization of microtubules within Sertoli cells, both considered to be due to self polymerization of exogenous tubulin.

(a)Base of Sertoli cell (broad arrow), extracellular matrix including collagen fibers (arrow heads), and myoid cells (asterisk). Decorated microtubules are seen in the extracellular matrix (short arrow), an artifactual location for microtubules.

(b) Close up view of decorated microtubules shown in (a). Collagen fibers of the extracellular matrix are seen. The same decorated microtubules are identified as in (a). Collagen fiber is identified with an arrowhead.

(c,d) Examples of haphazard orientation of microtubules found in Sertoli cells. These were not seen in Sertoli cells incubated initially on ice or at 22°C.

(e) Area of stalk of Sertoli cell, cut perpendicular to cell axis, observed from base to apex of the cell. In areas such as this, haphazardly organized microtubules are still present, but the majority of microtubules are caught in cross section and oriented in a clockwise direction, as shown here.

(f) Axoneme from same field as shown in (e).

bars: a = 1µm, b= 0.1µm, c= 1µm, d= 0.5µm , e= 0.2µm , f= 0.1µm.

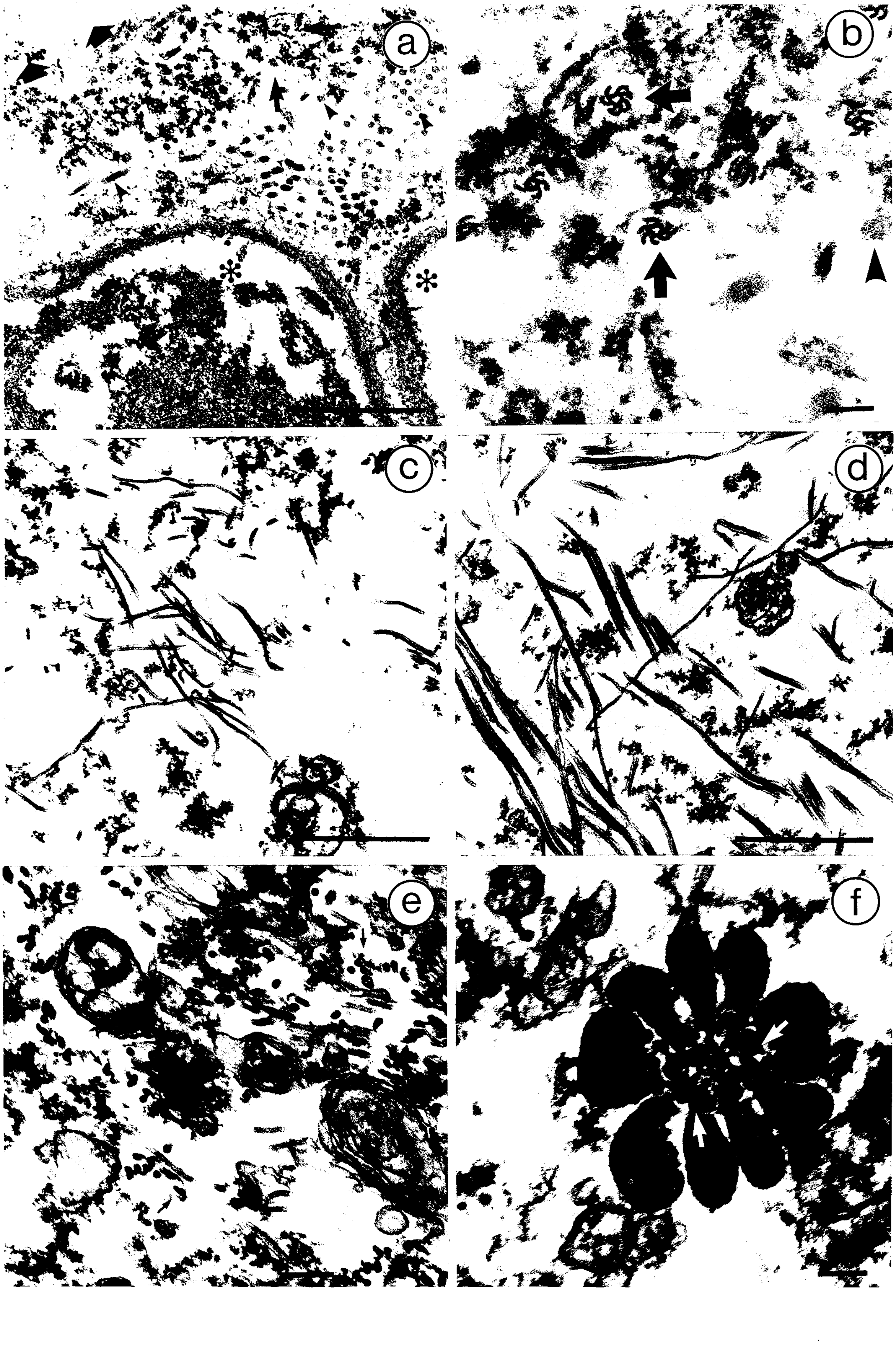
a
b
c
d
e
f

DISCUSSION

The specific findings of the microtubule polarity portion of this study are summarized in this section and conclusions drawn from the data are discussed. The implications of these findings and their relevance to the issue of microtubule-based spermatid translocation will be discussed more fully in chapter 4.

MICROTUBULE POLARITY IN SERTOLI CELLS

The results of this study lead to the conclusion that Sertoli cell microtubules are unipolar. Combining the counts from all montages from rat testis, an average of 95.4 % percent of Sertoli cell microtubules were oriented in one direction. This is well within the accepted range of reliability of microtubule polarity indicated by hook formation on microtubules of known polarity, a standard used to assert unipolar orientation of microtubules.

Sertoli cell microtubules are oriented with their minus-end directed toward the apical surface of the cell. Alternate L.M. and E.M. sections were used to monitor level of sampling within the apical portion of Sertoli cells and precautions were taken to ensure that section orientation was not lost during processing. The presence of sperm tail axonemes was used to verify the orientation of tissue sections, in most cases. When viewed from the base toward the tip of the spermatid tail, axonemal dynein arms are oriented in a clockwise direction. From that same perspective, viewing from the base to the apex of the epithelium, hooks on Sertoli cell microtubules form in a clockwise direction. The coexistence of clockwise oriented dynein arms, on sperm tail axonemes, and clockwise hook formation, on cytoplasmic microtubules, in the same sections, confirms the finding that the polarity of microtubules are oriented with their minus ends directed toward the apical surface of the cell.

The use of a number of modifications of the lysis/decoration parameters indicates that methods do not play a role in the quality of results reported here. The lysis/decoration buffer was variably disruptive of the tissue, both within and between samples. Nuclear decondensation occurred in some samples, as has been observed by others (Euteneuer and McIntosh, 1980). Because tissue preservation, as well as the complexity of hook decoration, varied with the depth of block sampled, it was clear that buffer penetration varied. In many samples, osmotic damage occurred in the form of selective condensation of germ cell cytoplasm. However, the latter feature facilitated counting of Sertoli cell microtubules. Regardless of the extent of tissue extraction or microtubule density, microtubule orientation was the same. The microtubule orientation in rat and squirrel testis were the same.

Hook formation was minimal on manchette microtubules and not seen on any of the sperm tail axonemes. The factors that are responsible for the remarkable stability of manchette and sperm tail axoneme microtubules may alter their potential to become decorated with the curved protofilament sheets. Manchette and sperm tail axoneme microtubules have been reported to contain detyrosinated and acetylated tubulins, while Sertoli cell cytoplasmic microtubules have been shown to be comprised exclusively of tyrosinated tubulins (Hermo et al., 1991). Detyrosination and acetylation are post translational modifications that occur in tubulins comprising more stable structures, but appear to be coincidental with microtubule longevity, rather than a cause of it. It may also be that hook formation is hindered by manchette MAPs and axonemal MAPs and associated structures.

In selecting the parameters of time and temperature, there was a trade off between the time required for tissue penetration and polymerization of exogenous tubulin. To confront the possible interpretation that cold incubation conditions resulted in preferential selection of a cold resistant population of microtubules, or alteration in polarity due to depolymerization and repolymerization, a number of preincubation and incubation temperature combinations were used. Initial preincubation conditions on ice or at 22°C were used to avoid self polymerization of exogenous tubulin, before it gained access to the Sertoli cell. To get a more complete picture, some of the experiments were carried out in which exogenous tubulin was omitted from the lysis/decoration buffer. This seemed reasonable because Sertoli cells have a very high concentration of microtubules, in most areas, and quite likely an adequate soluble tubulin pool, both of which may provide a source of tubulin for hook formation. The density of decorated microtubules was reduced following either with the use of cold preincubation or the omission of exogenous tubulin and were higher when preincubation was carried out at 22°C. Regardless of the incubation conditions used, the polarity indicated by hook decoration was the same.

To more closely approximate *in vivo* temperatures, experiments were also carried out using immediate incubation at 35°C. It was considered that if self polymerization of exogenous tubulin occurred, it would be with random polarity. Microtubules of haphazard orientation were seen in a supranuclear location of Sertoli cells when tissue was immediately incubated at 35°C, even though the tubulin was not added until immediately before incubation. Randomly oriented microtubules are not observed in the apical regions of Sertoli cells in control tissue. In addition, following the immediate warm incubation in lysis/decoration buffer with exogenous tubulin, decorated microtubules were observed in the interstitial space, decidedly an artifact. Counts were not made from tissue from experiments incubated immediately at 35°C. However, even in this group, microtubules from areas in which microtubules were largely parallel showed microtubule hook formation, consistent with the other data.

SUMMARY

In reviewing data from all of the experiments, the results consistently showed that Sertoli cell microtubules are oriented with the minus end directed toward the apical surface of the cell. Figure 2-11 illustrates these findings showing a Sertoli cell, with spermatids embedded in Sertoli cell crypts, sectioned in the apical portion of the cell, viewed from the base to the apex of the cell. The coexistence of clockwise oriented axoneme dynein arms and clockwise oriented cytoplasmic microtubule hooks is illustrated. The resulting model provides for cytoplasmic microtubules oriented with their minus-end directed toward the apex of the cell.

The implications of these findings are discussed in chapter 4.

Figure 2-11: Summary diagram of Sertoli cell microtubule polarity observations. This is a schematic summary of the results of hook formation following microtubule decoration of Sertoli cell microtubules. No attempt is made to represent a specific stage of the seminiferous epithelial cycle. **1.** A Sertoli cell as depicted in the model diagram sectioned to reveal a cross section of spermatids and surrounding microtubules. The resulting section (**2.**) shows the handedness of hook formation on decorated microtubules and the direction of axonemal dynein arms on axonemes. When the dynein arms are oriented in a clockwise direction, as shown, the section is being viewed from the base to the apical surface of the Sertoli cell, and microtubules are oriented with their minus-ends directed toward the apical surface of the cell.

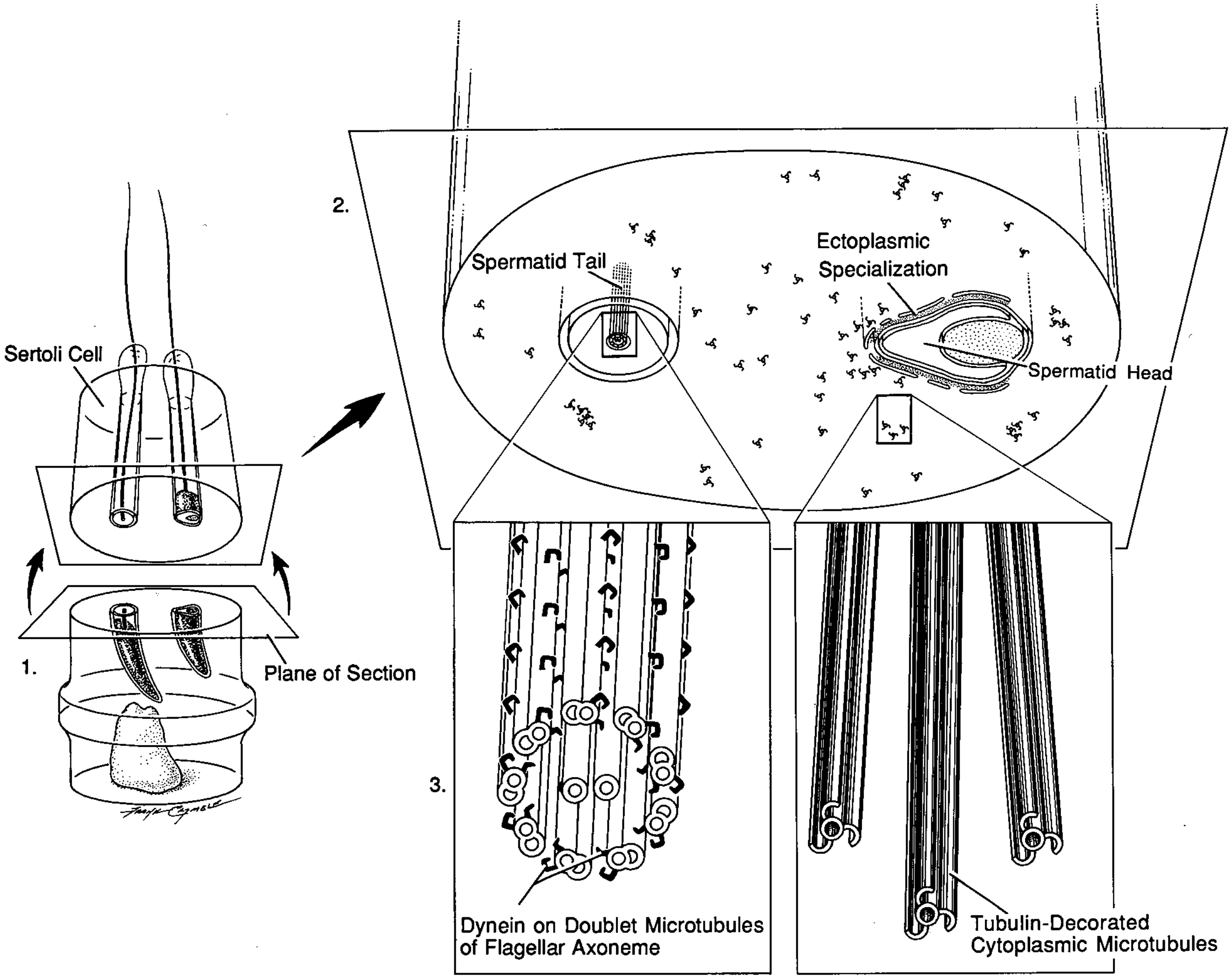
Sertoli Cell
1.
Plane of Section
2.
Spermatid Tail
Ectoplasmic Specialization
Spermatid Head
3.
Dynein on Doublet Microtubules of Flagellar Axoneme
Tubulin-Decorated Cytoplasmic Microtubules

CHAPTER 3

BINDING ASSAY

INTRODUCTION

The purpose of this section is first, to describe some of the methods used for the binding assay and second, to provide an outline for the approach used to answer the question: do microtubules bind to spermatid-ESs?.

BINDING ASSAY CRITERIA: COMPONENTS

Spermatid-ESs

It was necessary to develop a method for the isolation of spermatids, with their ESs consistently intact, in sufficient numbers for a binding assay. It has been shown that when spermatids are mechanically removed from the seminiferous epithelium, ESs remain intact and attached to isolated spermatids (Fig. 3:1 in Masri et al., 1987; Romrell and Ross, 1979; Fig 2 in Vogl et al., 1986; Grove and Vogl, 1989); that is, the spermatid with its membrane, the Sertoli cell membrane, the underlying actin network, and the ESER are stably linked and remain intact. This relationship is illustrated in Fig. 3-1. ESER has been shown to remain attached although it is subject to osmotic damage with some buffers. Isolation of Sertoli cell sheets in a PBS buffer (Vogl and Soucy, 1985), followed by pipetting to remove spermatids (Masri et al., 1987; Vogl et al., 1986; Grove and Vogl, 1989), used to investigate the molecular components of ESs, proved too vigorous for the ESER. The buffer did not protect the exposed ESER from osmotic effects. A more gentle isolation method was developed to ensure retention of ESs and buffer components adjusted to protect the ESER.

Following a method adapted from an earlier method of Perey and coworkers (1961) by Parvenen and Ruokonen (1982), individual seminiferous tubules were isolated and stages identified. Figure 3-2 illustrates this method of stage identification. Squashes were made from sections of the tubule to verify that spermatids could be expressed from all stages of the tubules using this method. The method of individual tubule isolation was then used throughout the binding assay, but sampling was not stage specific.

Figure 3-1: Isolation of spermatids-ESs from seminiferous epithelium with intact ESs: This diagram shows a spermatid situated in a Sertoli cell crypt that is lined with an ES. During spermatid isolation with a gentle squash technique, the spermatid is removed from the Sertoli cell carrying with it the ES: the Sertoli cell membrane, the intact actin filament network, and the ESER.

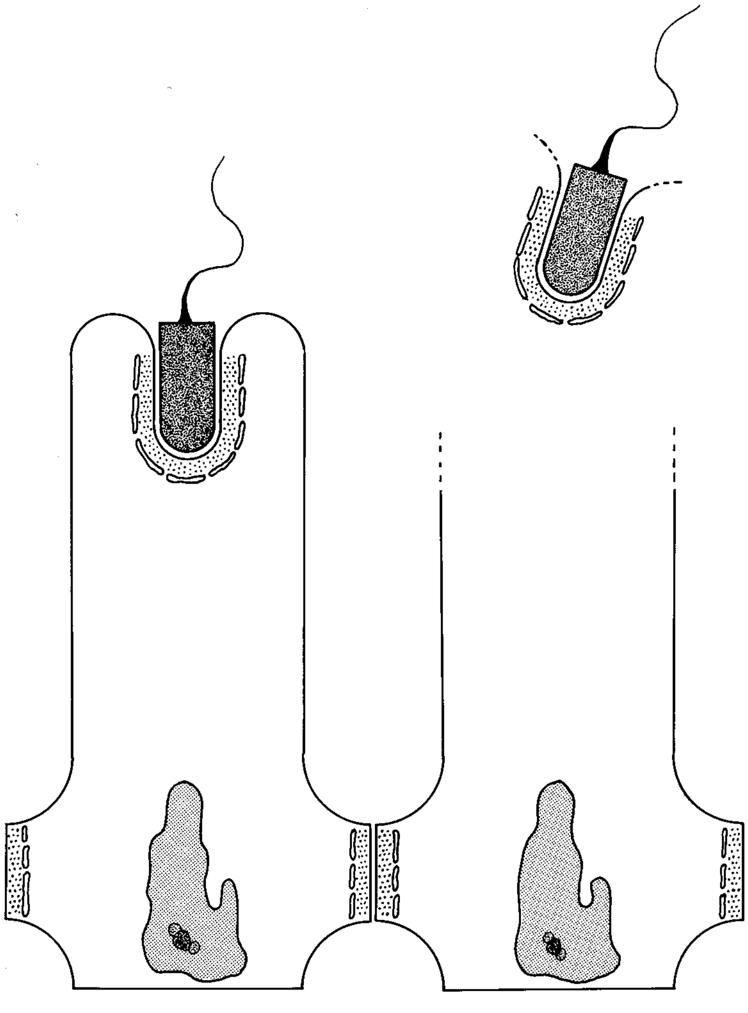

Figure 3-2: Transillumination methods of seminiferous cycle staging: This diagram shows the morphological criteria used to determine the stages in isolated single seminiferous tubules (adapted from Parvinen and Ruokonen, 1982). This method of identifying seminiferous epithelium stages in intact tubules allows for stage specific investigation of physiological and morphological events during spermatogenesis, and was used in this study to verify that spermatids could be recovered from all stages of spermatogenesis.

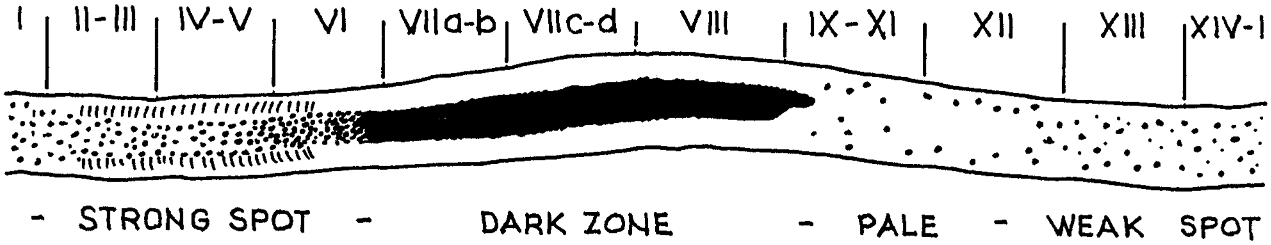
I
II-III
IV-V
VI
VIIa-b
VIIc-d
VIII
IX-XI
XII
XIII
XIV-1
- STRONG SPOT -
DARK ZONE
- PALE -
WEAK SPOT

Labelled microtubules

In preliminary studies, a 'topical' binding assay was developed. Isolated spermatids were allowed to adhere to a glass slide and then subjected to a number of binding conditions. The binding of exogenous microtubules and variety of MAP preparations to spermatids that had been adhered directly to glass slides was tested. Although some general trends could be seen, results were difficult to interpret and findings could not be quantified. It became apparent that to properly characterize spermatid-ES-microtubule binding, it was necessary to distinguish between the fate of added microtubules and endogenous microtubules that may have been retained either during isolation, from the treatment condition, or by nonspecific binding to the slide. A marker was needed to quantify binding, in order to demonstrate consistently when binding occurred and to characterize binding, in the presence of pharmacological agents that may potentially inhibit or enhance microtubule binding. To quantify spermatid-ES-microtubule binding, the measurement of labelled exogenous microtubules provided a means of 'ignoring' endogenous microtubules retained during isolation. Radiolabelled exogenous microtubules stabilized with taxol (^3MT_x) were used to provide a quantitative comparison of ^3MT_x-spermatid-ES binding under selected binding conditions.

BINDING ASSAY: ESTABLISHING THE CRITERIA

Development of the binding assay

An assay was developed in which spermatid-ESs were combined with ^3MT_xs and allowed to bind. In order to confine the measurement to bound microtubules, unbound microtubules had to be removed prior to counting. In order to measure microtubule binding to spermatid-ESs, after binding had occurred, it was necessary to separate spermatid-ESs from other cellular material that accompanied spermatid-ESs as they were isolated from the seminiferous tubule during the squash technique. Both of these requirements were addressed using centrifugation of the combined ^3MT_x and spermatid-

ESs, over a sucrose gradient, determining conditions that would enable the spermatid-ES, with their bound ^3MT_xs (^3MT_x - spermatid-ESs) to enter the gradient while ^3MT_xs alone did not.

Establishing that counts represented microtubules

It was necessary to show that label was incorporated, stably, into the exogenous microtubules, and that the label that become bound to spermatid-ESs was microtubule in origin. In this study, incorporation was measured by comparing counts before and after the removal of microtubules by centrifugation. It has been shown that microtubules, labelled by polymerization of purified tubulin in the presence of [^{3}H] GTP and taxol, remain stable (Wilson et al., 1985). Stoichiometric quantities of GTP are not required if microtubule assembly occurs in the presence of taxol. Stability was measured by comparing microtubule counts, pelleted from aliquots taken from the same stock, over time. The strategy, used to determine the proportion of counts that could be attributed to microtubule binding, was to remove microtubules from an aliquot of ^3MT_x stock and compare binding with and without microtubules.

CHARACTERISTICS OF BINDING

Reversal of binding.

Mechanoenzymes have ATPase activity and are removed from microtubules with nucleotides, ATP and GTP breaking kinesin-microtubule rigor bonds and ATP breaking cytoplasmic dynein-microtubule rigor bonds. Some of the putative motors are releasable with both GTP and ATP. Concentrations of ATP and GTP routinely used for release in MAP isolation, were used in this study.

Experiments to characterize ^3MT_x and spermatid-ESs binding

If binding could be demonstrated between ^3MT_x and spermatid-ESs, manipulation of binding, using conditions known to influence MAP-microtubule binding, could be used to characterize that binding. While there is a fair amount of information available about the ATPase activities and motility properties of the motor-microtubule site, less is known about its binding properties and even less is known about the binding at the motor organelle site (Brady and Pfister, 1991). In the absence of specific agents to test the nature of motor-microtubule binding, aside from nucleotide specificity, pharmacological agents that affect microtubule based motility, and mechanoenzyme ATPase activity were selected for these studies. Direct comparisons of binding, ATPase activity and motility are not valid. However, use of these agents provided some information as to the nature of the binding and a basis for comparison with other organelle-microtubule binding studies.

The concentrations of pharmacological agents were selected from a consensus of the levels that might distinguish between the two known families of motors. They included 2 mM NEM, 1mM EHNA, 10 and 100 μM vanadate, as well as 5 mM GTP and 10 mM MgATP. The effect of added Sertoli cell cytosol and rat testis MAPs were also tested.

LOCALIZATION OF LABEL

Morphological support for results of binding assay

In order for counts, in gradient fractions, to be considered representative of bound microtubules entering the gradient, it was necessary to determine if the binding occurred at ES sites. In that microtubules would be labelled with [^{3}H]-GTP, autoradiography of ^3MT_X combined with spermatid-ESs, was used to localize ^3MT_X - spermatid-ESs binding.

To examine the potential binding of microtubules at ESs, in this portion of the study:

1) A method was developed to isolate spermatids, with ESs attached, with a minimum of associated endogenous microtubules.

2) Microtubules were assembled from purified bovine brain tubulin, in the presence of [^{3}H]GTP and stabilized with taxol to be used as labelled exogenous

microtubules. The incorporation of label, stability, and length of the microtubules were checked.

3) Buffer conditions were defined to protect the ESER from osmotic effects and address the anticipated requirements for binding.

4) Differential centrifugation conditions were determined that met the criteria for measurement of exogenous microtubule binding to spermatid-ESs: enrichment for spermatid-ESs and separation of microtubules bound to spermatid-ESs from those that were not bound.

5) The validity of considering counts entering the gradient as microtubule binding was checked by determining the percent of counts that could be attributed to the microtubule component of ^3MT_X

6) ^3MT_X - spermatid-ES binding was quantified by counting the radiolabelled exogenous microtubules present with spermatid-ESs in the gradient fraction: binding assays.

7) The effect of nucleotides on ^3MT_X - spermatid-ES binding was examined for its potential as a tool to reverse binding.

8) ^3MT_X - spermatid-ES binding was characterized by imposing selected conditions including: the effect of varying substrate concentration; the possibility of turnover of binding; the effect of adding Sertoli cell cytosol or a cytoplasmic dynein enriched MAP preparation; and the effect of a selection of known mechanoenzyme inhibitors (10 mM MgATP, 5 mM GTP ± ATP depletion, 2 mM NEM, 1 mM EHNA, 1 mM AMPPNP, 10 μM vanadate, and 100 μM vanadate, and ATP depletion with 10 units/ml hexokinase with D glucose).

9) Label was localized by autoradiography, with and without the release of binding using 10 mM MgATP.

CALCIUM AS A PROPOSED REGULATOR

It has been proposed that the ESER may provide regulation of local events by selective uptake and release of calcium (Franchi and Camatini, 1985). Results of calcium localization studies in mouse (Kierszenbaum et al., 1971) and guinea pig testis (Franchi and Camatini, 1985) were contradictory. Mechanoenzymes are highly sensitive to calcium dependent proteases, released during tissue disruption, and therefore calcium is customarily removed from *in vitro* assays of cell motility by EGTA. Little is known about the effect of calcium on microtubule based transport. Microtubule based transport occurs in the presence of EGTA. To test the initial assumption, that calcium is sequestered by the ESER, the methods used for localization of calcium in mouse (Kierszenbaum et al., 1971) and guinea pig testis (Franchi and Camatini, 1985) were repeated in rat testis. In addition a number of other methods were used.

MATERIALS AND METHODS

MATERIALS

Animals

Rat testes used for the binding assay studies were from male Sprague Dawley rats, housed in animal care facilities at University of British Columbia or Brown University (Charles River CD). To ensure that all stages of spermatid development were well represented in tissue used in the binding assays, only mature rats of greater than 250 gms were used (Ekwall et al., 1984) for these experiments. Animals used for isolation of Sertoli cell cytosol and testis cytoplasmic dynein enriched MAP preparations were 21 days of age. Animals used in the binding assays were anesthetized with pentobarbital or killed with CO_2.

Chemicals and reagents

General

Unless otherwise indicated, all chemicals and reagents were obtained from Sigma chemical Co. (St. Louis Mo.). ^{3}H-GTP (NET-305 Guanosine 5'-triphosphate, tetrasodium salt, [8-5'-^{3}H] was from NEN Research Products Wilmington DE.

Buffers

A4M: 0.1 M MES (2[N-morpholino]ethane sulfonic acid), 1.0 mM EGTA (bis(ß-aminoethyl ether)-N,N^1-tetracetic acid), 0.5 mM $MgCl_2$, 4.0 M glycerol, pH 6.75. (plus protease inhibitors: 2 µg/ml leupeptin (4.2 µM), 0.1 mg/ml soybean trypsin inhibitor, and 0.2mM PMSF (phenyl-methylsulfonyl fluoride).

PEM: 0.1 M PIPES (piperazine-N, N-bis (2-ethane sulphonic acid), 1 mM $MgCl_2$, 1 mM EGTA, pH 6.9 (plus protease inhibitors: 10 μg/ml leupeptin, 0.5 μg/ml pepstatin,10 μg/ml soybean trypsin inhibitor and 0.5mM PMSF)

PEM 250: PEM with 250 mM sucrose (plus protease inhibitors 10μg/ml leupeptin, 0.5 μg/ml pepstatin, 10 μg/ml soybean trypsin inhibitor and 0.5 mM PMSF

PBS: phosphate buffered saline (0.15 M NaCl, 4.0 mM Na/K phosphate titrated to pH 7.3), 5 mM KCl).

MES: (0.1 M MES, 1 mM EGTA, 0.5 mM $MgCl_2$, 0.1 mM EDTA (ethylenediaminetetracetic acid), 1 mM MgATP and 20 μM taxol, pH 6.75) PIPES buffer -K:100 mM PIPES (titrated with KOH),1 mM EGTA, 1.0 M sucrose (or 250 mM if used in binding assay) plus protease inhibitors: 0.1 mg/ml soybean trypsin inhibitor, 2 μg/ml leupeptin, 2 μg/ml pepstatin

Primary antibodies:

5A6 monoclonal antibody to alpha tubulin and TuJ1 monoclonal antibody to beta tubulin were the generous gift of Dr. David L. Brown (Aitchison and Brown, 1986).

Secondary antibodies:

FITC - conjugated goat anti-mouse affinity purified IgG (Organon Teknika-Cappel, Malvern P.A.) was used as a secondary antibody to 5A6, and Tuj1. Mouse IgG, used in control, was purified from normal mouse serum (Sigma S3509) using an ImunoPure (G) IgG purification kit (PIERCE, Rockford Ill.).

Binding assay treatment reagents

AMPPNP: non hydrolyzable analogue of ATP (5'-adenylylimidodiphosphate)
Vanadate: sodium orthovanadate
EHNA: erythro-9-[3-(2-hydroxynonyl)] adenine
NEM: N-ethylmaleimide

Protease inhibitors were added to buffers from stocks, kept at -80°C. Concentrated PMSF in DMSO was added to buffer immediately before interacting with tissue by vigorous stiring.

METHODS

General protocols

Protein determinations

Protein concentrations were done by the methods of Lowry et al. (1951) or Bradford (1976) as indicated.

SDS PAGE gels

SDS PAGE gels were done according to Laemmli (1970), using 7% SDS PAGE minigels stained with Coomassie blue stain or 7.5% PhastGels (Phast Gel system Pharmacia LKB, Piscataway, N.J.), stained with silver stain (Phast gel method 3).

Isolation of ^{3}MTx - spermatid-ES binding assay components

Tubulin purification for binding assay

For this part of the study, tubulin was purified using a temperature dependent assembly, disassembly method using DEAE-Sephacel (Pharmacia) after the first temperature dependent cycle. This method provides equal purity but an improved yield over that used for microtubule decoration experiments described in chapter 2. Brains, from freshly killed steer, were placed immediately on ice and transported to the lab (approximately 20 minutes). Tissue was homogenized in a cold Waring blender in A4M buffer (75 ml/100 g of tissue) 2X for 15 seconds each at low speed and 30 seconds at high speed. Homogenate was centrifuged at 36,000 rpm (100,000 g), for 45 minutes, at 4°C, in 42.1 rotor. The crude supernatant was brought to 0.1 mM GTP and added to DEAE-Sephacel (1/2 original supernatant volume), which had been equilibrated with 1.0 M sodium glutamate, (pH 6.6) and mixed with DEAE-Sephacel by gentle rocking at 4°C for 45 minutes. It was then centrifuged at 2,800 rpm, for 2 minutes, in a IEC CRU 5000 centrifuge. The supernatant was discarded. The tubulin-bound Sephacel was washed by being resuspended in 1.0 M sodium glutamate with 0.1 mM GTP (pH 6.6), allowed to sit for 2 minutes, and respun at 2,800 rpm, for 2 minutes, all at 4°C. The wash step was repeated two more times, discarding the wash each time. Tubulin was then eluted from the Sephacel by incubating in 1/4 X original supernatant volume of 0.85 M NaCl with 1.0 M sodium glutamate and 0.1mM GTP (pH 6.6) for 20 minutes at 4°C. It was then spun at 2800 rpm, for 2 minutes in an IEC CRU 5000 centrifuge, at 4°C and collected eluate saved. The eluting proceedure was repeated 2 more times by gently resuspending the tubulin bound sephacel, incubating it for 10 minutes and spinning at 2800 rpm in IEC CRU 5000 centrifuge, for 2 minutes, each time saving the eluate. Excess Sephacel was centrifuged from the eluate. The eluate was brought to 1.0 mM GTP and the tubulin allowed to polymerize for 30 minutes at 37°C. The microtubules were centrifuged at 35,000 rpm (96,000g) at 37°C, for 30 minutes using a 42.1 rotor. The supernatant was discarded and the microtubule pellet resuspended and homogenized in 1/6 of original crude supernatant volume of 1.0 M sodium glutamate. The microtubules were depolymerized on ice for 30 minutes, centrifuged at 36,000 rpm (100,000 g), at 4°C, for 30 minutes, in 42.1 rotor. This "1X cycled" pure tubulin (MAP free) was either frozen in liquid nitrogen and stored at -80°C at this point (1X cycled tubulin), before the final recycle step, or recycled one more time before freezing (2X cycled tubulin). To recycle the1X tubulin, it was placed in 1M sodium glutamate with 1mM GTP, polymerized for 30 minutes at 37°C, centrifuged at 36,000 rpm (100,000 g), at 37°C, for 30 minutes, in 50Ti rotor. The pellet was resuspended and homogenized in small volume of PEM 250, depolymerized for 30 minutes on ice, and cleared at at 39,500 rpm (100,000g), at 4°C, for 30 minutes, using a 50 rotor. This purified "2X cycled" tubulin (MAP free) was aliquoted and frozen in liquid nitrogen, then stored at -80°C. Protein concentration was determined according to the method of Bradford.

Preparation of ^{3}HGTP labelled, taxol stabilized, microtubules (^3MT_x):

For the binding assays, 2X cycled tubulin was polymerized in the presence of ^{3}HGTP and taxol to produce labelled, stabilized microtubules as described by Wilson and co-workers (1985). All gradient solutions contained 20µM taxol to maintain microtubule stability in bound microtubules entering the gradient. Taking advantage of the fact that in the presence of taxol stoichiometric amounts of GTP are not required for polymerization (Vallee, 1982), a substoichiometeric amount of GTP (labelled plus unlabelled) was used to ensure complete incorporation of competent GTP into microtubules and therefore minimize the residual label left in solution. To label microtubules, ^{3}HGTP (1.0 µCi/50 µl of final microtubule solution) was included in the polymerization step (^3MT_x). MAP free microtubules were assembled by polymerization of purified bovine brain tubulin ([1X] = 1.6 mg/ml) at 37°C for 30 minutes in PEM 250 buffer, with 5 µM GTP, and 20 µM taxol (MT_x).

Length measurement of ^{3}HGTP labelled, taxol stabilized, microtubules (^3MT_x):

Microtubules, polymerized at 1X concentration (1.6mg/ml) in the presence of 20µM taxol and 5µM GTP, (as prepared for binding assays but without ^{3}HGTP label) were examined using negative stain electron microscopy techniques and microtubule lengths determined. Microtubules were placed on carbon coated EM grids, negatively stained with 1% aqueous uranyl acetate and observed using Phillips 300 EM at 60 kv. They were photographed, using Agfa plate film, and lengths were measured directly from the negatives. Using the negative, montages were formed, where necessary, to measure the longer microtubules. All microtubules, for which both ends were clearly visible, were measured in 14 fields, a total of 103 microtubules.

Spermatid-ES isolation

Figure 3-3 illustrates a 'poke and squash method' developed for isolation of spermatid-ESs. Testes were removed, decapsulated and placed in PEM 250 on ice. Seminiferous tubules were carefully teased apart to increase access of cold buffer. Under a dissecting microscope, approximately 15 mm lengths of individual seminiferous tubules were removed from the testis and placed on an ice cold glass slide. Care was taken to avoid overlap of tubules. The slide was replaced on ice frequently during the isolation to avoid having the spermatids warmed by the microscope lamp. Tubules were poked at approximately 3 mm intervals and covered with a glass coverslip. Spermatids were expressed from the tubules by very gently pressing the coverslip onto the slide (under direct observation of the dissecting scope). The coverslip was removed and, using fine forceps, all seminiferous tubules were removed from the slide and coverslip and discarded. Using a minimum of PEM 250 buffer, the remaining isolate was gently rinsed, from both the slide and coverslip, into a cold collecting container and kept cold until just before use. For stage specific isolation, the testis was incubated in PEM 250 with 2mg/ml collagenase for 3 minutes, teased gently apart, and rinsed in PEM 250, without collagenase, before isolating individual seminiferous tubules. Staging of seminiferous tubule seqments was done according to Parvinen and coworkers (Parvinen and Tapani-Perttula, 1972; Parvinen and Ruokonen,1982), as elaborated by Kangasneimi and coworkers (1990). A complete wave of seminiferous epithelium, from one dark zone-pale zone change-point to the next, was identified. The wave was cut into four segments, based on the transillumination pattern of pale zone (stages IX to XII), weak zone (XIII and I), strong spot zone (II to VI), and dark zone (VII and VIII). The segments were placed on a microscope slide, gently squashed, and immediately visualized by phase microscopy, to determine if spermatids could be recovered from all stages.

Figure 3-3. Spermatid-ESs isolation. Steps for spermatid-ESs isolation are indicated in the figure. The essential features of this isolation technique are 1) Tissue is kept cold at all steps, including being returned onto ice repeatedly while being handled on microscope, to encourage depolymerization of endogenous microtubules. 2) The seminiferous tubules are arranged on the slide such that they do not overlap, to ensure that pressure is applied evenly to the tubules. 3) Holes are poked in the seminiferous tubules to allow spermatids to exit all along the tubule, reducing the pressure required to get a good yield. This can be observed under the microscope. 4) Tissue is recovered from both the slide and the coverslip. 5) A minimum amount of buffer is used to rinse tissue from slide and coverslip, to discourage dilution of cytosolic factors. Spermatids are allowed to settle and the cold buffer is taken from the top for each rinse, to reduce the total amount of buffer added.

Spermatid - ES Isolation

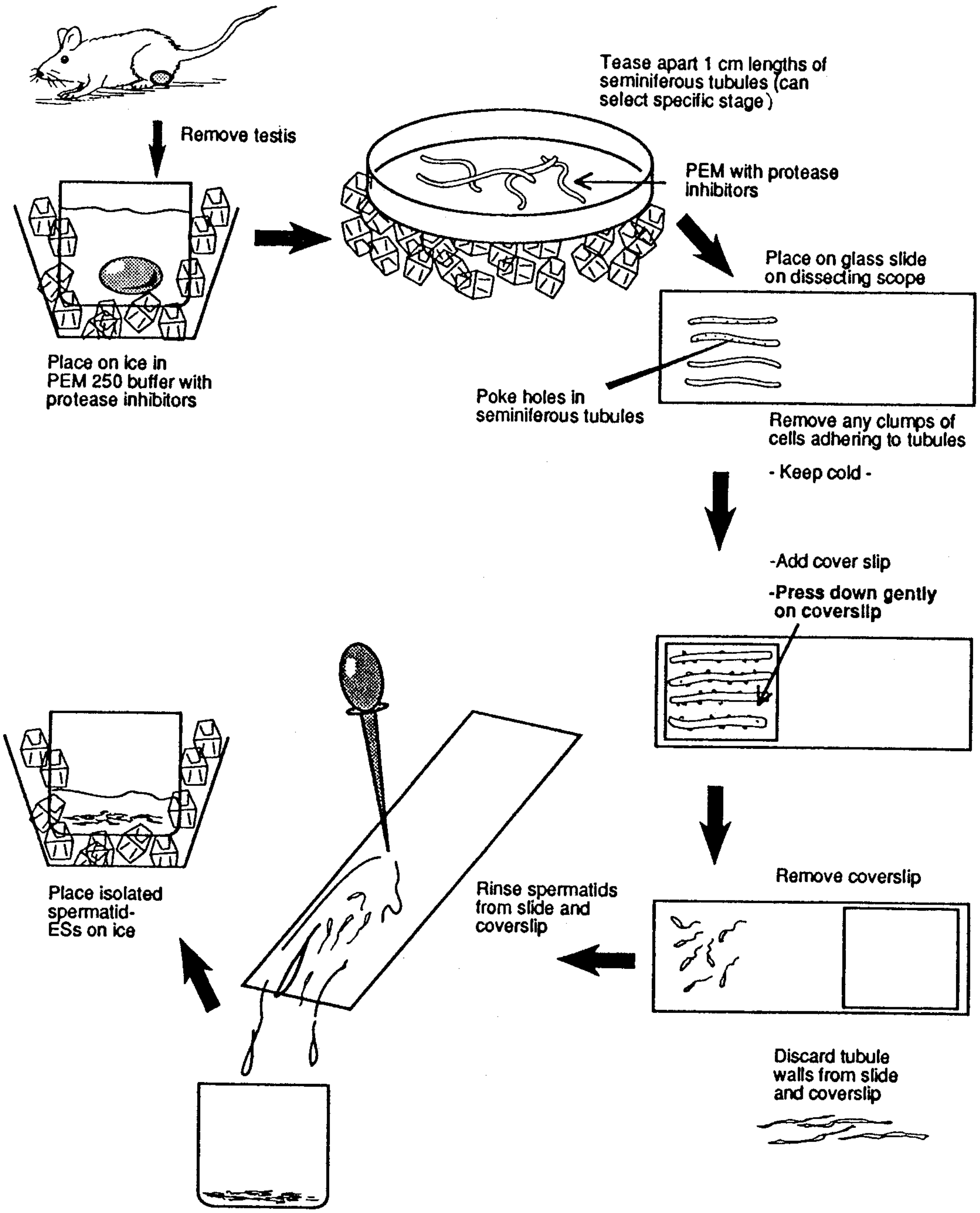
Remove testis
Place on ice in
PEM 250 buffer with
protease inhibitors
Tease apart 1 cm lengths of
seminiferous tubules (can
select specific stage)
PEM with protease
inhibitors
Place on glass slide
on dissecting scope
Poke holes in
seminiferous tubules
Remove any clumps of
cells adhering to tubules
- Keep cold -
-Add cover slip
-Press down gently
on coverslip
Remove coverslip
Discard tubule
walls from slide
and coverslip
Rinse spermatids
from slide and
coverslip
Place isolated
spermatid-
ESs on ice

Binding assay: preparation

Sample preparation for binding assay

Figure 3-4 illustrates the method used for the binding assays. Labelled and stabilized microtubules were prepared using 1 µCi/50 µl of tubulin (^3MT_X). Isolated spermatid-ESs were prepared under cold conditions and kept on ice. Spermatid-ESs were quickly brought to room temperature and combined with ^3MT_X, at a ratio of 1:2 (^3Mt_X:spermatid-ESs) (in most cases 50 µl:100 µl) and either used immediately (time=0) or allowed to incubate at room temperature for the duration indicated by the experiment. Samples made up in this way are referred to as '**no treatment controls**', serving as a basis for comparison with treated groups. To avoid dilution of sample or gradient solutions, all treatment solutions were added at 100X the final concentration, to both sample and gradient solutions.

Gradient preparation for binding assay

Gradients were prepared from stock solutions immediately before each spin. Stocks of 60, 45 or 30% sucrose in PEM buffer, with freshly added protease inhibitors and 20 µM taxol, were used for the gradients. Treatments, such as 10 mM MgATP that were added to samples, were also included in all levels of the gradient on which the treated sample was to be loaded, to prevent reversal of binding by dilution of the agent being tested. (Treatments with: added excess cold microtubules; dynein enriched MAPs; Sertoli cell cytosol, and different concentrations of MTs or supernatants, were not included in the gradients.) Each gradient consisted of 150 µl of PEM60%, 200 µl PEM45%, 200 µl PEM30%, layered from bottom to top. Gradients were loaded with 150 µl of sample: 50 µl ^3MT_X +100 µl spermatid-ESs (exceptions are noted).

Figure 3-4. Binding assay: methods: This figure illustrates the method used for running binding assays. Labelled microtubules (^3MT_Xs) are assembled by adding tritium labelled GTP (^3HGTP) at 1 µci/50 µl tubulin stock, to tubulin in PEM250 plus taxol and GTP buffer, and polymerized for 30 minutes at 37°C. Spermatid-ESs, are quickly warmed to room temperature and immediately combined with ^3MT_Xs at 50 µl ^3MT_X for each 100 µl of spermatid-ES preparation. Gradients are assembled immediately prior to the spin for which they are to be used. If the tissue is to be treated, treatment agent is added (from 100X concentration stock) to each sucrose stock for those gradients. Gradient levels are marked with an indelible pen (that will not bleed color into the scintillation fluid) after the application of each level of sucrose, to provide markers for accurate cutting of the gradient after freezing. The spermatid-ES + ^3MT_X mixture is loaded onto the sucrose gradient (150 µl/ gradient). The gradients are centrifuged in a Beckman SW 65 rotor (3 bucket rotor), for 5 minutes, at room temperature (the spin conditions must be verified for the centrifuge used). Gradients are removed from the rotor, inspected, and immediately frozen at -70°C. The frozen gradients are cut as shown in the figure, midway between sample/30% and 30/45%, and between 30/45 and 45/60% interfaces. 4.5 mls of scintillation fluid (plus 500µl dH_2O/sample) are added to each sample and counts/minute determined. Combined counts from the 30/45%, and 30/45 and 45/60% gradient fractions are expressed as a percent of the total count.

Binding Assay

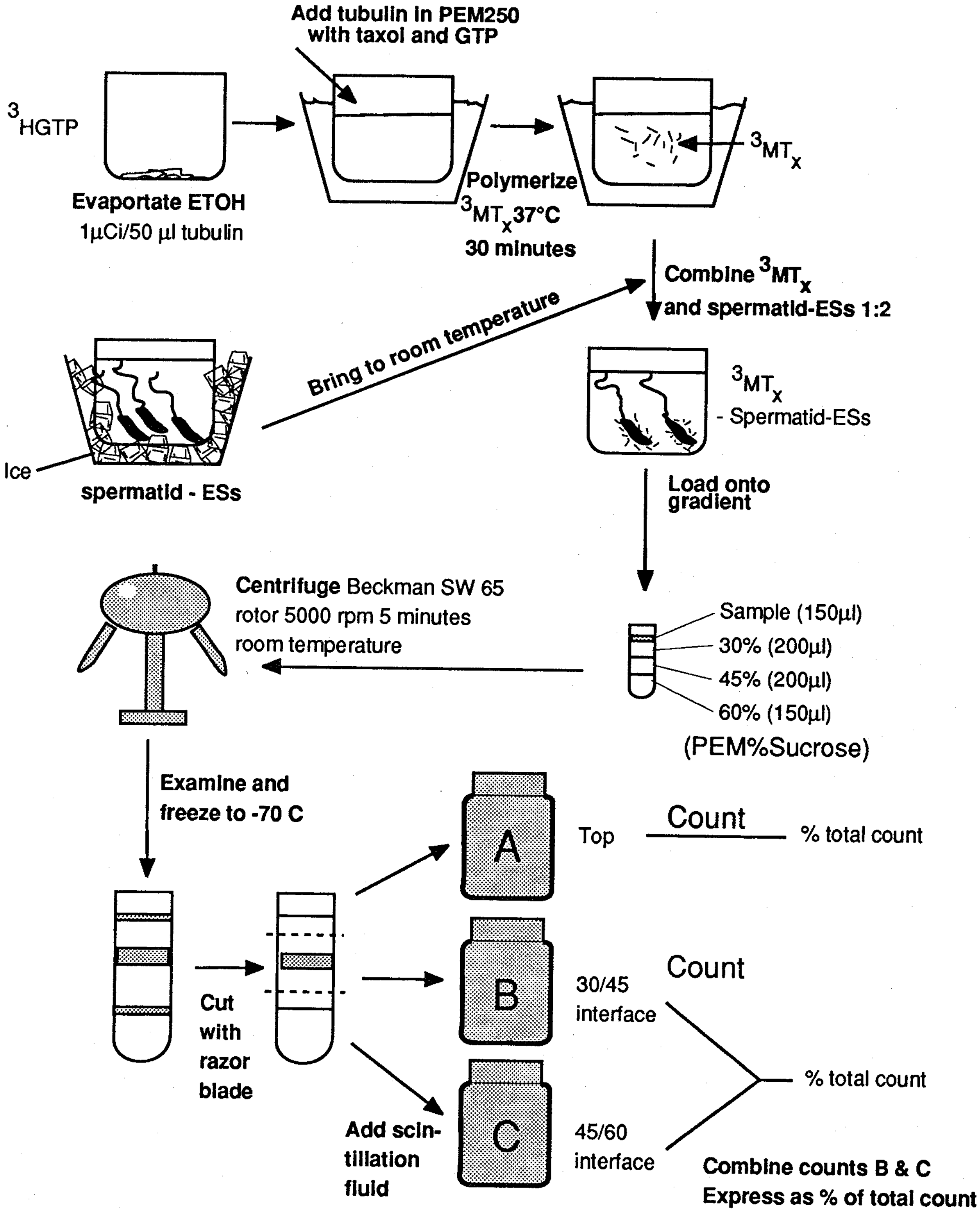
Add tubulin in PEM250
with taxol and GTP
^{3}HGTP
Evaportate ETOH
1μCi/50 μl tubulin
Polymerize
^{3}MT$_x$ 37°C
30 minutes
^{3}MT$_x$
Combine ^{3}MT$_x$
and spermatid-ESs 1:2
Bring to room temperature
Ice
spermatid - ESs
^{3}MT$_x$
- Spermatid-ESs
Load onto gradient
Centrifuge Beckman SW 65
rotor 5000 rpm 5 minutes
room temperature
Sample (150μl)
30% (200μl)
45% (200μl)
60% (150μl)
(PEM%Sucrose)
Examine and
freeze to -70 C
Cut
with
razor
blade
Add scin-
tillation
fluid
A
Top
Count
% total count
B
30/45
interface
Count
C
45/60
interface
% total count
Combine counts B & C
Express as % of total count

Binding assay: methods

Running the binding assays

The time required for isolation of fresh spermatid-ESs was a limiting factor on the volume of sample that could be used in the binding assays. The SW 65 rotor (Beckman), with #356860 adaptors, provided the ideal volume (800 µl capacity) for the gradients. Because preliminary experiments indicated that it was imperative that centrifuge conditions were constant from spin to spin, the same ultracentrifuge (Beckman L7-55) and rotor (Beckman SW 65) were used for all binding assays. A defined proceedure for ultracentrifugation was followed, duplicating the rate of acceleration, timing by use of "hold" option, precise duration of spin (verified by revolutions on meter), and rate of deceleration.

Use of the SW 65 rotor (with 3 buckets) dictated that only three experimental conditions could be included in any spin, one being the 'no treatment control' that served as a basis of comparison for other conditions in any given spin. Gradients were prepared immediately before each spin. 150 µl of sample were loaded onto the sucrose gradients, spun at 5000 rpm, for 5 minutes, at 22°C. The gradients were inspected and immediately frozen to -80°C. A number of techniques that potentially could introduce error such as: methods of sampling from gradients, effects of freezing, means used to standardize the spin conditions, and effect of gradient solutions on scintillation fluid, were checked.

Binding assays: experimental design

Design of binding assay experiments (general)

Experiments were designed around the constraints of 3 gradients/spin. Consideration was given to an apparent time course of binding and different effects of adding treatments before or after binding was established. In general, three conditions, one being the 'no treatment control' and the other two being treatment conditions, were repeated throughout the entire experiment (see Figs. 3-17 and 3-18 for an example of a short experiment employing the general design). A 'no treatment control' was included in every spin, unless the effect of a second treatment was imposed simultaneously on 'no treatment' and the other two treated samples in the same spin (for example, 10 mM ATP effect on 'no treatment control, 10 μM vanadate and 100 μM vanadate). In that case, the 'no treatment control' value was extrapolated from the 'no treatment control' values of the previous and subsequent spins. This experimental design was used to test 10 mM MgATP, 2 mM NEM, 1 mM EHNA, 1 mM AMPPNP, 5 mM GTP (with and without ATP depletion), 10 and 100 μM vanadate, ATP depletion with 18units/ml hexokinase and D glucose, cold 5X [MT_x] competition (or microtubule depleted supernatant), 1X [^3MT_x] supernatant, Sertoli cell cytosol and cytoplasmic dynein enriched testis MAP preparation. Spins to test the effect of 10 mM MgATP on all these conditions were included.

Experiments for which total sample added to gradients was not 150 μl

In experiments in which treatment material could not be added at 100X concentration (for example, competition with the addition of 5X cold microtubules) total volume of sample was greater than 150 μl. The effect of dilution, by the treatment material, was controlled for by the addition of equal amounts of buffer to the 'no treatment control'.

Direct effect of treatments on microtubules

To rule out the possibility that treatments influenced binding by a direct affect on microtubules, each treatment was added directly to aliquots of polymerized microtubules. Treated microtubules were pelleted in a Beckman airfuge and the microtubule mass in the pellet compared with 'no treatment' microtubules to look for any direct effects of treatments on microtubules.

Design of matched experiments

A series of experiments were designed to look at the effects of a number of binding inhibitors on early and established binding, matching as closely as possible for time and spermatid-ES and microtubule concentration. They were carried out with a first series of spins using samples to which treatments had been added before binding was begun (early binding) followed by a second series using samples treated at least 2 hours after binding had begun (established binding). This was achieved by dividing each of the $^{3}MT_{X}$ stock and the isolated spermatid-ES stock in half. For "early binding", treatments were added to the aliquot of spermatid-ESs and then combined with the $^{3}MT_{X}$. This was time = 0. For the second series, "established binding", the $^{3}MT_{X}$ and spermatid-ES samples were combined at time = 0, but treatments were not added until after the first series of spins were complete, that is at the end of the "early binding" runs. For both the early binding and established binding series, the first gradient was prepared immediately before treatments were added so that data from the first spins could capture the earliest possible effects of treatment. The effect of 10 mM MgATP was tested in each group. For this series of matched experiments, the microtubule concentration was 0.5X.

Design of [MT] experiment

Figure 3-5 shows the design of the microtubule concentration experiment. To test the MT concentration effect on ^{3}MT - spermatid-ES binding, a stock of $^{3}MT_{X}$ was assembled at 10X tubulin concentration (1X[^{3}MT= 1.6mg/ml, ie 0.53 mg/ml in final assay sample). Stocks of 0.1X, 0.25X, 0.5X, 1.0X, 3.0X, and 10X [$^{3}MT_{X}$] were diluted from the 10X [$^{3}MT_{X}$] stock. Polymerization was done before dilution as polymerization properties depend on tubulin concentration.

Figure 3-5. Microtubule concentration experiment: strategy: This figure shows the design of the microtubule concentration experiment. Three things were determined: 1) the effect of microtubule concentration [T] on ^3MT_X-spermatid-ES binding (binding assay); 2) the reliability of the assumed tubulin concentrations (concentration assay); and 3) any loss of counts from pelleted microtubules between spin 1 and 6 (cycling of label)(stability of label). Tubulin was polymerized at 10 X concentration and all dilutions made from that stock (hence data expressed in absolute counts). [T]= tubulin concentration in microtubule samples. The binding assay was carried out as described earlier, using the tubulin from each of tubulin concentration stocks with a 1 X sample included in every spin to act as the control. For the concentration assay, counts and tubulin concentrations were determined directly from tubulin concentration stocks, verifying that assumed dilutions were reliable. To test the stability of label, samples from each tubulin stock was tested, timed to coincide with spins 1 and 6. At each time period, three samples from each stock were spun over 15% PEM sucrose cushions, in a Beckman airfuge, at maximum speed, for 30 minutes. From these airfuge spins, counts of pelleted microtubules were determined as shown. Pelleted microtubule counts showed that counts pelleted from the samples did not change during the experiment; label does not cycle from the taxol polymerized microtubules.

Figure 3-5: Microtubule concentration experiment

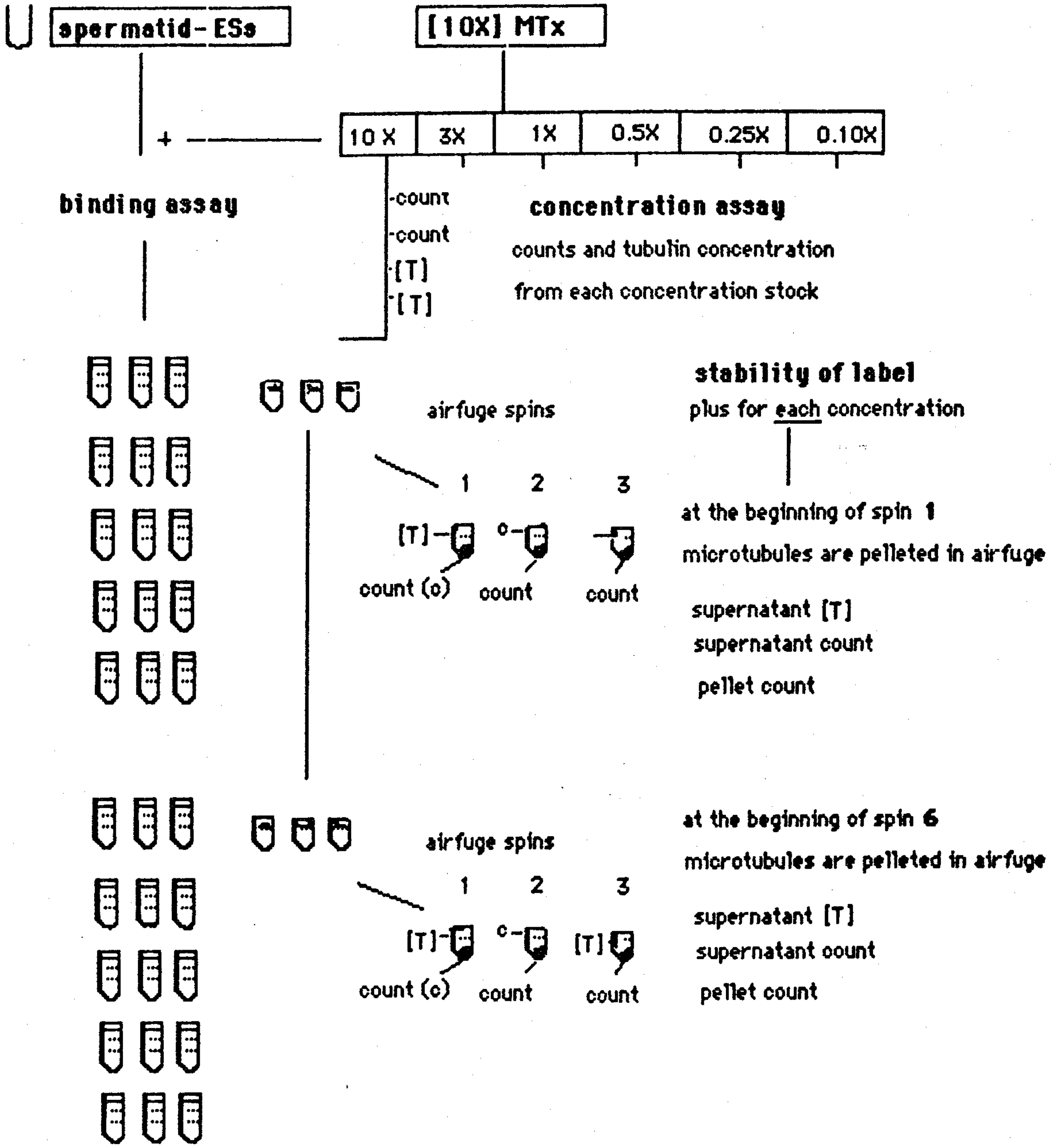
spermatid-ESs
[10X] MTx
+
10X
3X
1X
0.5X
0.25X
0.10X
binding assay
-count
-count
-[T]
-[T]
concentration assay
counts and tubulin concentration
from each concentration stock
stability of label
plus for each concentration
airfuge spins
1
2
3
[T]
c
count (c)
count
count
at the beginning of spin 1
microtubules are pelleted in airfuge
supernatant [T]
supernatant count
pellet count
airfuge spins
1
2
3
[T]
c
[T]
count (c)
count
count
at the beginning of spin 6
microtubules are pelleted in airfuge
supernatant [T]
supernatant count
pellet count

Samples from each concentration stock were used in two ways: 1)binding assays were done to test the effect of MT concentration on ^3MT_X-spermatid-ES binding, and 2) tubulin concentration and MT incorporation assays were run, concurrently with the binding assays, to verify tubulin concentration and label stability (Fig. 3-5).

1) Binding assays: Samples from each of the 0.1, 0.25, 0.5, 3X and 10X ^3MT concentrations were added to the spermatid ESs. The resulting ^3MT - spermatid-ESs were allowed to bind for 1.5 hrs (established binding) and tested for binding on sucrose gradients. Samples from each [^3MT] were loaded onto the gradients four times in varied order, except the 1X [^3MT_X] - spermatid-ES sample which served as the 'no treatment control' for each of the ten spins.

2) Protein concentration and label incorporation: For this part of the experiment, MT protein concentrations were determined (Bradford) and scintillation counts made from each ^{3} MT_X stock. This allowed the comparison between the number of counts in samples loaded in each of the binding assays with the number of counts in samples directly aliquoted from the stock, to verify the tubulin concentration in each stock. To test for possible cycling of microtubules over the time period of the experiment, and therefore loss of label, three samples were taken to coincide with the beginning of the binding assay spins and three more to coincide with the midpoint of the binding assay spins. In each case, 50 µl of sample was pelleted over a 125 µl cushion of 15% sucrose in PEM in a Beckman airfuge, at full speed (130,000 to 150,000 rpm), for 20 minutes. Percent incorporation of tubulin into microtubules was determined for each sample and total counts were done for each of the six samples at each concentration. The counts and protein checks verified that the measured protein concentrations of the samples were consistent with the assumed concentration for the binding assays,(0.1X - 10 X), that the percent incorporation into pellets was essentially the same at all ^3MT_X concentrations, and that there was no turnover in the microtubules, ie, the label did not cycle out of the pellet during the experiment.

Topical binding assay

In preliminary experiments, an attempt was made to carry out the binding assay directly on acid cleaned, polylsysine coated glass slides, evaluating binding by the presence of antitubulin staining on spermatid heads. Spermatid-ESs were isolated at the selected temperature and then spun through a cushion of 30% sucrose in a Beckman airfuge at maximum speed for 3 minutes. The isolated spermatid-ESs were collected from the bottom of the tube, placed on glass slides, and allowed to settle for fifteen minutes. Spermatid-ESs were then reacted with microtubules directly on the slide, using a variety of conditions and temperatures. While some trends were observed with these assays, they were replaced with the radiolabelled technique for three reasons. 1) To show that binding occurs, it was deemed necessary to demonstrate that exogenous microtubules (labelled in the gradient assays) could be bound. The topical assays did not distinguish between exogenous and endogenous microtubules. 2) Because microtubules attached to slides, their presence could not unambiguously be interpreted as binding. 3) The radiolabelled gradient assays could be quantified.

Preparation of treatment materials used in binding assays

Isolation of rat testis crude supernatant for cytoplasmic dynein enriched MAP preparation

Rat testis crude supernatant and cytoplasmic dynein enriched MAPs were prepared after the method of Neely and Boekelheide (1988). Testes were removed, from 25 CO_2 killed rats (21 days of age), decapsulated, and put immediately into iced A4M buffer with protease inhibitors (see *buffers*). Testes were homogenized using Dounce homogenizer at 1300 rpm (3-5 times up and down) with 1:1 buffer:testis by wt (yield SN volume about 40 mls). The resulting homogenate was spun at 36,000 rpm (100,000g) at 4°C, for 30 min, in a 42.1 rotor. The supernatant was frozen in liquid nitrogen and stored at -80°C until required for cytoplasmic dynein enriched MAP preparation.

Isolation of cytoplasmic dynein enriched MAP preparation from crude supernatant

Crude supernatant from rat testes (42 mls) was thawed and cleared by centrifugation at 40,000 rpm (130,000g), at 4°C, for 45 minutes, in a 42.1 rotor. The supernatant was brought to 20 μM taxol and underlayed with 25% sucrose in MES buffer (see *buffers*) using an 18 g needle. The supernatant was incubated for 10 minutes at 37°C to initiate the tubulin polymerization, then returned to ice for a further 20 minutes. (Microtubule polymerization is stablilzed from this point on by 20 μM taxol). Microtubules were pelleted at 36,000 rpm (100,000g) at 4°C, for 30 minutes in 42.1 rotor. The pellet was resuspend in MES buffer plus 20μM taxol (about 1/10 vol of testes homogenate), gently homogenized and placed on ice for 5 minutes. Microtubules were again pelleted at 36,000 rpm, at 4°C, for 30 minutes in a 50 rotor (75,000 g). The pellet was resuspended (in same vol about 1/20 original testis vol) in MES buffer with 20μM taxol, and 5 mM GTP and 5 mM $MgCl_2$, homogenized gently, and allowed to sit at room temperature for 10 minutes. After a further 5 minute incubation at 37°C, it was spun at 36000 rpm, (90,000 g) at 29°C , for 30 minutes with type 50 Ti rotor. The pellet was resuspended in 1/20 volume of MES buffer with 20 μM taxol, 1mM GTP, 1 mM $MgCl_2$ and 1 mM ATP, gently homogenized, and allowed to sit for 10 minutes at room temperature and then for 5 minutes at 37°C. It was again spun for 36,000 rpm, (90,000 g) at 29°C , for 30 minutes with type 50 Ti rotor. MAPS were eluted from the microtubules by resuspending the pellet in MES buffer (1/20 of original supernatant volume) with 20 μM taxol, 1 mM GTP and 10 mM $MgCl_2$ and 10 mM ATP. Following gentle homogenization, microtubules were incubated for 15 minutes at room temperature, then10 minutes at 37°C, and spun for 30 minutes at 29°C at 36000 rpm, in a 50 Ti rotor. This supernatant contained ATP eluted cytoplasmic dynein (HMW2) enriched rat testis MAPs. The cytoplasmic dynein enriched MAP fraction was salt eluted on exocellulose GF5 40-100 μM desalting gel (Pierce) at 4°C into PEM 250 and used for binding assays immediately after being removed from the column (concentration = 210 μg/ml). For binding assays, cytoplasmic dynein (HMW2) enriched rat testis MAPs were loaded at 1/100 dilution final concentration = 2.1μg/ml sample. This HMW2 MAP enriched preparation (considered to be MAP 1C or cytoplasmic dynein) has been shown to be present, independent of the development of mature germ cells, and is considered to be of Sertoli cell origin, as it was present in Sertoli cell enriched preparations from two rat models of germ cell depleted testes (Neely and Boekelheide, 1988).

Sertoli Cell enriched isolation from 21 day old rats

Testes were removed from 21 day old rats, immediately placed into CMF Hanks (Hanks balanced salt solution: calcium and magnesium free), and washed 3X with sterile CMF Hanks. Testes were then decapsulated and moved into fresh CMF Hanks, and minced. Testes pieces were transfered to a solution of: 1.9 ml 40X trypsin, 0.5 mg DNase I, and 48.1 ml CMF Hanks and incubated for 30 min at 32.5°C on a rotating table at 150 rpm, with occasional added swirling. Tissue was poured into a 50 ml centrifuge tube and allowed to sediment for 5 min. The supernatant was discarded. 20 ml HBSS were added to the tubules, which were then pipetted 10-15 times with a 10 cc pipette and allowed to sediment for 5 minutes. The supernatant was removed. The pelleted tubule fragments were added to 35 ml of CMF Hanks with; 45mg collagenase, 0.6mg DNase I, and 30 mg hyaluronidase. The fragments were incubated for 60 min at 32.5°C, rotating at 150 rpm with occasional swirling, then poured into a 50 ml centrifuge tube and spun at 1000 rpm in a clinical centrifuge for 3 minutes. The supernatant was removed and 0.1% soybean trypsin inhibitor added to the pellet 0.35ml in 35ml DMEM/F12 (pen/strep, gent., L- glutamine). The cells were pipetted 10-15 times with a 10cc pipette to break up the pellet, and spun down at 1000 rpm for 3 minutes. The supernatant was discarded and the cells resuspend in 20ml F12/DMEM (pen/strep, gent., L- glutamine). Cells were pipetted 10 times to break up any cell clumps.

Preparation of cytosol: Sertoli cell enriched preparation from 21 day rat testis

Sertoli cells, isolated from 21 day old rats as described above, were washed once in 20 mM HEPES-KOH, 1mM EDTA, 1 mM $MgCl_2$ pH 7.4 and resedimented by centrifuging at 1000 g for 5 min. The supernatant was removed and 1 volume of 100 mM PIPES-K, 250 mM sucrose with protease inhibitors pH 6.9 was added. The cells were homogenized using a Dounce homogenizer and centrifuged for 10 min at 43,000g at 4°C. The supernatant was collected and recentrifuged, at 50,000 rpm (150,000g), at 4°C, for 90 minutes in a 50 Ti rotor, to obtain the Sertoli cell enriched cytosolic extract. The extract was frozen in liquid nitrogen and stored at -80°C. 10μl PMSF (from100 mM stock) per ml buffer was added just prior to use.

Data collection for binding assays

Frozen gradients were cut into three fractions with a razor blade as shown in Fig. 3-4. Each fraction was place in a scintillation vial, mixed with 500 μl of deionized water and 4.5 mls of scintillation fluid (Optifluor: Packard) mixed well until clear, allowed to settle, and counted. Counts were always very low in the 45/60 fraction compared with the 30/45 fraction. Any changes in that trend could be traced back to faults in gradient assembly. Because this pattern was consistent and no differences in cell content were noted between the fractions, data from the 30/45 and 45/60 fractions were combined for analysis. Data from any gradients in which the appearance of inspected gradients, spin duration, control values, or counts loaded, cast doubt on the spin were not included.

Total counts loaded onto gradients were consistent throughout any given experiment, indicating that sample did not change over time. Variability of counts in gradient fractions for 'no treatment controls' was low within any experiment. However, there were differences in 'no treatment counts' between experiments. Counts are expressed as a percent of the same spin 'no treatment control', thereby reducing the effects of between experiment variability.

Sucrose concentration was determined to have no effect on the scintillation fluid. Repeat counts in a second counter or in the same counter after a period of 12 hrs, indicated that there were no spurious effects of chemiluminesence or counter efficiency.

Data analysis

For the determination of significant main effects of experimental treatments, data was analyzed by analysis of variance (ANOVA); significance at $P < 0.05$. Where ANOVA showed significant main effects, Tukey's paired tests were used for between group comparisons.

Immunohistochemistry

Immunofluoresence: sample preparation and microscopy (5A6: anti-tubulin).

Spermatid isolate was adhered to acid-cleaned polylysine coated glass slides. It was then fixed in 3.7% paraformaldehyde in PEM 250 for 10 min, rinsed 3 times, 5 minutes each, in PEM 250 and plunged into -20°C acetone for 5 minutes. Slides were left to airdry briefly after which tissue was rehydrated with 0.1% BSA/PBS for 5 minutes. Non-specific sites were blocked with 5% normal goat serum in 0.1% BSA/PBS for 30 min. Tissue was incubated with primary antibody (diluted in 0.1% BSA/PBS with1 % normal goat serum) for 60 minutes at 37°C in moisture chambers, then rinsed 3 times with 0.1% BSA/PBS at 5 minutes/wash. Tissue was incubated with FITC congugated goat anti mouse secondary antibody (diluted in 0.1% BSA/PBS with1% normal goat serum) for 45 minutes, in moisture chambers, at room temperature, washed 3 times with 0.1% BSA/PBS for 5 minutes/ wash, mounted in 50% glycerol with p-phenylenediamine (Johnson and Nogueira Araujo, 1981), and sealed with clear nail polish. Slides were kept at 4°C in the dark and photographed within 24hrs of staining.

Antibody final dilutions were: 5A6 anti alpha tubulin (1:4000), and TuJ1 anti beta tubulin (1:10,000) for primary anti-tubulin antibodies and FITC - congugated anti mouse IgG (1:200) for the secondary antibody. Controls used were: normal mouse serum, IgG purified from normal goat serum, 0.1% BSA/PBS with1% normal goat serum substituted for primary antibodies or both (no 1°, no 2°, no 1° and no 2°), and tubulin block for 5A6.

Rhodamine phalloidin staining

For actin staining, rhodamine phalloidin (1:200) was used (and tissue processed as described above, eliminating the primary antibody steps. For dual staining rhodamine phalloidin was added at the same time as the secondary antibody.

Preparation of normal mouse IgG: control for 5A6 anti-tubulin antibody

Mouse IgG was isolated from normal mouse serum (Sigma) using an ImunoPure (G) IgG purification Kit (PIERCE, Rockford Ill). Normal mouse serum (Sigma S3509) was clearified by centrifugation in clinical centrifuge at maximum speed for 15 minutes. It was then diluted 1:1 with ImmunoPure Immobilized Protein G column and was equilibrated with binding buffer. Serum was applied to the column, which had been washed with 10 ml binding buffer. Normal mouse IgG was eluted from the column with 6 mls of elution buffer, monitoring 1 ml fractions with A280 (Gilforld spectrometer) to locate IgG fraction. IgG fraction was desalted on desalting column using equilibration buffer (kit) and eluted with PBS. Resulting IgG was concentrated back to original volume using centricon microconcentrator (AMICON).

Autoradiography of binding assay

Autoradiography: methods

Tissue was prepared as described for binding assay for no treatment control and 10mM MgATP treated groups. Samples which had not been enriched on gradients and samples recovered from the combined 30/45 and 45/60 interfaces were processed for autoradiography. Microtubules were labelled using 10 µCi/50 µl of tubulin at1X concentration (10X that used in binding assays). To avoid possible morphological damage by freezing, tissue for autoradiography was drawn slowly from the 30/45 and 45/60 interfaces using a Hamilton syringe pushed through a small hole made in the wall of the centrifuge tube. To provide a count check on the material used for autoradiography, binding assays were done using parallel samples from the 'no treatment controls' and 10 mM MgATP treated groups. 10 mM MgATP reduced binding to 20% of 'no treatment controls'.

Samples for autoradiography were placed directly on acid washed glass slides and after being allowed to adhere, were fixed with 3.7% paraformaldehyde in PEM 250, incubated for 5 minutes in -20°C acetone, rinsed in PEM 250 and allowed to air dry overnight. Using deflected red light, slides were dipped in melted emulsion at 40°C (Kodak), allowed to dry for 30 minutes and suspended in light proof boxes containing silica gel dessicant pouches. Boxes were wrapped in 3 layers of foil and stored at 4°C. For development, slides were brought to room temperature, removed from the boxes under deflected red light, developed in Kodak D19 (diluted to 50% with dH2O) for 3 minutes, placed in stop bath of 8ml Kodak stop indicator/50 ml dH20 for 30 seconds, fixed in 25% sodium thiosulfate for 5 minutes, and rinsed for 30 minutes. Slides were dehydrated in ascending series of ethanol (70, 95, 95, 100, and 100%), placed in 2 changes of xylene, and the coverslip mounted with permount. Before photographing, emulsion was scraped from the back surface of the glass slides with a razor blade.

Periodic development determined that the optimum exposure time for silver grain development was 3 weeks.

A number of observations cast doubt on the reliability of carrying out quantative measures for the autoradiography experiments. Firstly, during processing for immunocytochemistry, it was observed that spermatid loss occurred at each rinse step. In addition, spots were seen associated with small amorphous clumps in autoradiography slides. Together these observations suggested that the ^3MT_X- spermatid-ESs, that had adhered to the glass slide, may be disturbed by processing. Secondly, when ^3MT_X-spermatid-ESs were exposed to either paraformaldehyde or acetone, total counts in gradient fractions were reduced over controls. This was suprising in that under any other treatment conditions, the total counts loaded were consistent. (see results).

The following experiment was done to check the effects of processing (rinse steps and acetone and paraformaldehyde treatment) on ^3MT_X- spermatid-ES binding. MT_X-Spermatid-ES (cold MT_X) sample was allowed to bind. Three conditions, 10 mM MgATP, ATP depleted with hexokinase and D-glucose, and 'no-treatment control' were each sampled in the following ways 1) before being put onto the gradient (pre-gradient processed), 2) after being removed from the gradient but unfixed (post gradient unprocessed) and 3) after being removed from the gradient and processed for either 5A6 anti tubulin, without primary antibody or with 5A6 and rhodamine phalloidin for dual localization of tubulin and actin (post gradient processed). Fixative proceedure was the same as that used for immunhistochemistry described earlier. Slides were examined and photographed immediately following the experiment on a Zeiss axiovert fitted with filters for FITC and rhodamine and with DIC optics.

Electron Microscopy

Routine electron microscopy

For experiments described in this chapter, tissue processed for electron microscopy was immersion fixed using 1.5% glutaraldehyde and 1.5%

paraformaldehyde. Following initial fixation, tissue was processed for electron microscopy as described in Chapter 2. Any temperature or buffer variations are described with the results.

Methods for calcium study

For these studies, potassium antimony (EM Sciences) was boiled in dH_2O (pH 8.6), cooled to room temperature and centrifuged at 10,000 rpm (16,000g) at 20°C for 30 minutes in a GSA rotor (Sorval) to remove insoluble precipitate. All EM fixation in this series involved tissue preparation, and fixation, followed by routine dehydration and embedding (see Chapter 2 for routine dehydration, embedding, and sectioning). For all experiments, tissue was observed with and without stain (uranyl acetate and lead citrate for 6 minutes each) to distinguish antimonate from metal stain, both visually and with elemental analysis. Calcium localization micrographs were photographed on a Phillips 300 electron microscope, from thin sections that had been stained with uranyl acetate and lead citrate to show ESER membranes.

The literature is repleat with potassium antimony precipitation methods for calcium localization. Three other calcium precipitation methods were tried. Only potassium antimony consistently gave positive results.

Method 1: (Tandler et al., 1970; Kierszenbaum et al., 1971) Fresh decapsulated rat and squirrel testes and hearts were cut into aproximately 1 mm cubes, and incubated at room temperature in 2% potassium antimony, in deionized, distilled water, for 6 hrs. (Potassium antimonate acts as a primary fixative). The blocks were then hardened in 5% paraformaldehyde in potassium antimony, for 16 hours, at room temperature, and washed 2X 15 minutes in dH_2O. Samples were post fixed in cold 2% osmium tetroxide (OsO_4) in dH_2O for 1 hour (parallel samples were processed with OsO_4 excluded. Samples were rat testis, squirrel testis and rat heart muscle.

Method 2: (Klein et al., 1972; as used by Franchi and Camatini, 1985). Rat testis was cut into blocks and incubated in 2% glutaraldyhyde with 2% potassium antimony in 0.01M acetic acid for 4 hours, on ice. Tissue was washed 3X with cold .01M actic acid with 2% potassium antimony, postfixed in 1% OsO_4 with potassium antimony (pH 7) for 1 hour, washed with cold .01M acetic acid with 2% potassium antimony, 3X 10 minutes each and processed for EM.

Method 3: (Borgers et al. 1981). The proceedure is the same as method 1 except: potassium antimony incubation was for 12 hours and was preceeded by a 30 minute HEPES-NaCl buffer (137 mM NaCl and 10 mM Hepes) preincubation step with either; buffer only, 5mM EGTA, or 4 mM calcium chloride at room temperature. The preincubated tissue was rinsed briefly in one change of potassium antimony to remove excess preincubation solutions and then incubated in fresh potassium antimony.

Method 4: (Spicer et al. 1969) Rat and squirrel testes and hearts were cut into cubes, and incubated for 1 hour at 4°C in 2.5% potassium antimony with 1% OsO_4 (pH 7.4 with acetic acid), dehydrated and embedded. A variation on this method (Cramer and Gall, 1979) using 2% potassium antimony incubation for 1 hour on ice, was also tried.

Three other methods were tried which have been used with limited success in the literature.

Method 5: In this method, oxalate is used, to bind calcium, and antimony, to produce an electron dense precipitate (Borgers et al., 1977). Tissue was immersed in 3% glutaraldehyde with 90mM oxalate at 4°C (pH 7.4), rinsed for 24 hours with 7.5% sucrose with 90mM oxalate at 4 °C, post fixed for 2 hours with 1% OsO_4 and 2% potassium antimony in 0.1N acetic acid at 4°C.

Method 6: NHA (N,N-Naphthaloylhydroxylamine) is used to precipitate calcium (Zechmeister, 1979).

Method 7: Tetrabutylamonium fluoride method (Poenine and Epel, 1987). Block of rat testis and rat striated muscle were incubated in100mM tetrabutylamonium fluoride with 1% glutaraldehyde in 25mM Hepes buffer (pH 7.2) at room temperature, for 15 minutes, rinsed in the same buffer with glutaraldehyde removed, post fixed on ice in same buffer with 1% OsO_4 and processed for EM.

RESULTS

This portion of the work consists of a combined biochemical and morphological approach to study the binding potential between microtubules and isolated spermatid-ES complexes. The purpose of these experiments was to: 1) define the components of the binding assay, 2) establish and test the criteria set for the binding assay, 3) characterize binding under a number of different conditions and 4) determine the location of label in the assay.

COMPONENTS OF THE BINDING ASSAY

Spermatid-ESs

Isolation of spermatids, by gentle poking and squashing of seminiferous tubule segments, resulted in a crude isolate comprised of spermatids from different stages of spermiogenesis. In order to determine that spermatids could be recovered from a range of epithelial stages, including when they are deeply placed in Spermatid crypts, spermatids were isolated from segments of seminiferous tubules, using the transillumination method (see methods). The squash method yielded spermatids from each of the segments. Figure 3-6: a-e shows the phase contrast microscopic appearance of spermatids immediately after they had been squashed from the tubule segments while they were still clustered together and surrounded by cytoplasm. To better visualize the spermatid head, they are also shown after spermatids from these isolates had been separated from one another. Figure 3-6:f is the DIC image of a general stage isolate after it had been rinsed from the slide. While spermatids remain still closely associated with one another, the phase contrast image highlights mainly the nuclei of spermatid heads. When spermatids are separated from the surrounding cell material, their phase contrast image changes. The outline of the acrosome can then more readily be seen, giving the impression of a larger spermatid head, with a slightly greater curvature. It

Figure 3-6. Appearance of spermatid-ESs isolate. Spermatid-ES were isolated from defined stages of seminiferous epithelium to verify that all stages of elongate spermatids can be recovered using the seminiferous tubule squash method. To facillitate separation, clumps of seminiferous tubule were incubated for 3 minutes in PEM 250 with 2mg/ml collagenase, and then rinsed with PEM 250 (without collagenase). Complete waves of seminiferous tubules were teased from the clump and transillumination pattern zones from one dark-zone to pale-zone change point, to the next, were identified (see introduction for explanation of zones). To examine spermatids squashed from different stages, waves were cut into four zones (see figure 3-2): 'pale zone' (stages IX to XII), 'weak spot zone' (XIII and I), 'strong spot zone' (II to VI), and 'dark zones' (VII and VIII) and isolated from each of the four segments by very gentle squashing. (a-e) phase contrast (f) DIC micrographs; tissue unfixed.

(a) Isolate from weak spot zone: stages XIII to I, spermatid steps XIII to XV,

(b) Separation of spermatids from isolate preparation in (a) to visualize individual spermatids. The acrosome identified only as a pale corona in (a) is more visible in (b) (arrow). During these stages (spermatid steps XIII to XV), phase image of flagella become thicker.

(c) Tissue from stages II to VI (strong spot zone): late spermatid steps XVI to XVIII. During these stages elongate spermatids achieve their deepest position within Sertoli cell crypts.

(d) Spermatid separated from the isolate in (c) showing long strands (arrowhead) typically seen extending from heads of spermatid-ESs isolated under warm conditions. The acrosome extends beyond the anterior tip of the nucleus. Together, these features give the isolated spermatid in (d) a more curved appearance than those that are still associated with surrounding cytoplasm. The dorsal surface of the nucleus (small white arrow) can be distinguished from a strand extending along the dorsal surface (arrow head).

(e) Individual spermatids in looser association with the isolate than surrounded them in (c) providing better visualization of the more completely developed flagellum .

(f) DIC image of multistage isolate, after being rinsed onto slide. Note the spermatids are surrounded with other cellular material in addition to the spermatids.

bars: a-e = 10 μm, f = 20 μm.

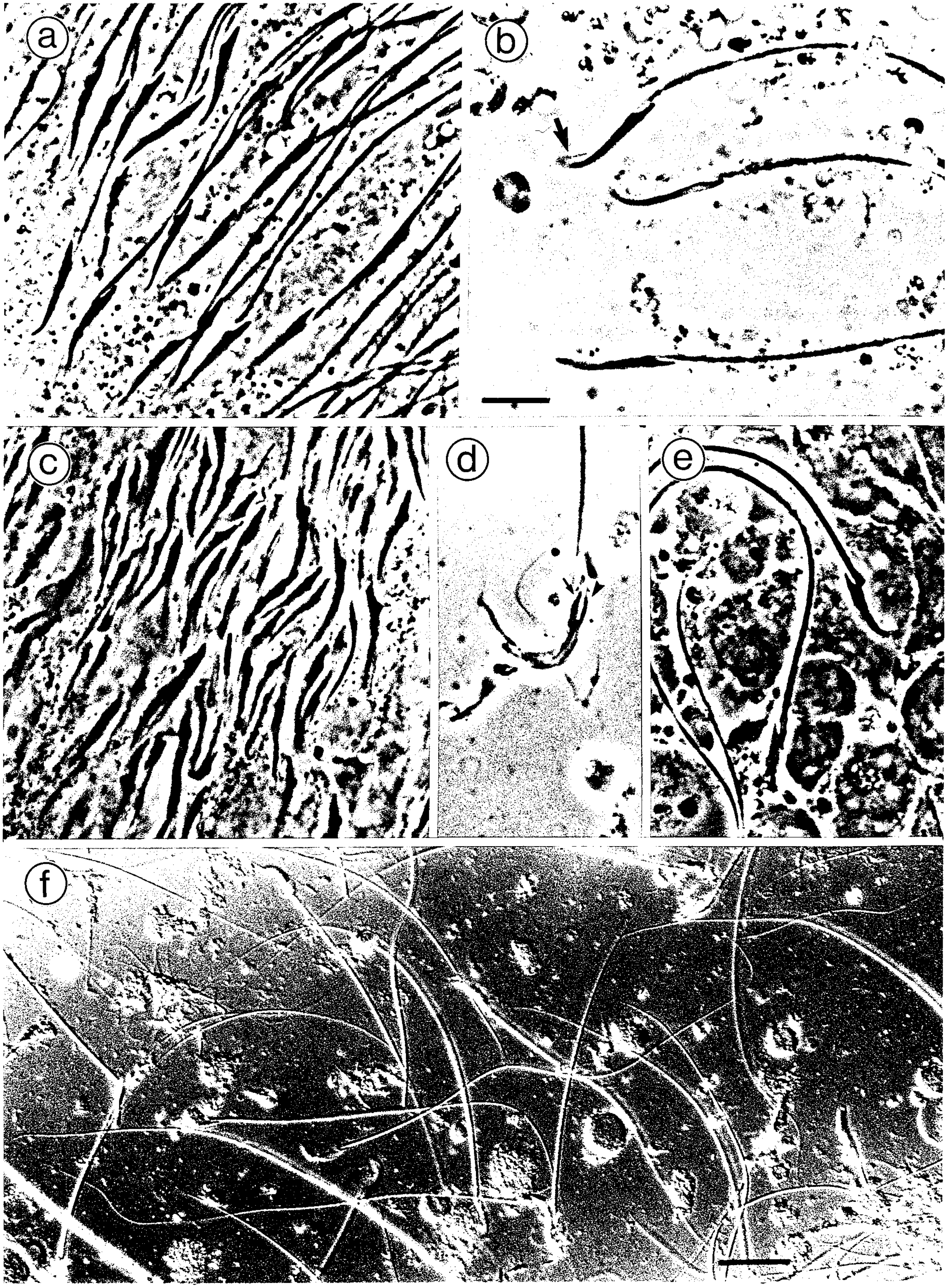
a
b
c
d
e
f

is not known whether being removed from the confines of the cytoplasm results in actual increase in curvature. It was found that spermatids could be removed from all four segments of epithelium using the squash method, that their appearance is slightly different when viewed in isolation, and that a wide range of stages are represented in the general isolate. Although it is to be expected that binding characteristics may vary between stages, determining which stages bind microtubules was beyond the scope of this study.

In addition to elongate spermatids, the crude isolate contained round spermatids, nuclei, organelles, and other cell components (Fig 3-6: f). Differential centrifugation of the crude isolate, on a 30/45/60% sucrose gradient at high speed: 100,000g for 45 minutes (Beckman Ti50 rotor, 36,000 rpm) or (Beckman SW40 rotor, 27,000 rpm) and very low speed (5000 rpm for 5 minutes), all yielded an elongate spermatid-ES enriched isolate that accumulated mainly at the 30/45 interface. Figure 3-16 shows spermatid enrichment from a crude spermatid isolate before (a) and after (b,c,d) using spin conditions ultimately chosen for the binding assays. Much of the cell debris has been removed.

When spermatids are mechanically removed from the seminiferous epithelium, the Sertoli cell ESs remain attached (Masri et al., 1987; Romrell and Ross, 1979; Grove and Vogl, 1989). For the binding assay, it was necessary to verify that, during the squash method of spermatid-ES isolation, ESs remain attached and intact.

In ESs, actin consists of a highly stable and ordered array of filaments that encompass all but the most posterior portion of the spermatid head. It has been well established spermatid heads stain intensely with rhodamine phalloidin, a stain for filamentous actin, only when ESs are present (Vogl et al., 1986). Isolated spermatids demonstrated the bright actin staining surrounding spermatid heads, indicating the presence of ESs (Fig. 3-7). The ES actin staining pattern did not coincide with that of the spermatid nucleus but provided a wider sillhoutte, accommodating the acrosome, that did not extend the full length of the nucleus posteriorly, (compare the outline of the

Figure 3-7. Actin staining associated with the heads of isolated spermatids: Spermatid-ESs. Spermatids, isolated by the squash method, stain for actin with rhodamine phalloidin in a pattern consistent with the location of ESs. Spermatids, shown here, were isolated by the squash method, (under warm conditions) and centrifuged on a sucrose gradient to give an enriched spermatid-ES preparation. Phase (a,c,f) and fluorescence (b,d,e,g,h) images of spermatids stained with rhodamine phalloidin to identify filamentous actin (b,d,g). Actin staining (b) surrounds the spermatid head but does not extend the full length of the nucleus posteriorly. A dotted line superimposed on the phase image in (a) indicates the location of the ES identified by actin staining in (b). (Note the difference in position between the caudal end of the spermatid nucleus and the actin staining of the ES). These data indicate that ESs remain attached to spermatids when they are isolated by this method.

(c) Phase contrast image of an isolated spermatid-ES, dual stained with rhodamine phalloidin for filamentous actin (d) and 5A6 antibody for tubulin (e) showing that endogenous tubulin is present but differs in distribution from that of actin. The tubulin positive strand extending from the spermatid head is a common finding in warm isolated spermatid-ESs (double arrows) and is not seen in the actin staining. Spermatid-ESs at this stage, a time when tubulobulbar processes are forming but actin staining gives evidence of presence of ESs, are at the apex of the epithelium, and may retain elements of the apical process during isolation.

(f) Spermatozoa or very late stage spermatid, identified in the phase image by its highly condensed and acutely curved nucleus, negative for both (g) actin and (h) tubulin staining. This is consistent with the fact that ESs are no longer present on late stage spermatids at the time of spermiation and that the actin and tubulin staining are not staining structures on the spermatid itself.

bars: a-h = 10 µm.

201

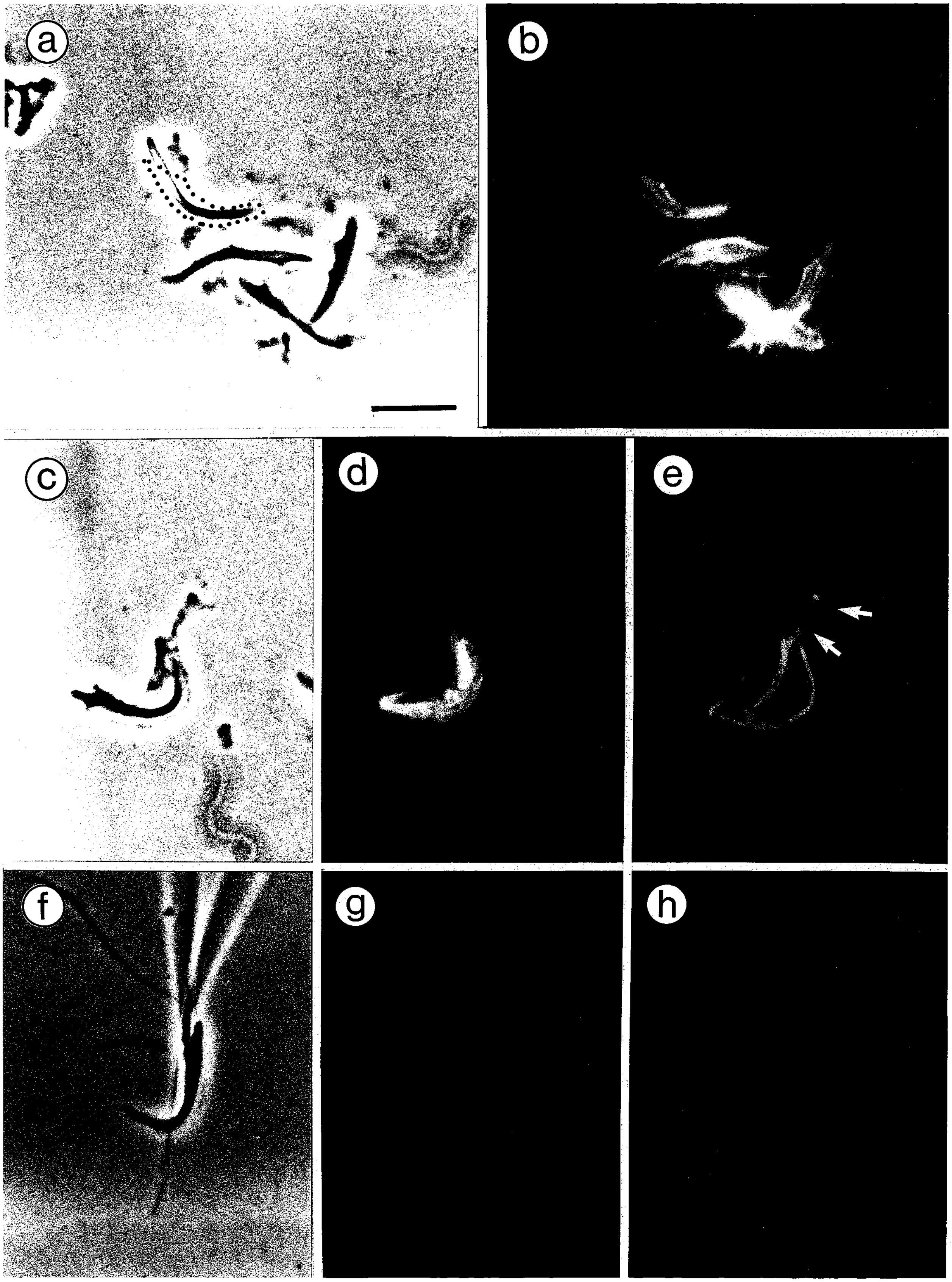

spermatid nucleus, indicated by black dots, with the actin staining pattern (Fig.3-7a,b). As expected, spermatids at a stage immediately prior to spermiation, identified by their highly curved heads, do not stain intensely for actin because the ESs have degraded by the time spermatids are released (Fig. 3-7 f-h).

Ectoplasmic specialization endoplasmic reticulum: ESER

The outer face of the ER is not readily removed from the actin component. In an attempt to establish conditions which would ensure that the inner, cytoplasmic face of the ESER was not lost, a sucrose containing buffer was used. On phase images the heads appeared to have some material around the heads. $DIOC_6$, a stain initially thought to be ER specific, stained all membranes and organelles including mitochondria indiscriminately, proving a poor tool to identify ESER. For EM of these spermatids, the tissue was pelleted in an Eppindorf centrifuge at every step of preparation. Loose spermatids were lost during wash steps and those in the pellet condensed with adjacent material around the head, making it more difficult to demonstrate the full shape of the ER. Spermatid-ESs, isolated in 100 mM sucrose PEM buffer showed some dilation of the ER when processed for EM (Fig. 3-8 a,b). As a result of the prolonged centrifugation required when preparing the 250 mM sucrose, material became collapsed, and the ER was flattened, leaving only thin profiles of ESER visible (Fig. 3-8 c).

Endogenous microtubules remain attached during warm isolation

Isolation temperature used during spermatid-ES isolation is important to the presence of endogenous microtubules. "Warm isolation" was done at room temperature, and kept somewhat warm by the microscope lamp. Ice was not used in any step. Phase images of spermatids isolated under warm conditons revealed long strands extending, from the anterior and posterior aspects of the spermatid head, parallel to the long axis of the spermatid. Figure 3-9 shows the phase appearance and anti-tubulin antibody 5A6 staining of isolated spermatids using the warm (a-h) and cold isolation (i-l) methods. (Controls for this antibody are shown in Figs. 3-10 and 3-11). Long strands, seen associated with the heads of the warm isolated spermatids, were positive for tubulin staining, suggesting that endogenous microtubules remain attached to the heads with this isolation.

For "cold spermatid-ES isolation", every attempt was made to keep the isolate cold throughout the proceedure. The testis was placed on ice immediately after being removed from the animal, and tubule segments were teased apart in ice cold buffer. The slide used on the microscope stage to poke and squash the tubule segments was cold and was replaced on ice as necessary, during the procedure. The isolated spermatids were immediately rinsed with ice cold buffer and kept cold in a collecting dish until used (methods Fig. 3:3). Following cold isolation, the long strands were generally absent and the staining with tubulin was greatly reduced or absent. Occasionally, some endogenous microtubules remained. For the radiolabelled binding assays in this study, all spermatid-ES isolations were done using the cold isolation method to reduce bound endogenous microtubules. These data suggest that endogenous microtubules, under warm isolation conditions, remain associated with the spermatid head and support the hypothesis that microtubules bind to spermatids.

To explore the relationship of the tubulin staining strands with actin staining ESs, isolated spermatids (warm isolation) were dual stained with rhodamine phalloidin and 5A6 (anti-tubulin antibody with FITC 2^{o} mouse IgG probe). Staining indicated that both tubulin and actin were present but formed different patterns. Figure 3-7: c,d,e show an isolated spermatid-ES stained for both actin and tubulin. Tubulin stain extends, as do the strands seen in the phase image, beyond the confines of the ES, delineated by actin staining. Late stage spermatids and spermatozoa lack both actin and tubulin staining, consistent with the loss of ESs just prior to spermiation (Fig. 3-7 f,g,h). The acutely curved head and lack of tubulobulbar processes, of this image, suggests that the spermatid/spermatozoa has been isolated immediately before, or after, spermiation.

Figure 3-8. ESER remains attached to spermatid head following spermatid-ES isolation. Electron micrographs of the fine structure of spermatid-ESs that have been isolated in ice cold PEM containing sucrose. The ER remains attached to spermatids although it remains somewhat dilated when PEM with 100 mM sucrose concentration is used.

(a, b) ESER of spermatids isolated in PEM with 100 mM sucrose (PEM 100). ESER (arrows) remains attached to the actin component of the ectoplasmic specialization (arrowheads).

(c) Cistern of ER surrounding spermatid heads (arrows) following isolation in PEM with 250 mM sucrose (PEM 250).

bars: a= 1 µm , b = 0.5 µm , c = 0.5 µm.

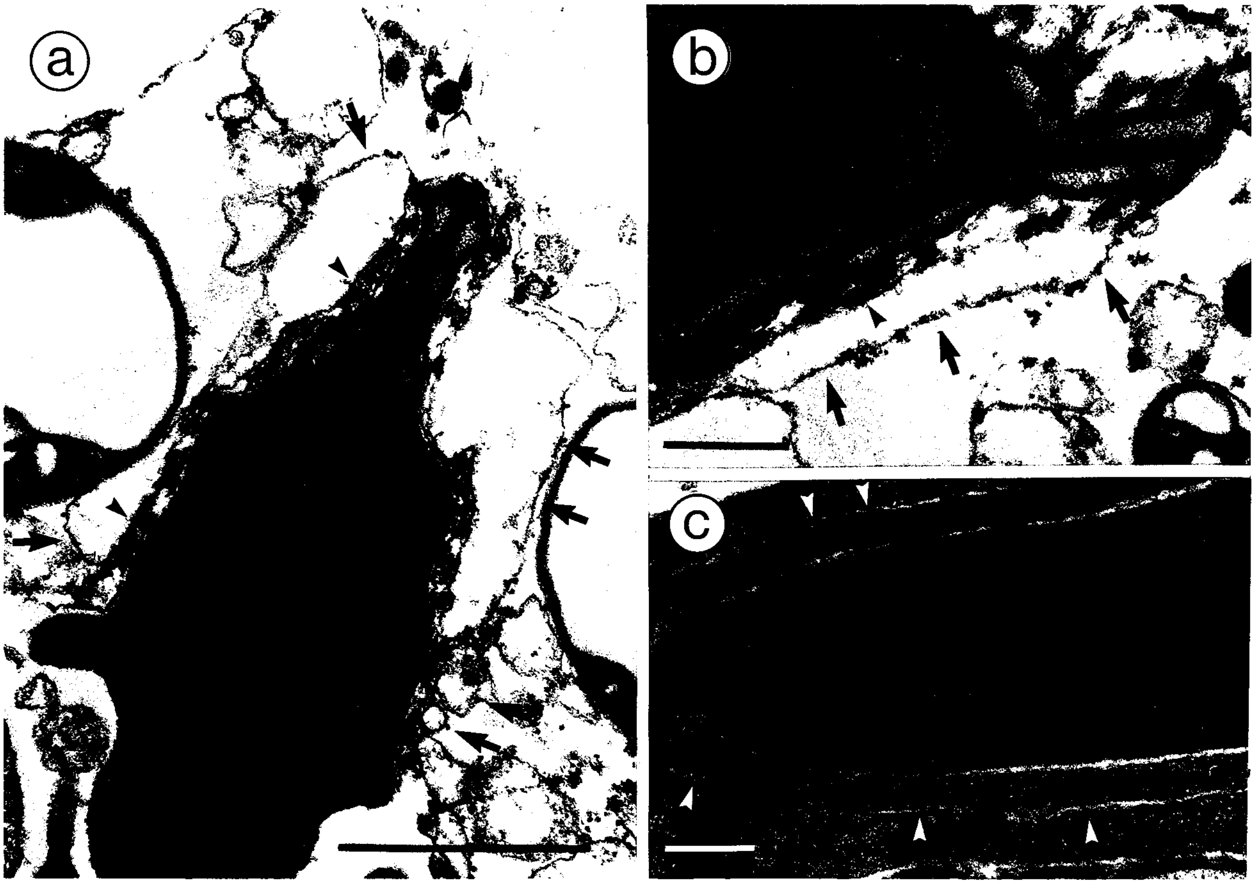
a
b
c

Figure 3-9. Tubulin staining pattern on spermatid-ESs isolated under warm or cold conditions. Spermatid-ESs, when isolated under warm conditions, retain endogenous tubulin in strands associated with the spermatid head.

(a,b; c,d; e,f; g,h) Phase contrast images and tubulin staining pattern of spermatid ESs isolated under warm conditions.

(i,j; k,l) Phase contrast images and tubulin staining pattern following isolation of spermatid-ESs under cold conditions. When spermatid-ES isolation is carried out on ice, the tubulin staining pattern is altered or lost.

bars: a-l = 10 μm.

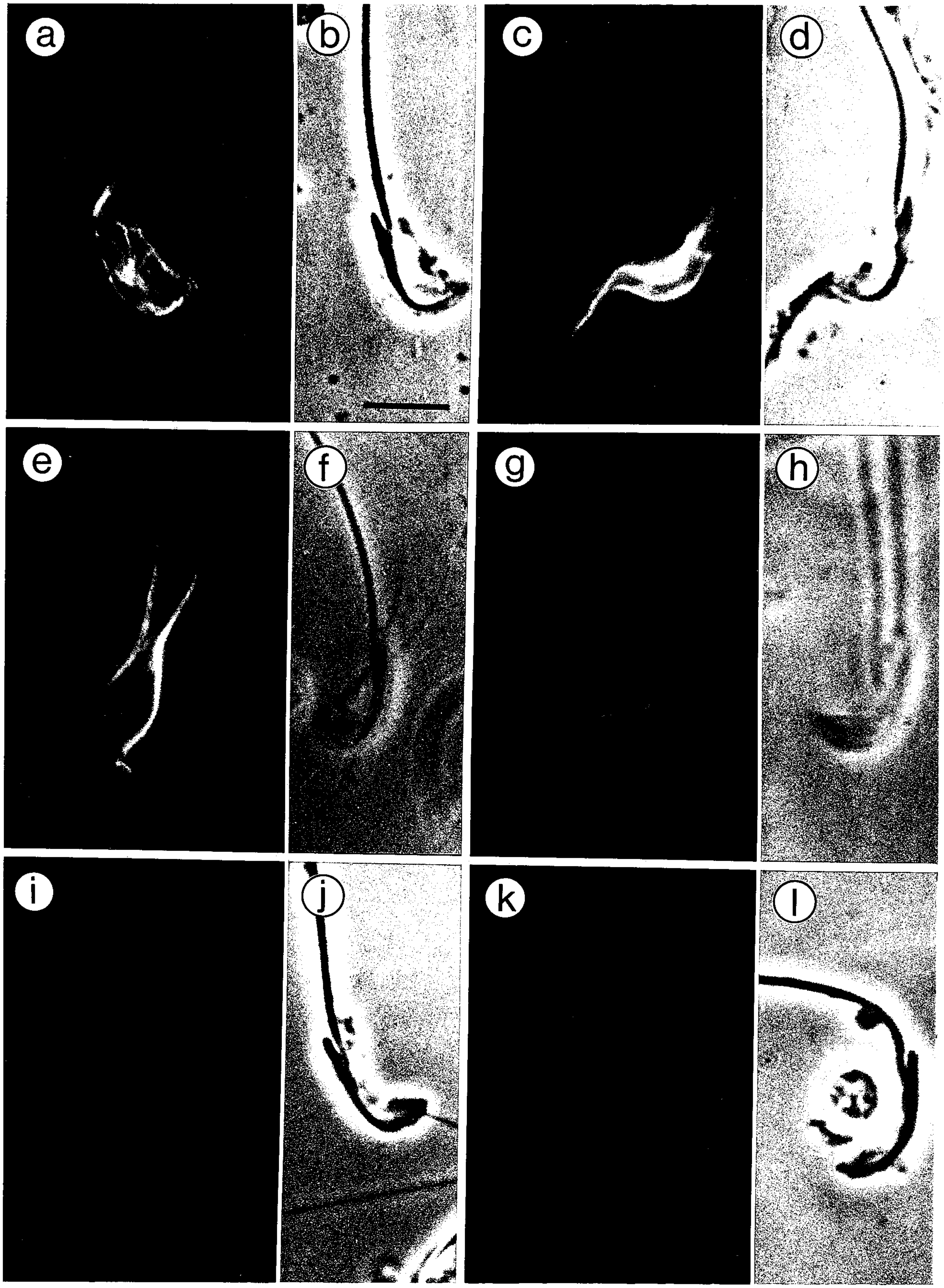
a
b
c
d
e
f
g
h
i
j
k
l

Figure 3-10. Control figure for 5A6 antibody staining for tubulin (1). Spermatid-ESs in these micrographs isolated under warm conditions (endogenous tubulin only). These micrographs show phase contrast and fluorescence images of samples spermatid-ESs stained for tubulin using 1° monoclonal antibody to alpha tubulin 5A6 and FITC conjugated goat- anti mouse 2° antibody (IgG). All 1° and 2° antibody buffers contained 1% normal goat serum and 0.1% bovine serum albumin in phosphate buffered saline. Purified mouse IgG was reacted with testis sections processed in the same way as the spermatid-ESs shown in this figure and there was no evidence of non specific staining seen. The 5A6 tubulin antibody consistently stained both Sertoli cell and exogenous bovine brain microtubules.

(a,b) Immunocytochemical staining with 1° monoclonal antibody 5A6 for alpha tubulin and FITC congugated goat anti mouse 2° antibody.

(c, d; e, f) 1° antibody is omitted from buffer.

(g,h) 1° and 2° antibodies are omitted from buffer

(i,j) 1° antibody is replaced with normal mouse serum. Remnant of tissue is included to show that non-specific staining of tissue does not occur .

bars: a-j = 10 μm

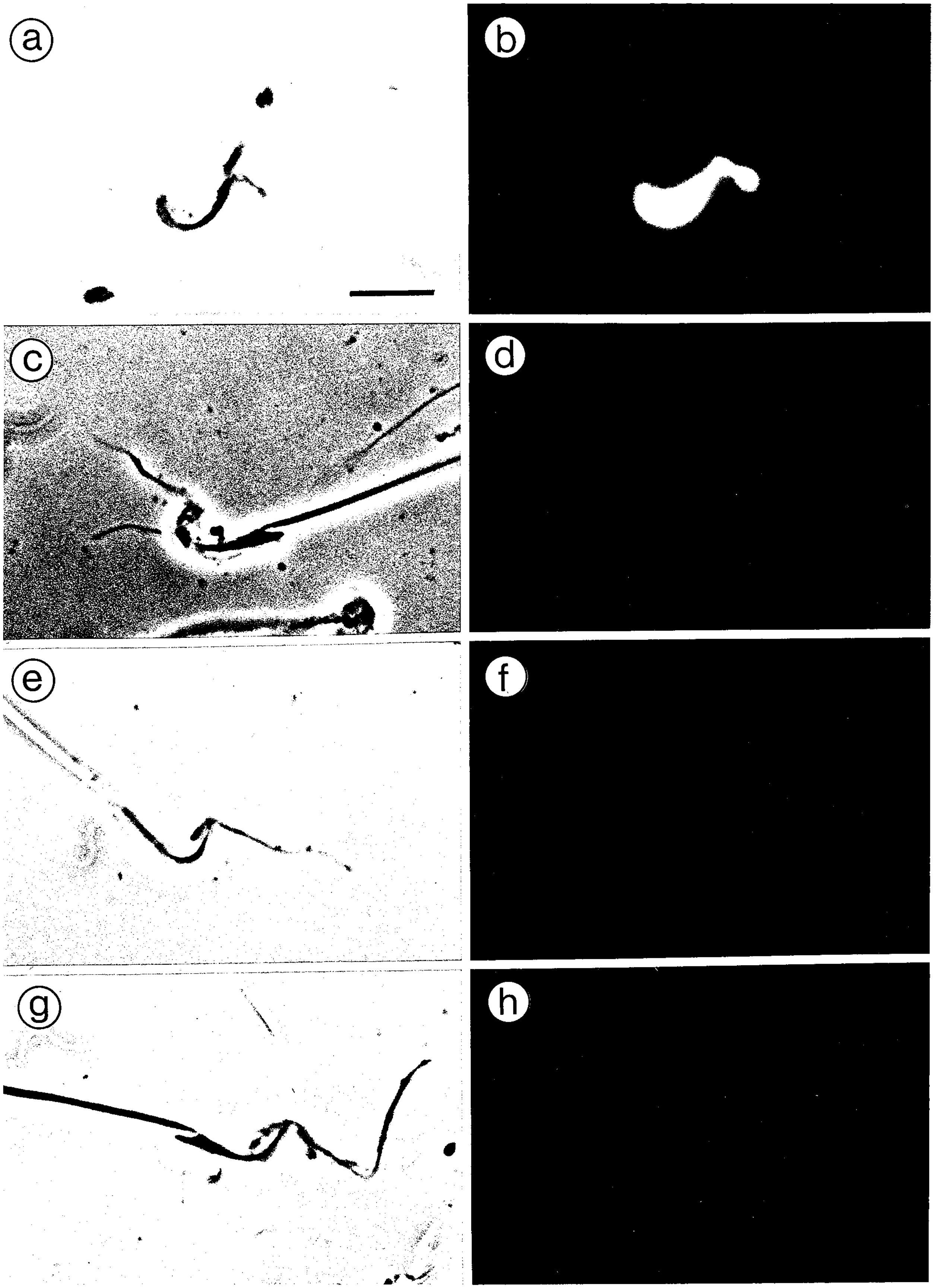
a
b
c
d
e
f
g
h

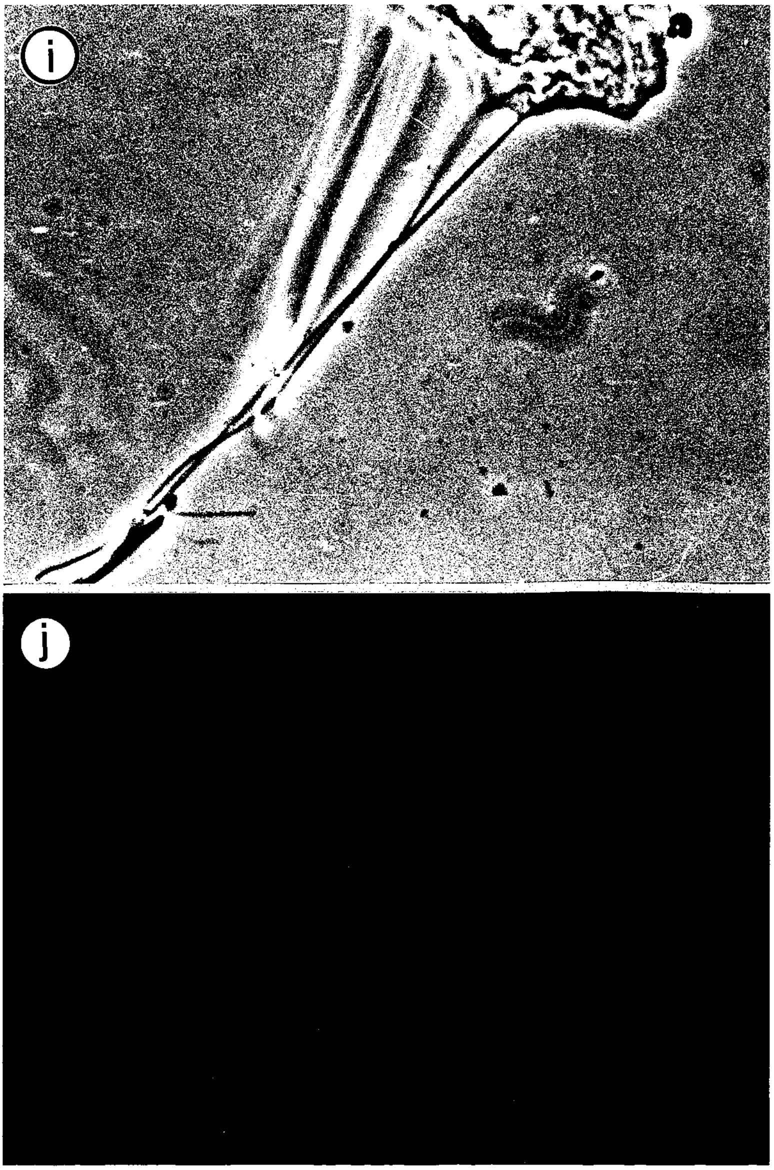
i
j

Figure 3-11. Control figures for 5A6 antibody staining for tubulin (2). (a,b; i,j) Phase and fluorescence images of spermatid-ESs isolated under warm conditions (endogenous tubulin only) stained with 5A6 monoclonal antibody to alpha tubulin using the same spermatid-ES isolation conditions as shown in Fig. 3-10.

(c,d; e,f) Tublin block of 5A6 antibody. No staining was seen when excess tubulin was added to the 5A6 antibody before reacting with spermatids.

(g,h) Tuj1 monocloncal antibody to beta tubulin (gift from David Brown). Staining pattern for Tuj1 antibody to beta tubulin was the same as for 5A6 antibody to alpha tubulin.

bars: a-j = 10 µm.

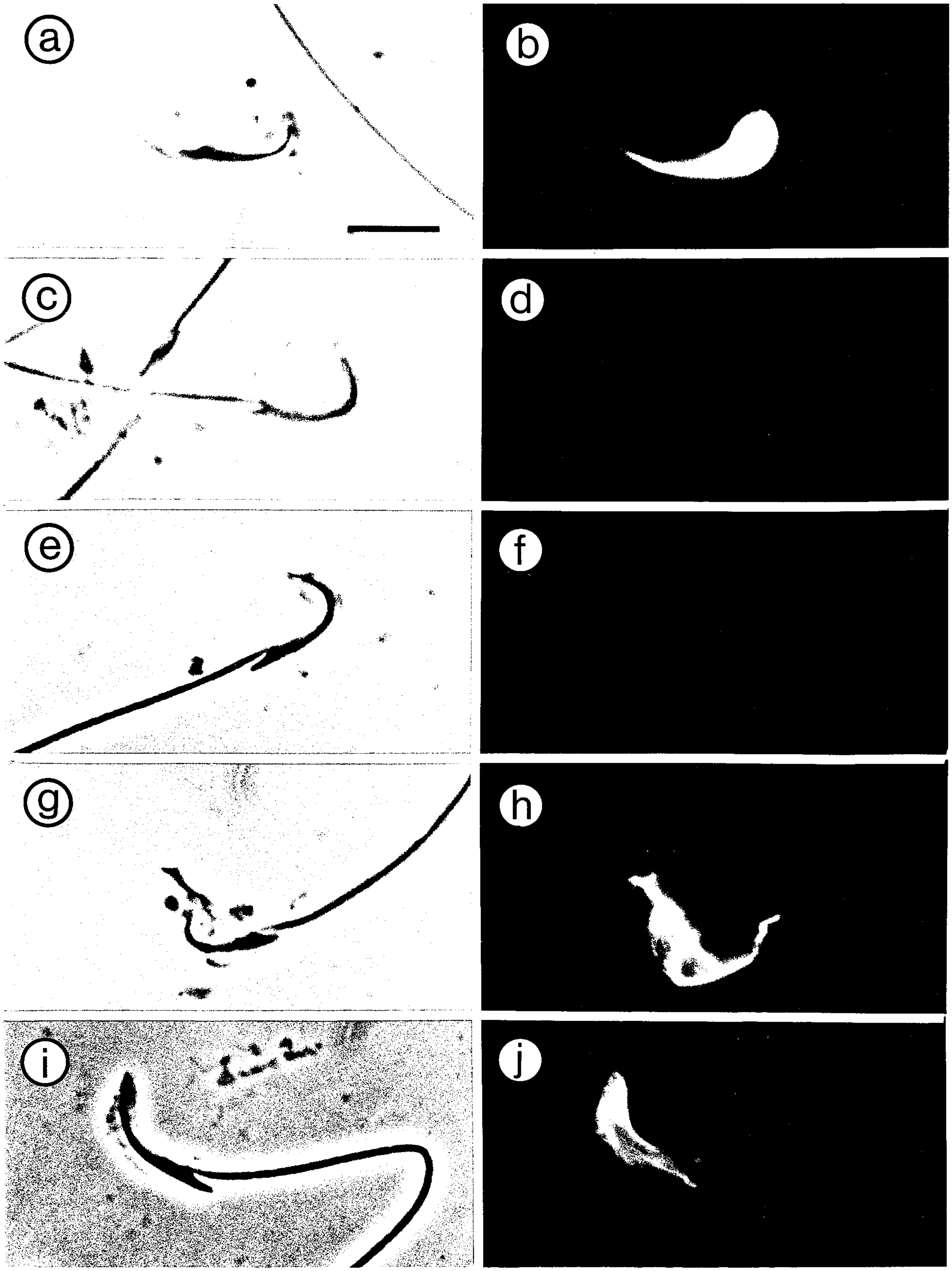
a
b
c
d
e
f
g
h
i
j

Microtubule isolation and measurements

Tubulin that is polymerized in the presence of taxol yields short stable microtubules (Schiff et al., 1979; Horowitz et al., 1981; Vallee, 1982). Figure 3-12 shows taxol polymerized bovine brain microtubules, an unlabelled equivalent of those used in the binding assays. Negative stain EM highlights the protofilament structure of microtubules (Fig 3-12 e). Of the 103 microtubules measured, over 14 fields, the mean length was 2.8 ±1.2 µm. The length of taxol stabilized microtubules measured here would be approximately 15 to 20% of the length of the spermatid head. Tubulin staining associated with spermatids removed from the sucrose gradient generally conformed to the shape of the spermatid head. They were never seen to form the long strands seen in spermatids isolated under warm conditions. In a "topical binding" experiment in which an excess of additional cytoplasmic dynein enriched MAPs, and taxol polymerized microtubules were added to isolated spermatid-ESs directly on the slide, the anti-tubulin stained microtubules associated with a spermatid can be seen as short strands (Fig. 3-12: b,c).

Labelling exogenous microtubules

Taxol reduces the critical concentration for microtubule assembly and stabilizes the polymer to depolymerizing conditions of cold or microtubule disrupting agents (Schiff et al, 1979, Horowitz et al., 1981). In the presence of taxol, microtubule polymerization is able to proceed without added nucleotides (Vallee 1982; Paschal et al., 1991). Microtubules, for binding assays, were assembled from purified brain tubulin in the presence of a substochiometric amount of GTP (5 µM) plus ^{3}HGTP (1 µCi/50µl tubulin) and 20 µM taxol. This ensured maximum incorporation of competent ^{3}HGTP into exogenous microtubules before they were added to the spermatid-ES preparation.

Figure 3-12. Length and structure of taxol stabilized microtubules used for MT_x - Spermatid-ES. MAP-free microtubules assembled from purified bovine brain tubulin (1.6 mg/ml) for 30 minutes at 37°C in the presence of 20 µM taxol. The resulting polymerized and taxol stabilized microtubules were stained with 1% aqueous uranyl acetate on parlodian and carbon coated copper EM grids, and visualized on a Phillips 300 at 80 kv. Fields of positively stained microtubules were photographed, (including consecutive fields to encompass the longer microtubules) and microtubule lengths counted from the negatives.

(a, d) EM micrographs of positively stained taxol polymerized microtubule images such as those from which microtubule lengths were determined.

(b, c) Phase and 5A6 anti tubulin fluorescence micrographs of a cold isolated spermatid-ES, allowed to adhere to a polylysine coated slide and then incubated with taxol stabilized microtubules in the presence of a cytoplasmic dynein enriched MAP preparation from rat testis. (See 'topical binding assay' in methods). The short exogenous microtubules which extend from the spermatid head are seen to particular advantage in this figure (arrow). The short taxol assembled microtubules, in this figure, contrast with the long tubulin positive strands of endogenous microtubules associated with the head of the spermatids isolated under warm conditions.

(e) EM image of negatively stained taxol polymerized microtubules showing the fine strands of tubulin protofilaments (small arrows). bars: a and d = 1 µm, b and c = 10µm, e = 0.1µm.

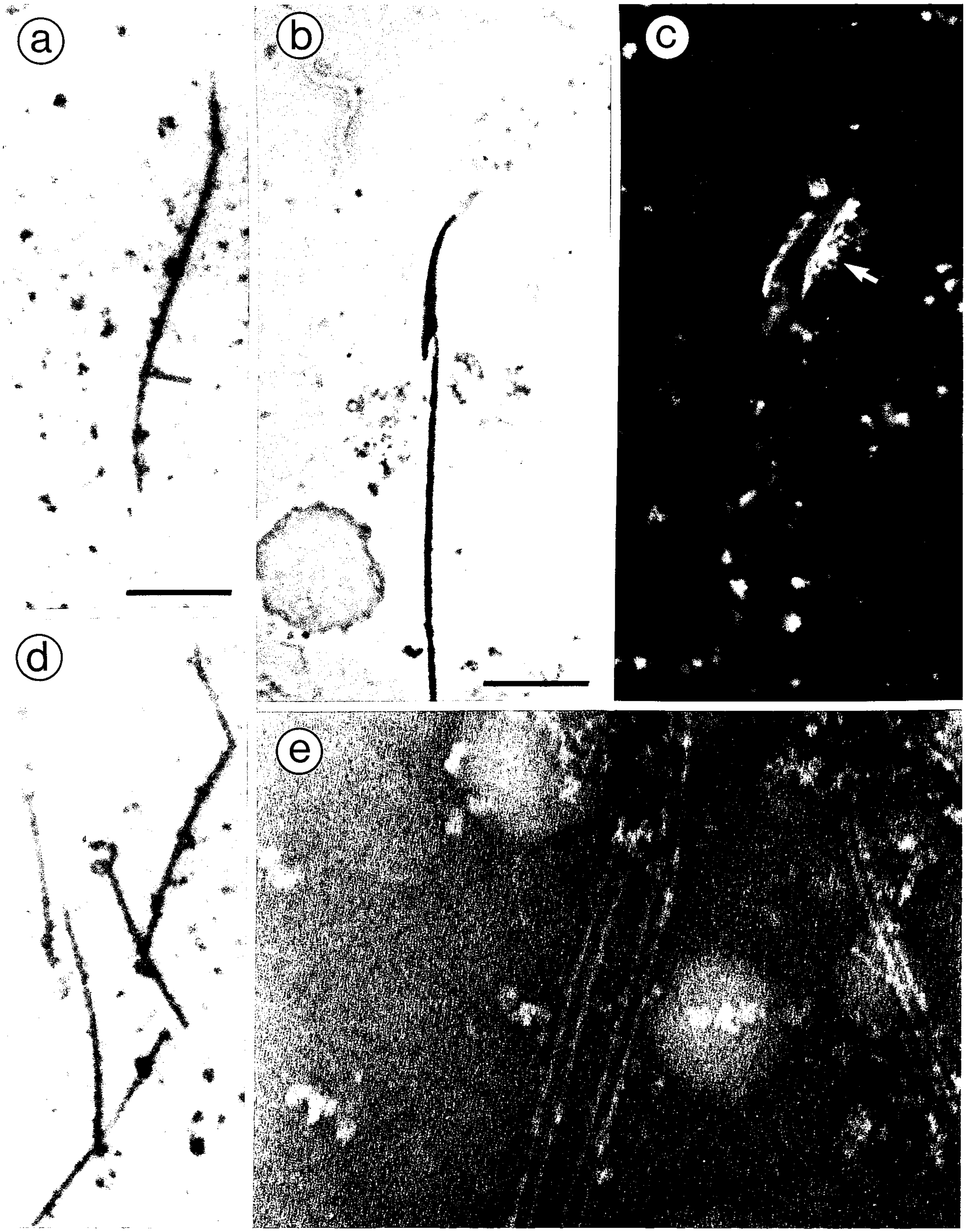
a
b
c
d
e

Incorporation of label and stability of microtubules over time

The percent of total label that pelleted with microtubules (sample pelleted over a 15% sucrose cushion in Beckman airfuge at maximum speed for 30 minutes), was taken to be the percent incorporation of label. In untreated, taxol stabilized microtubules, prepared for binding assays, this was 43 ± 9.2%. Taxol stabilization prevents cycling of the label from the exogenous microtubules (Wilson and coworkers, 1985). The quantity of label present in microtubules, aliquoted from the same stock, pelleted from samples collected beginning at time = 0 hrs; or time = 2 hrs remained constant. Furthermore, an "apparent" decline in binding over the duration of the experiment would have been expected if the label was being cycled from bound exogenous microtubules; "apparent" because it would be label, not microtubules that would be declining. No such effect was observed.

Microtubule stability: effect of agents for characterization of microtubule binding

To ensure that changes in microtubule - spermatid-ES binding were not due to direct microtubule injury by the respective agents, incorporation of label was measured in microtubules exposed to agents used to characterize binding. The incorporation of label in all of the agents was within 98% ± 8% of the incorporation of the untreated microtubules in same spin controls. This was well within the variability of sampling for pelleted microtubules.

BINDING ASSAY: ESTABLISHING THE CRITERIA

In a series of "topical binding" experiments, immunohistochemistry was used to examine binding of exogenous microtubules to isolated spermatids that had been adhered to glass slides. Using this method, the results were difficult to interpret because some endogenous microtubules remained and observations could not be quantitated. These experiments indicated that, to characterize spermatid-microtubule binding, an unambiguous method using labelled exogenous microtubules was required to characterize spermatid-ES-microtubule binding.

Buffer conditions

As described above, a number of buffer conditions were examined to protect the ESER from hypo-osmolar effects. PEM with 250 mM sucrose was deemed to be of sufficient osmolarity to isolate spermatid-ESs with the ESER intact. Protease inhibitors were added to protect protease sensitive MAPs that might be present and required for binding (Wiche, 1989).

When crude spermatid-ES isolate was placed on a discontinuous sucrose gradient including 30, 45 and 60% sucrose, and spun at 92000g for 45 minutes (4°C or 29°C), spermatids-ESs were primarily found at the 30/45 interface, with a minor amount at the 45/60 interface. There was no discernable difference in the stages of spermatids present at the 30/45 and the 45/60 interface; however, the occasional cluster of spermatid heads and a rare fragment of tubule wall were found at the lower level. Inspection of material from the bottom of the gradients indicated that material did not migrate through the 60% sucrose. Using SDS PAGE gel electrophoresis, it was determined that during high speed spins taxol stabilized microtubules were present at all levels of the gradient, with the greatest concentration at the 30/45 interface.

The need for spin parameters in which spermatids would consistently enter the gradient, while unbound microtubules would not, was satisfied by a short duration, low speed spin. Figure 3-13 is a SDS PAGE gel of fraction samples from gradients loaded with spermatid-ESs, spermatid-ESs incubated with ^3MT_X, and ^3MT_X alone, spun at 5,000 rpm for 5 minutes. It was determined that any increase in speed or time (over 5,000 rpm for 5 minutes) allowed taxol stabilized microtubules to enter the gradient (Fig. 3-14 and 3-15). Spins of 5,000 rpm for 5 minutes did not. Figure 3-14 (bottom) shows an SDS PAGE gel of spermatid-ESs + ^3MT_X samples using three different spin conditions. The 5,000 rpm for 5 minutes provided a maximum amount of tissue at the 30/45 interface.

Using the ultracentrifuge with Beckman SW65 rotor, spermatid-ESs migrated into the gradient, collecting mainly at the 30/45 interface with only a minor amount collecting at the 45/60 interface (Figs. 3-13 and 3-14). Although the force used was available from other centrifuges, precise control of the acceleration and decceleration time, duration and total number of cycles available in the ultracentrifuge were critical to consistency between spins and maintenance of the criteria: ^3MT_X - spermatid-ESs enter the gradient and ^3MT_X alone do not. To that end, the same centrifuge was used for all binding assay experiments. Using the SW65 Beckman rotor with adaptors for a sucrose gradient capacity of 550µl and a sample load of 150 µl accommodated the problem of small yield from spermatid-ES isolation. Although results from the 30/45 and 45/60 interface were eventually pooled, the two levels of sucrose were counted separately as an internal check. The count in the 45/60 fraction was always very small compared with that in the 30/45 fraction. Use of the three levels of sucrose meant that the occasional error in the construction of the gradient could be caught on visual inspection and the data deleted. Such errors were also obvious in the fraction counts.

Spermatid-ES enrichment by gradients

The primary purpose for putting the sample for the binding assay on a sucrose gradient was to 'wash out' unbound microtubules. It simultaneously had the effect of enriching the fraction for spermatid-ESs, leaving much of the other cellular material behind. Figure 3-16 shows the composition of a spermatid isolate before being applied (Fig. 3-16a) and after being recovered (Fig. 3-16 b,c,d) from the gradient.

Figure 3-13. Testing for microtubule migration using sucrose gradients in MT_X - spermatid-ES binding assays.

Spermatid-ESs, MT_X- spermatid-ESs, and MT_X alone, were centrifuged on discontinuous 30, 45, and 60 % sucrose gradients at 5,000 rpm for 5 minutes (Beckman Ultracentrifuge model L7-55). Samples were prepared from tissue recovered from the 45/60, 30/45, and sample/30% sucrose interfaces and loaded onto 7.5% SDS polyacrylamide gels. Gels were stained with comassie blue stain.
(Lane 1) Molecular weight markers (carbonic anhydrase 29 kD, egg albumin 45 kD, bovine albumin 66 kD, phosphorylase B 97.4 kD, beta galactosidase 116 kD, and Myosin 205 kD.)(Electrophoresis is from top to bottom of gel).

(Lanes 2, 3, and 4) Isolated spermatid-ES samples, recovered from 45/60, 30/45 and sample/30 % sucrose gradient interfaces respectively.

(Lanes 5, 6, and 7) Isolated spermatids, to which taxol polymerized bovine brain microtubules had been added; from 45/60, 30/45 and sample/30 % sucrose gradient interfaces respectively. Arrow indicates tubulin in lane 7. (Lanes 8, 9, and 10) Taxol polymerized microtubules only, recovered from 45/60, 30/45 and sample/30 % sucrose gradient interfaces respectively.

Proteins from spermatid-ESs collect mainly at the 30/45 interfaces (lanes 3 and 6). Tubulin is also present in these fractions, possibly darker in lane 6. Tubulin is present in the 30%/45% fraction in the spermatid-ES samples when MT_Xs are added (lane 7) but not in 30%/45% fractions when the spermatid-ES samples do not have added MT_Xs (lane 4). There was no tubulin found to enter the gradient, that is, in the 30/45 or 45/60 fractions, when spermatid-ESs were not present. Tubulin loaded onto the gradient without spermatids (lanes 8, 9 and 10) remains in sample/30 fraction. These data indicated that MT_Xs do not enter the gradient, except in the presence of spermatid-ESs, under these spin conditions.

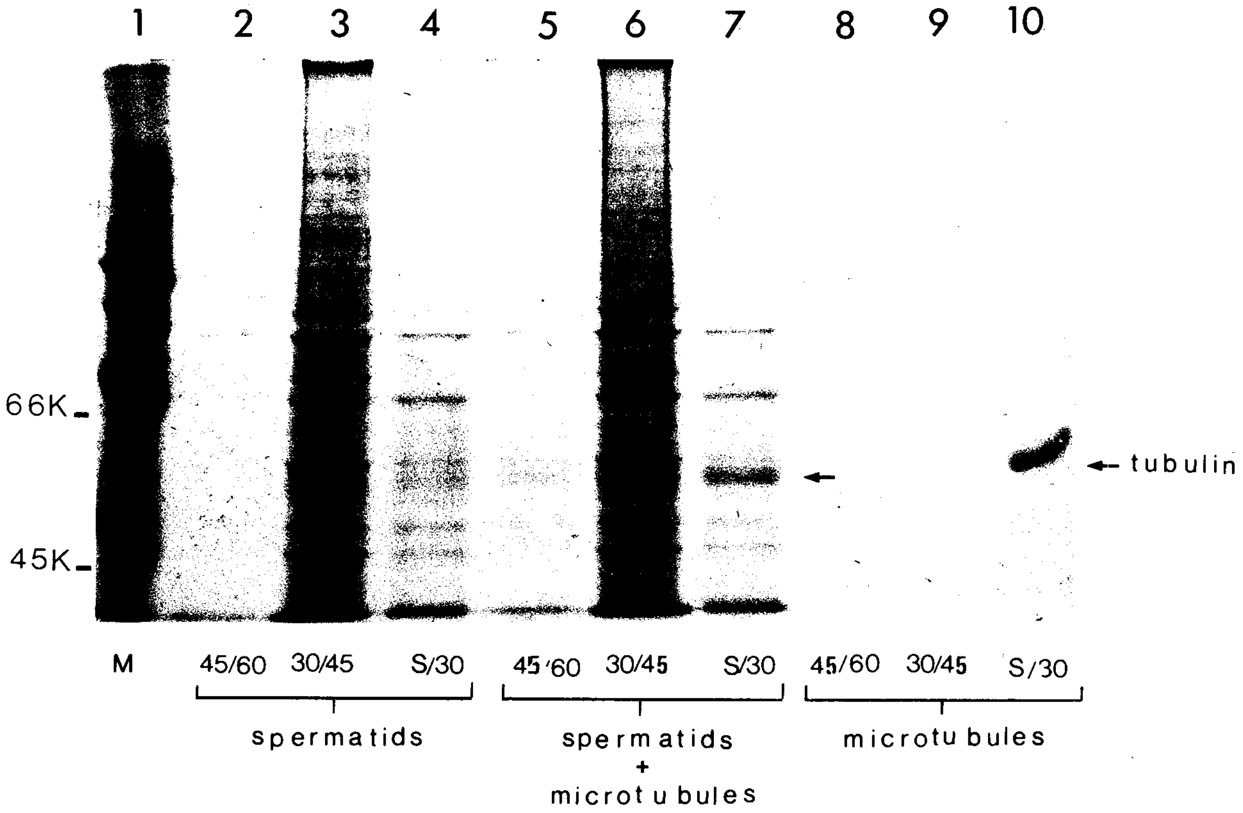
1
2
3
4
5
6
7
8
9
10
66K
45K
tubulin
M
45/60
30/45
S/30
45/60
30/45
S/30
45/60
30/45
S/30
spermatids
spermatids
+
microtubules
microtubules

Figure 3-14. Establishing spin criteria for binding assay: SDS page gels:

Gel data from a variety of the spin parameters tested to determine optimum parameters for maximum migration of MT_X - spermatid-ESs but without migration of MT_X alone. The format and lane assignments for the four gels in the upper part of this plate are exactly the same as those shown in the previous figure.

(*upper left and upper right*) Gels used to test the contents of gradient fractions under spin conditions ultimately used in the binding assays (in which MT_X- spermatid-ESs samples were spun at 5000 rpm for 5 minutes). Spin criteria of requiring that unbound microtubules do not migrate into gradient fractions, are met with these parameters.
(*middle left*) Gel testing spin parameters, 15000 rpm, 5 minutes.
(*middle right*) Gel testing spin parameters, 5000 rpm for 30 minutes.

At 5000 rpm for 5 minutes, tubulin was present only in the sample/30% fraction (*lane 10*). At both 15000 rpm for 5 minutes and 5000 rpm for 30 minutes tubulin was present in both the 30%/45% (*middle left, lane 9 and middle right lane 9*) and sample/30% fractions (*middle left, lane 10 and middle right lane 10*). These data indicated that the spin conditions of 5,000 rpm for 5 minutes fit the criteria that spermatid-ES enter the gradient while microtubules alone do not.

(*lower gel*) SDS PAGE gel loaded with gradient fractions from three different spermatid-ES + MT_X binding assays.

To compare the amounts of MT_X-spermatid-ESs that enter the gradient using these spin conditions, the 45/60, 30/45 and sample/30 interfaces were collected from each assay. (lanes 2,3,4) 45/60, 30/45 and sample/30 interfaces from assay spun at 5,000 rpm for 30 minutes. (lanes 5,6,7) 45/60, 30/45 and sample/30 interfaces from assay spun at 15,000 rpm for 5 minutes. (lanes 7,8,9) 45/60, 30/45 and sample/30 interfaces from assay spun at 5,000 rpm for 5 minutes. The majority of MT_X-spermatid-ESs were found in the 30/45 interface, when using the parameters: 5000 rpm for 5 minutes. The 5000 rpm for 5 minutes satisfied two criteria: adequate entry of MT_X bound spermatid-ESs and no entry of MT_X alone. These data were consistent with radiolabelled data.

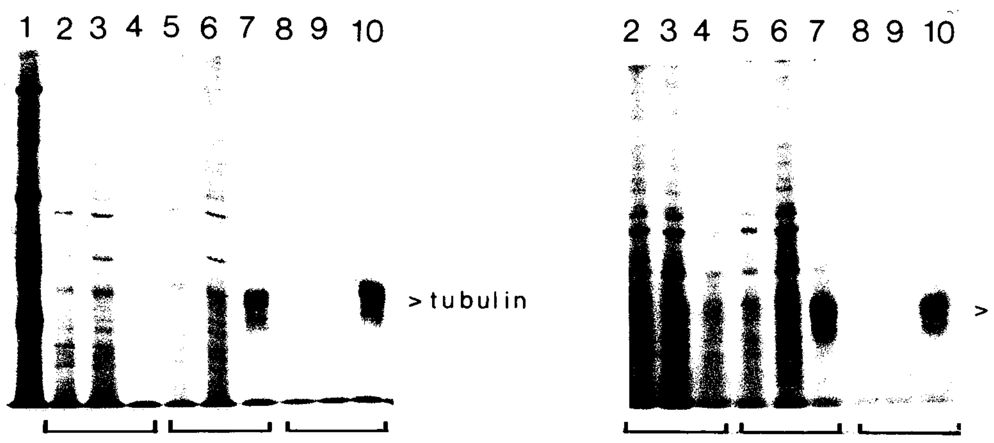
1 2 3 4 5 6 7 8 9 10
> tubulin
2 3 4 5 6 7 8 9 10
>

5,000 rpm, 5 min

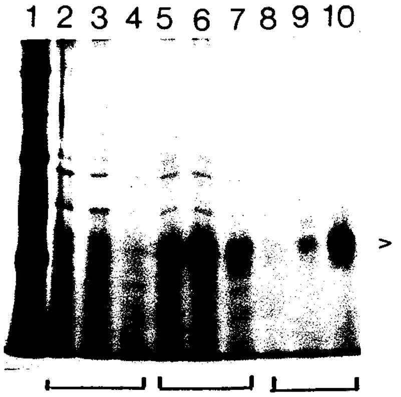
1 2 3 4 5 6 7 8 9 10
>

15,000 rpm, 5 min

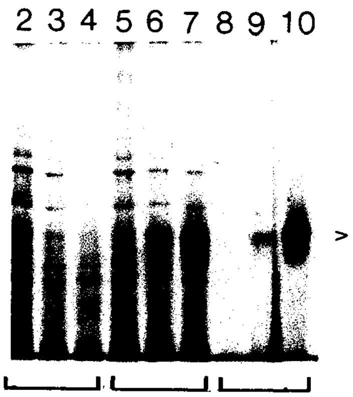
2 3 4 5 6 7 8 9 10
>

5,000 rpm, 30 min

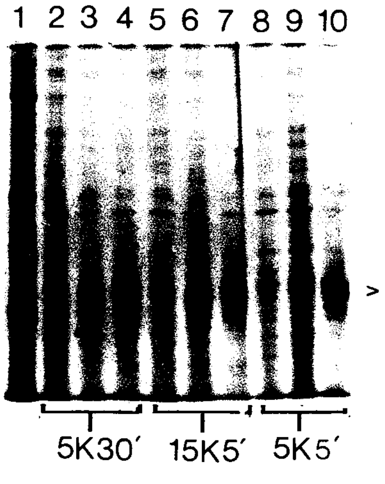
1 2 3 4 5 6 7 8 9 10
>
5K30′
15K5′
5K5′

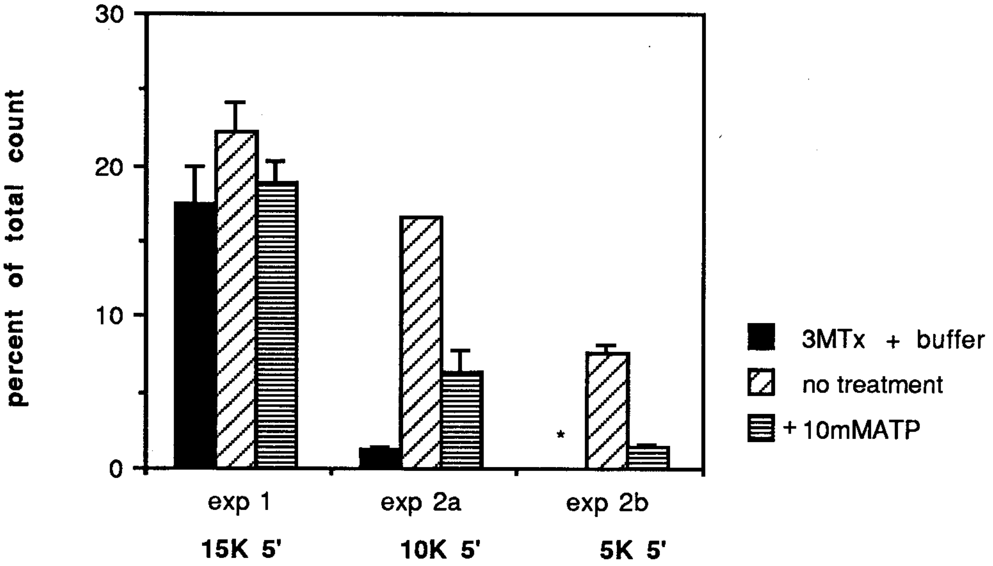

Figure 3-15. Test of differential centrifugation conditions for binding assay using ^3MT_x counts. The previous figure provides SDS gel evidence that microtubule protein is not detected in the gradient in the absence of spermatid-ESs. This data gives evidence that counts, associated with microtubules are not detected in the gradient when loaded without spermatid-ESs. A number of different centrifugation conditions were tested which could provide for migration of labelled microtubules bound to spermatid-ESs and at the same time not result in the migration of unbound microtubules. Data are give for three of the conditions tested and expressed as a percent of the total label that entered the gradient using 15,000 (15K5'), 10,000 (10K5') and 5,000 rpm (5K5') for 5 minutes for each spin. One sample each of: labelled microtubules + buffer (^{3}MTx); ^{3}MTx + isolated spermatids (no treatment control); ^{3}MTx-spermatid-ESs + 10mM MgATP (+10mM ATP), was included in each spin. Centrifugation at 5,000 rpm for 5 minutes met the required criteria. (* indicates 0.0% counts entering gradient, which do not register on the graph.) This illustrates the importance of using spin criteria that eliminate the counts from microtubules entering the gradient.

Controls: "same spin controls" in every spin

The Beckman SW65 rotor, has only three buckets, limiting the number of conditions that can be spun together to three. An untreated control ('same spin control') was included in each spin. Sample size and therefore 'total counts loaded' were equivalent, in all gradients for a given experiment (exceptions are noted). Figure 3-17, 3-18 and Table III-I show a short experiment that is illustrative of the general experimental design, results, and method of expressing data. Measures of ^3MT_X-spermatid-ESs entering the gradient are combined counts from fractions 30/45 and 45/60, expressed as the percent of total counts from all three fractions: 'percent of total count'. To examine the treatment effect of an agent, it was necessary to factor out, between-experiment variability and variability caused by time. These effects would be reflected in 'no treatment control' spins. For that data, each count from a treated group was expressed as a fraction of the count from the 'no treatment control' from the same spin: 'fraction of same spin control'.

Initially, one gradient with ^3MT_X and buffer only, was included in each run to check for migration of microtubules alone. Consistently, no label was found in these gradients. This was then checked only periodically. None of the treatment agents used to characterize ^3MT_X - spermatid-ES binding caused migration of ^3MT_X and buffer alone.

Epididymal sperm, with or without added microtubules, did not migrate in the same way, on the sucrose gradient, as spermatid-ESs, making them inappropriate as a control.

Sampling

High variablity was encountered when spermatid-ESs were sampled using the top, side or bottom access to the gradients. Tissue was also damaged passing through the needle (see discussion of autoradiography experiments). Contamination of label occurred and not all the material was recovered. Gradients were fast frozen and cut into three fractions (mid way between S/30 and 30/45 and between 30/45 and 45/60

Figure 3-16. Centrifugation of crude spermatid-ES isolate on a discontinuous 30-45-60% sucrose gradient results in enrichment of spermatid-ESs. DIC appearance of spermatid-ESs isolate (without added tubulin) before and after being enriched on a sucrose gradient, using the same conditions as the binding assay.

(a) DIC appearance of spermatid-ES isolate prior to being enriched by a sucrose gradient.

(b, c and d) DIC appearance of the spermatid-ES isolate shown in (a) after being enriched on the sucrose gradient. Samples shown here were collected by syringe from the 30/45 % sucrose interface and are unfixed. Figures (b and c) show typical appearance of isolated material. Figure (d) shows clusters of cellular material that is seen in some fields. In (d) spermatid heads can be seen in the cluster.

bars: a-d = 20μm.

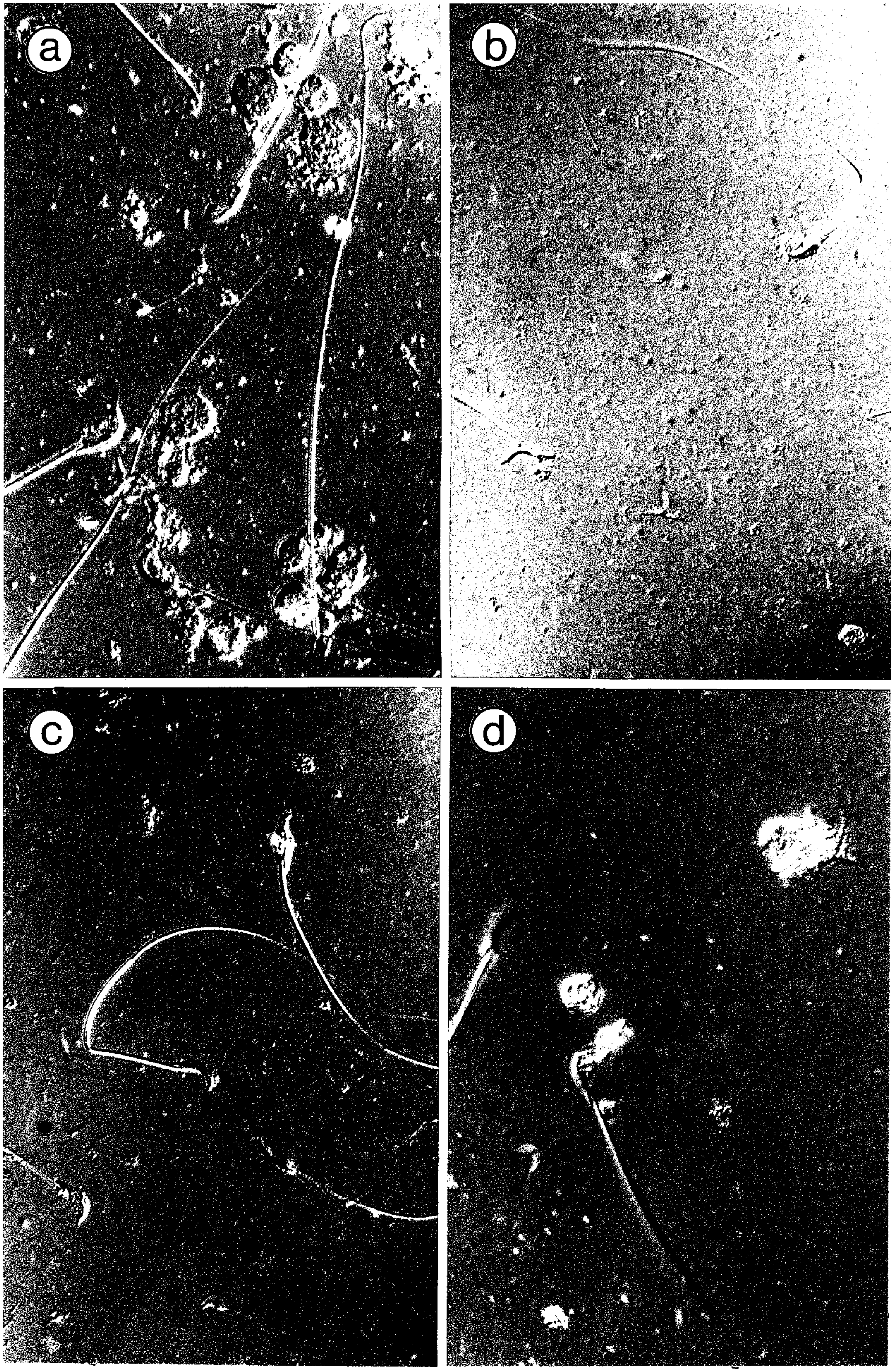
a
b
c
d

Figure 3-17. Binding assay: method: short sample experiment. Design of a short experiment that typifies the binding assay experiments used throughout this study. $^{3}MT_{X}$ were combined with isolated spermatid-ESs (1:2) to give $^{3}MT_{X}$ - spermatid-ESs, or with buffer (1:2) to give $^{3}MT_{X}$+ buffer. The $^{3}MT_{X}$ - spermatid-ESs were further divided into 'no treatment control' and $^{3}MT_{X}$ - spermatid-ES with added 10 mM MgATP groups. Gradients were prepared immediately before each spin. Three conditions were tested in each spin. A 'no treatment control' was used in every spin. Initially a $^{3}MT_{X}$ with buffer was included in each spin, however, with the repeated result that $^{3}MT_{X}$ did not enter the gradient, this condition was replaced by other treatments in later experiments. A typical 'treatment', 10 mM MgATP, was used in this experiment.

(*Early vs late binding)* For 'early' binding experiments, the $^{3}MT_{X}$ - spermatid-ESs were loaded immediately onto the gradient for the first spin. For established binding, $^{3}MT_{X}$ - spermatid-ESs binding was allowed to proceed for at least 1 hour before being assayed. Binding in this experiment is early binding.

(*Early vs late treatment*) For early treatment, the 10 mM MgATP was added at the same time as the $^{3}MT_{X}$ and the first spin begun as quickly as possible. When treatment was imposed on established binding, treatment was added to $^{3}MT_{X}$ - spermatid-ESs the after the established binding period. Treatment in this experiment is on early binding.

Experimental Design

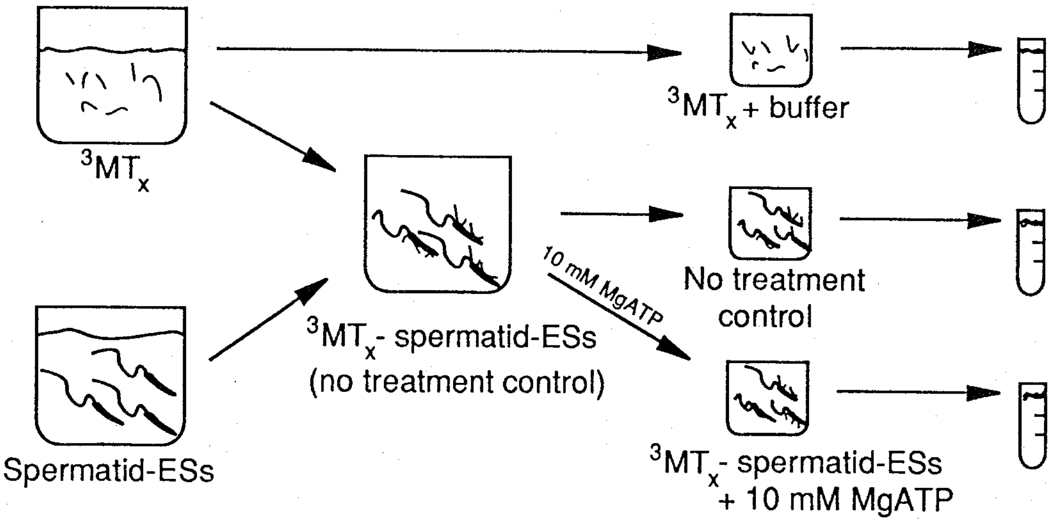
^3MT_x
Spermatid-ESs
^3MT_x- spermatid-ESs
(no treatment control)
^3MT_x + buffer
No treatment
control
10 mM MgATP
^3MT_x- spermatid-ESs
+ 10 mM MgATP

Tab. III-I. Sample data from binding assay

spin	no treatment	10 mM MgATP	3MTx + buffer	% same spin control
1	7.0	1.6	0.0	23
2	7.2	1.6	0.0	22
3	8.1	1.4	0.0	17
4	8.2	1.5	0.0	18

This short binding assay consisted of four spins having one gradient of each condition: ^3MT_X - spermatid-ESs only (untreated), ^3MT_X - spermatid-ESs with 10 mM MgATP, and ^3MT_X with buffer alone, in each spin. Samples were incubated for 30 minutes before first spin to allow time for ^3MT_X - spermatid-ES binding. Gradients were spun at 5,000 rpm for 5 minutes. Data represents counts that were collectively found in 30/45 and 45/60 gradient fractions, expressed as a percent of total counts loaded onto gradient. Each value from the 10 mM MgATP group is expressed as a fraction of the same spin control (column % same spin control).

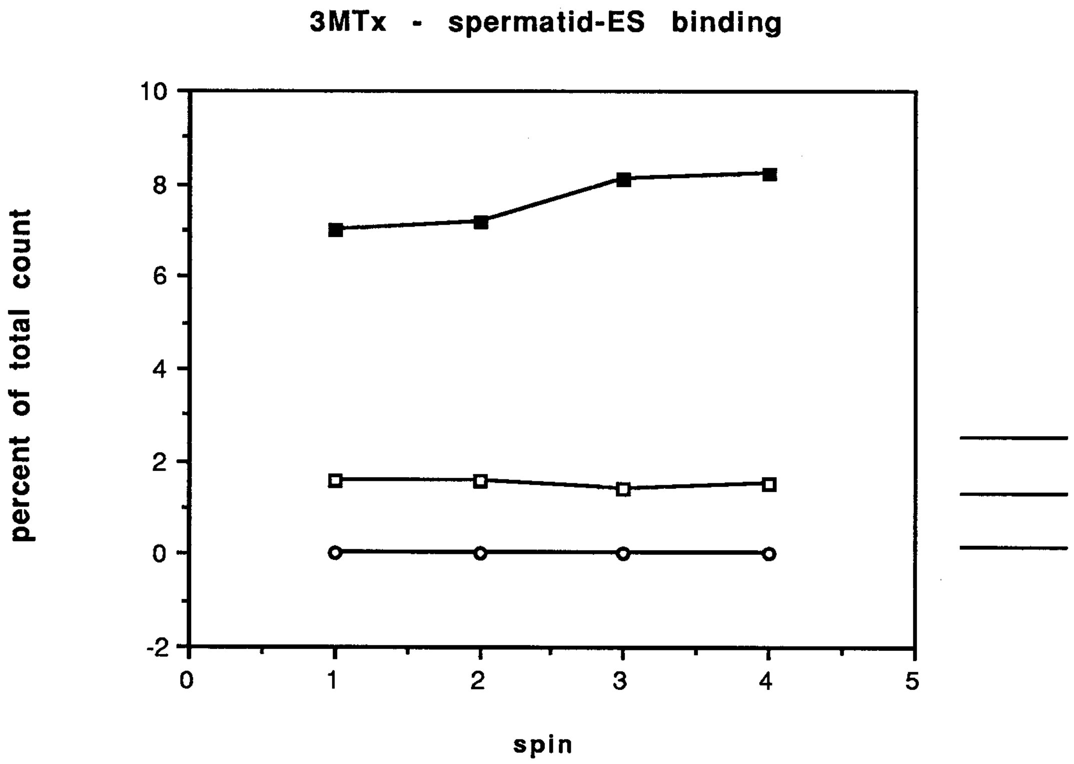

Figure 3-18. Results of sample binding assay. ^3MT_X with buffer only (*open circle*), ^3MT_X with spermatid-ESs treated with 10 mM Mg ATP (*open square*) and same spin controls (*solid square*) are shown as a function of spin number and expressed as a percent of same spin control (See Table III-I). ^3MT_X with buffer only do not enter the gradient. 10 mM MgATP significantly reduces binding.

interfaces) with a razor blade to circumvent these sampling inconsistencies. Because repeated freezing and thawing of gradients is an accepted method to produce continuous gradients, gradients of different colors were processed to see if the freezing caused any mixing of the gradient levels. No mixing occured. Problems frequently encountered in scintillation counting, chemiluminesence and interaction of gradient components with scintillation fluid, also were checked.

BINDING ASSAY: RESULTS

Microtubules bind to spermatid-ESs

The first evidence of spermatid-ES-^3MT_X binding, in the assays, was the presence of counts in gradient fractions using conditions in which ^3MT_X alone could not enter the gradient. Figures 3-17, 3-18 and Table III-I show the data from a short experiment in which the effects of: ^3MT_X+ buffer; spermatid-ES + ^3MT_X (no treatment); and spermatid-ES + ^3MT_X +10 mM MgATP are compared. In this experiment, ^3MT_X and spermatid-ESs were incubated for 30 minutes before the spins were started. ^3MT_X did not enter the gradient alone as shown by the 0% counts in the gradient. Spermatid-ESs entered the gradient and with them, radioactive counts, evidence of labelled microtubules. Assuming that the label represents microtubules, and that the binding is to spermatid-ESs (the major component of the gradient fraction), two findings central to this study are supported by these data: 1) Binding occurs between microtubules and spermatid-ESs and 2) this binding can be reversed by treatment with 10mM MgATP. The assumption that the label represents microtubules is examined first.

Label entering the gradient with sperimatid-ESs is primarily from microtubules

In order to equate counts entering the gradient with microtubules bound to spermatid-ESs, it was necessary to determine what percent of the counts present in the gradient could be attributed to microtubule and non microtubule associated label. The reasoning was that, if all microtubules were removed from the ^3MT_X sample by pelleting, the remaining label would constitute non microtubule associated label in the sample. 1200 µl of ^3MT_X sample were spun over a PEM15% sucrose cushion at 50,000 rpm for 30 minutes and the top 900 µl were recovered as '^3MT_X supernatant' (^3MT_XSN). The percent of count remaining in the supernatant after pelleting averaged 52.5%, suggesting that at least 47.5 % of the label was incorporated into microtubules of sufficient size to be pelleted (tubulin concentration was reduced by 90% by pelleting). This was consistent with microtubule incorporation values generally. The ^3MT_XSN was then substituted for ^3MT_X. Controls were ^3MT_X+ buffer and ^3MT_X-spermatid-ESs. Removing labelled microtubules from ^3MT_X sample has the effect of lowering the total counts loaded onto the gradients. For these experiments, binding was therefore expressed as 'absolute counts entering the gradient' (rather than % of total counts). Table III-II summarizes the results of these experiments. These data indicate that the majority of counts entering the gradient are associated with labelled microtubules.

Figure 3-19 shows the microtubule and non microtubule components of binding over time. There is an increase in counts entering the gradient over the first two time points of sequential spins. Calculations show that in both these points, nonmicrotubule component is 25% of microtubule component. This raised the question of a time course in binding.

There is a time course to 3MTx - spermatid-ES binding

When the data from 'no treatment controls' from each experiment were expressed over time, (plotted on a composite graph), a pattern of binding emerged that was typically lower at early time points before achieving a plateau. In order to define this time course, count data from 'no treatment controls' of seven experiments, matched in their time courses, were plotted over time (Fig 3-20). In these experiments, ^3MT_x and spermatid-ESs were mixed (time = 0 minutes), immediately placed on the sucrose gradient, and the first spin begun (early binding). Data from the spins were found to be different, by analysis of variance, when grouped into either 15 or 30 minute intervals ($P < 0.05$) (Fig 3-21). Pairwise comparisons using Tukey's test showed that the first 15 minute interval was different from all but the second, and the second was different from most but not all of the others. When they were grouped into 30 minute intervals, the first interval was different from the others and none of the others were different from each other. This indicates that there is a time course to the binding and with lower binding in the first 30 minutes and a plateau occuring by approximately 60 minutes. This time course pattern was found to be consistent with a composite scatter plot of the other experiments in the binding study that had included measures during early binding.

Nucleotides reverse binding

Some MAPs can be released from microtubules with nucleotides, a fact that is utilized routinely for the isolation of MAPs (Wiche, 1989), in particular mechanoenzymes.

The effect of 10mM MgATP on ^3MT_x - spermatid-ES binding was tested in 20 experiments. In some experiments 10 mM MgATP was a prime focus of the experiment (one of the two treatment conditions being examined). In the other experiments it was tested episodically to measure ATP release on other agents under study. The mean reduction of binding by 10mM MgATP was determined for each experiment. The method of expressing the binding is shown in table III-I. Counts (combined 30/45 and 45/60 fractions) are expressed as percent of total count. In order to compare the effect of treatments, such as ATP, in a number of different experiments, the percent of total count is then expressed as a ratio of "no treatment, same spin control" values. Figure 3-18 and Table III-I show that ^3MT_x - spermatid-ES binding is reduced by the addition of 10 mM MgATP. Over 20 experiments, 10 mM Mg ATP reduced binding to 36 ± 13%

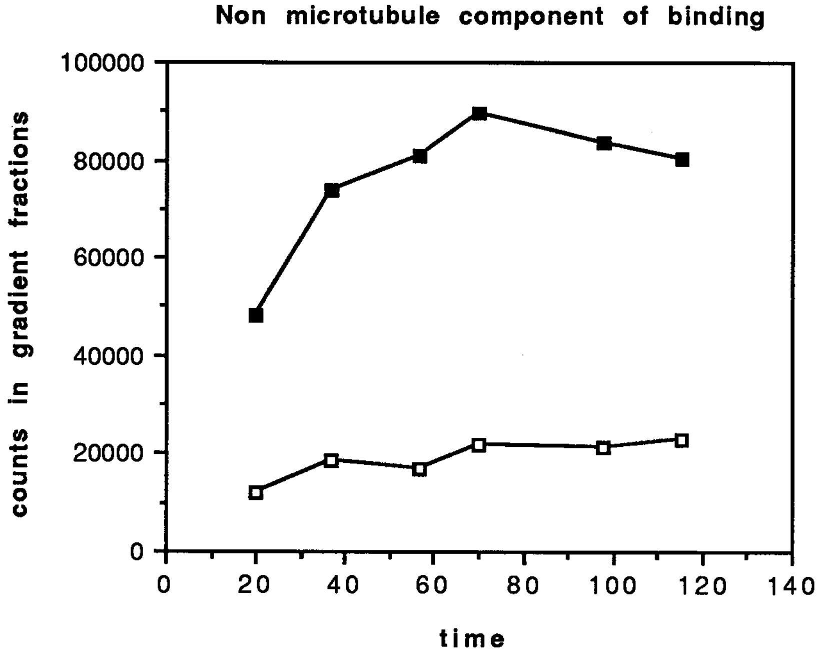

Figure 3-19. Non-microtubule component of binding. Spermatid-ESs reacted with ^3MT_X (*solid squares*) or microtubule depleted ^3MT_X (^3MT_XSN) (*open squares*). An initial increase in binding is seen in both ^3MT_X-spermatid-ES and ^3MT_XSN-spermatid-ES binding. The average percent of binding attributed to microtubule component of binding was 75%.

Table III-II. Non-microtubule component of binding: summary

	experiment 1	experiment 2
final tubulin concentration in control sample	0.53 mg/ml (1x)	0.27mg/ml (0.5X)
percent of binding accounted for by nonmicrotubule component of sample incubated with spermatid-ESs*	25 ± 2 %	8 ± 2%
calculated percent of binding accounted for by microtubule component of sample incubated with spermatid-ESs	75 ± 2 %	92 ± 2 %
percent of label entering the gradient accounted for by non microtubule component in the absence of spermatid-ESs+	0.0 %	0.0%
percent of label incorporated into microtubule component	48%	47%

'Non-microtubule component' is the supernatant from the same labelled microtubule sample as that used for the control but first having been depleted of microtubules by high speed centrifugation substituted for the ^3MT_X sample in spins with spermatid-ESs* or with buffer only+. Controls were ^3MT_X + spermatid-ESs ('no treatment control') and ^3MT_X + buffer. The percent of label accounted for by non-microtubule component is the percent of binding in the microtubule depleted supernatant divided by the percent of binding in the control sample. Percent incorporation of label into microtubules was calculated as counts removed by centrifugation/original counts in microtubule sample before centrifugation. Results indicate that at least 75-92% of counts entering gradient can be attributed to the microtubule component of the label. Microtubule-depleted sample with buffer only (replacing spermatid-ESs) does not enter the gradient (no counts in gradient fractions).

Figure 3-20. Time course of ^3MT_X - spermatid-ES binding: overlay plots of time course from matched experiments. The source of these data is the ^3MT_X - spermatid-ES controls from seven experiments, matched with respect to microtubule concentration and time course of binding. ^3MT_X and isolated spermatid-ESs were combined at time = 0 minutes. For each time point, the percent of counts entering the gradient is expressed as a ratio of the experiment mean. Each experiment has been assigned a different symbol.

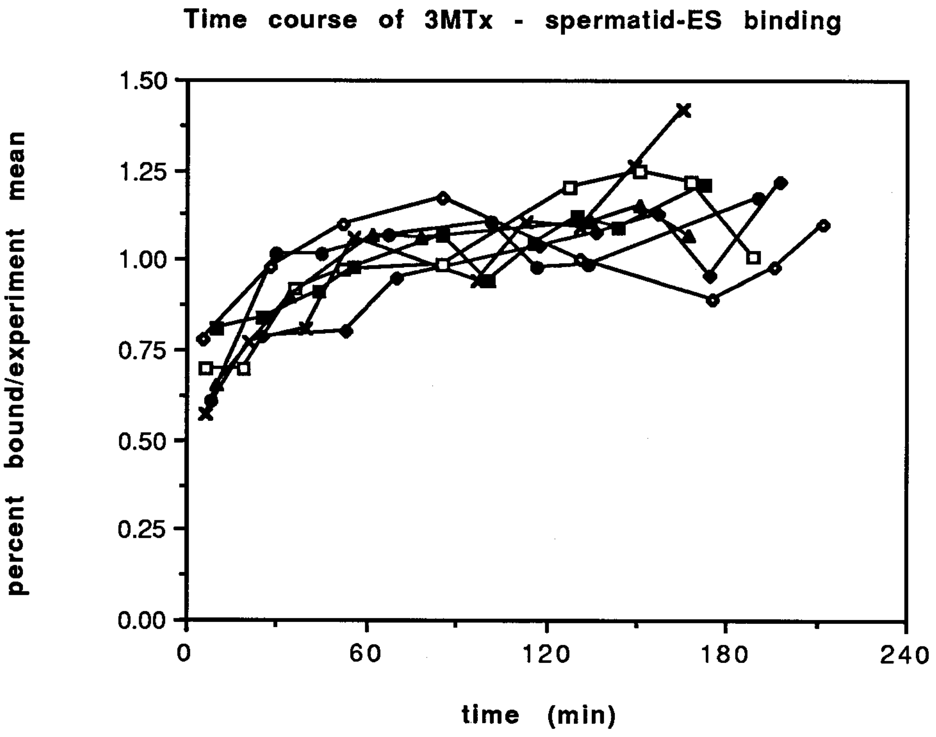
Time course of 3MTx - spermatid-ES binding
percent bound/experiment mean
1.50
1.25
1.00
0.75
0.50
0.25
0.00
0
60
120
180
240
time (min)

Figure 3-21. Time course of ^3MT_X - spermatid-ES binding: collapsed data. Values from Fig. 3-20 shown above have been collapsed into 15 minute intervals. Plot lines have been removed. Solid line indicates mean time line for the seven experiments. The time course for these seven matched experiments is consistent with a similar composite graph for the time course for all of the binding assays done in this study (not shown). There is a significant increase in binding during the first hour.

Time course of 3MTx - spermatid-ES binding (15min intervals)

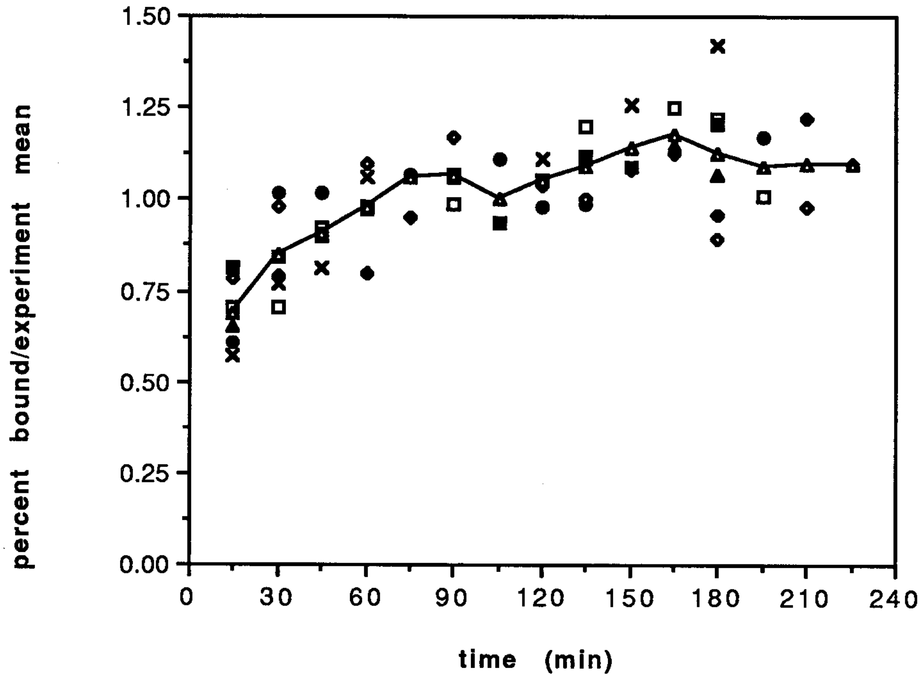

of same spin controls. Release appeared to be immediate (within the time constraints of this assay) and occured whether the ATP was added before or after binding has become established.

Support for the binding assay evidence of release by 10 mM MgATP is shown in Figures 3-22 and 3-23. Parallel samples using ^3MT_X or MT_X were incubated with spermatid-ESs, with or without 10 mM MgATP, run on gradients and processed for scintillation counting (labelled), or recovered with a needle and processed for anti tubulin immunofluoresence (unlabelled). The anti-tublin staining pattern was present in controls but essentially disappeared from MT_X - spermatid-ES + 10 mM MgATP group. Unlike the antibody staining controls seen in Figures 3-10 and 3-11, there are small remnants of staining around the spermatid head, consistent with the findings of the binding assays. The binding assay run parallel to the immunofluoresence showed a reduction to 31% of controls in 10 mM MgATP treated group.

5mM GTP is used to selectively release the mechanoenzyme, kinesin, from microtubules (Vallee, 1982). In five experiments, 5mM GTP reduced ^3MT_X - spermatid-ES binding to 43 ± 21% of controls. This compares with 10mM MgATP release values of 36 ± 14%. When 10mM MgATPATP and 5mM GTP were compared directly in the same spins, the two effects were not significantly different.

To address the possibility of the reconstitution of ATP from GTP by nucleoside diphosphokinase activity in which the phosphate from GTP is bound to ADP, GTP in the presence of 18 units/ml hexokinase and 10 mg/mlD glucose was tested. The binding was not different between the two groups.

As described with the 10 mM MgATP group data, a number of factors may be contributing to the variability in nucleotide binding release encountered. However, when 10 mM MgATP and 5 mM GTP were combined, the binding was always reduced to less than half of the binding that remained after treatment with either nucleotide alone. In some way, the effect was additive. Figure 3-24 illustrates the comparison of 10 mM MgATP, 5 mMGTP and their combined effects.

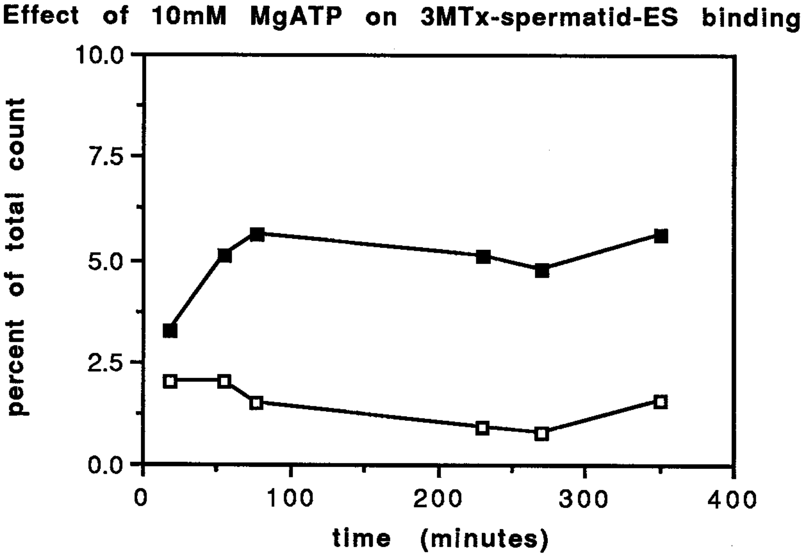

Figure 3-22. Effect of 10 mM MgATP on ^3MT_X - spermatid-ES binding. Reduction of binding following treatment with 10 mM MgATP (open squares). Treatment with 10 mM MgATP and the initiation of binding were both at time = 0 minutes. Microtubule concentration in final samples was 0.53 mg/ml. The typical time course of binding of the untreated group ^3MT_X - spermatid-ESs, resulting in an increase in binding during the first hour, is seen in the control group (closed squares). In this experiment, reduced binding by ATP treatment is evident by the first spin (at 18 minutes) and maintained. The mean ratio of 10 mM Mg ATP/same spin control values for this experiment is 27.4 ± 10.5 that is, only 27% of the binding remains after treatment with 10 mM MgATP (first spin omitted in calculation to avoid time effect).

Figure 3-23. Reduction in tubulin staining on MT_X - Spermatid-ESs binding after treatment with 10 mM MgATP. Paired DIC and fluorescence micrographs of isolated spermatids incubated with exogenous microtubules (MT_X - spermatid-ESs) that have been stained with 5A6 anti tubulin monoclonal antibody.

(a,b) MT_X - spermatid-ESs untreated control

(c,d; e,f; g,h) MT_X - spermatid-ESs treated with 10 mM MgATP. Unlike the complete absence of staining in controls for 5A6, these spermatids, treated with 10 mM MgATP, retain remnants of staining for tubulin in some cases (arrow), but staining is greatly reduced compared with the untreated controls. This is consistent with the count data from binding assays.

bars: a-h = 10 μm.

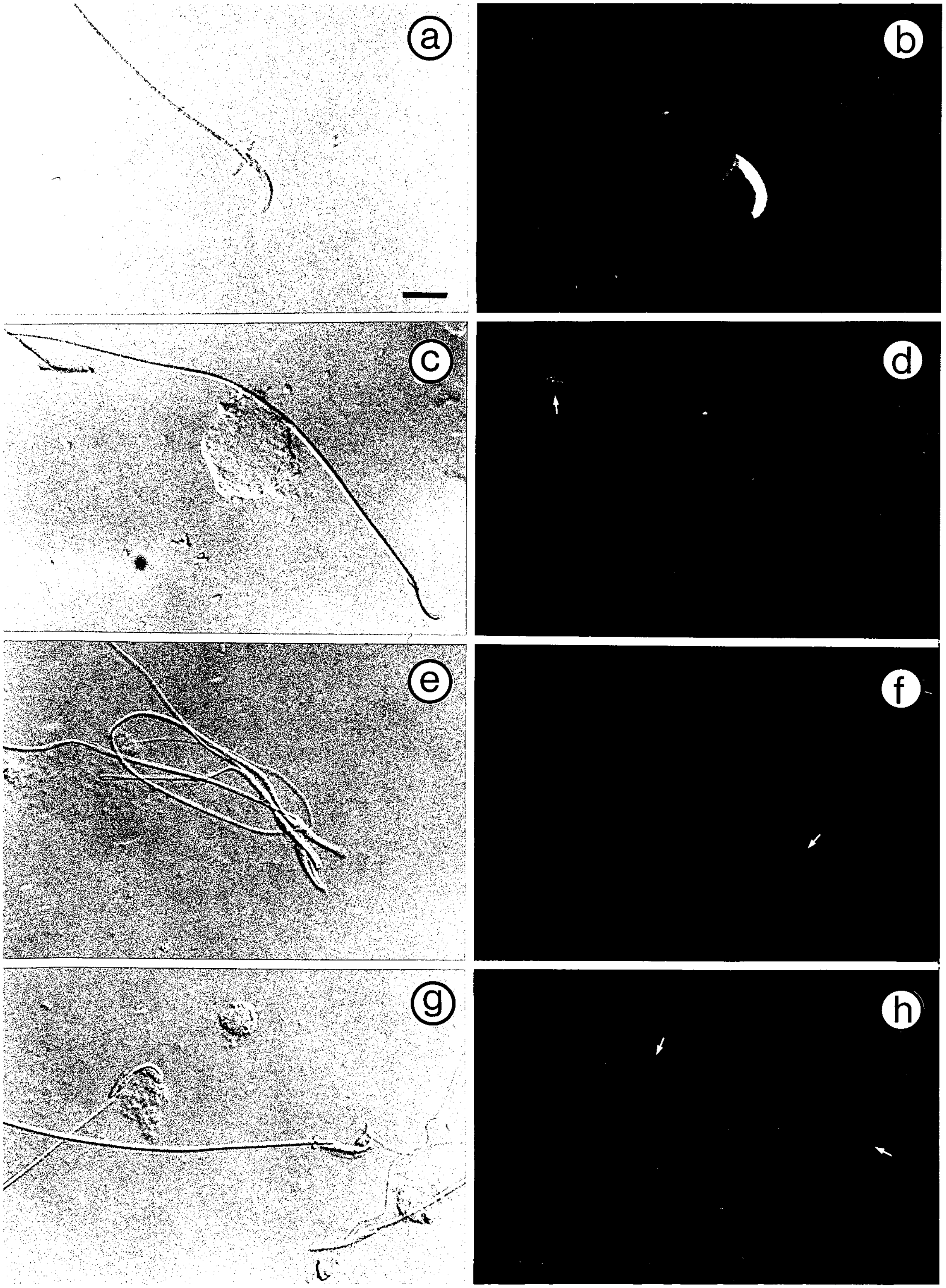
a
b
c
d
e
f
g
h

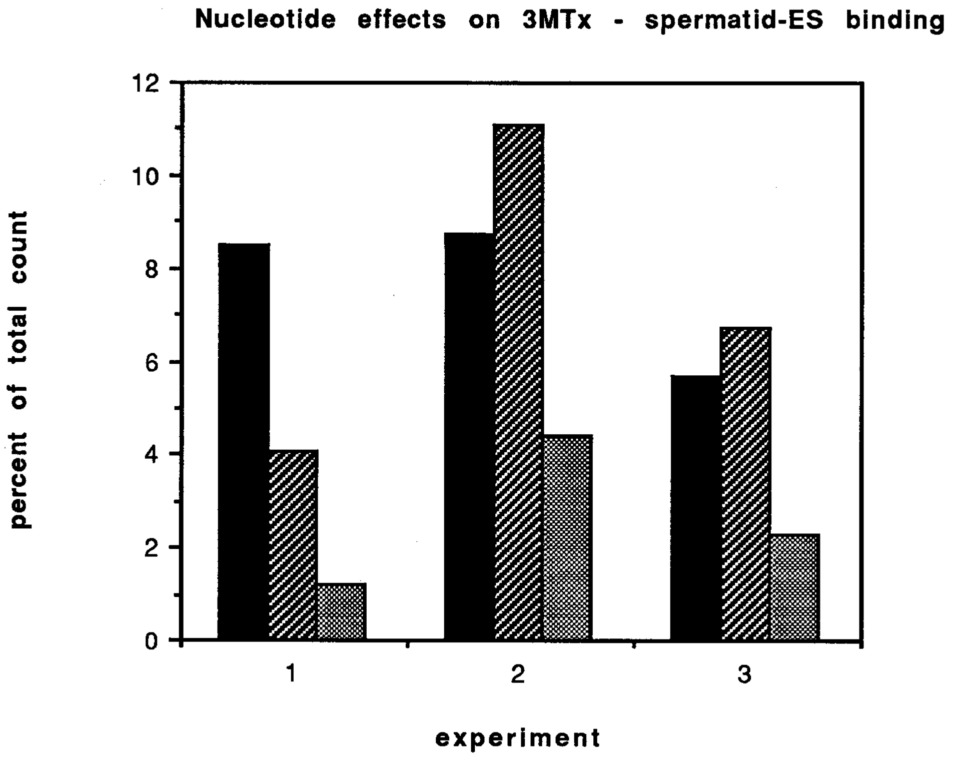

Figure 3-24. Comparison of nucleotide effects on ^3MT_X - spermatid-ES binding. Effects of 10 mM Mg ATP (*solid bar*), 5 mM GTP (*diagonal hatched bar*) and 10 mM MgATP+5 mM GTP combined (*fine hatched bar*) in the same spins. These data indicate that, under the conditions used in these binding assays, the two nucleotides combined reduce ^3MT_X - spermatid-ES binding to a greater degree than either alone.

The effect of ATP depletion on ^3MT_x-spermatid-ES binding

Another aspect of the nucleotide question to be considered was that if ATP reduces binding, will the complete depletion of ATP increase binding? Exogenous ATP was not added to the 'no treatment control groups' to avoid a possible ATP induced release. However, low levels of ATP of the capacity to regenerate ATP might retained in the spermatid-ES isolate. Because the degree to which ATP was present and its change over time could not monitored, an ATP depleting system in which hexokinase (18u/ml) and D glucose (10mM) were used to exhaust endogenous ATP was added to the spermatid-ES isolate (and to the gradient solutions).

Figure 3-25 shows 6 experiments in which the effect of ATP depletion was examined. When these 6 experiments are compared by analysis of variance, only experiments 1 and 6 are significantly different from the controls. Although experiment 5 appears to be reduced, due to the variability of measures, there is no statistical difference registered by analysis of variance. These results are consistent with the notion that in some cases the residual nucleotide is low and in others, there is sufficient ATP regenerating capability or residual ATP that there is a change in binding values when an ATP depletion system is introduced. Again, the ATP question appears to be complex. What is clear is that high concentrations of MgATP produce a release of binding and complete depletion of ATP contributes to an increase in binding in some preparations.

Microtubule concentration has a nonlinear effect on binding

The initial assumption of the binding was that it would be analogous to actin-myosin rigor and therefore not dynamic (not cycling), a condition one would expect in a purified motor-microtubule system *in vitro*. This was predicated on the finding that ATP is required for microtubule based, organelle transport *in vivo* and *in vitro* (Vale, 1987; Cohn et al., 1987; Shimizu et al., 1991). Evidence presented so far suggests that

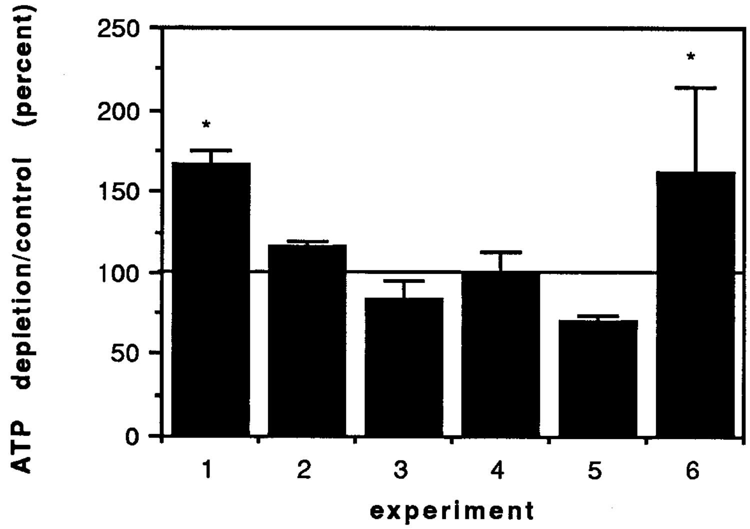

Figure 3-25. ATP depletion effect on ^3MT_X - spermatid-ES binding. Effect of ATP depletion on ^3MT_X - spermatid-ES binding in six experiments. Hexokinase and D glucose were added to buffers used in six ^3MT_X - spermatid-ES binding assay experiments, to deplete any residual ATP. Analysis of variance between ATP depleted group and controls for the six experiments indicates that binding was significantly increased by ATP depletion in experiments 1* and 6*, but not significantly different from controls in experiments 2-5. Line at 100% indicates control values. Although experiment 5 would appear to be significantly reduced from the control value, analysis of variance of all the groups compared with the variance of no spin controls, indicates that it is not.

^3MT_X-spermatid-ES binding is stable, with a time course that establishes a plateau ofbinding and an increase in binding with the removal of ATP. If that is so, then it is reasonable to expect that the effect of varying the substrate concentration would result in a linear increase in binding to a point of saturation, which would then plateau in spite of further increases in substrate concentration. ^{3}MTx - spermatid-ES binding does not fulfill that prediction.

Some variability is to be expected in the spermatid composition and between isolations. When comparing binding in the presence of a fixed concentration of tubulin while varying the spermatid-ES concentration from the same isolate, there is a linear relationship between spermatid-ES concentration and binding. This is illustrated in Figure 3-26. This leads to the assumption that, at these concentrations, an increase in available binding sites results in a proportional increase in binding.

Based on the linear relationship of spermatid-ES concentration to binding at a fixed microtubule concentration, if the number of binding sites was held constant (sampling from the same isolate) then a rigor-like binding would predict a linear relationship between binding and microtubule concentration, until saturation of available binding sites occured. Figure 3-5 shows the design of a study done to check the relationship between tubulin concentration and binding, using spermatid-ESs sampled from the same isolate. A number of precautions were taken. To ensure that incorporation of label into microtubules was not influenced by microtubule concentration, label was incorporated at the 10X concentration and all dilutions made from the same 10X stock. Binding was allowed to become established before the first spins were begun. The microtubule concentration experiment was designed to check three technical considerations: 1) do the microtubules retain their label over the duration of the experiment? 2) is the sampling of the tubulin concentrations reliable? 3) do the counts reflect the tubulin concentration? The first question was addressed by comparing the counts and their respective tubulin concentrations early and late in the experiment. There was no loss of counts or microtubule concentration, verifying that

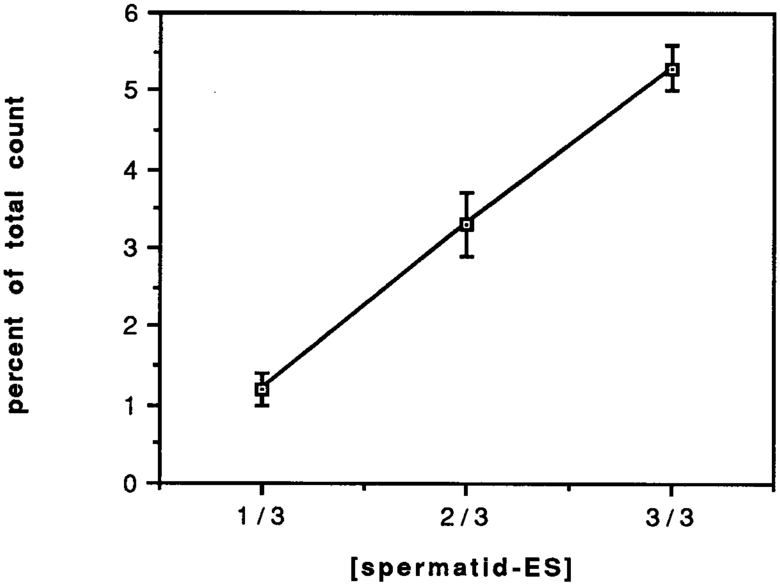

Figure 3-26. Effect of varying spermatid-ES concentration on ^3MT_X - spermatid-ES binding. Spermatid-ESs from the same isolation were diluted to 1/3 and 2/3 of controls. To avoid an effect of time, binding was allowed to proceed for two hours before [spermatid-ES] effects were tested. Samples from each of the three concentrations were included in each spin.

label does not cycle from the microtubules. This was consistent with previous findings (Wilson et al., 1985) and the known stability of taxol stabilized microtubules (Schiff et al., 1979; Horowitz et al., 1981; Vallee, 1982). Secondly, microtubule concentration in stocks did not change with repeated sampling, although there was, understandably, more variability in sampling with the lowest concentrations. Thirdly, the counts from both the assays and the microtubule concentration determination portion of the study varied in direct proporation to the assumed tubulin concentration from the stock solutions. Because dilutions were made after the label had been incorporated such that the counts loaded reflected the tubulin concentration being tested, the 'total counts' loaded on each gradient were (unlike the other assays) not equivalent. For this reason, binding data is expressed in absolute 'counts' rather than 'percent of counts loaded'.

The results of the binding assay using different microtubule concentrations are shown in Figs. 3-27 and 3-28. Binding increases with increasing tubulin concentration in a non linear manner. The slope of binding vs microtubule concentration changes at 1X concentration (Fig.. 3-28). One of a number of possible explanations is that there may be at least one low and one high affinity binding site being assayed. The binding does not show evidence of saturation even at the very high microtubule concentrations used. An attempt was made to explore the kinetics of this binding, plotting the bound/free versus bound and drawing a Scatchard plot to calculate the Km. It became evident that this system would need to be defined more precisely before the kinetics could be studied; not enough is known about the binding to make the assumptions required for kinetic analysis. These data suggest that the binding is not rigor-like; that turnover of binding may be occuring. If turnover was occuring, the introduction of excess amounts of unlabelled microtubules would replace the labelled microtubules reducing apparent binding.

^3MT_X - spermatid-ES binding is dynamic

The shape of the plot of substrate concentration vs binding suggested that ^3MT_X-spermatid-ES binding in this system, may not be static, but may be in dynamic

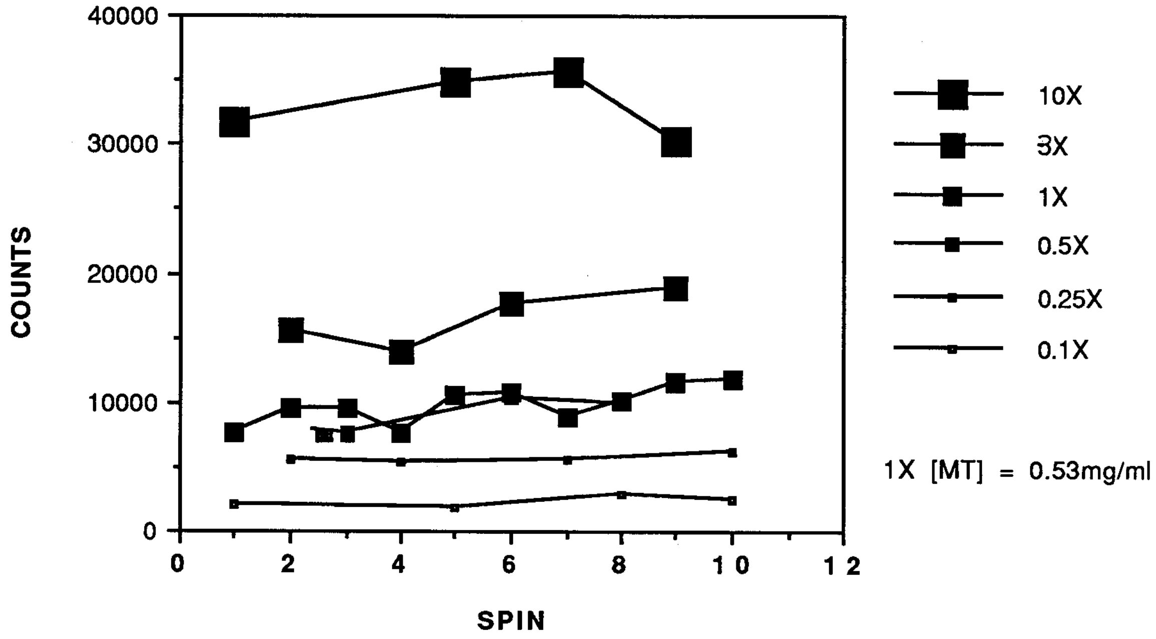

Figure 3-27. Effect of varying microtubule concentration on ^3MT_X-spermatid-ESs binding. Counts from combined 30/45 and 45/60 gradient fractions of ^3MT_X-spermatid-ESs binding using six different microtubule concentrations. Radiolabelled microtubules were polymerized and stabilized with taxol at 10X concentration (10 X 1.6 mg/ml = 16.0 mg/ml), then diluted into 0.1 to 10X samples. (Samples loaded on the gradient were 50µl ^3MT_X : 100µl spermatid-ESs). Final concentrations in binding assay, ie. after adding spermatid-ESs, were 0.1 X to 10 X (0.53 mg/ml). Microtubule concentration were assigned in varying order for two tubes, the third one being a 1X [^3MT_X] sample that was included in each spin, to act as a control. Due to randomization, two samples of 0.5X were included in spin 3: the values were the same and they have been placed side by side. Data is expressed as counts that were recovered from the gradient. Counts loaded were proportional to the [^3MT_X] because the [^3MT_X] samples were diluted after the microtubules had been polymerized and stabilized. Counts entering the gradient increased with increasing [^3MT_X].

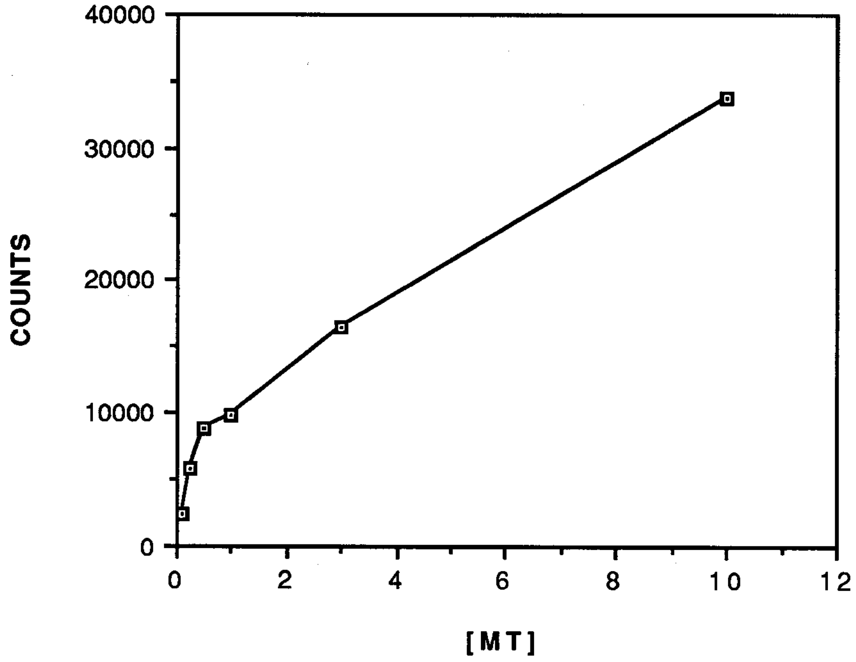

Figure 3-28. ^3MT_X-spermatid-ESs binding expressed as a function of microtubule concentration. With the concentration of spermatid-ESs held constant, ^3MT_X - spermatid-ESs binding increases with the increase in [^3MT_X]. The rate of increase is nonlinear and does not show saturation at microtubule concentrations used.

Table III-III. Effect of the addition of excess cold label: 5X cold taxol stabilized microtubules on ^3MT_x - spermatid-ES binding

^3MT_x concentration	competition by dilution by cold 5X MT_x	competition by displacement by cold 5X MT_x
1.0X	48 ± 10 %	46 ± 3 %
0.5X	18 ± 5 %	24 ± 2 %

To test the effect of competition of unlabelled microtubules (cold) with labelled microtubule-spermatid-ES binding, excess unlabelled microtubules (50µl/ gradient of 5X concentration of unlabelled microtubules MT_x) were added either at the onset (dilution) or after established binding (displacement) of 50µl of ^3MT_x and 100 µl spermatid-ESs. 50 µl of buffer only were added to the controls to compensate for the addition of 50µl of ^3MT_x. 1X tubulin concentration = 1.6 mg/ml (before being added to the spermatid-ESs). Competition of cold label at the onset of binding would have the same effect as diluting the labelled microtubules at a time when binding sites are equally available to labelled and non labelled microtubules. Competition after the establishment of binding (here over 1 hour) indicates the degree to which the unlabelled microtubules are able to displace already bound ^3MT_x. These experiments show that microtubules bound to spermatid-ESs can be displaced, suggesting a turnover of binding.

Table III-IV. Effect of the non-microtubule component of 5X cold taxol stabilized microtubule sample on ^3MT_x - spermatid-ES binding

^3MT_x concentration	competition by dilution by supernatant from cold 5X MT_x	competition by displacement by supernatant from cold 5X MT_x
1.0X	83 ± 8 %	94 ± 6 %
0.5X	68 ± 8 %	69 ± 11 %

The purpose of this part of the study was to determine the effect of the microtubule and non microtubule components of cold competition. Aliquots of non labelled 5X microtubules were pelleted and the **supernatant** used as a microtubule-depleted control for the experiments described above. These data indicate that it is primarily the microtubule component of the excess cold label (5X cold MT_x) that is responsible for the effect of competition to ^3MT_x - spermatid-ESs binding.

In both tables, figures quoted are percent of same spin control

equilibrium. To test this, binding (no treatment control) was compared with apparent binding (competition by the addition of an excess of unlabelled microtubules). ATP was not added to the system, nor was it depleted: the isolate was the same as for 'no treatment controls' of all the binding assays. If the excess of unlabelled microtubules are added at the onset of binding, they simply represent a dilution of label by competing directly for the available sites. The reasoning was: if unlabelled microtubules are added after binding has become established, the unlabelled microtubules will need to replace already bound labelled microtubules. A change in apparent binding would indicate turn over of binding. Eventually the number of labelled microtubules may approach that in the diluted group, but only if the system is dynamic. To avoid the effects of dilution of spermatid-ESs by the addition of microtubules, buffer, equal to the volume of added unlabelled microtubules, was added to the controls. This has the effect of increasing the microtubule concentration in the test sample while decreasing it in the control. However, the result of the minor changes in tubulin concentration, according to the data presented above, would be to increase binding, the opposite effect expected if unlabelled microtubules compete with labelled microtubules. Table III-III shows the effects of cold competition of 5 fold concentration of microtubules added to compete with labelled microtubules. The binding was reduced following competition with added excess unlabelled microtubules. This would suggest that labelled microtubules had been removed, and replaced by unlabelled microtubules.

If microtubules are responsible for the reduced binding by competition, then removing them from the competing sample should eliminate the competition effect. As had been done to measure the microtubule component in the labelled binding, the unlabelled sample was centrifuged to remove pelletable microtubules leaving a $5XMT_X$supernatant. Table III-IV shows the dilution and competition effects of the non-microtubule component of $5XMT_X$sample on binding. Comparison of tables III-III and III-IV indicate that the majority of the competition effect can be attributed to microtubules.

Characterization of ^{3}MTx - spermatid-Es binding

If ^3MT_X - spermatid-ES binding, like that of cytoplasmic dynein and kinesin, can be reversed by added nucleotides, it most likely posesses ATPase activity. However, because binding can be competed off by unlabelled microtubules, it may be undergoing a slow turnover. In order to further characterize ^3MT_X-spermatid-ES binding, it was measured in the presence of agents known to affect MT-mechanoenzyme interaction. As described in Chapter 1, the effects of a variety of agents that have been used to characterize mechanoenzyme activity and binding to microtubules depends on the conditions of the binding, the source of the mechanoenzyme and the nature of the activity being tested (for example: motility vs ATPase activity). Very few studies have examined the effect of these inhibiting agents on binding directly. The plan here was to select a number of agents that are known to alter MAP-microtubule interactions and use them to characterize ^3MT_X-spermatid-ES binding with a view to comparing these properties with other organelle-MT binding, bearing in mind that these agents may be affecting more than one site and/or protein.

A number of agents (see table III-V) were used to test their affect on ^3MT_X-spermatid-ES binding. A series of experiments were then carried out using these agents in a design matched in time course, including early and established binding, and as nearly as possible in substrate concentration, to characterize ^{3}MTx - spermatid-ES binding. Based on the assumption that a high affinity binding may be occuring at the lower tubulin concentrations, the matched series were carried out with 0.5X microtubule concentration. Results from these experiments showed the effects were similar at 1X and 0.5X microtubule concentrations.

The agents used to characterize binding were: 10 and 100 μM vanadate, 2 mM NEM, 1 mM EHNA, 1 mM AMPPNP, added cytoplasmic dynein enriched MAP prep, Sertoli cell enriched cytosol, unlabelled excess microtubules, 5 mM GTP (with and without depletion), and ATP depletion with hexokinase and D glucose. The effect of 10 mM MgATP

Figure 3-29. Characterization of ^3MT_X - spermatid-ESs binding: matched experiments. Data from a series of experiments designed to re-examine a number of treatments using conditions matched as closely as possible for substrate concentration and time course (see methods). Each experiment included an early binding series in which inhibitors were added to spermatid-ESs immediately before combining ^3MT_X and spermatid-ESs, and an established binding series in which binding was allow to become established before adding the inhibitor. It provides for the characterization of binding with respect to a number of properties of ^3MT_X - spermatid-ESs binding. ***In all of the graphs in this figure, solid squares (-■-) are 'no treatment controls' (^3MT_X - spermatid-ESs).***

(top left) "cold 5X MT_X competition" shows the 'apparent' decrease in binding following cold competition by the addition of an excess of unlabelled microtubules (-□-) and the supernatant from the excess cold microtubules binding (-▲-).

(top right) Binding with added Sertoli cell cytosol from 21 day old rat testis (■--■), and cytoplasmic dynein enriched testis MAP preparation (-□-). ANOVA shows that overall, the effects of adding either the Sertoli cell cytosol or the cytoplasmic dynein enriched MAP preparation are not significant. While there did appear to be an increase in binding in the presence of early addition of cytoplasmic dynein enriched MAP preparation, at each time period, it was not significant by ANOVA at the concentration used.

(middle left) ^3MT_X - spermatid-ES binding is significantly decreased with 100µm vanadate (-▲-) but not 10µm vanadate (-□-).

(middle right) ^3MT_X - spermatid-ES binding is significantly decreased with 2 mM NEM (-□-) but not 1mM EHNA (-▲-). The late treatment group is joined by dotted line. The spin at 190 minutes is from the early treatment group.

(bottom left) ^3MT_X - spermatid-ES binding is significantly reduced by 5 mM GTP (-○-) with or without ATP depletion. The addition of ATP depletion enzymes hexokinase and substrate D-glucose to GTP (to remove any contamination of ATP in the GTP) did not change the result (-▲-).

(bottom right) ^3MT_X - spermatid-ES binding was not significantly altered by the nonhydrolyzable ATP analogue AMPPNP (-□-).

unlabelled 5X MTx competition

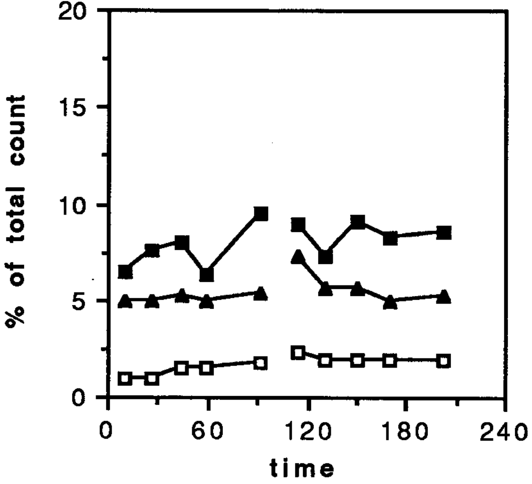

Sertoli cell cytosol and cytoplasmic dynein enriched MAPs

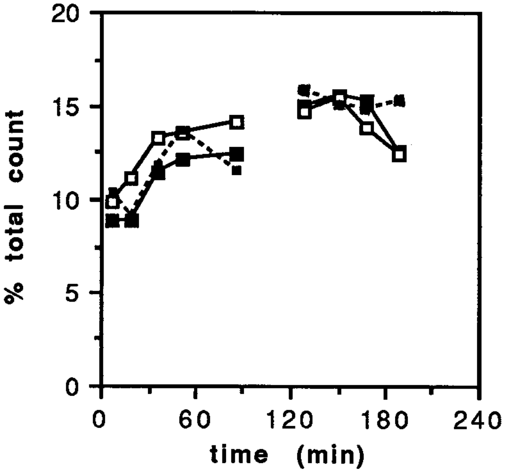

10 μM and 100 μM vanadate

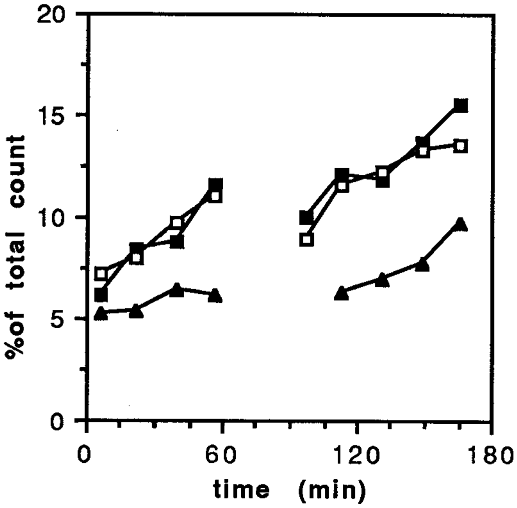

2mM NEM and 1mM EHNA

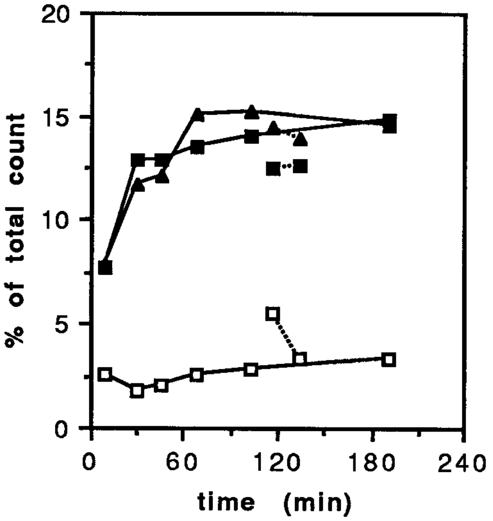

5mM GTP+/- ATP depletion

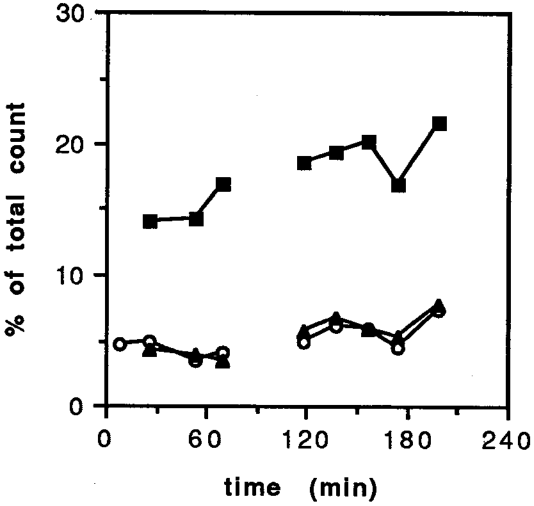

1 mM AMPPNP

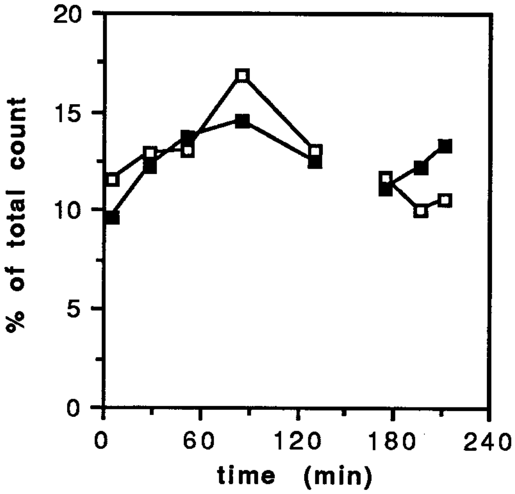

Table III-V. Effects of selected agents on ^3MT_X- spermatid-ES binding

CHARACTERIZATION OF ^3MT_X - SPERMATID-ES BINDING		
Condition tested	**Early binding**	**Established binding**
10 mM MgATP	↓	↓
5 mM GTP	↓	↓
5 mM GTP + ATP depletion	↓	↓
1 mM AMPPNP	↔	↔
10 µM vanadate	↔	↔
100 µM vanadate	↓	↓
1 mM EHNA	↔	↔
2 mM NEM	↓	↓
Sertoli cell enriched cytosol	↔	↔
Cytoplasmic dynein enriched MAPs	↔	↔
excess unlabelled microtubules	↓	↓

This chart summarizes the effects of a numbers of selected treatments on ^3MT_X-spermatid-ES binding. Changes in binding, which were found to be significant by ANOVA and pairwise comparisons using Tukey's test (at $p= \leq .01$) are indicated as ↓ decreased, ↑ increased or ↔ unchanged.

was tested on all these treatments. The effects of these agents are shown in Table III-V. Those indicated as changed were significantly different from same spins controls by analysis of variance of all experiments involving that agent. To illustrate the nature of these differences, sample data from the matched series of experiments are shown in Figure 3-29.

All agents were tested at the onset of binding and after binding had become established. Only the dynein enriched MAP preparation showed any difference between early and late binding; however, its effect on binding was not statistically significant at this dynein concentration. The effect of treatment is not affected by timing. It may be that the dynamic nature of the binding eliminates any effect of early or late use of the agent as a factor in binding.

LOCALIZATION OF LABEL TO SPERMATID HEADS

Labelled microtubules are localized to the spermatid-ES

There are a number of pieces of evidence that support the contention that microtubules bind to spermatid-ESs. 1) Under the assay conditions, microtubules do not enter the gradient alone, 2) The major source of label found in gradient fractions is from microtubules, 3) The presence of label in the gradient fraction is reduced with the addition of 10 mM MgATP, 4) Label can be competed away with excess cold microtubules. 5) Binding is dependent on substrate concentration, and 6) Binding is inhibited by some of the same inhibitors that affect other MAPs. Morphological data shows that spermatid ESs are highly enriched in gradient fractions. It follows that the microtubules are attaching to the spermatid-ESs and with an enzyme profile that is influenced by agents that similarly affect known mechanoenzymes. However, none of this data directly addresses the question: Are microtubules binding to the head of the spermatid, that is to the zone covered by ESs? It has been shown here, that isolated spermatid-ESs stain for actin and, following cold isolation, stain weakly and variably for tubulin, but, when isolated under warm conditions, retain long strands of tubulin positive structures.

Autoradiography experiments were carried out to localize the label, taken to be a correlate for exogenous microtubules. Tissue was prepared for the autoradiography experiments in the same way as for the binding assay, except to avoid deleterious effects of freezing, gradients were sampled from the side of the centrifuge tube with a syringe. Pre-gradient samples (stock as loaded onto gradient) and samples that had been treated with 10 mM MgATP were included in the study. Parallel binding assays were run.

In the pre-gradient samples, label was associated with a number of structures, including spermatids, round structures and clumps of debris. After being enriched and "washed" by the gradient the amount of label (due to unbound microtubules and nonspecific label) was reduced, and primarily observed in association with two structures, spermatid heads and amorphous clusters of unknown origin. Bearing in mind that microtubules do not enter the gradient on their own, any 'free' label is likely to be primarily from two sources: 1) background picked up by the emulsion, or by contamination (preliminary experiments showed some contamination occurs when sampling from the side) and 2) label released after entering the gradient, including labelled microtubules that have come free from attached spermatids. A series of experiments were done to examine the content of amorphous clusters to see if they contained ESs, as defined by having a coexistence of actin and tubulin (see below).

Micrographs in Fig. 3-30 are paired DIC and bright field images to show the distribution of label in pre-gradient samples. DIC images allow for identification of the morphology of the structures and brightfield enhances the identification of label. Figure 3-31 shows paired images from gradient material from 'no treatment controls'. Label was seen associated with spermatid heads as would be predicted for 3MTx - spermatid-ES binding. Very little label was seen associated with the (membrane covered) spermatid tail. Figure 3-32 shows paired images of gradient material from 10 mM

Figure 3-30. Localization of label in ^3MT_X - spermatid-ES binding from pre-gradient autoradiography samples. Localization of label in ^3MT_X - spermatid-ES binding was followed, by autoradiography.

(a, b; c, d) Localization of radioactive label, from ^3MT_X, on spermatid-ES isolate, after being allowed to develop in the dark for three weeks. Paired DIC and bright field images have been included to show the structure and highlight the spots produced by development of emulsion by beta particles emitted from [^{3}H]GTP label incorporated into exogenous microtubules. These micrographs illustrate the location of the label in ^3MT_X - spermatid-ESs samples before being loaded onto gradients. Label is associated with spermatid head (*arrows*) as well as other cellular material.

bars: a-d = 10 µm.

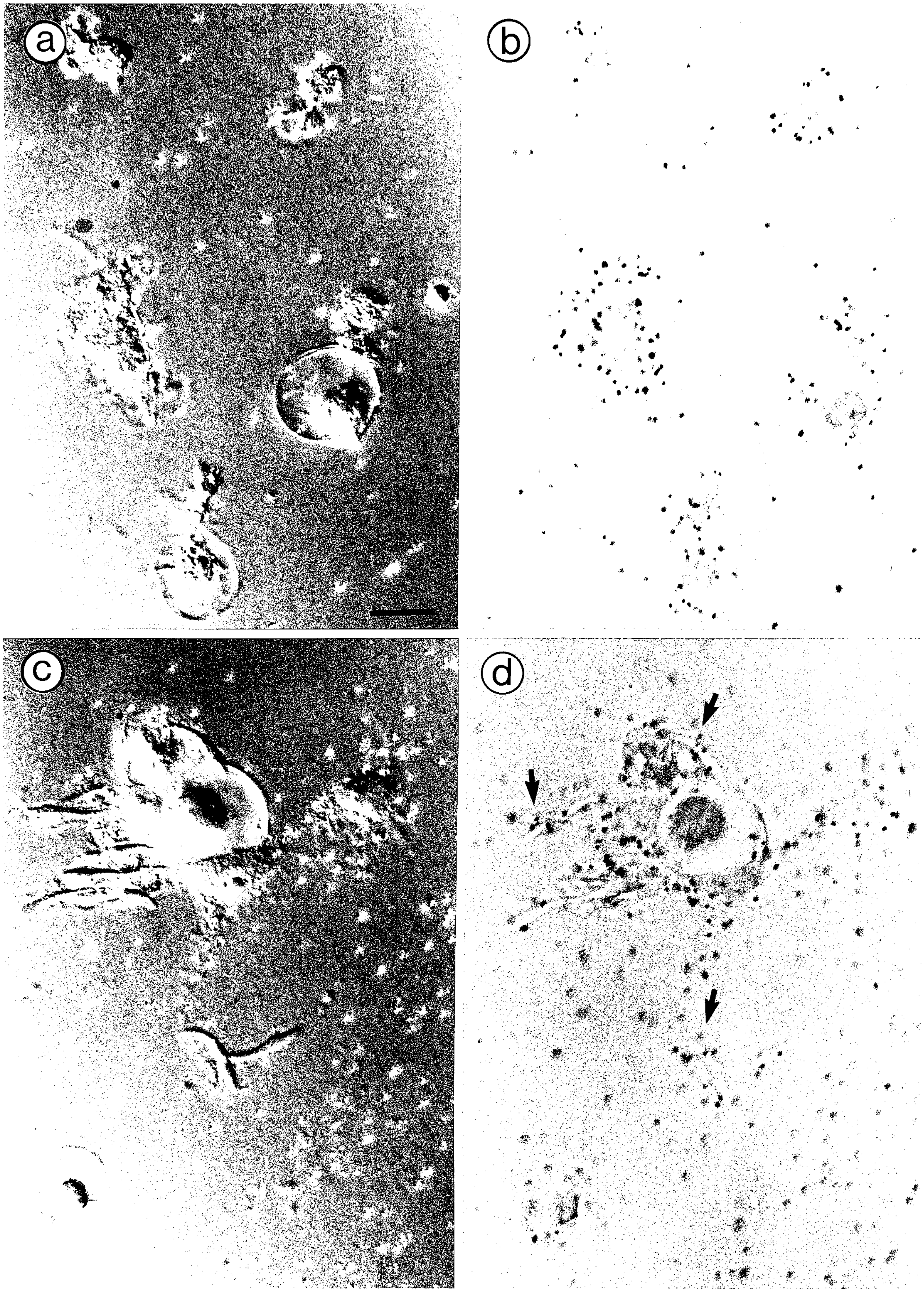
a
b
c
d

Figure 3-31. DIC and brightfield micrograph pairs to show localization of label in $^{3}MT_{X}$ - spermatid-ES binding from gradient autoradiography samples.

(a,b; c,d; e,f) Paired DIC and bright field images of label in $^{3}MT_{X}$ - spermatid-ES binding, sampled from the 30/45 gradient fraction, in autoradiography experiments sampled at three weeks. DIC images show the spots produced by $^{3}MT_{X}$ label (*white dots*) and the structures with which they are associated. While DIC images allow for the better visualization of structure, bright field images enhance the visualization of the autoradiography spots (*black spots*). Label was mainly associated with two types of structures, the heads of spermatids (*arrows*) and amorphous clumps as shown in e and f (*arrow heads*).

bars: a-f = 10 μm.

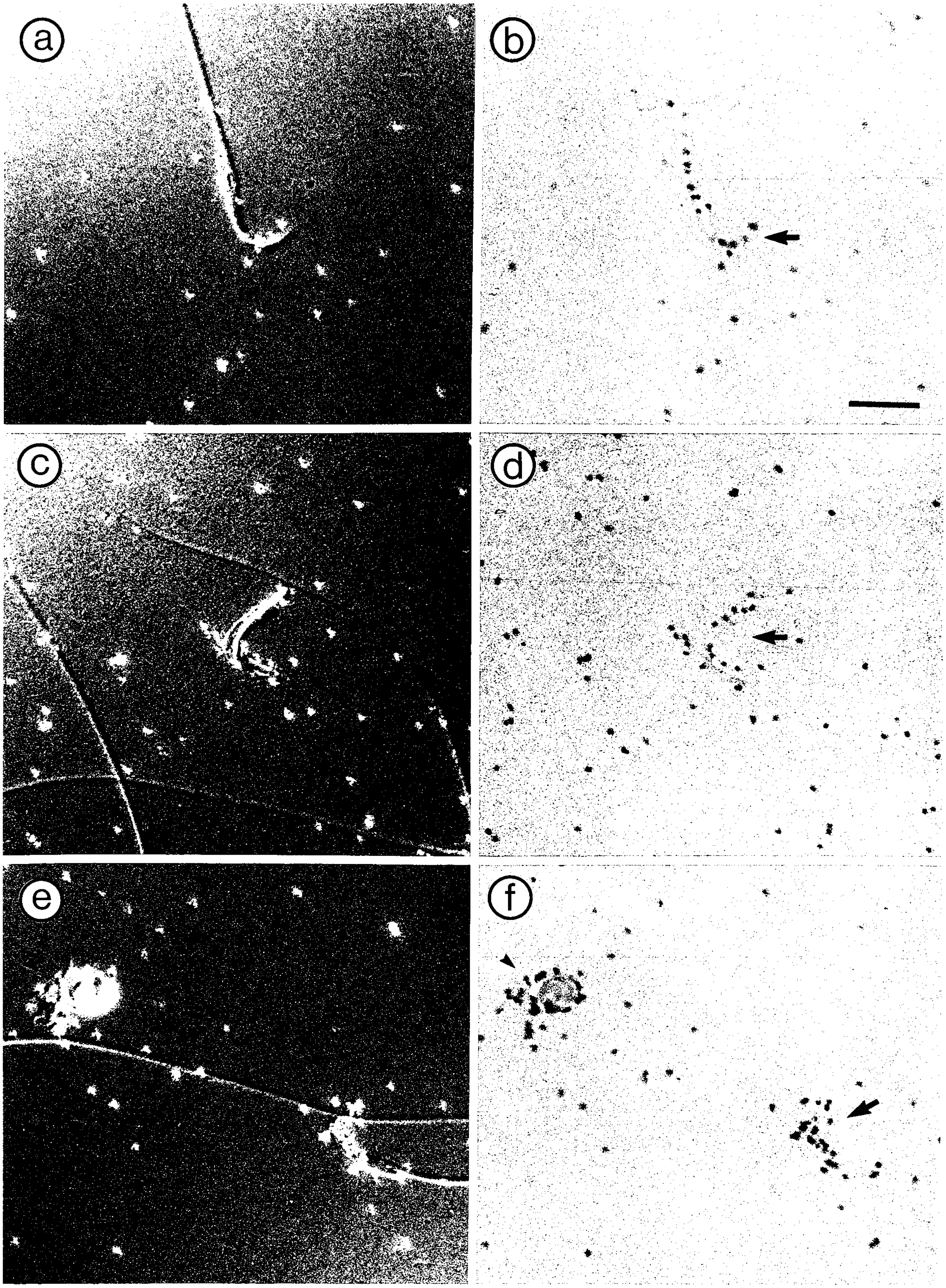
a
b
c
d
e
f

Figure 3-32. DIC and brightfield micrographs pairs to show localization of label in ^3MT_X - spermatid-ES binding, in the presence of 10 mM MgATP, in gradient autoradiography samples. These paired DIC and brightfield images (a,b; c,d; e,f) show the limited association of labelled ^3MT_X with spermatid heads, following treatment with 10 mM MgATP. Label is seen as white spots in DIC images (a,c,e) and black spots in bright field images (b,d,f). The three samples show the effect of ATP on a range of spermatid stages. Comparison of these results with those of the previous figure shows that label that is associated with spermatid heads in ^3MT_X - spermatid-ES binding is markedly reduced with the addition of 10 mM MgATP.
bars: a and b = 10 μm.

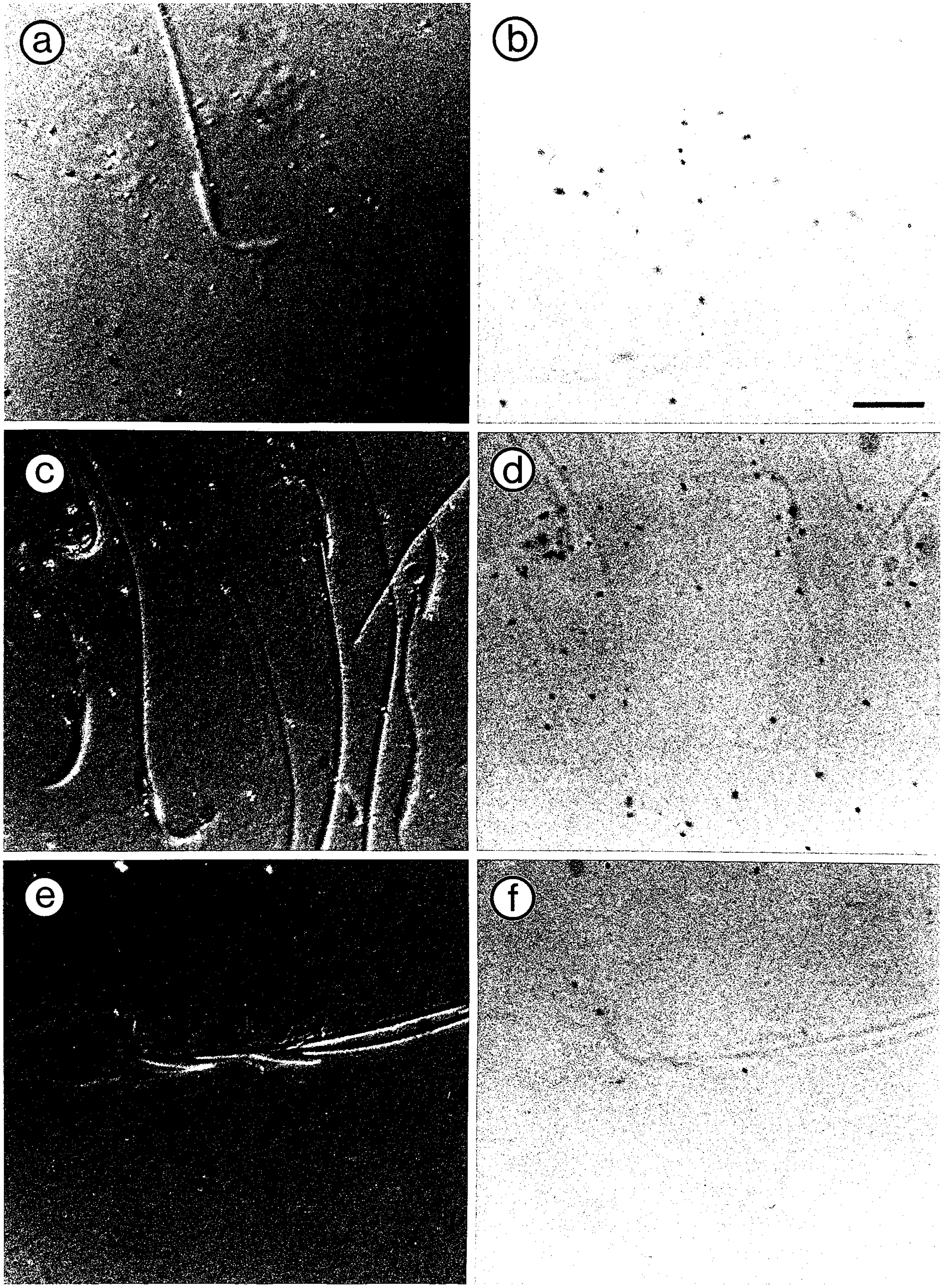
a
b
c
d
e
f

MgATP treated samples. Label is greatly reduced and is not associated with spermatid heads to the same degree as in untreated samples.

These results are consistent with those described earlier, (Fig. 3-23) in which the 5A6 anti tubulin antibody staining was observed on 10mM MgATP treated material and no treatment controls from gradient fractions. The tubulin staining was greatly reduced following treatment with 10mM MgATP. Unlike controls without primary antibody, some remnants of tubulin staining remained.

Actin and tubulin dual staining of amorphous clusters

In some areas, label was associated with amorphous clusters of unknown material. In some DIC images, varying the focus revealed what appeared to be heads, embedded in some of the larger clusters. Similarly processed tissue (without label) was stained with rhodamine phalloidin to identify actin, to see if ESs were present in amorphous clusters. Figure 3-33 shows head shaped actin staining, in some clusters, indicating that some of the larger clusters may contain ESs. Figure 3-33: c,d show clumping of material that occasionally occured following processing of gradient material. Figure 3-33: g,h shows the round cells that were sometimes present, but did not stain for actin.

It was reasoned that if microtubules were brought into the gradient on ESs, tubulin would only be present on actin staining structures. On the other hand, not all actin staining structures would necessarily have tubulin. Figure 3-34 shows dual staining of samples from 'no treatment control' gradient fractions, stained to identify both tubulin and actin. Most spermatids heads stained for both actin and tubulin. Those structures that stained for tubulin, also stained for actin. However, those that stained for actin did not always have associated tubulin (see Fig. 3-33: d,e,f, for a head that has lost its tubulin staining, and Fig. 3-33: g.h.i for cellular material that is positive for actin but not tubulin). These may have been ESs that had been separated from the spermatid heads during processing.

Figure 3-33. Actin staining of amorphous clusters, like those seen in the autoradiography slides, show that ESs are frequently present in the clusters. Amorphous clusters, found in gradient fractions, stained with rhodamine phalloidin for filamentous actin. Clusters are similar to those seen in gradient fractions in autoradiography experiments. These experiments were carried out to answer the question: Are there ESs in the clusters seen in autoradiographs? Shown is material from samples that had been recovered, by needle, from gradients and fixed and treated with cold acetone, as was done for autoradiography samples.

(a,b; , c,d; e,f; g,h) are DIC and fluorescence micrograph pairs that show the structure and filamentous actin staining of structures similar to clusters seen in the autoradiographs. Many of the clusters stained for actin and, in addition, the shape of spermatid heads can be seen in many of the DIC images (arrows). Not all clusters stained for actin see e,f and g,h pairs (arrowheads). Many of these clusters appear to contain spermatid heads or remnants of ESs.

bars: a-h = 20 μm.

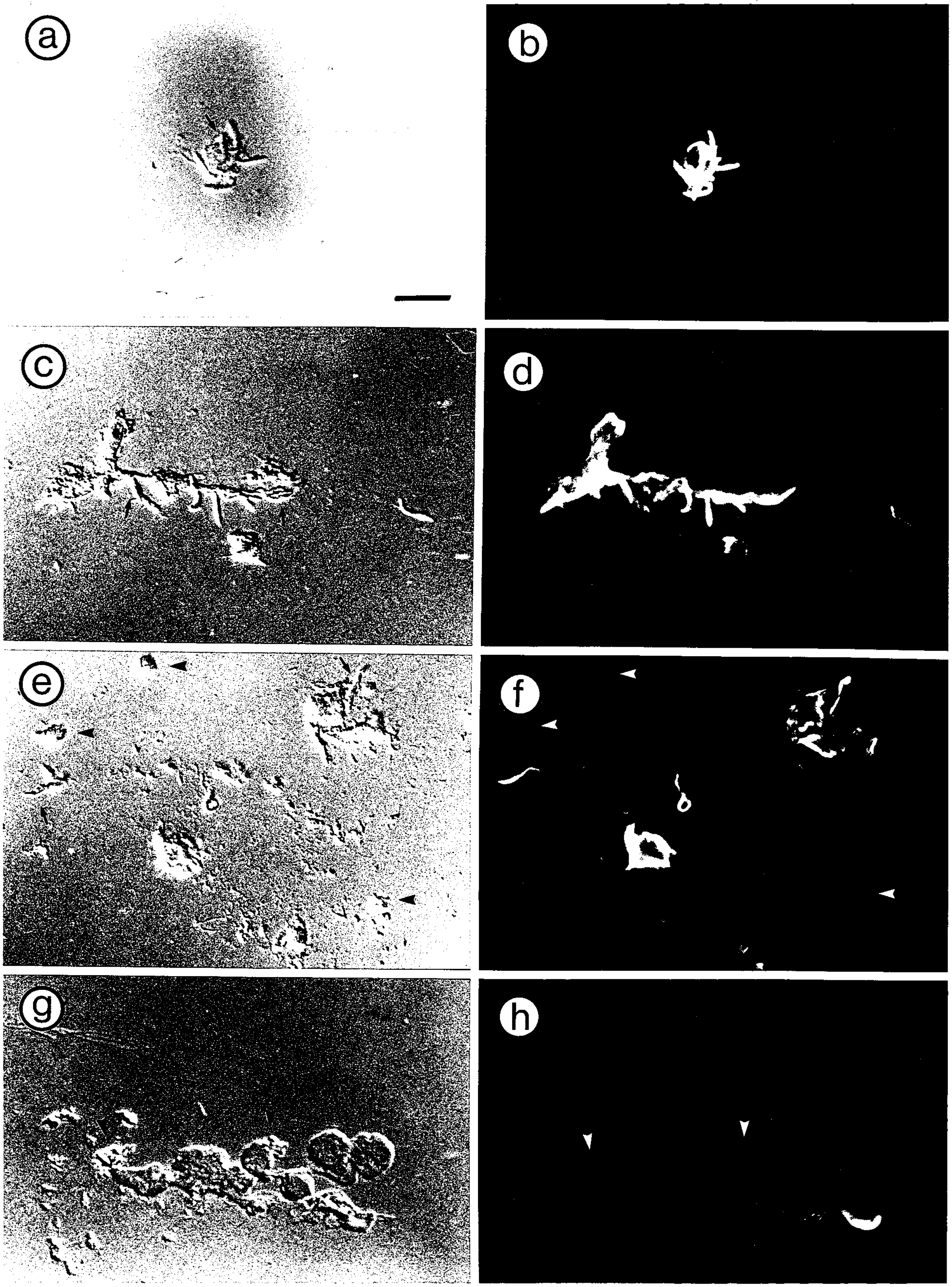
a
b
c
d
e
f
g
h

Figure 3-34. $^3MT_{X}$ - spermatid-ESs stain for both actin and tubulin. Dual staining of $^3MT_{X}$ - spermatid-ESs showing the presence of both actin and tubulin in $^3MT_{X}$ - spermatid-ES and in other structures that may be remnants of ESs that have adhered to the polylysine coated slides. (a, d, g) phase contrast images; (b, e, h) staining for tubulin; (c, f, i) staining for actin. The dual staining shows that in all structures where tubulin staining is positive, actin staining is also positive. The reverse is not the case: not all actin staining is accompanied by positive tubulin staining (*arrows*) see spermatid head that stains for actin but not tubulin in figs (d-f). Note the clusters that stain for actin but not tubulin in figs (g-i). This would suggest that these structures may contain ESs with associated microtubules, possibly disturbed by processing. Although ESs may be present without microtubules, microtubules are not present without the ES (*actin*).

bars: a-i= 25 μm.

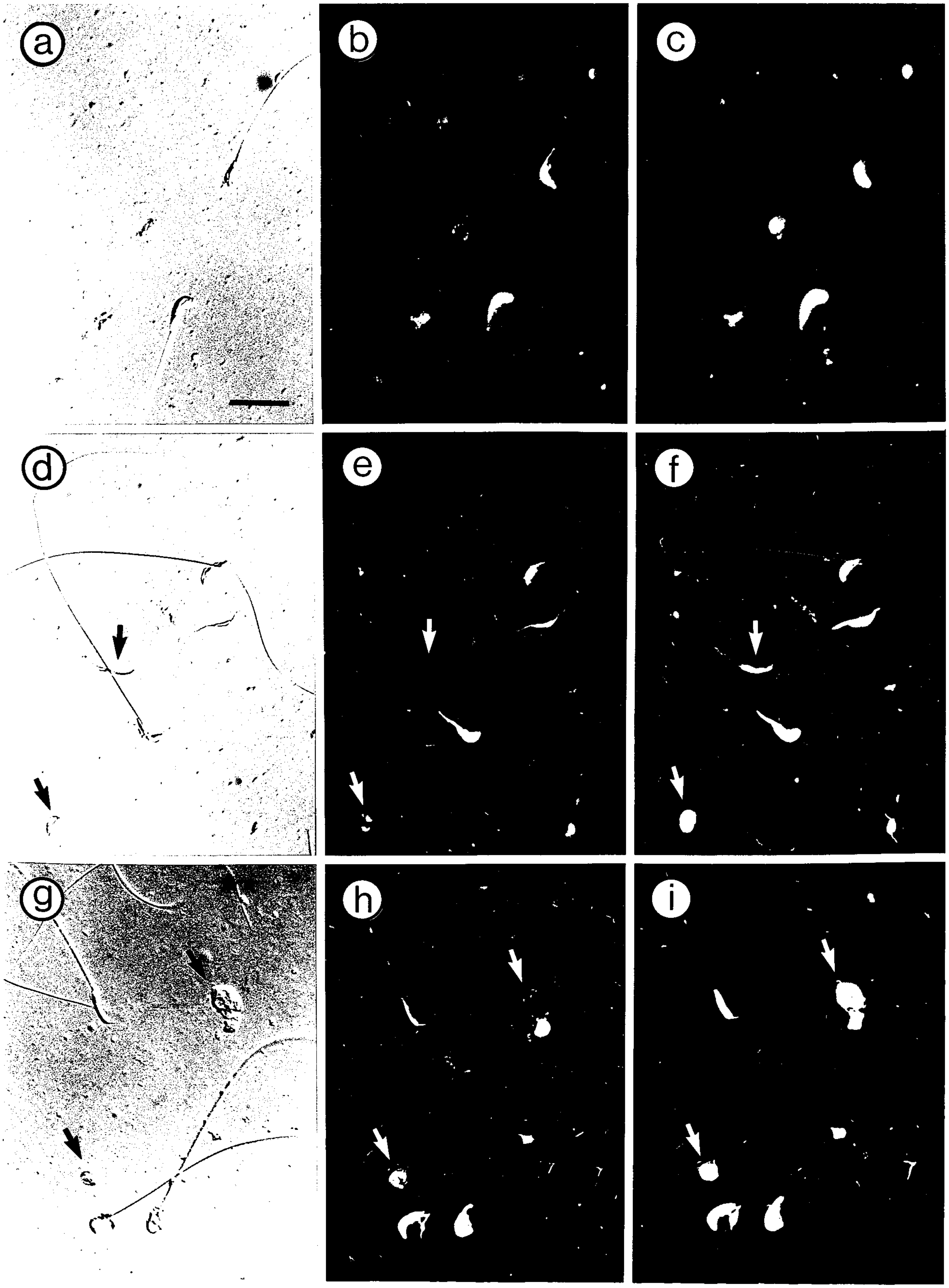
a
b
c
d
e
f
g
h
i

Pursuit of a proposed regulation of events around the spermatid-ES

Elongating spermatids are transported in two directions during spermatogenesis, toward the base of the epithelium between stages IV and V and returned to the lumen during stage VI. The function of this basal migration is not known; nor is its regulation. Equally, the means of regulating microtubule based transport in systems generally, is not known. In the axon, minus-end and plus-end directed transport occurs in the presence of kinesin and cytoplasmic dynein, each exclusive in their direction of transport. It is not known how their direction is specified. There is very little information as to whether motors coexist on the same organelles, how the appropriate motor is activated, or how its direction is assigned. Based on the evidence that endoplasmic reticulum plays a calcium sequestering role in cells generally (Somlyo, 1984), it has been proposed that ER serves to produce local microenvironments for the regulation of the multitude of calcium-dependent events in cells which may include microtubule-based transport (Burton et al., 1985). The ESER is situated between two cytoskeletal elements, actin and microtubules differentially sensitive to calcium. Using precipitation of calcium by antimonate, Franchi and Camatini (1985) reported that calcium is sequestered in the ESER, in the guinea pig; however, work by Kierszenbaun and coworkers (1971) showed localization of calcium in early spermatids, and a double line of extracellular precipitate, but no Sertoli cell deposits, surrounding late spermatids, in the mouse. To explore the role of the ESER, an attempt was made to verify the findings of a calcium sequestering activity of the ESER. A variety of protocols were used in an attempt to demonstrate the reported calcium uptake in the ESER.

The pyroantimonate methods gave mixed results (methods 1-4) which depended on the technique and did not support, nor refute a conclusion that calcium is sequestered in ESER (Fig. 3-35,36 and 37). Method one (Kierszenbaum et al., 1971; Tandler et al., 1970), used by Kierszenbaum and coworkers to show an intercellular distribution of potassium antimonate adjacent to late spermatids in mouse testis, demonstrated the same intercellular distribution in rat testis. The double lines of precipitate described, in mouse testis, were seen only occasionally in rat tissue and were within the Sertoli cell- late spermatid intercellular space. If the method, using prolonged fixation with antimonate and hardening with paraformaldehyde (Kierszenbaum et al., 1971; Tandler et al., 1970), was completed with incubation in OsO_4 (Fig. 3-35), no precipitate was seen in the ESER. Without the final OsO_4, there was a loss of membranes and more dispersion of precipitate (not shown). If the tissue was preincubated with calcium chloride or EGTA, it was not materially changed (method: 3). Antimony was included in the prefixation rinse after the EGTA incubation, and being able to successfully compete with EGTA for calcium, may have stabilized the calcium location. The EGTA preincubation may not have performed its initial intent, to act as a control in which calcium ions were removed.

The second method, incorporating fixation in combined 2% glutaraldehyde and 2% K-pyrantimonate (Klein et al., 1972) as used by Franchi and Camatini, to show intercellular and ER location of antimonate in quinea pig testis, showed very limited precipitate in the ESER and a wide spread distribution of precipitate throughout intercellular space (Fig. 3-36). Although there was only limited vesiculation of ESER in these sections, it contrasts with the data presented by Franchi and Camatini in which the ESER is highly vesiculated. In addition they show widening of the intercellular space, a finding not seen in this study.

The fourth method, most frequently used in calcium localization studies, consisted of incubation in combined antimony and OsO_4. With this method there was considerable vesiculation of ESER, which often contained precipitate. However, precipitate was also spread throughout the cytoplasmic space and was not present in the intercellular space (Fig. 3-37). The high degree of vesiculation of the ESER, and the presence of precipitate throughout cell, casts doubt on whether the precipitate is identifying calcium in the ER or has actually been captured after precipitate formed.

The three other methods tried gave poor results. No precipitate was seen in testes or cardiac muscle with method 5: oxalate antiomny method of Borgers et al., 1977). Using the NHA method, described by Zechmeister (1979), no precipitate was seen in rat testis or cardiac muscle. Using the tetrabutylamonium fluoride method (Poenine and Epel, 1987), deposits of precipitate coalesced into large deposits that bore no relationship to any specific structure. No data is shown from these methods.

These results, using the precipitation of calcium antimony to localize calcium in testis, in part, replicate previous findings and extend the information on localization of calcium in testis. However, taken together, they are contradictory and indicate that this method does not provide satisfactory evidence of celcium sequestration by the ESER.

Figure 3-35: Localization of calcium in seminiferous epithelium (Method 1). Micrograph of rat testis, treated with potassium antimony for calcium localization (method 1).

(a) Using method 1, precipitate is almost exclusively in an intercellular (arrow heads) location, with occasional evidence of entry into the cell (long arrow), but not localized within ESER (short arrows).

(b) A higher magnification of the area marker with a large arrow in (a) shows the precipitate to be between the germ cell membrane (on the left of the precipitate) and Sertoli cell membrane (on its right). Microfilaments and the endoplasmic reticulum of the ES are seen just deep to the Sertoli cell membrane.

(c) Rat cardiac muscle (control for method 1) shows antimony is present in the sarcoplasmic reticulum and in intracellular location (small arrows). Antimony has had to cross the cardiac myofiber membrane to precipitate calcium within the sarcoplasmic reticulum or in the myofibrillar space, as shown here.

bars: a = 1 µm, b = 0.25 µm, c = 1 µm.

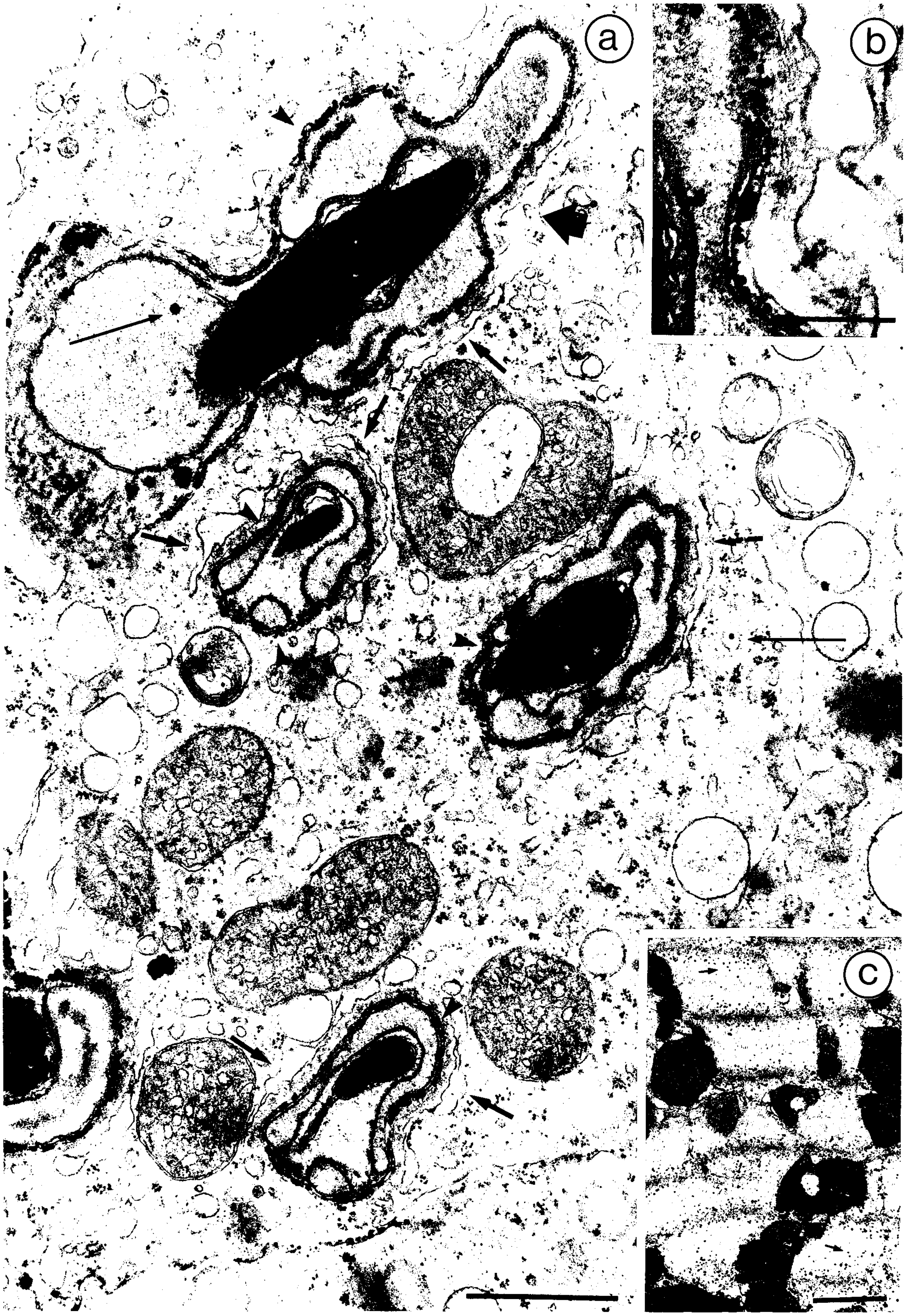
a
b
c

Figure 3-36: Localization of calcium in the seminiferous epithelium (Method 2). Micrograph of rat testis treated with potassium antimony using method 2.

(a) Extensive intercellular precipitate (short arrows), occasional ESER precipitate (arrowhead) and large deposits in intracellular vesicles are seen surrounding late spermatids.

(b) Antimony depostis mainly in intracellular vesicles (long arrows) and intercellular location.

(c) ESER does not contain antimony, but intercellular deposts are seen (short arrows).

bars: a = 1 μm, b = 1 μm, c = 0.5 μm, d = 0.5 μm.

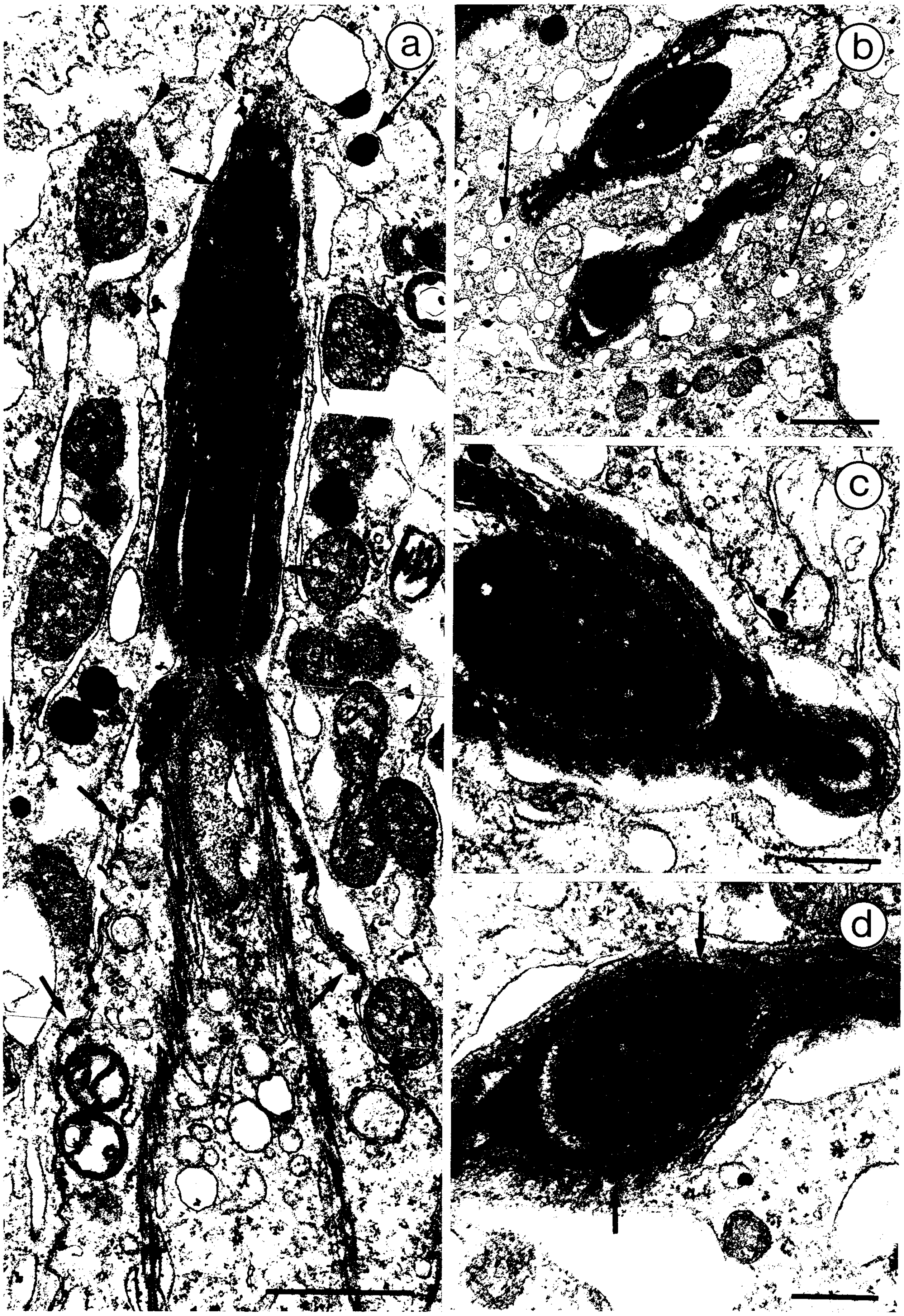
a
b
c
d

Figure 3-37: Localization of calcium in seminiferous epithelium (Method 4), Localization of antimony precipitate using a method mostly commonly used in calcium localization experiments. Here precipitate is in ESER in some areas (small arrowhead) but not others (large arrowheads). It is also located in vesicles in the cytoplasm (short arrows) as well as being 'free' in the cytoplasm (long arrows). The light background of the cytoplasm suggests that the cytoplasm has been extracted from this cell and the 'free' calcium may be attached to remaining cytoskeleton. Extensive vesiculation of the ESER occurs with this method and with longer incubation, membranes are lost.

bars: a,b = 0.5 μm.

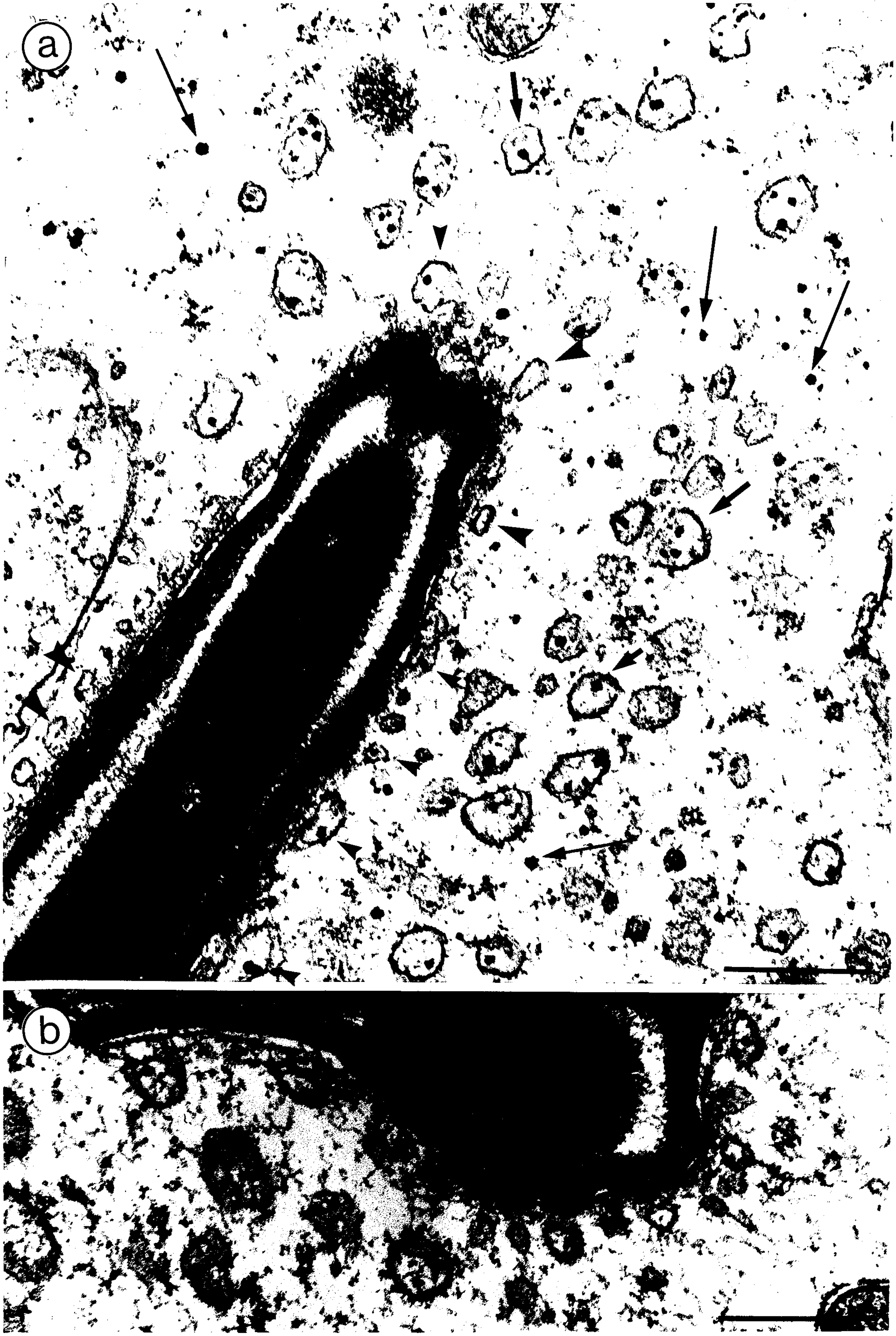
a
b

DISCUSSION

The findings of this part of the study, designed to test binding between Spermatid-ESs and microtubules, are summarized here. The results and specific conclusions that can be drawn from these findings are summarized in this section. The implications of these findings and their relevance to the proposal that spermatids are transported through the seminiferous epithelium by a microtubule-based transport mechanism are discussed in Chapter 4.

COMPONENTS OF THE BINDING ASSAY

Spermatid-ESs

The components used in the binding assays, isolated spermatid-ESs and labelled taxol assembled bovine brain microtubules, were acceptable representatives of their *in vivo* counterparts: spermatids with ESs and Sertoli cell microtubules. The spermatid-ES isolation method developed for the binding assays, involving poking and then gentle squashing of the seminiferous epithelium, yielded spermatids from all stages. Isolation of spermatids from segments of seminiferous tubules that had been staged by transillumination, showed that all stages of elongate spermatids could be recovered by this spermatid isolation technique. This was further supported by the presence of all spermatid stages in the isolated tissue as seen in the micrographs from this study. The presence of ESs on isolated spermatids was indicated by bright actin staining with rhodamine phalloidin, in a shape characteristic of ES distribution, and by microfilament networks, in electron micrographs. These observations are consistent with the findings of others in which ESs remained intact during mechanical isolation of spermatids (Romrell and Ross, 1979; Franke et al., 1978; Grove and Vogl, 1989; Masari et al., 1987; Vogl, et al., 1986), with profiles of ESER still attached. When removed from the confines of Sertoli cells, in buffers without sucrose, the ESER tends to dilate, and in some cases break into smaller vesicles, still attached to the actin network. Some dilation of the ESER was still present in EMs of spermatids isolated in PEM buffer with 100 mM sucrose. Therefore, to protect the ESER further from osmotic effects, 250 mM sucrose was used in all buffers, as employed by Pratt to protect organelles from osmotic damage in the isolation of vesicle-microtubule complexes (Pratt, 1986).

Endogenous microtubules, were retained during isolation of spermatid-ESs under warm conditions, and seen as long strands that extended beyond the ends of spermatid heads, with anti-tubulin immunofluoresence. These were largely removed during isolation under cold conditions. In contrast, exogenous microtubules stabilized with taxol, used in the binding assay were seen closely associated with the spermatid head, using the same tubulin probe. This is consistent with the exogenous microtubules, assembled with taxol for this study, being an average length of of 2.8 μm (about 15 to 20% of the length of the spermatid heads). Endogenous microtubules, depolymerized during the cold isolation, may have reassembled; however, they would be unlabeled and therefore 'ignored' by the binding assay. Immunocytochemical staining of spermatid-ESs, that had been incubated with exogenous microtubules and recovered from gradients, indicated that tubulin was present only on spermatids that stained positively for filamentous actin. Not all actin containing structures stained for tubulin. This suggests that the presence of ESs was necessary for the presence of microtubules, but microtubules were not present without ESs.

Labelled, taxol polymerized microtubules remained stable throughout the assay. Exogenous microtubules were labelled with $[^3H]$GTP. Assembled from bovine brain tubulin, in the presence of taxol and substoichiometric amounts of $[^3H]$GTP, they incorporated an average of 43 ± 9.2% of the available label. The number of counts left in the supernatant by pelleted, labelled microtubules, divided by the number of total counts in the ^3MT_X sample, (X100) was taken as the percent of label incorporated into microtubules, bearing in mind that some microtubules may be of insufficient length to pellet. Some breakdown of GTP during storage and preparation steps could be anticipated. Label did not cycle from microtubules during the time of the experiment, indicating that the microtubules were stable. Similar microtubule stability was reported by Wilson and coworkers (Wilson et al., 1985) and is further supported by the observation that binding did not appear to decline over the course of the binding assay experiments. If microtubules were cycling and thereby losing their label, there would have been an 'apparent' reduction in binding (detected by counts), but not real binding of labelled and unlabeled microtubules. Microtubule stability was unchanged in the presence of all agents used to characterize microtubule binding and therefore did not contribute to the changes in binding that occurred with these agents.

THE BINDING ASSAY MEASURES MICROTUBULE- SPERMATID BINDING

Effects of the sucrose gradient

SDS gel electrophoresis and scintillation counts from gradient fractions, indicated that microtubules did not enter the gradient alone, with the differential centrifugation parameters used in these assays. In addition to 'washing out' of unbound microtubules, the sucrose gradient served to provide a fraction enriched for spermatid-ESs, having separated them from the other cellular components of the isolate. Therefore, the counts in the gradient were primarily associated with spermatid-ESs.

Counts represent microtubule binding

The possibility remained that even though microtubules became labelled, other sources of label such as breakdown products of [^{3}H]GTP may have taken part in non specific binding with spermatid-ESs and thereby entered the gradient. To address this possibility, it was necessary to determine what proportion of the label that entered the gradient, in these assays, could be attributed to microtubules. Microtubules were removed from ^3MT_x stock, by pelleting, giving a 'microtubule free' ^3MT_x supernatant. Measurement of binding with ^3MT_x or with 'microtubule free' ^3MT_x supernatant, in the same spins, provided a measure of the microtubule and non-microtubule components of the label that entered the gradient sample and therefore the microtubule and non-microtubule components of binding. Between 75-92% of counts found in the gradient fractions could be attributed to labelled microtubules. Taken together, these data support the interpretation that: 1) the majority of counts present in the gradient are associated with spermatid-ESs can be attributed to microtubules, and 2) that the majority of counts represent specific ^3MT_X-spermatid-ES binding.

MAP isolation procedures, particularly for mechanoenzymes, take advantage of the fact that high concentrations of nucleotides can be used to release microtubule binding proteins from microtubules. In this study, the reduced number of counts present in the gradient fractions, following the addition of 10 mM MgATP, supports the interpretation that it was microtubules that were bound to spermatid-ESs. Furthermore, binding is directly influenced by changes in either spermatid-ES or microtubule concentration, supporting the interpretation that spermatid-ESs and microtubules are both involved in the binding.

Binding time course

After an initial increase during the first hour, binding remained relatively stable over the course of the experiment, in untreated controls. Scheel and Kreis (1991), in an assay of endocytic carrier vesicle-microtubule binding report a similar time course, with an increase in binding over the first 45 minutes. This may represent the time required for the system to stabilize. There was an expected variability between experiments. This was dealt with, in part, by expressing binding as a percent of same spin controls. Similarly, the effects of treatment agents showed some variability between experiments: therefore, the significance of treatment effects was tested by analysis of variance.

Effects of added nucleotide

The amount of ATP, present or being replenished in the spermatid-ES isolate was not known. Hexokinase uses ATP as its exclusive substrate for the breakdown of D-glucose and is widely employed as a tool to deplete ATP from the cell contents. In this study, ATP depletion from spermatid-ES isolate resulted in increased microtubule binding in some, but not all, binding assays to which it had been added. A possible interpretation is that binding may have increased as a result of ATP depletion, in some cases and in the others, that either the ATP was not depleted sufficiently to affect binding, or that ATP, (or the capacity for its renewal) was already very low, in those samples.

The concentrations of nucleotides, 10 mM MgATP and 5 mM GTP, chosen to test for binding release in the binding assays were guided by experiments in which nucleotides were used to release mechanoenzymes from microtubules during mechanoenzyme isolation (Paschal et al., 1987). The effect of 10 mM MgATP was tested in virtually all binding assays in this study, both on 'no treatment controls' as well as on the treated groups. Binding was reduced in every case. The addition of 10 mM MgATP reduced binding to an average of 36 ± 13% of 'no treatment controls'. Although the values from these data tended to cluster into two groups, the differences between these two groups could not be determined from the available data. 5 mM GTP reduced binding to 43 ± 21% of controls. In preparations containing cytosolic enzymes, nucleosidase diphosphokinase activity removes the terminal phosphate from available nucleotides to reconstitute ATP. This can result in the presence of ATP in GTP containing solutions (Paschal et al., 1989; Vallee et al, 1989). In assays in which 5 mM GTP was added, in the presence of hexokinase and glucose to deplete ATP, binding was not different from the addition of GTP alone. Increasing the Mg concentration did not change the GTP effect (1mM $MgCl_2$ was present in all buffers). The effect of 10 mM MgATP and 5 mM GTP were not statistically different when they were compared in the same spins. However, when they were combined, binding was reduced to less than one half of that of either agent alone. One of a number of explanations for the apparent additive effect of ATP and GTP is that the effects of the two nucleotides may be mediated at different binding sites. What is evident is that high levels of both ATP and GTP reduce ^3MT_X-spermatid-ES binding. AMPPNP, a non hydrolyzable analogue of ATP did not significantly change binding. It is of interest to note that, in experiments testing AMPPNP effects, values were somewhat lower than in controls; however, taking into account the between experiment variability, the difference was not significant.

Competition by unlabeled microtubules

Under the conditions of these assays, competition by excess unlabeled microtubule competition may indicate that there was slow turnover of ^3MT_X-spermatid-ES binding. This is based on the evidence that label is not cycling from microtubules and labelled microtubules can be competed away by the addition of excess unlabeled microtubules. The turnover was unlike the rapid turnover that would occur during the dynamic binding and release in microtubule based motility, in which case insufficient rigor complexes would have formed to detect binding. However, it suggests that these events are ATP dependent and potentially dynamic. Competition by unlabeled microtubules supports the contention that the label in gradient fractions is microtubule in origin.

CHARACTERIZATION OF BINDING

^3MT_X-spermatid-ES binding was reduced by 2 mM NEM and high concentrations of vanadate, but unchanged by EHNA, low concentrations of vanadate, and the addition of Sertoli cell enriched cytosol and MAP enriched preparations. Binding was reversible with the addition of MgATP and GTP and unchanged with AMPPNP. Depletion of ATP by hexokinase and D-glucose increased binding in some preparations. The relevance of these observations are discussed in Chapter 4.

LOCALIZATION OF ^3MT_X-SPERMATID-ES BINDING

Label associates with spermatid heads

Data from the binding assays supported the contention that microtubules were able to bind to isolated spermatid-ESs, but did not localize the binding. The autoradiography data indicated that the label, shown to be primarily microtubule origin in gradients, was associated with two structures in autoradiographs.

In pre-gradient samples, label was more intense and widely distributed than in gradient samples. This is in keeping with the presence of both bound and unbound microtubules. In the pre-gradient samples, label was associated with spermatid heads but not exclusively. In gradient samples, where unbound microtubules were not present, label was associated mainly with the heads, but not the tail of spermatids. Immunocytochemical staining of material, treated in the same manner as the autoradiography samples, showed that the microtubules are localized to the heads of MT_X-spermatid-ES complexes. Taken together, these data support the conclusion that the label is indicative of microtubules and that they bind to spermatid heads

On autoradiographs, the label on ^3MT_X-spermatid-ESs treated with 10 mM MgATP is reduced in number and is no longer associated with microtubule heads. This provides further support for the specificity of binding to the spermatid head. There are a number of possible explanations for the retention of some label in ^3MT_X-spermatid-ESs treated with 10 mM MgATP. Because 10 mM MgATP is included in the gradient solutions, further microtubule release may occur in the gradient. Also, it was observed in preliminary experiments that sampling gradient fractions from the side of the tube, as was done for the autoradiography experiments, results in some contamination by label. Finally, as explained below, rinse steps tended to wash spermatids from slides, possibly separating ESs from the spermatid heads. For these reasons, the observations were not quantified.

Localization to amorphous clusters

Label associated with small amorphous clusters of unknown composition. To determine the source of these clusters and their composition, two approaches were used. The first was to see if the clusters were present in the gradient samples or if they had formed as a result of processing. Samples of gradient fractions were observed with DIC microscopy before any processing was carried out. Only occasional clusters were observed in those samples. However, after processing for immunofluoresence, clusters were observed more frequently, often containing DIC images of spermatid heads. These were thought to be effects of rinsing of the slides during preparation. The concentration of spermatids was reduced by processing, indicating that spermatids were being displaced from the slide. The second approach was to determine if the clusters contained ESs, either having been separated from the spermatid heads, or clumped together during processing. The presence of actin, detected with rhodamine phalloidin, was considered to be evidence of the presence of ESs. Samples, treated in the same manner as the autoradiography samples, were double stained to identify actin and tubulin. Actin and tubulin were frequently associated with amorphous clusters, suggesting that they may contain ESs that were associated with material that accumulated during processing, or separated from spermatids. This is consistent with an observed loss of spermatids, from glass slides, during processing. Moreover, tubulin staining did not occur without actin, suggesting that the presence of microtubules required ESs.

ANTIMONY PRECIPITATION EVIDENCE OF CALCIUM IN ESER IS INCONCLUSIVE

The contradictions between reports of calcium localization in guinea pig (Franchi and Camatini, 1985) and mouse (Tandler et al., 1970) testis may be related to the techniques used, rather than species differences. The methods of antimony precipitation to localize calcium, used in these studies were repeated in rat testis with similarly contradictory results in the same species. The use of other techniques, all of which have been used to localize calcium in a variety of tissues, increased the range of possible interpretations. Method 3, was developed to address the possibility that calcium ions moved from their *in vivo* location as a result of treatment with fixatives. In this case the antimony acts as the primary fixative, with aldehyde fixatives added after antimony has precipitated calcium in its *in vivo* location. That would indicate that calcium, in significant amounts to be identified, is only present in the intercellular space. The tissue preservation is better in these sections. The fact that antimony acts as the primary fixative and that it identifies intracellular calcium in cardiac muscle, suggests, but does not prove, that it is not prevented from entering the cell. It may be that calcium enters the cell in tissue which loses membrane before it is fixed and vesiculation surrounds calcium that would otherwise be in the intercellular space. The enormous range of variations in antimony precipitation methods used to localize calcium may be an index to the difficulty interpreting this technique. The only conclusion available from this work is that corroborative methods are needed before it can be accepted that calcium is present in the ESER.

CHAPTER 4

DISCUSSION

INTRODUCTORY REMARKS

The purpose of this study has been threefold: firstly, to determine the polarity of Sertoli cell microtubules; secondly, to examine the potential for binding between ESs and microtubules; and lastly, to characterize that binding. It has been shown in this study, that Sertoli cell microtubules are oriented with their minus-ends directed toward the apical surface of the cell. This observation has important implications for the Sertoli cell and for cells generally. Data from the MT-spermatid-ES binding assays, reported here, indicate that ESs are able to bind microtubules. The binding can be released by ATP and GTP, and shares properties with organelle-microtubule binding in other systems. These findings are consistent with a role for microtubules in positioning spermatids within the seminiferous epithelium and the hypothesis of a microtubule-based transport mechanism for spermatid translocation.

MICROTUBULE POLARITY IN SERTOLI CELLS

In a number of recent reviews of the mechanisms involved in the organization of intracellular organelles (Kreis, 1990; Kelly, 1990a,b; Schroer and Sheetz, 1991), the authors have emphasized the importance of microtubule orientation to organelle distribution, in particular, the need to account for the observation that microtubules in polarized epithelial cells may be organized differently than those in many cell types on which the classical model has been based. In view of the microtubule dependence of many cellular events, many of which are mediated by mechanoenzymes with a preferred direction of transport, the orientation of cytoplasmic microtubules has important consequences for these events, particularly in epithelial cells.

The hook decoration method has been used to determine microtubule polarity in a number of cells and cell free systems. Unipolar microtubule arrays have been demonstrated in cat post-ganglionic sympathetic fibers (Heidemann et al., 1981), chicken sensory neurites (Bacallo et al., 1989), rat hippocampal neurons and frog olfactory neurons (Baas et al., 1988; Burton and Paige, 1981), angelfish and teleost melanophores (Euteneuer and McIntosh, 1981; (Phillips and Satir, 1988), teleost photoreceptors (Troutt and Burnside, 1988a) and heliozoan axopodia (Euteneuer and McIntosh, 1981), sunfish retinal pigmented epithelial cells (Troutt and Burnside, 1988b), Madin Darby canine kidney (MDCK) cells (Bacallao et al., 1989), and *Drosophila* wing epidermal cells (Mogensen et al., 1989). The only exception to the unipolar distribution of cytoplasmic microtubules, reported thus far, are the bipolar microtubule arrays that have been described in dendrites ((Baas et al., 1988; Burton, 1988). Interestingly, in developing nerve processes all neuronal microtubules are unipolar and have their positive end directed toward the cell periphery until the first sign of dendritic specific morphology, at which time dendrite microtubules become bipolar (Baas et al., 1989).

In the majority of cell types studied, cytoplasmic microtubules all oriented with their minus-ends radiating from a supranuclear microtubule organizing center and their plus-end directed toward the cell periphery. The cell types in which this microtubule orientation has been demonstrated include: cat post-ganglionic sympathetic fibers Heidemann et al., 1981), chicken sensory neurites (Bacallao et al., 1989), rat hippocampal neurons and frog olfactory neurons (Baas et al., 1988; Burton, 1981), angelfish and teleost melanophores (Euteneuer and McIntosh, 1981; McNiven and Porter, 1986), teleost photoreceptors (Troutt and Burnside, 1988a) and heliozoan axopodia (Euteneuer and McIntosh, 1981). Recently, a few exceptions to this plus-end out microtubule pattern have been reported, describing cells in which microtubules are oriented with their minus-ends directed peripherally. These include sunfish retinal pigmented epithelial cells (Troutt and Burnside, 1988b), Madin Darby canine kidney (MDCK) cells (Bacallao et al., 1989), and *Drosophila* wing epidermal cells (Mogensen et al., 1989). Sertoli cells share their 'unusual' polarity with these cells.

In the classic cell model (Kreis, 1990; Kerr, 1991a,b) of cellular organization, microtubules are thought to be nucleated from centrosomal MTOCs (typically located centrally in a perinuclear position), stabilized at their proximal minus-ends, and growing at their peripherally-directed plus-ends (Kirschner, 1980). There are exceptions to this pattern. Microtubules of developing dendrites switch from a unipolar distribution, with their plus-end directed peripherally, to a bipolar distribution in the absence of a demonstrable MTOC. Similarly, amputated neurite segments are capable of reorienting their microtubules in the absence of any known MTOC (Baas et al. 1987). In those cells in which microtubules have been shown to be oriented with their minus-ends out, microtubule-MTOC relationships are atypical. In retinal pigmented epithelial cells and MDCK cells, both with their MT minus-end directly peripherally, cytoplasmic microtubules do not appear to associate with perinuclear centrosomes (Trout and Burnside, 1988b). Nucleating centers may relocate to an apical position, as has been demonstrated in *Drosophila* wing cells (Mogensen et al., 1989), an epithelial cell in which microtubules are oriented with their minus-ends directed toward the apical surface of the cell Mogensen et al., 1989). While it is clear MTOCs, with their paired centrioles and centrosomal material, are capable of nucleating microtubule, other microtubule organizing mechanisms probably exist. A recent report of the nucleating capacity of gamma tubulin in the absence of a MTOC (Joshi et al., 1991) is potentially such a mechanism.

Sertoli cell microtubules occur parallel to the long axis of the cell and extend from the body into apical processes (Amlani and Vogl, 1988, Vogl, 1988). Although paired centrioles have been reported in a supranuclear position (Nagano, 1966) in Sertoli cells, microtubules do not appear to arise from a central point. The distribution of centrosomal material has not been described in Sertoli cells. Further studies are needed to determine the source of microtubule nucleation in Sertoli cells.

Other than in the cultured MDCK cell, the results reported here are the only example of mammalian epithelial tissue for which microtubule polarity has been determined. Although the cells that have been reported to share their minus-end out microtubule polarity with Sertoli cells are from a diverse group of organisms, they share at least one feature, they are all epithelial cells. The finding that MDCK cells reorganize their microtubule polarity as they establish cell polarity (Pepperkok et al., 1990; Bré et al., 1990; Bacallo et al., 1989) has given rise to a new model, the parallel model for microtubule organization in epithelial cells (Schroer and Sheetz, 1991). Based on the limited examples that have been reported, Schroer and Sheetz (1991) have suggested that the minus-end out polarity, reported here for Sertoli cells, may not be unusual. They have proposed three models of intracellular organization based on microtubule organization: 1) the radial model: in which microtubules radiate from a nucleating center with their plus ends directed peripherally, typical of many cultured cells (Kreis, 1991; Kelly, 1990a,b); 2) the linear model: in which microtubules are arranged in series with slight overlap at their ends, unipolar in their orientation, as found in axons (Burton and Paige, 1981), and 3) parallel: microtubules arranged in a parallel configuration with their minus ends directed toward the apical surface of the cell in polarized epithelial cells(Mogensen et al., 1989; Troutt and Burnside, 1988b; Bacallao et al, 1989; Redenbach and Vogl., 1991).

There are a number of possible consequences of the polarity of cytoplasmic microtubules. As described earlier, the transport and distribution of most membrane bounded organelles depend on a microtubule-based transport system, as does the entire "continuous intracellular circulatory system" (Heuser, 1989) of the cell. Furthermore there is evidence that microtubule polarity plays a vital role. Amputation of embryonic chicken sensory neurites (Baas et al., 1987) or teleost melanophore arms (McNiven et al., 1984) results in a reversal of the microtubule polarity at the cut end within the amputated segments. In severed melanophore processes, a similar reversal of microtubule polarity coincides precisely with the reversal of pigment aggregation in the distal cut end (McNiven and Porter, 1986). It is not known what factors institute or regulate these changes in microtubule polarity. However, there is some signal to reestablish a functional pattern. This relationship between polarity and function implies that once the mechanoenzymes and their regulating signals are in place, the polarity of the microtubules is critical.

It is increasingly apparent that the distribution of cellular organelles is primarily based on a preferential direction of transport of specific organelles (Black and Baas, 1989; Kelly, 1990a,b; Kreis, 1990) presumably mediated by mechanoenzymes that have a preferred direction of transport. Therefore the polarity of microtubules will influence the distribution of organelles in the cell. It will be interesting to see whether organelles in polarized cells that exhibit a minus-end out polarity, have a unique distribution, or whether they employ different motors for their positioning than their counterparts in non-polarized cells.

Reorientation of microtubules to a minus-end out pattern, in epithelial cells, appears to be linked to the establishment of cell polarity. The formation of cell-cell junctions and the development of polarity, in cultured MDCK (epithelial) cells, immediately precedes the reorganization of microtubules (Bacallao et al., 1989). Therefore the new microtubule pattern is probably a response to rather than a cause of polarization. Following their reorganization, microtubules have greater stability (Bré et al., 1990; Pepperkok et al., 1990). The apical migration of electron dense material is proposed to be centrosomal material that assumes a microtubule nucleating role, in the apical region of the cell, following cell polarization of MDCK cells. It is not known what mechanisms are responsible for the change in organelle position during the establishment of cell polarity, or with the change to bidirectional polarity of dendrite microtubules, at the first sign of dendrite specific morphology (Baas et al., 1988, 1989). However, the coincidence of the alteration of microtubule polarity with changes in tissue specific morphology suggests a causal relationship.

In secretory cells, the assignment of secretory products, as well as apically or basally targeted membrane proteins to their appropriate surface, may depend on the polarity of microtubules and the mechanoenzymes and the regulatory proteins that are available. It will be interesting to determine the microtubule orientation for cells that have more than one active secretory surface. With the basal targeting of proteins being a bulk flow phenomenon, apical targeting may be a departure from the constitutive pattern, imposed by special constraints of polarization.

Sertoli cell microtubules are likely to participate in the same microtubule dependent functions as other cells, with their microtubule polarity influencing these events. The minus end-out orientation may have a causal relationship with the establishment of cell polarity, as Sertoli cells assume their epithelial morphology. As described earlier, during spermatogenesis, Sertoli cell organelles undergo marked stage dependent positional changes of cellular organelles including repositioning of the Golgi and elements of ER. Sertoli cells are secretory cells (Griswold, 1988), assuming the responsibility for establishing an environment to maintain viable spermatogenic cells through release of secretory products into the seminiferous tubule lumen, which is continuous with the adluminal compartment that houses spermatids. Much of the secretory pathway is microtubule dependent in cells generally, and can also be expected to be microtubule dependent in Sertoli cells. Many of the Sertoli cell secretory products are moved to the seminiferous tubule lumen, toward the microtubule minus-end. The elaborate shape changes that occur during spermatogenesis would require active membrane recycling. This pathway is, in part, microtubule dependent (See Schroer and Sheetz, 1991; Kreis, 1990) and would involve an important role for Sertoli cell microtubules. In addition, the lysosomal pathway, also partially microtubule dependent, is active and stage dependent in Sertoli cells as they not only dispose of their own unwanted cellular end products, but are responsible for the elimination of nonviable spermatogenic cells and residual bodies. In view of the range and extent of microtubule dependent activities occurring in Sertoli cells, incurred by both the added responsibility imposed by continuous stage dependent changes and the responsibility assumed for many nurturing functions on behalf of the spermatogenic cells, it is not surprising to find that Sertoli cells possess an abundance of microtubules. It follows that they would also possess an abundance of the required microtubule associated proteins to mediate these functions. Furthermore, with Sertoli cell microtubules directed with their minus-end out, an abundance of minus end-directed motors could be expected. Consistent with this is the finding that a high concentration of MAPs is present in testis (Neely and Boekelheide, 1988; Collins and Vallee, 1989) and Sertoli cell enriched fractions, including the minus-end directed motor, cytoplasmic dynein (Neely and Boekelheide; 1988).

MTx-SPERMATID-ES BINDING

Sertoli cells are thought to mediate the translocation of spermatids within the seminiferous epithelium. The events of spermatogenesis are highly complex and they are not readily amenable to manipulation *in vivo*. For this reason, an *in vitro* system has been developed to examine the potential for spermatid-ES-microtubule interaction. This approach has been rewarding for the study of microtubule-based transport generally (Vale et al., 1985a-d).

There are three methods in common use to test organelle-microtubule interactions *in vitro*. The first is the use of binding assays (Pratt, 1986; Suprenant and Dentler, 1982; Van der Sluij et al., 1990; Scheel and Kreis, 1991a,b; Rothwell et al., 1989; Sherline et al., 1977). These involve assaying the interaction of organelles with microtubules under selected conditions, usually by direct observation or differential sedimentation. The advantage of the binding assay is that it can be used in less defined systems and is often the place to start in systems with many unknown components or in cases where the questions being asked defy simplification of the components. The second means of testing microtubule-organelle interaction is the motility assay (Vale and Toyoshima, 1989). These assays are particularly useful when the elements involved are small and amenable to observation with DIC video enhanced microscopy. Many organelle transport systems are either simple, or well defined, allowing for studies to be carried out *in vitro*. Motility assays are most useful in systems that can be readily manipulated, and have the advantage of providing information about the whole mechanochemical cycle, allowing for the study of dynamic parameters. The third method is a biochemical progression from the first two and involves characterization of the ATPase activity of the enzyme. This generally requires that the motor be isolated (Paschal et al., 1987; Pratt, 1986a, 1991).

The advantage of the binding assay is that it can be used to test the interaction of organelles with microtubules before the participating partners have been defined, in order to find out what characteristics can be used to further test the interaction. It therefore tests the potential for microtubule binding and can be used to partially characterize that binding. The S1 crude supernatant that Vale and coworkers (1985d) isolated from axoplasm contained factors that transport vesicles in both directions, participants from two separate events. Not unlike the early *in vitro* studies of squid axoplasm, binding assays in less defined systems are testing all the motors present in the system, collectively. Similarly, the spermatid-ES isolation technique samples from all stages of spermatogenesis. Because the transport of spermatids toward the base of the epithelium and toward the apical surface involve a different directions of transport and different stages of spermatogenesis, it is reasonable to predict that there may be more than one motor to mediate these events. The method of spermatid isolation used in this study recovers spermatid-ESs from all stages. It is important to remember that the results of the binding assays in this study represent ^3MT_x-spermatid-ES binding properties of all stages in combination.

The wealth of information that has been gained from the ATPase activity assays and motility assays to study mechanoenzyme behavior has contributed to the study of more complex systems. Bindings assays are being employed to look at specific organelle-microtubule interactions in an attempt to test whether those organelles may be part of microtubule dependent pathways (see Schroer and Sheetz, 1991a). There are a number of studies, using binding assays, that closely parallel the method used in this study, and provide some comparison for the data presented here (Pratt, 1986; Suprenant and Dentler, 1982; Van der Sluij et al., 1990; Scheel and Kreis, 1991a,b; Rothwell et al., 1989; Sherline et al., 1977). Details of these studies have been described in an earlier section: binding assays, chapter 1.

Mechanoenzymes share three properties by which they can be identified (Scholey et al., 1988): 1) formation of enzyme cytoskeleton interactions in absence of ATP. 2) dissociation of that interaction with nucleotide, usually ATP, and 3) cytoskeleton activated ATPase activity. The binding assays used in this study provide evidence of the first two properties in microtubule-spermatid-ES interactions: that binding occurs, and that it is releasable with nucleotides. Without the isolation of the linking protein(s) ATPase activity could not be measured in this system. Here, binding in the absence of added ATP and dissociation with nucleotides, taken together with an apparent turnover of binding, support, but do not prove that the linking protein is a mechanoenzyme.

Spermatid-ES complexes share their potential to stably bind microtubules with all of the organelle-microtubule binding assays described earlier. This bound state is analogous to the arrest of motility and depression of ATPase activity that occurs in the absence of ATP and transport and increased ATPase activity in the presence of ATP, that are measured in motility assays and ATPase activitiy assays respectively. The kinesin-microtubule interaction is releasable by ATP and GTP but the dynein-microtubule interaction is releasable only with ATP. ^3MT_X spermatid complexes were releasable with both 5 mM GTP and 10 mM ATP. An unexpected finding was the greater release that occurred with a combination of ATP and GTP, compared with either alone. Although this could be a dose dependent effect, most mechanoenzyme isolation techniques employ the levels of nucleotide used in this study, on the assumption that they are in excess of what is required for maximum release (Paschal et al., 1991; Neely and Boekelheide, 1988). One possible interpretation is that ATP and GTP are acting at different sites and therefore have an additive effect. Of six binding assays cited earlier, five formed rigor complexes that were releasable with ATP. Of the three in which GTP and ATP release were both tested, two showed release with both nucleotides The common interpretation is that in the absence of ATP, rigor complexes form and that with the addition of ATP (and in some cases GTP), there is a decrease in motor-microtubule affinity and rigor is released (Lasek and Brady, 1985; Chiocotin and Johnson, 1989; Hackney, 1988).

Rickard and Kreis (1991) offer an alternate explanation that arose from an inconsistency in their data. They have identified a 170kD microtubule binding protein "pp170" that mediates binding between exocytic vesicles and microtubules. (Rickard and Kreis, 1991; Scheel and Kreis 1991a.b) Initially pp170 was found to be released from microtubules by ATP and GTP in crude preparations, but not with affinity purified protein. They have extended their findings to show that nucleotide dependent release requires cytosolic extracts. Furthermore, they report that 170 kD-microtubule binding is regulated by phosphorylation of 170 kD (also referred to as pp170), by cytosolic kinases in the present of excess ATP. Removal of ATP restricts kinase activity. Phosphatases in the cytosol dephosphorylate the pp170 protein, resulting in the dephosphorylated form and its release from microtubules. Scheel and Kreis (1991a,b) have used a novel binding assay, employing an affinity matrix of microtubules complexed to magnetic beads and exposed to endocytic vesicles, to show that pp 170 is likely the protein that mediates endocytic carrier vesicle-microtubule binding. They interpret the cytosol requirement as a need for a source of kinases and phosphatases to regulate the on/off cycling. The endocytic carrier vesicle-microtubule binding is releasable with ATP and GTP, presumably, not as a stimulus for the mechanochemical cycle, but to provide for phosphorylation of pp170- to achieve the off state.

Depletion of ATP frequently increases the formation of rigor complexes and is used to increase mechanoenzyme binding in both organelle and microtubule-based mechanoenzyme isolation. In this study ATP depletion produced mixed results, increasing binding in two of six experiments, leaving it unchanged in four. Because the basal level of ATP was not monitored in these assays the basal level is not known. It may be that the residual ATP or the possible regeneration of ATP, was already sufficiently low to maximize binding in four of the six experiments. There appears to be some turnover of binding occurring, evidenced by the competition with excess unlabeled microtubules, but it is slow enough to provide enough rigor complexes to detect binding.

Microtubule-spermatid-ESs were unaffected by AMPPNP.

In most experiments AMPPNP reduced binding slightly but accounting for variance, the reduction was not significant. In the presence of AMPPNP, kinesin-like motors would be predicted to increase the formation of rigor complexes, while a dynein-like motor would slightly decrease binding. If kinesin were present, an increase in binding may be expected because of the slow release of ADP from kinesin (the rate limiting step), which occurs after ATP hydrolysis and before kinesin-microtubule separation. If dynein were present, a decrease in binding would be expected because of the relative ineffectiveness of AMPPNP as a substitute for ATP in releasing rigor complexes with dynein or myosin (Penningroth, 1989). Although dynein-microtubule rigor complexes would be released with ATP, they are less effectively released with AMPPNP.

In the binding assays cited earlier, three groups tested the effect of NEM on binding: two found reduced binding at 1-5 mM levels. Kinesin is less sensitive to NEM than dynein but the results of experiments vary. NEM is a sulfhydral alkylating agent that interferes with transport by altering SH groups before the motor interacts with the cytoskeleton. Its reduction in binding is therefore approximately analogous to a reduction in motility. In this study, 2mM NEM reduced microtubule spermatid-ES binding. Although NEM is used as a probe for dynein-like motors, it can potentially interfere with any SH group and therefore its specificity is poor (Penningroth, 1989).

EHNA is a structural analogue of adenosine and is a more effective inhibitor of dynein than kinesin. It has been shown to reduce ATPase activity in cytoplasmic dynein in testis at 4 mM but not at 0.4mM (Neely and Boekelheide, 1988). It was ineffective in changing binding in this binding assay. It was not used in the binding assays described above.

The addition of cytosol from Sertoli cells or MAP enriched fractions from testis did not alter binding, in this study. It is possible that the linking protein(s) were already present in sufficient amounts for maximum binding or that the concentration of proteins in the added fractions used in this assay were too low.

The reduced binding with 100 μM vanadate, in this study, is more puzzling. The effects of vanadate on motility and ATPase activity occur at lower levels for cytoplasmic dynein than for kinesin, although they are quite variable between systems. In motility assays, vanadate blocks ATP by forming ADP-vanadate complexes from ATP and then occupying an adjacent site effectively limits access of ATP, reducing transport but increasing rigor formation. In this study, $^{3}MT_{X}$-spermatid-ES binding was reduced by 100 µM vanadate, but not significantly reduced by 10 µM vanadate. Porter and Johnson (1989) describe the potential for vanadate and ADP to partially mimic the effect of ATP in dissociating rigor complexes in dynein microtubule binding. If dynein was involved in this binding assay, this effect may explain the reduced binding by high concentrations of vanadate (Porter and Johnson, 1989)

Binding increased with increased microtubule concentration. Even in the presence of very high concentrations of microtubules saturation did not occur. The change in slope of binding with increased microtubule concentration may reflect the existence of two binding sites one of high and one of low affinity, or more than one enzyme.

The results of the binding assay suggest that spermatid ESs bind to microtubules and are released by ATP and GTP. As has been the case with other organelle-microtubule binding assays, the characteristics of $^{3}MT_{X}$-spermatid-ES binding do not align with a single known motor. They share properties with both dynein and kinesin. The ATP effects, on $^{3}MT_{X}$-spermatid-ES binding, are similar to those that occur with kinesin or dynein type motors, (for reviews see Vale, 1987,1990; McIntosh and Porter, 1989), but they are also similar to the the binding properties of pp170 that have, upon further investigation been shown to be regulated by phosphorylation/dephosphorylation, and may not have microtubule-based transport capabilities (Rickard and Kreis, 1991; Scheel and Kreis, 1991a,b). As has been done by Kreis and coworkers, additional approaches are required to determine if the linking protein in $^{3}MT_{X}$-spermatid-ES binding is a motor.

Considering the complexity of the microtubule-spermatid-ES system, as isolated for this study, it is possible that more than one motor (and/or accessory or microtubule binding protein) may contribute simultaneously to the binding properties described here. What is clear is that $^{3}MT_{X}$-spermatid-ES binding shares two properties with known motors: it binds to microtubules and it can be released with nucleotides. The third property, whether it participates in microtubule-based transport, requires further study. The findings presented here do not prove, but are consistent with the spermatid-ES microtubule binding being mediated by a mechanoenzyme.

The localization of tubulin with immunofluoresence or radiolabelled microtubule by autoradiography, indicate that microtubules associate with spermatid-ESs. This evidence is further supported by the microtubule release by ATP using these parameters.

SUPPORT FOR THE MODEL

Organelle-microtubule binding in cells generally provides for the positioning of organelles and translocation along functional pathways. Microtubule spermatid-ES binding has been tested in this study because of a suspected function in the positioning and translocation of spermatids within the seminiferous epithelium. The evidence presented here provides two additional pieces of information for the proposed model of microtubule based-spermatid translocation. First, that Sertoli cell microtubules are oriented with their minus-ends directed toward the apical surface of the cell, and secondly, that binding occurs between ESs and microtubules. Figure 4-1 is a diagramatic representation of these findings and Figure 4-2 depicts the ES-microtubule linkage as a motor. Two possible motor complexes are illustrated in which the motor-ER binding may be either direct, or mediated through an accessory membrane protein. Further evidence is needed to determine whether the binding is indeed a mechanoenzyme capable of spermatid-Es transport along microtubule tracks.

Vogl et al (1991a) have described four domains that make up ESs. A fifth domain is provisionally described at the ER microtubule site. The data presented here support the possibility that the cytoplasmic domain with its microtubules and links to the ESER are in fact a functional part of ectoplasmic specializations.

Figure 4-1: Summary diagram of microtubule-based spermatid translocation model. This is the microtubule-based spermatid translocation model presented in chapter 1. The results of the microtubule polarity study, that Sertoli cell microtubules are oriented with their minus-ends directed toward the apical surface of the Sertoli cell, have been added to the model.

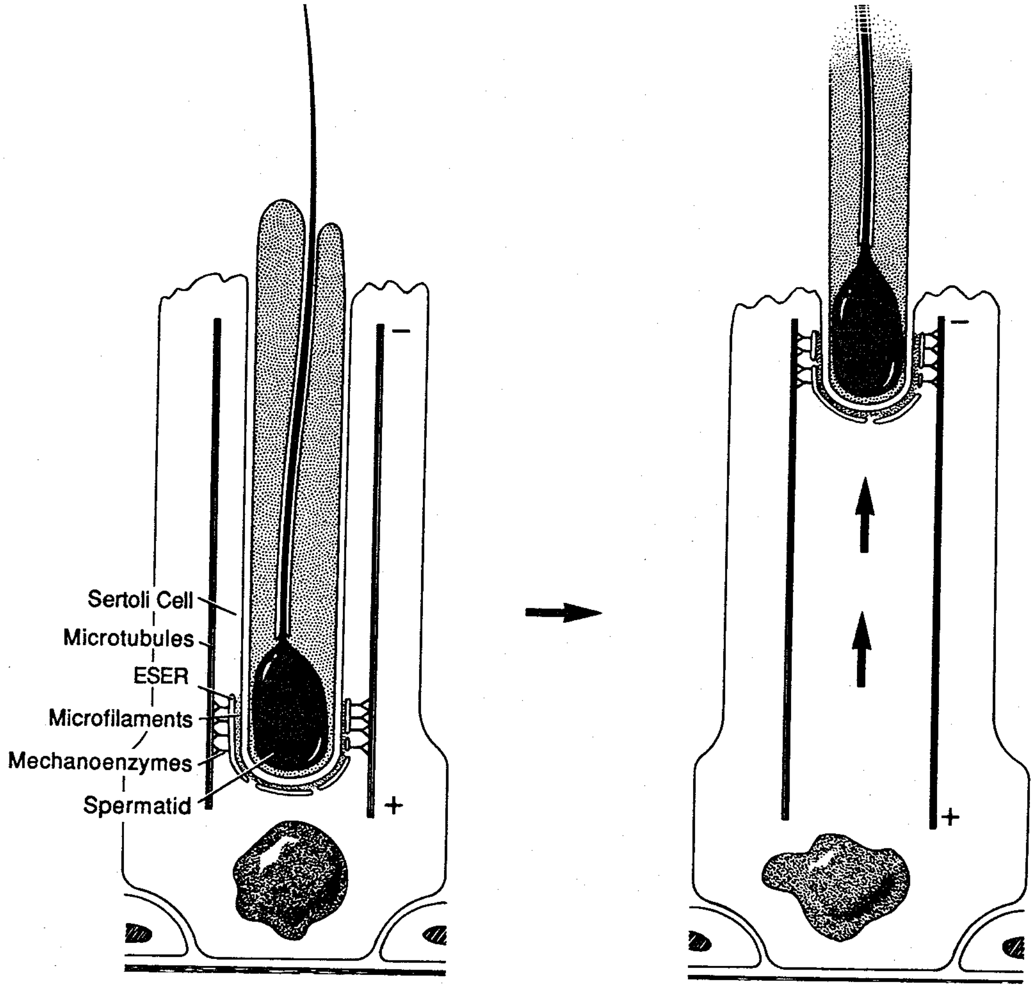
Sertoli Cell
Microtubules
ESER
Microfilaments
Mechanoenzymes
Spermatid
−
+
−
+

Figure 4-2: Summary diagram of microtubule-spermatid-ES binding: This diagram illustrates the structural details of apical ESs in Sertoli cells. The structural link from the ESER, across the actin network, to the Sertoli cell and spermatid membranes are shown. A microtubule situated on the cytoplasmic face of the ESER is shown bound to the ESER, consistent with the results of the MT-spermatid-ES binding assays. Two possible formats for the linkage are shown, one in which the linking protein provides a direct linkage, and one in which binding is mediated by an integral membrane protein receptor. The details of this linkage are speculative. That microtubule-spermatid-ES binding is releasable with nucleotides and shares some properties with known mechanoenzymes suggests that the linking protein may be a motor. These findings suggest that the cytoplasmic domain is a functional component of ESs.

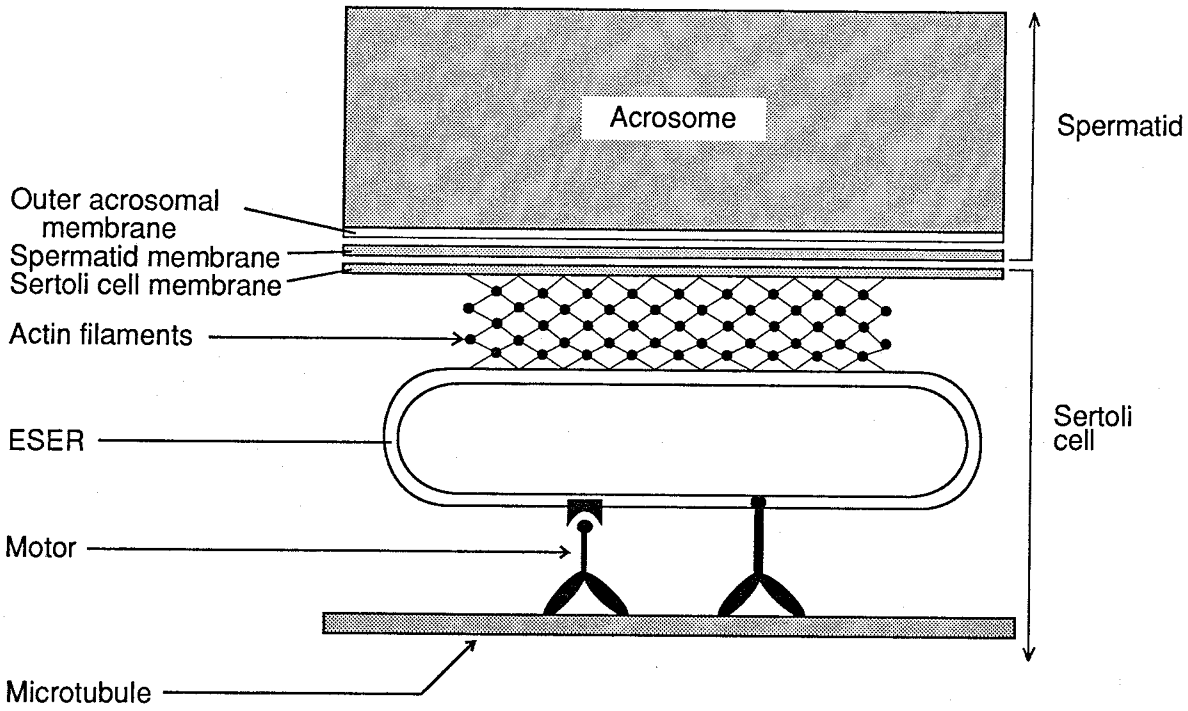
Acrosome
Spermatid
Outer acrosomal membrane
Spermatid membrane
Sertoli cell membrane
Actin filaments
ESER
Sertoli cell
Motor
Microtubule

BIBLIOGRAPHY

Achler, C.,D. Filmer, C. Merte and D. Drenckhahn. 1989. Role of microtubules in polarized delivery of apical membrane proteins to the brush border of the intestinal epithelium. *J. Cell Biol.* 109: 179-189.

Allan, V.J. and R.D. Vale. 1991. Cell cycle control of microtubule-based membrane transport and tubule formation *in vitro. J. Cell Biol.* 113 (2): 347-359.

Allen, C., and G.G. Borisy. 1974. Structural polarity and directional growth of microtubules of *Chlamydomonas* flagella. *J. Cell Biol.* 90: 381-402.

Allen, R.D., N.S. Allen, and J.L. Travis. 1981a. Video-enhanced contrast differential interference contrast (AVEC-DIC) microscopy: a new method capable of analyzing microtubule related motility in the reticulopodial network of *Allogromia laticollaris. Cell Motil.* 1: 291-302.

Allen, R.D., J. Metuzals, I. Tasaki, S.T. Brady and S.P. Gilbert. 1982. Fast axonal transport in squid giant axon. *Science* 218: 1127-1128.

Allen, R.D., J.L. Travis, J.H. Hayden, N.S. Allen, A.C. Breuer and L.J. Lewis. 1981b. Cytoplasmic transport: moving ultrastructural elements common to many cell types revealed by video-enhanced microscopy. Cold Spring Harbour Symposium on Quantitative Biology. 46:85-89.

Allen R.D., D.G. Weiss, J.H. Hayden, D.T. Brown, H. Fujiwake, and M. Simpson. 1985. Gliding movement of, and bidirectional transport along, single native microtubules from squid axoplasm: evidence for an active role of microtubules in cytoplasmic transport. *J. Cell Biol.* 100: 1736-1752.

Amlani, S., and A.W. Vogl. 1988. Changes in the distribution of microtubules and intermediate filaments in mammalian Sertoli cells during spermatogenesis. *Anat. Rec.* 220: 143-160.

Amos, L.A. 1987. Kinesin from pig brain studied by electron microscopy. *J. Cell. Sci.* 87: 105-111.

Baas, P.W, M.M. Black, and G.A. Banker. 1989. Changes in microtubules polarity orientation during the development of hippocampal neurons in culture. *J. Cell Biol.* 109 (6): 3085-3094.

Baas, P.W, J.S. Deitch, M.M. Black, and G.A. Banker. 1988. Polarity orientation of microtubules in hippocampal neurons: uniformity in the axon and nonuniformity in the dendrite. *Proc. Natl. Acad. Sci.* 85: 8335-8339.

Baas, P.W., L.A. White, and S.R. Heidemann. 1987. Microtubule polarity reversal accompanies regrowth of amputated neurites. *Proc. Natl. Acad. Sci.* 84: 5272-5276.

Bacallao, R., C. Antony, C. Dotti, E. Karsenti, E.H.K. Stelzer, and K. Simmons. 1989. The subcellular organization of Madin-Darby canine kidney cells during the formation of a polarized epithelium. *J. Cell Biol.* 109: 2817-2832.

Balch, W.E. 1989. Biochemistry of interorganelle transport. *J. Biol. Chem.* 264 (29): 16965-16968.

Bergen, L.C., and G.G. Borisy. 1980. Head-to-tail polymerization of microtubules *in vitro.* electron microscope analysis of seeded assembly. J. *Cell Biol.* 84(1): 141-50.

Bershadsky, A.D., and J.M. Vasiliev. 1988a. Cytoskeleton and internal organization of the cell. *In* Cytoskeleton. Plenum Press, N.Y. 19: 167-201.

Bershadsky, A.D., and J.M. Vasiliev. 1988b. Reorganization of Cytoskeleton. *In* Cytoskelton. Plenum Press, N.Y.: 217-250.

Bershadsky, A.D., and J.M. Vasiliev. 1988c. Systems of microtubules. *In* Cytoskeleton. Plenum Press, New York. 73-131.

Black, M.M., and P.W. Baas. 1989. The basis of polarity in neurons. *Trends in Neurosci.* 12(6): 211-214.

Bloom, G.S., M.C. Wagner, K.K. Pfister, P.L. Leopold and S.T. Brady. 1989. Involvement of microtubles and kinesin in the fast axonal transport of membrane-bounded organelles. *In* Cell Movement: Kinesin, Dynein, and Microtubule Dynamics. Vol

2. F.D. Warner and J.R. M^{c}Intosh, editors. Alan R. Liss Inc., New York. 321-333.

Boekelheide K., M.D. Neely, and T.M. Sioussat. 1989. The Sertoli cell cytoskeleton: a target for toxicant induced germ cell loss. *Toxicol Appl. Pharmicol.* 101: 373-389.

Bomsel, M., R. Parton, S.A. Kuznetsov, T.A. Schroer and J. Gruenberg. 1990. Microtubule- and motor- dependent fusion *in vitro* between apical and basolateral endocytic vesicles from MDCK cells. *Cell* 62:719-731.

Borgers, M., M. DeBrabander, J. van Reempts, F. Awouters, and W.A. Jacob. 1977. Intranuclear microtubules in lung mast cells of guinea pigs in anaphylactic shock. *Lab. Invest.* 37 (1): 1-9.

Borgers, M., F. Thoné, and J.M. van Nueten, 1981. The subcellular distribution of calcium and the effects of calcium-antagonists as evaluated with a combined oxalate-pyroantimonate technique. *Acta Histochem. Suppl. XXIV*, S. 327-332.

Borisy, G.G., 1978. Polarity of microtubles of the mitotic spindle. *J. Mol. Biol.* 124: 565-70.

Borisy, G.G., and L.C. Bergen. 1982. A direct method for analyzing the polymerization kinetics at the two ends of a microtuble. *Meth. Cell Biol.* 24: 171-187.

Borisy, G.G., J.M. Marcum, J.B. Olmstead, D.B. Murphy, and K.A. Johnson. 1974. Purificatrion of tubulin and associated high molecular weight proteins from porcine brain and characterization of microtubule assembly *in vitro. Ann. N. Y. Acad. Sci.* 253: 107-132.

Bornens, M., M. Paintrand, J. Bergs, M.C. Marty, and E. Karsenti. 1987. Structural and chemical characterization of isolated centrosomes. *Cell Motil. Cytoskeleton.* 8: 238-249.

Bradford, M.M. 1976. A rapid method for the quantitation of microgram quantities of protein utilizing the principle of protein-dye binding. *Anal. Biochem.* 72: 248-254.

Brady, S.T. 1985. A novel brain ATPase with properties expected for the fast axonal transport motor. *Nature*. 317: 73-75.

Brady, S.T., R.J. Lasek and R.D. Allen. 1982. Fast axonal transport in extruded axoplasm from squid giant axon. *Science*. 218: 1129-1131.

Brady, S.T., and K.K. Pfister. 1991. Kinesin interactions with membrane bounded organelles *in vivo* and *in vitro*. *J. Cell Sci.* Supp. 14: 103-108.

Brady, S.T., K.K. Pfister, G.S. Bloom. 1990. A monoclonal antibody against kinesin inhibits both anterograde and retrograde fast axonal transport in squid axoplasm. *Proc. Natl. Acad. Sci.* 87 (3): 1061-1065.

Bré, M.H., R. Pepperkok, A.M. Hill, N. Levilliers, W. Ansorge, E.H.K. Stelzer and E. Karsenti. 1990. Regulation of microtubule dynamics and nucleation during polarization in MDCK II cells. *J. Cell Biol.* 111 (6):3013-3021.

Brinkley, B. R. 1985. Microtubule organizing centers. *Annu. Rev. Cell Biol.* 1: 145-172.

Brinkley, B.R., S.M. Cox, D.A. Pepper, L. Wible, S.L. Brenner, and R.L. Pardue. 1981. Tubulin assembley sites and the organization of cytoplasmic microtubles in cultured mammalian cells. *J. Cell Biol.* 90: 554-562.

Brökelmann, J. 1963. Fine structure of germ cells-and Sertoli cells during the cycle of the seminiferous epithelium in the rat. *Zeitschrift für Zellforschung*. 59: 820-850.

Bulinski, J.C. and G.G. Gundersen. 1991. Stabilization and post-translational modification of microtubules during cellular morphogenesis. *BioEssays*.13 (6): 285-293.

Burnside B. 1989. Microtubule sliding and the generation of force for cell shape change. *In* Cell Movement: Kinesin, Dynein and Microtubule Dynamics. Vol 2. F. D. Warner and J. R. M^{c}Intosh, editors. New York: Alan R. Liss Inc. 169-189.

Burton, P.R. 1988. Dendrites of mitral cell neurons contain microtubules of opposite polarity. *Brain Res.* 473: 107-115.

Burton, P.R., and L.A. Laveri. 1985. The distribution, relationships to other organelles, and calcium-sequestering ability of smooth endoplasmic reticulum in frog olfactory axons. *J. Neurosci.* 5 (11): 3047-3060.

Burton, P.R., and J.L. Paige. 1981. Polarity of axoplasmic microtubules in the olfactory nerve of the frog. *Proc. Natl. Acad. Sci.* 78 (5): 3269-3273.

Cherry, L.M. and T.C. Hsu. 1984. Antitubulin immunofluoresence studies of spermatogenesis in the mouse. *Chromosoma.* 90: 265-274.

Chilcote, T.J., and K.A. Johnson. 1989. Microtubule-dynein cross-bridge cycle and the kinetics of 5'-Adenylyl Imidodiphosphate (AMPPNP) binding. *In* Cell Movement: The Dynein ATPases. Vol 1. F.D. Warner, P. Sater, I.R. Gibbons, editors. Alan R. Liss Inc., N. Y.: 235-250.

Christensen, A.K. 1965. Microtubules in Sertoli cells of the guinea pig testis. *Anat. Rec.* 151: 335a.

Clermont, Y. 1972. Kinetics of spermatogenesis in mammals: seminiferous epithelium cycle and spermatogonial renewal. *Physiol. Rev.* 52 (1): 198-236.

Clermont, Y., J. M^{c}Coshen and L. Hermo. 1980. Evolution of the endoplasmic reticulum in the Sertoli cell cytoplasm encapsulating the heads of late spermatids in the rat. *Anat. Rec.* 196: 83-99.

Clermont, Y., and A. Rambourg 1978. Evolution of the endoplasmic reticulum during rat spermiogenesis. *Am. J. Anat.* 151: 191-212.

Cohn, S.A., A.L. Ingold, and J.M. Scholey. 1987. Correlation between the ATPase and microtubule translocating activities of sea urchin egg kinesin. *Nature.* 328: 160-163.

Cohn, S.A., A.L. Ingold, and J.M. Scholey. 1989. Quantative analysis of sea urchin egg kinesin-driven microtubule motility. *J. Biol. Chem.* 264(8): 4290-4297.

Cole, A., M.L. Meistrich, L.M. Cherry, and P.K. Trostle-Weige. 1988. Nuclear and manchette development in spermatids of normal and *azh/azh* mutant mice. *Biol. of Reprod.* 38: 385-401.

Collins, C.A., and R.B. Vallee. 1989. Preparation of microtubules from rat liver and testis: cytoplasmic dynein is a major microtubule associated protein. *Cell Motil. Cytoskeleton.* 14: 491-500.

Cramer E. B., and J. I. Gallin. 1979. Localization of submembranous cations to the leading end of human neutrophils during chemotaxis. *J. Cell Biol.* 82: 369-379.

Dabora, S.L., and M.P. Sheetz. 1988. The microtubule-dependent formation of a tubulovesicular network with characteristics of the ER from cultured cell extracts. *Cell.* 54: 27-35.

Dedman, J.R., B.R. Brinkley, and A.R. Means. 1979. Regulation of microfilaments and microtubules by calcium and cyclic AMP *In* Advances in Cyclic Nucleotide Research. Vol. 11. P. Greengard, G.A. Robinson, editors. Raven Press, N. Y.: 131-174.

Duden, R., W.C. Ho, V.J. Allan and T.E. Kreis. 1990. What's new in cytoskeleton-organelle interactions? Relationship between microtubules and the Golgi-apparatus. *Path. Res. Pract.* 186 (4): 535-541.

Dym, M. 1977. The role of the Sertoli cell in spermatogenesis. *In* Male Reproductive System. R.D. Yates and M. Gordon, editors. Masson Pub. Co., St. Paul. 155-169.

Dym, M. and Y. Clermont. 1970. Role of spermatogonia in the repair of the seminiferous epithelium following irradiation of the rat testis. *Am. J. Anat.* 128: 265-282.

Dym, M., and D.W. Fawcett. 1970. The blood-testis barrier in the rat and the physiological compartmentation of the seminiferous epithelium. *Biol. Reprod.* 3: 308-326.

Ekwall, H., Å. Jansson, P. Sjöberg, and L. Plöen. 1984. Differentiation of the rat testis between 20 and 120 days of age. *Arch of Androl.* 13: 27-36.

Ellisman, M.A. and K.R. Porter. 1980. Microtrabecular structure of the axoplasmic matrix: visualization of crosslinking structures and their distribution. *J. Cell Biol.* 87:464-479.

Euteneuer, U., L.T. Haimo, and M. Schliwa. 1989a Microtubule bundles of *Reticulomyxa* networks are of uniform polarity. *Eur. J. Cell Biol.* 49 (2): 373-376.

Euteneuer, U., K.B. Johnson and M. Schliwa. 1989b. Photolytic clevage of cytoplasmic dynein inhibits organelle transport in *Reticulomyxa*.. *Eur. J. Cell Biol.* 50: 34-40.

Euteneuer U., and J.R. M^{c}Intosh. 1981a. Polarity of some motility-related microtubules. *Proc. Natl. Acad. Sci.* 78(1): 372-376.

Euteneuer, U., and J.R. M^{c}Intosh. 1981b. Structural polarity of kinetochore microtubules in PtK1 Cells. *J. Cell Biol.* 89: 338-345.

Evans, L., T.J. Mitchison, and M.W. Kirschner. 1985. Influence of the centrosome on the structure of nucleated microtubules. *J. Cell Biol.* 100: 1185-1191.

Fawcett, D.W. 1975. Ultrastructure and function of the Sertoli cell. *In* Handbook of Physiology, Section 7, Endocrinology, Vol. 5: Male Reproductive System. R.O. Greep, editor. Williams and Wilkins, Baltimore, pp. 21-55.

Fawcett, D.W., W.A. Anderson, and D.M. Phillips. 1971. Morphogenic factors influencing the shape of the sperm head. *Dev. Biol.* 26(2): 220-251.

Fleming, T.P., and M.H. Johnson. 1988. From egg tp epithelium. Ann. Rev. Cell Biol. 4: 459-85.

Flickinger, C., and D.W. Fawcett. 1967. The junctional specializations of the Sertoli cells in the seminiferous epithelium. *Anat. Record.* 158: 207-222.

Forman, D.S., K.J. Brown, and D.R. Livengood. 1983. Fast axonal transport in permiablized lobster giant axon is inhibited by vanadate. *J. Neurosci.* 3(6): 1279-1288.

Franchi, E., and M. Camatini. 1985. Morphological evidence for calcium stores at Sertoli-Sertoli and Sertoli-spermatid interrelations. *Cell Biol. Int. Rep.* 9 (5): 441-446.

Franke, W.W., C. Grund, A. Fink, K. Weber, B.M. Jockusch, H. Zentgraf, and M. Osborn. 1978a. Location of actin in the microfilament bundles associated with the junctional specializations between Sertoli cells and spermatids. *Biol. Cell.* 31: 7-14.

Franke, W.W., C. Grund, and E. Schmid. 1979. Intermediate-sized filaments present in Sertoli cells are of vimentin type. *Eur. J. Cell Biol.* 19: 269-275.

Franke, W.W., M. Hergt, and C. Grund. 1987b. Rearrangement of the vimentin cytoskeleton during adipose conversion: formation of an intermediate filament cage around lipid globules. *Cell.* 49: 131-141.

Gelfand, V. I. 1989. Cytoplasmic microtubular motors. *Curr. Opin. Cell Biol.* 1: 63-66.

Gibbons, I.R. 1988. Dynein ATPases as microtubule motors. *J. Cell Chem.* 263(31): 15837-15840.

Gilbert, S.P., R.D. Allen, and R.D. Sloboda. 1985. Translocation of vesicles from squid axoplasm on flagellular microtubules. *Nature.* 315: 245-248.

Gilbert, S.P., and R.D. Sloboda. 1989. A squid dynein isoform promotes axoplasmic vesicle translocation. *J. Cell Biol.* 109: 2379-2394.

Gilbert, S.P., and R.D. Sloboda. 1984. Bidirectional transport of fluorescently labeled vesicles introduced into extruded axoplasm of squid *Loligo pealei. J. Cell Biol.* 99: 445-452.

Gilbert, S.P., and R.D. Sloboda. 1986. Identification of a MAP2-like ATP-binding protein associated with axoplasmic vesicles that translocate on isolated microtubules. *J. Cell Biol.* 103: 947-956.

Gilula, N.B., D.W. Fawcett, and A. Aoki. 1976. The Sertoli cell occluding junctions and gap junctions in mature and developing mammalian testis. *Dev. Biol.* 50: 142-168.

Gondos, B. 1984. Germ cell differentiation and intercellular bridges. *In* Ultrastructure of Reproduction. J. VanBlerkom, P.M. Motta, editors. Martinus Nyhoff Pub. Boston.

Gravis, C.J. 1979. Interrelationships between Sertoli cells and germ cells in the Syrian hamster. *Z. mikrosk-anat. Forsch. Leipzig.* 93 (2): S 321-342.

Gravis, C.J. 1980. Ultrastructural observations on spermatozoa retained within the seminiferous epithelium after treatment with dibutyrl cyclic AMP. *Tiss. Cell.* 12 (2): 309-322.

Greer, K. and J.L. Rosenbaum. 1989. Post-translational modifications of tubulin. *In* Cell Movement: Kinesin, Dynein and Microtubule Dynamics, Vol 2. F. D. Warner and J. R. M^{c}Intosh, editors. New York, Alan Liss Inc. 47-66.

Griswold, M.D. 1988. Protein secretions of Sertoli cells. *Int. Rev. of Cyt.* 110: 133-156.

Grove, B.D., D.C. Pfeiffer, S. Allen, and A.W. Vogl. 1990. Immunofluorescence localization of vinculin in ("junctional ") ectoplasmic specializations of rat Sertoli cells. *Am. J. Anat.* 188: 44-56.

Grove, B. D., and A. W. Vogl. 1989. Sertoli cell ectoplasmic specializations: a type of actin-associated adhesion junction? *J. Cell Sci.* 93: 309-323.

Hackney, D.D. 1988. Kinesin ATPase: rate-limiting ADP release. *Biochem.* 85: 6314-6318.

Hackney, D.D., A.S. Malik, and K.W. Wright. 1989. Nucleotide-free kinesin hydrolyzes ATP with burst kinetics. *J. Biol. Chem.* 264(27): 15943-15948.

Haimo, L.T. 1982. Dynein decoration of microtubules-determination of polarity. *Meth. Cell Biol.* 24: 189-206.

Hall, E.S., J. Eveleth and K. Boekelheide. 1991. 2, 5-hexanedione exposure alters the rat Sertoli cell cytoskeleton in intermediate filaments and actin. *Toxicol. Appl. Pharacol.*:111(in press).

Handel, M.A. 1979. Effects of colchicine on spermiogenesis in the mouse. *J. Embryol. Exp. Morph.* 51: 73-83.

Hayden, J.H., R.D. Allen, and R.D. Goldman. 1983. Cytoplasmic transport in keratocytes: direct visualization of particle translocation along microtubules. *Cell Motil.* 3 (1): 1-19.

Heidemann, S.R. 1991. Microtubule polarity determination based on formation of protofilament hooks. *Meth. in Enzymol.* 196: 469-477.

Heidemann, S.R., and U. Euteneuer. 1982. Microtubule polarity determination based on conditions for tubulin assembly *in vitro. Meth. Cell Biol.* 24 : 207-216.

Heidemann, S.R., J.M. Landers, and M.A. Hamborg. 1981. Polarity orientation of axonal microtubules. *J. Cell Biol.* 91: 661-665.

Heidemann, S.R., and J.R. M^{c}Intosh. 1980. Visualization of the structural polarity of microtubules. *Nature.* 286: 517-519.

Heidemann, S. R., G.W. Zieve, and J.R. M^{c}Intosh. 1980. Evidence for microtubule subunit addition to the distal end of mitotic structures *in vitro. J. Cell Biol.* 87: 152-159.

Heins, S., Y.H. Song, H. Willie, E. Mandelkow, and E.M. Mandelkow. 1991. Effect of MAP2, Map2C, and tau on kinesin-dependent microtubule motility. *J. Cell Sci.* Supp. 14: 121-124.

Hermo L., R. Oko and N. B. Hecht. 1991. Differential post-translational modifications of microtubules in cells of the seminiferous epithelium of the rat: a light and electron microscope immunocytochemical study. *Anat Rec.* 229: 31-50.

Heuser, J. E. 1989. Mechanisms behind the organization of membranous organelles in cells. *Curr. Opin. in Cell Biol.* 1: 98-102.

Hirokawa, N. 1982. Cross-linker system between neurofilaments, microtubules and membranous organelles in frog axons revealed by the quick-freeze, deep-etching method. *J. Cell Biol.* 94: 129-142.

Hirokawa, N., K.K. Pfister, H. Yorifuji, M.C. Wagner, S.T. Brady, and G.S. Bloom. 1989. Submolecular domains of bovine brain kinesin identified by electron microscopy and monoclonal-antibody decoration. *Cell.* 56: 867-878.

Hirokawa, N., R. Sato-Yoshitake, N. Kobayashi, K.K.Pfister, G.S. Bloom, and S.T. Brady. 1991. Kinesin associates with anterogradely transported membranous organelles *in vivo. J. Cell Biol.* 114 (2): 295-302.

Hirokawa, N., R. Sato-Yoshitake, T. Yoshida, and T. Kawashima. 1990. Brain dynein (MAPIC) localizes on both antergradely and retrogradely transported membranous organelles *in vivo. J Cell Biol.* 111: 1027-1037.

Hisanaga, S., H. Murofushi, K. Okuhara, R. Sato, Y. Masuda, H. Sakai, and N. Hirokawa. 1989. The molecular structure of adrenal medulla kinesin. Cell Motil. *Cytoskeleton.* 12: 264-272.

Ho, W.C., V.J. Allan, G. van Meer, E.G. Berger and T.E. Kreis. 1989. Reclustering of scattered Golgi elements occurs along microtubules. *Eur. J. Cell Biol.* 48: 250-263.

Hollenbeck, P.J. 1989a The distribution, abundance, and subcellular localization of kinesin. *J. Cell Biol.* 108 (6): 2335-2342.

Hollenbeck, P.J. 1989b. The transport and assembly of the axonal cytoskeleton. *J. Cell Biol.* 108: 223-227.

Horio,T., and H. Hotani. 1986. Visualization of the dynamic instability of individual microtubules by dark-field microscopy. *Nature.* 321: 605-607.

Horowitz, S.B., L. Lothstein, J.J. Manfredi, W. Mellado, J. Parness, S.N. Roy, P.B. Schiff, L. Sorbara, and R. Zeheb. 1986. Taxol: Mechanisms of action and resistance. *Ann. N. Y. Acad. Sci.* 733-744.

Horwitz, S.B., J. Parness, P.B. Schiff, and J.J. Manfredi. 1981. Taxol: a new probe for studying the structure and function of microtubules. *Cold Springs Harbor Symposium on Quantitative Biology.* 46 (1): 209-226.

Houliston, E., S.J. Pickering, and B. Maro. 1987. Redistribution of microtubules and pericentriolar material during the development of polarity in mouse blastomeres. *J. Cell Biol.* 104: 1299-1308.

Hoyle, H.D., and E.C. Raff. 1990. Two *Drosophila* beta tubulin isoforms are not functionally equivalent. *J. Cell Biol.* 111: 1009-1026.

Idriss, H., D.K. Stammers, C.K. Ross and R.G. Burns. 1991. The dynamic instability of microtubules is not modulated by alpha Tubulin Tryosinylation. *Cell Motil. Cytoskeleton.* 20: 30-37.

Inoué, S. 1981. Video image processing greatly enhances contrast quality, and speed in polarization-based microscopy. *J. Cell Biol.* 89: 346-356.

Inoué, S. 1986. Video Microscopy. New York, Plenum Press.

Joshi, H.C., M.J. Palacio, and D.W. Cleveland. 1991. Gamma tubulin is required for *in vivo* microtubule nucleation. *J. Cell Biol.* 115(3): 170a abst. 991.

Kangasniemi, M., A Kaipia, P. Mali, J. Toppari, I. Huhtaniemi, and M. Parvinen. 1990. Modulation of basal and FSH-dependent cyclic AMP production in rat seminiferous tubules staged by an improved transillumination technique. *Anat. Rec.* 227: 62-76.

Kelly, R.B. 1990a. Association between microtubules and intracellular organelles. *Curr. Opin. in Cell Biol.* 2: 105-108.

Kelly, R.B. 1990b. Microtubules, membrane traffic, and cell organization. *Cell* 61: 1-3.

Kerr, J.B. 1988. An ultrastructural and morphometric analysis of the Sertoli cell during the spermatogenic cycle of the rat. *Anat. Embryol.* 179: 191-203.

Kierszenbaum, A.L., C.M. Libanati, and C.J. Tandler. 1971. The distribution of inorganic cations in mouse testis. *J. Cell Biol.* 48: 314-323.

Klein, R.L., S.S. Yen, and A. Thureson-Klein 1972. Critique on the K-pyroantimonate method for semiquantitative estimation of cations in conjunction with electron microscopy. *J. Histochem. Cytochem.* 20 (1) 65-78.

Koonce, M.P., U. Euteneuer, and M. Schliwa. 1986. *Reticulomyxa*: a new model system of intracellular transport. *J. Cell Sci.* Suppl. 5: 145-159.

Koonce, M.P., and M. Schliwa. 1985. Bidirectional organelle transport can occur in cell processes that contain single microtubules. *J. Cell Biol.* 100: 322-326.

Kreis, T. E. 1990. Role of microtubules in the organization of the Golgi apparatus. *Cell Mot. Cytoskeleton.* 15: 67-70.

Kuriyama, R. 1984. Activity and stability of centrosomes in Chinese hamster ovary cells in nucleation of microtubules *in vitro. J. Cell Sci.* 66: 277-295.

Kuznetsov, S.A.M, and V.I. Gelfand. 1986. Bovine brain kinesin is a microtubule-activated ATPase. *Proc. Natl. Acad. Sci.* 83: 8530-8534.

Lacey, M.L. and L.T. Haimo. 1992. Cytoplasmic dynein is a vesicle protein. *J. Biol. Chem.* 267: (in press - March).

Laemmli. U. K. 1970. Clevage of structural proteins during the assembly of the head of bacteriophage T4. *Nature* 227: 680-685.

Lasek, R.J., and S.T. Brady. 1985. Attachment of transported vesicles to microtubules in axoplasm is facilitated by AMP PNP. *Nature.* 316: 645-647.

Leblond, C.P. and Y. Clermont. 1952a. Definition of the stages of the cycle of the seminiferous epithelium in the rat. *Ann. N. Y. Acad. Sci.* 55: 548-573.

Leblond, C.P., and Y. Clermont. 1952b. Spermiogenesis of rat, mouse, hamster and guinea pig as revealed by the periodic acid-fuchsin sulfurous acid technique. *Am. J. Anat.* 90:167-215.

Lee, J.C. 1982. Purification and chemical properties of brain tubulin. *Meth Cell Biol.* 24: 9-30.

Lee, C., M. Ferguson and L.B. Chen. 1989. Construction of the endoplasmic reticulum. J. *Cell Biol.* 109: 2045-2055.

Linden, M., B.D. Nelson, D. Loncar and J.F. Leterrier. 1989. Studies on the interaction between mitochondria and the cytoskeleton. *J. Bioen. and Biomem.* 21 (4): 507-518.

Lowry, O.H., N.J. Rosebrough, A.L. Farr, and R.J. Randall. 1951. Protein measurement with the Folin phenol reagent. *J. Biol. Chem.* 193: 265-275.

Lye, R.J., C.M. Pfarr, and M.E. Porter. 1989. Cytoplasmic dynein and microtubule translocators. *In* Cell Movement: Kinesin, Dynein, and Microtubule Dynamics. Vol

2. F.D. Warner and J.R. M^{c}Intosh, editors. Alan R. Liss Inc., New York. 141-154.

Lye, R.J., M.E. Porter, J.M. Scholey, and J.R. M^{c}Intosh. 1987. Identification of a microtubule-based cytoplasmic motor in the nematode C. elegans. *Cell.* 51(2): 309-18.

Magre, S. and A. Jost. 1991. Sertoli cells and testicular differentiation in the rat fetus. *J. Elect. Microsc. Tech.* 19: 172-188.

Mali, P., M.J. Welsh, J. Toppari, K.K. Vihko, and M. Parvinen. 1985. Cell interactions in the rat seminiferous epithelium with special reference to the cellular distribution of calmodulin. *Med. Biol.* 63: 237-244.

Malik, F. and R. D. Vale 1990. A new direction for kinesin. *Nature* 347: 713-714.

Mandelkow, E., and E.M. Mandelkow. 1989a. Microtubule structure and tubulin polymerization in *Curr. Opin. Cell Biol.* 1: 5-9.

Mandelkow, E. and E.-M. Mandelkow. 1989b. Tubulin, microtubules, and oligomers: molecular structure and implications for assembly. *In* Cell Movement: Kinesin, Dynein, and Microtubule Dynamics. Vol 2. F.D. Warner and J.R. M^{c}Intosh, editors. Alan R. Liss Inc., New York. 23-45.

Margolis, R.L. 1982. Measurement of steady-state tubulin flux. *Meth. Cell Biol.* 24: 145-158.

Masri, B.A., L.D.Russell, and A.W. Vogl. 1987. Distribution of actin in spermatids and adjacent Sertoli cell regions of the rat. *Anat. Rec.* 218: 20-26.

M^{c}Beath, E. and K. Fujiwara. 1989. Coalignment of microtubules, cytokeratin intermediate filaments, and collagen fibrils in a collagen-secreting cell system. *Eur. J. Cell Biol.* 50: 510-521.

M^{c}Donald, H.B., and L.S.B. Goldstein. 1990. Identification and characterization of a gene encoding a kinesin-like protein in *Drosophila.*. *Cell.* 61: 991-1000.

M^{c}Donald, H.B., R.J. Stewart, and L.S.B. Goldstein. 1990. The kinesin-like ncd protein of *Drosophila* is a minus-end directed microtubule motor. *Cell*: 1159-1165.

M^{c}Intosh, J. R. and M. E. Porter. 1989. Enzymes for microtubule-dependent motility. *J. Biol. Chem.* 264 (11): 6001-6004

M^{c}Intosh, J.R. and U. Euteneuer. 1984. Tubulin hooks as probes for microtubule polarity: an analysis of the method and an evaluation of data on microtubule opolarity in the mitotic spindle. *J. Cell Biol.* 98: 525-533.

M^{c}Keithan, T. W. and LJ. L. Rosenbaum. 1984. The biochemistry of microtubules. *Cell Muscle Motil.* 5: 255-288.

M^{c}Niven, M.A., M. Wang, and K.R. Porter. 1984. Microtubule polarity and the direction of pigment transport reverse simulataneously in surgically severed melanopore arms. *Cell.* 37: 753-765.

M^{c}Niven, M.A., and K.R. Porter. 1986. Microtubule polarity confers direction to pigment transport in chromatophores. *J. Cell Biol.* 103: 1547-1555.

Means, A.R., J.R. Dedman, J.R. Tash, D. J. Tindall, M. Van Sickle, and M.J. Welsh. 1980. Regulation of the testis Sertoli cell by follicle stimulating hormone. *Annu. Rev. Physiol.* 42: 59-70.

Mitchison, T.J. and M.W. Kirschner. 1984a. Dynamic instability of microtubule growth. *Nature.* 312: 237-242.

Mitchison, T.J. and M.W. Kirschner. 1984b. Microtubule assembly nucleated by isolated centrosomes. *Nature.* 312: 232-237.

Mogensen, M. M., J. B. Tucker, and H. Stebbings. 1989. Microtubule polarities indicate that nucleation and capture of microtubules occurs at cell surfaces in *Drosophila. J. Cell Biol.* 108: 1445-1552.

Moralis, C., Y. Clermont, and N.J. Nadler. 1986. Cyclic endocytotic activity and kinetics of lysosomes in Sertoli cells of the rat: a morphometric analysis. *Biol. of Reprod.* 34: 207-218.

Moralis, C., and Y. Clermont. 1982. Evolution of Sertoli cell process invading the cytoplasm of rat spermatids. *Anat. Rec.* 203: 233-244.

Na, G.C., and S.N. Timasheff. 1982. Physical properties of purified calf brain tubulin. *Meth. Enzymol.* 85: 393-416.

Nagano, T. 1966. Some observations on the fine structure of the Sertoli cell in the human testis. *Zeitschrift für Zellforschung.* 73: 89-106.

Neeley, M.D., H.P. Erickson and K. Boekelheide. 1990. HMW-2 the Sertoli cell cytoplasmic dynein from rat testis, is a dimer composed of nearly identical subunits. *J. Biol. Chem.* 265 (15) 8691-8698.

Neely, M. D., and K. Boekelheide. 1988. Sertoli cell processes have axoplasmic features: an ordered microtubule distribution and an abundant high molecular weight microtubule-associated protein (cytoplasmic dynein). *J. Cell Biol.* 107: 1767-1776.

Neighbors, B.W., R.C. Williams, and J.R. M^cIntosh. 1988. Localization of kinesin in cultured cells. *J. Cell Biol.* 106: 1193-1204.

Nicander, L. 1963. Some ultrastructural features of mammalian Sertoli cells. *J. Ultrast. Res.* 8: 190-191a.

Nicander, L. 1967. An electron microscopical study of cell contacts in the seminiferous tubules of some mammals. *Zeitschrift für Zellforschung.* 83: 375-397.

Ogawa, K., H. Hosoya, E. Yokota, T. Kobayashi, Y. Wakamatsu, K. Ozato, S. Negishi, and M. Obika. 1987. Melanoma dynein: evidence that dynein is a general motor for microtubule-associated cell motilities. *Eur. J. Cell Biol.* 43: 3-9.

Okabe, S., and N. Hirokawa 1989. Axonal transport. *Curr. Opin. Cell Biol.* 1: 91-97.

Olmstead, J.B. 1986. Microtubule-associated proteins. *Annu. Rev. Cell Biol.* 2: 421-457.

Parvinen, M., and A. Ruokonen. 1982. Endogenesis steroids in the rat seminiferous tubules. Comparison of the stages of the epithelial cycle isolated by transillumination-assisted microdissection. *J. Androl.* 3: 211-220.

Parvinen, M., and T. Vanha-Perttula. 1972. Identification and enzyme quantitation of the stage of seminiferous epithelial wave in the rat. *Anat. Rec.* 174: 435-450.

Paschal, B.M., H.S. Shpetner and R.B. Vallee. 1987. MAP 1C is a microtubule-activated ATPase which translocates microtubules *in vitro* and has dynein-like properties. *J. Cell Biol.* 105: 1273-1282.

Paschal, B.M., H.S. Shpetner, and R.D. Vallee. 1991. Purification of brain cytoplasmic dynein and characterization of its *in vitro* properties. *Meth. in Enzymol.* 196: 181-191.

Paschal, B.M., and R.B. Vallee. 1987. Retrograde transport by the microtubule-associated protein MAP1C. *Nature* 330: 181-183.

Penningroth, S.M. 1989. Chemical inhibitors of the dynein adenosine triphosphatases. *In* Cell Movement: The dynein ATPases, Vol I. F.D. Warren, P. Satu, I.R. Gibbons, editors. Alan R. Liss, Inc., New York: 167-179.

Pepperkok, R., M.H. Bré, J. Davoust. and T.E. Kreis. 1990. Microtubules are stabilized in confluent epithelial cells but not in fibroblasts. *J. Cell Biol.* 111 (6): 3003-3012.

Perey, B., Y. Clermont, and C.P. Leblond. 1961. The wave of the seminiferous epithelium in the rat. *Am. J. Anat.* 108: 47-77.

Pfarr, C.M, M. Cove, P.M. Grissom, T.S. Hays, M.E. Porter, and J.R. McIntosh. 1990. Cytoplasmic dynein is localized to kinetochores during mitosis. *Nature* 345: 263-265.

Pfeiffer, D.C., S. Delhar, S.W. Byers, and A.W. Vogl. 1991. Evidence that an integrin may be present at specialized sites ('ectoplasmic specializations') of intercellular adhesion in the seminiferous epithelium. *J. Cell Biol.* 115(3): p 482a abst. 2803.

Pfeiffer, D. S. and A. W. Vogl., 1991. Evidence that vinculin is co-distributed with actin bundles in ectoplasmic ('junctional') specializations of mammalian Sertoli cells. Anat. Rec. 231: 89-100.

Pfister, K. K., M. C. Wagner, D. L. Stenoien, S. T. Brady, and G. S. Bloom. 1989b. Monoclonal antibodies to kinesin heavy and light chains stain vesicle-like structures, but not microtubules, in cultured cells. *J. Cell Biol.* 108 (4): 1453-1463.

Plöen, L, and E.M. Ritzén. 1984. Fine structural features of Sertoli cells. *In* Ultrastructure of reproduction. J. Van Blerkom, P.M. Motta, editors. Martinus Nijhoff Pub., Boston. 67-74.

Poenie, M. and D. Epel. 1987. Ultrastructural localization of intracellular calcium stores by a new cytochemical method. *J. Histochem. Cytochem.* 35 (9): 939-956.

Porter, K.R. 1966. Cytoplasmic microtubules and their functions. *In* Ciba Foundation Symposium on Principles of Biomolecular Organizations. G.E.W. Wolstenholme and M. O'Connor, editors. London: J & A Churchill Ltd. 308-345.

Porter, M. E. and K. A. Johnson. 1989. Dynein structure and function. *Annu. Rev. Cell Biol.* 5:119-151.

Porter, M.E., J.M. Scholey, D.L. Stemple. G.P.A. Vigers, R.D. Vale, M.P. Sheetz, and J.R. M^{c}Intosh. 1987. Characterization of the microtubule movement produced by sea urchin egg kinesin. *J. Biol. Chem.* 262 (6): 2794-2802.

Pratt, M. M. 1980. The identification of a dynein ATPase in unfertilized sea urchin eggs. *Dev. Biol.* 74: 364-378.

Pratt, M.M. 1986a. Purification of cytoplasmic dynein from *Strongylocentrotus* sea urchin eggs. *Meth. Enzymol.* 134: 325-337.

Pratt, M.M. 1986b. Stable complexes of axoplasmic vesicles and microtubules: protein compositon and ATPase activity. *J. Cell Biol.* 103: 957-968.

Pratt, M.M. 1989. Cytoplasmic dynein and related adenosine triphosphatases.*In* Cell Movement: Kinesin, Dynein, and Microtubule Dynamics. Vol 2. F.D. Warner and J.R. M^{c}Intosh, editors. Alan R. Liss Inc., New York. 115-124.

Pudney, J. 1986. Fine structural changes in Sertoli and Leydig cells during the reproductive cycle of the ground squirrel *Citellus lateralis*. *J. Reprod. Fert.* 77: 37-49.

Purvis, K., and V. Hansson. 1981. Hormonal Regulation of Spermatogenesis. *Int. J. Andrology* Supp.3: 81-143.

Rambourg, A., Y. Clermont, and L. Hermo. 1979. Three-dimensional architecture of the Golgi apparatus in Sertoli cells of the rat. *Am. J. Anat.* 154: 454-476.

Rattner, J.B., and B.R. Brinkley. 1972. Ultrastructure of mammalian spermiogenesis. III the organization and morphogenesis of the manchette during rodent spermiogenesis. *J. Ultrastru. Res.* 41: 209-218.

Redenbach, D.M. and A.W. Vogl. 1991. Microtubule polarity in Sertoli cells: a model for microtubule-based spermatid transport. *Eur. J. Cell Biol.* 54:277-290.

Redenbach, D.M., K. Boekelheide, and A.W. Vogl. 1991. Dynamic binding of spermatid-ES complexes to microtubules: a model of microtubule based spermatid translocation in mammalian Sertoli cells. *J. Cell Biol.* 115: 40 abst. 229.

Rickard, J.E. and T.E. Kreis. 1991. Binding of pp170 to microtubules is regulated by phosphorylation. *J. Biol. Chem.* 266 (26) 17597-17605.

Rickard, J.E. and T.E. Kreis. 1990. Identification of a novel nucleotide-sensitive microtubule-binding protein in HeLa cells. *J. Cell Biol.* 110 (5): 1623-1633.

Ritzen, E.M., C. Boitani, and M. Parvinen. 1981a. Cyclic secretion of proteins by rat seminiferous tubules depending on the stage of spermatogenesis. *Int. J. of Andrology.* 3: 51-58.

Ritzen, E.M., V. Hansson, and F.S. French. 1981b. The Sertoli cell. *In* The Testis. H. Burger and D. de Kretsen, editors. Raven Press. New York. 175-194.

Romrell, L.J. and M.H. Ross. 1979. Characterization of Sertoli cell-germ cell junctional specializations in dissociated testicular cells. *Anat. Rec.* 193 (1):23-42.

Ross, M.H. 1976a. Sertoli-Sertoli junctions and Sertoli-spermatid junctions after efferent ductule ligation and lanthanum treatment. *Am. J. Anat.* 148: 49-56.

Ross, M.H. 1976b. The Sertoli cell junction specialization during spermiogenesis and at spermiation. *Anat. Rec.* 186: 79-104.

Ross, M.H. and J. Dobber. 1975. The Sertoli cell junctional specializations and their relationship to the germinal epithelium as observed after efferent ductule ligation. *Anat. Rec.* 183: 267-292.

Rothwell, S.W., W.A. Grasser, and D.B. Murphy. 1985. Direct observations of microtubule treadmilling by electron microscopy. *J. Cell Biol.* 101: 1637-42.

Rothwell, S.W., J. Nath, and D.G. Wright. 1989. Interactions of cytoplasmic granules with microtubles in human neutrophils. *J. Cell Biol.* 108: 2313-2326.

Russell, L.D. 1977a. Desmosome-like junctions between Sertoli and germ cells in the rat testis. *Am. J. Anat.* 148: 301-312.

Russell, L.D. 1979a. Further observations on tubulobulbar complexes formed by late spermatids and Sertoli cells in the rat testis. *Anat. Rec.* 194 (2): 213-232.

Russell, L.D. 1977b. Movement of spermatocytes from the basal to the adluminal compartment of the rat testis. *Am. J. Anat.* 148: 313-328.

Russell L.D. 1977c. Observations on rat Sertoli ectoplasmic ("junctional") specializations in the association with germ cells of the rat testis. *Tissue Cell* 9: 475-498.

Russell, L.D. 1979b. Observations on the inter-relationships of Sertoli cells at the level of the blood-testis barrier: evidence for formation and resorption of Sertoli Sertoli tubulobulbar complexes during the spermatogenic cycle of the rat. *Am. J. Anat.* 155: 259-280.

Russell, L. D. 1980. Sertoli-germ cell interactions: a review. *Gamete Res.* 3: 179-202.

Russell, L.D. 1979c. Spermatid-Sertoli tubulobulbar complexes as devices for elimination of cytoplasm from the head region of late spermatids of the rat. *Anat. Rec.* 194 (2): 233-246.

Russell, L.D. 1984. Spermiation-the sperm release process: Ultrastructural observations and unresolved problems. *In* Electromicroscopy in Biology and Medicine. J. van Berkhon and P. Motta editors. Martinus Nijhoff, Boston. 46-66.

Russell, L.D., A. Bartke and J.C. Goh. 1989a. Postnatal development of Sertoli barrier, tubular lumen and cytoskeleton of Sertoli and myoid cells in the rat, and their relationship to tubular fluid secretion and flow. *Am. J. Anat.* 184: 179-189.

Russell, L.D., and Y. Clermont. 1976. Anchoring device between Sertoli cells and late spermatids in rat seminiferous tubules. *Anat. Rec.*185 (3): 259-278.

Russell, L.D., R.A. Ettlin, A.P. Sink a Hikim, and E.D. Clegg. 1990. Histological and Histopathological Evaluation of the Testis. Cache River Press, Clearwater, Florida.

Russell, L.D., and J.C. Goh. 1988. Localization of alpha-actinin in the rat testis: preliminary observations. *In:* Development and function of one reproductive organs. Ares-Serno Symposium. M. Parvinen, I. Huhtanieme and L. Pelliniemi, editors. Rome Ans Serono Symp. Rev no. 14. Vol. II: 237-244.

Russell, L.D., J.C. Goh, R.M.A. Rashed, and A.W. Vogl. 1988. The consequences of actin disruption at Sertoli ectoplasmic specialization sites facing spermatids after *in vivo* exposure of rat testis to cytochalasin D. *Biol. of Reproduction.* 39: 105-118.

Russell, L.D., I.P. Lee, R. Ettlin, and R.N. Peterson. 1983a. Development of the acrosome and alignment, elongation and entrenchment of spermatids in procarbazine-treated rats. *Tiss. Cell.* 15 (4): 615-626.

Russell, L.D. and J.P. Malone. 1981. A study of Sertoli-spermatid tubulobulbar complexes in selected mammals. *Tiss. Cell.* 12(2): 263-285.

Russell L.D., J.P. Malone and D.S. MacCurdy. 1981. Effect of the microtubule disrupting agents, colchicine and vinblastine, on seminiferous tubule structure in the rat. *Tiss. Cell.*13 (2): 349-367.

Russell, L.D., P. Myers, J. Ostenburg, and J. Malone. 1980. Sertoli ectoplasmic specializations during spermatogenesis. *In* Testis Development Structure and Function. C. Steinberger and E. Steinberger, editors. Raven Press N. Y. 55-63.

Russell, L.D., and R.N. Peterson. 1985. Sertoli Cell Junctions: Morphological and functional correlates. *Int. Rev. Cytol.* 94: 177-211.

Russell, L.D., N.K. Saxena, and T.T. Turner. 1989b. Cytoskeletal involvement in spermiation and sperm transport. *Tiss. Cell.* 21(3): 361-79.

Russell, L.D., M. Tallon-Doran, J.E. Weber, V. Wong, and R.N. Peterson. 1983b. Three-dimensional reconstruction of a rat stage V Sertoli cell: III a study of specific cellular relationships. *Am. J. Anat.* 167: 181-192.

Saez, J.M., E. Tabone, M.H. Perrard-Sapori, and M.A. Rivarola. 1985. Paracrine role of Sertoli cells. *Med. Biol.* 63: 225-236.

Sammak, P.J., and G.G. Borisy. 1988. Direct observations of microtubule dynamics in living cells. *Nature*. 332: 724-726.

Scheel, J., and T.E. Kreis. 1991a. Motor protein independent binding of endocytic carrier vesicles to microtubules. *J. Biol. Chem.* 266 (27): 18141-18148.

Scheel, J., and T.E. Kreis. 1991b. Motor protein independent binding of endocytic carrier vesicles to microtubules. *J. Cell Biol.* 115 (3): 478a (abst. 2779).

Schelanski, M.L., F. Gaskin, and C.R. Cantor. 1973. Microtubule assemby in the absence of added nucleotides. *Proc. Natl. Acad. Sci.* 70: 765-768.

Schiff, P.B., J. Fant, and S. B. Horwitz. 1979. Promotion of microtubule assembly *in vitro* by taxol. *Nature* 277: 665-667.

Schliwa, M. 1984. Mechanism of intracellular organelle transport. *In* Cell, and Muscle Motility, vol 5. J. W. Shaw, editor. New York, Plenum Press.1-81.

Schliwa, M., T. Shimizu, R.D. Vale, and U. Euteneuer. 1991. Nucleotide specificities of anterograde and retrograde organelle transport in *Reticulomyxa* are indistinguishable. *J. Cell Biol.* 112: 1199-1203.

Schnapp, B.J. 1986. Viewing single microtubules by video light microscopy. *Meth. Enzymol.* 134: 561-573.

Schnapp, B.J. and T.S. Reese. 1989. Dynein is the motor for retrograde axonal transport or organelles. *Proc. Natl. Acad. Sci.* 86 (5): 1548-1552.

Schnapp, B.J., R.D. Vale, M.P. Sheetz, and T.S. Reese. 1986. Microtubules and the mechanism of directed organelle movement. *Ann. N.Y. Acad. Sci.* 466: 909-918.

Schnapp, B.J., R.D. Vale, M.P. Sheetz and T.S. Reese. 1985. Single microtubules from squid axoplasm support bidirectional movement of organelles. *Cell* 40: 455-462.

Scholey, J.M., S.A. Cohn, and A.L. Ingold. 1989. Biochemical and mobile properties of sea urchin egg kinesin: Relationship to the pathway of the kinesin-microtubule ATPase. *In* Cell Movement: Kinesin, Dynein, and Microtubule Dynamics. Vol 2. F.D. Warner and J.R. M^{c}Intosh, editors. Alan R. Liss Inc., New York.

Schroer, T.A., B.J. Schnapp, T.S. Reese and M.P. Sheetz. 1988. The role of kinesin and other soluble factors in organelle movement along microtubules. *J. Cell Biol.* 107: 1785-1792.

Schroer, T. A. and M. P. Sheetz. 1991a. Functions of microtubule-based motors. *Annu. Rev. Physiol.* 53: 629-652.

Schroer, T.A., and M.P. Sheetz. 1989. Role of Kinesin and Kinesin-associated proteins in organelle transport. *In* Cell Movement: Kinesin, Dynein, and Microtubule Dynamics. Vol 2. F.D. Warner and J.R. M^{c}Intosh, editors. Alan R. Liss Inc., New York. 295-306.

Schroer, T.A., and M.P. Sheetz. 1991b. Two activators of microtubules-based vesicle transport. *J. Cell Biol.* 115 (5): 1309-1318.

Schroer, T. A., E. R. Steuer and M. P. Sheetz. 1989. Cytoplasmic dynein is a minus end-directed motor for membranous organelles. *Cell* 56:937-946.

Schulze, E., D.J. Asai, J.C. Bulinski and M. Kirschner. Posttranslational modification and microtubule stability. *J. Cell Biol.* 105:2167-2177, 1987.

Sertoli, E. 1865. Dell' esistenza di particolari cellule ramificate nei canalicoli seminiferi del testicolo umano. B.P. Setchell, translator. *Morgagni.* 7: 31-39.

Sheetz, M.P., R.D. Vale, B. Schnapp, T. Schroer and T. Reese. 1986. Vesicle movements and microtubule-based motors. *J. Cell Sci.* Suppl. 5: 181-188.

Sheetz, M.P. 1989. Kinesin structure and function *In* Cell Movement: Kinesin, Dynein, and Microtubule Dynamics. Vol 2. F.D. Warner and J.R. M^{c}Intosh, editors. Alan R. Liss Inc., New York. 277-285.

Sheetz, M.P., E.R. Steuer, and T.A. Schroer. 1989. The mechanism and regulation of fast axonal transport. *Trends in Neurosci.* 12 (11): 474-8.

Sherline, P., Y.C. Lee, and L.S. Jacobs. 1977. Binding of microtubules to pituitary secretory granules and secretory granule membranes. *J. Cell Biol.* 72: 380-389.

Shpetner, H.S., B.M. Paschal, and R.B. Vallee. 1988. Characterization of the microtubule-activated ATPase of brain cytoplasm dynein (MAPIC). *J. Cell Biol.* 107 (3): 1001-1009.

Skoufias, D. A., T.L. Burgess, and L. Wilson. 1990. Spacial and temporal colocalization of the Golgi Appatatus and microtubules rich in detyrosinated tubulin. *J. Cell Biol.* 111: 1929-1937.

Slautterback, D.B. 1963. Cytoplasmic microtubules. I. Hydra. J. Cell Biol. 18: 367-388.

Sloboda, R.D., and S.P. Gilbert. 1989. Microtubule-associated proteins and intracellular particle motility. *In* Cell Movement: Kinesin, Dynein, and Microtubule Dynamics. Vol 2. F.D. Warner and J.R. M^{c}Intosh, editors. Alan R. Liss Inc., New York. 223-232.

Smith, R.S. 1972. Detection of organelles in myelinated nerve fibres by dark-field microscopy. *Can. J. Physiol. & Pharm.* 50: 467-469.

Smith, R. S. 1980. The short-term accumulation of axonally transported organelles in the region of localized lesions of single myelinated axons. *J. Neurocytol.* 9: 39-65.

Soltys, B.J., and G.G. Borisy. 1985. Polymerization of tubulin *in vivo*: direct evidence for assembly onto microtubule ends and from centrosomes. *J. Cell Biol.* 1682-1689.

Somlyo, A.P. 1984. Cellular site of calcium regulation. *Nature* 309: 516-517

Spicer, S. S., J. H. Hardin, and W. B. Greene. 1969. Nuclear precipitates in pyroantimonate-osmium tetroxide-fixed tissues. *J. Cell Biol.* 39: 216-221.

Stebbings, H. 1988. Microtubule motors: cytoplasmic dynein graduates. Nature. 336: 14-15.

Stebbings, H. and C. Hunt. 1983. Microtubule polarity in the nutritive tubes of insect ovarioles. *Cell Tissue. Res.* 233: 133-141.

Stephens, R.E. 1986a. Isolation of embryonic cilia and sperm flagella. *Meth. Cell Biol.* 27: 217-227.

Sterns, T., L. Evans, and M. Kirschner. 1991. Gamma-tubulin is a highly conserved component of the centrosome. Cell 65: 825-836.

Steuer, E.R., L. Wordeman, T.A. Schroer, and M.P. Sheetz. 1990. Localization of cytoplasmic dynein to mitotic spindles and kinetochores. *Nature.* 345: 266-8.

Suarez-Quian, C.A., and M. Dym. 1984. Further observations on the microfilament bundles of Sertoli cell junctional complexes. *Ann. N. Y. Acad. Sci.* 438: 476-480.

Summers, K., and M.W. Kirschner. 1979. Characteristics of the polar assembly and disassembly of microtubules observed *in vitro* by darkfield light microscopy. *J. Cell Biol.* 83 (1): 205-17.

Suprenant, K.A., and W.L. Dentler. 1982. Association between endocrine pancreatic secretory granules and in-vitro-assembled microtubules is dependent upon microtubule-associated proteins. *J. Cell Biol.* 93: 164-174.

Tandler, C. J., C. M. Libanati, and C. A. Sanchis. 1970. The intracellular localization of inorganic cations with potassium pyroantimonate. *J. Cell Biol.* 45: 355-366.

Tash, J.S. 1989. Protein phosphorization: the second messenger signal transducer of flagellar motility. *Cell Motil. Cytoskeleton.* 14: 332-339.

Timasheff, S.N., and L.M. Grisham. 1980. *In vitro* assembly of cytoplasmic microtubules. *Annu. Rev. Biochem.* 49: 565-591.

Terasaki, M., J. Song, J. R. Wong, M. J. Weiss and L. B. Chen. 1984. Localization of endoplasmic reticulum in living and glutaraldehyde-fixed cells with fluorescent dyes. *Cell* 38: 101-108.

Tilney, L.G. 1971. How microtubule patterns are generated. *J. Cell Biol.* 51: 837-854.

Tindall, D.J., D.R. Rowley, L. Murthy, L.I. Lipshultz, and C.H. Chang. 1985. Structure and biochemistry of the Sertoli cell. *Int. Rev. Cytol.* 94: 127-149.

Troutt, L.L., and B. Burnside. 1988a. Microtubule polarity and distribution in Teleost photoreceptors. *J Neurosci.* 8(7): 2371-2380.

Troutt, L.L., and B. Burnside. 1988b. The unusual microtubule polarity in teleost retinal pigment epithelial cells. *J. Cell Biol.* 107: 1461-1464.

Ueno, H., and H. Mori. 1990. Morphometrical analysis of Sertoli cell ultrastructure during seminiferous epithelial cycle in rats. *Biol. of Reprod.* 43: 769-776.

Ueno, H., Y. Nishimune, and H. Mori. 1991. Cyclic localization change of Golgi Apparatus in Sertoli cells induced by mature spermatids in rats. *Biol. of Reprod.* 44: 656-662.

Vale, R. D. 1987. Intracellular transport using microtubule based motors. *Annu. Rev. Cell Biol.* 3: 347-378.

Vale, R. D. 1990. Microtubule-based motor proteins. *Curr. Opin. Cell. Biol.* 2: 15-22.

Vale, R.D. and L.S.B. Goldstein. 1990. One motor, many tails: an expanding repertoire of force-generating enzymes. *Cell* 60: 883-885.

Vale, R.D. and H. Hotani. 1988. Formation of membrane networks *in vitro* by kinesin-driven microtubule movement. *J. Cell Biol.* 107 (6): 2233-2241.

Vale, R.D., T.S. Reese and M.P. Sheetz. 1985a. Identification of a novel force-generating protein, kinesin, involved in microtubule-based motility. *Cell.* 42: 39-50.

Vale, R.D., B.J. Schnapp, T. Mitchison, E. Steuer, T.S. Reese and M.P. Sheetz. 1985b. Different axoplasmic proteins generate movement in opposite directions along microtubules *in vitro. Cell.* 43:623-632.

Vale, R.D., B.J. Schnapp, T.S. Reese and M.P. Sheetz. 1985c. Movement of organelles along filaments dissociated from the axoplasm of the squid giant axon. *Cell.* 40: 449-454.

Vale, R.D., B.J. Schnapp, T.S. Reese, and M.P. Sheetz. 1985d. Organelle, bead, and microtubule translocations promoted by soluble factors from the squid giant axon. *Cell.* 40: 559-569.

Vale, R.D., and Y.Y. Toyoshima. 1989. *In vitro* mobility assays for kinesin and dynein. *In* Cell Movement: Kinesin, Dynein, and Microtubule Dynamics. Vol 2. F.D. Warner and J.R. M^{c}Intosh, editors. Alan R. Liss Inc., New York. 287-294.

Vallee, R.B. 1990. Molecular characterization of high molecular weight microtubule-associated proteins: some answers, many questions. *Cell Mot. Cytoskeleton.* 15: 204-209.

Vallee, R. B. 1986a. Purification of brain microtubules and microtubule-associated proteins using taxol. *Meth. Enzymol.* 134: 104-115.

Vallee, R.B. 1986b. Reversible assembly purification of microtubules without assembly promoting agents and futher purification of tubulin, microtubule-associated proteins and MAP fragments. *Meth. in Enzymol.* 134: 89-105.

Vallee, R.B. 1982. Taxol-dependent procedure for the isolation of microtubules and microtubule-associated proteins (MAPS). *J. Cell Biol.* 92: 435-442.

Vallee, R.B., and G.S. Bloom. 1984. High molecular weight microtubule-associated proteins (MAPS). *Mod. Cell Biol.* 3: 21-75.

Vallee, R.B., B.M. Paschal, and H.S. Shpetner. 1989a. Characterization of microtubule-associated protein (MAP) 1C as the motor for retrograde organelle transport and its identification as Dynein. *In* Cell Movement: Kinesin, Dynein, and Microtubule Dynamics. Vol 2. F.D. Warner and J.R. M^{c}Intosh, editors. Alan R. Liss Inc., New York. 211-222.

Vallee, R.B., H.S. Shpetner, and B.M. Paschal. 1989b. The role of dynein and other microtubule activated ATPases in mitosis. *Prog. Clin. Biol. Res.* 318: 205-15.

Vallee, R.B., H.S. Shpetner, and B.M. Paschal. 1989c. The role of dynein in retrograde transport. *Trends in Neurosci.* 12 (2): 66-70.

van der Sluijs, P., M. K. Bennett, C. Antony, K. Simons and T. E. Kreis. 1990. Binding of exocytic vesicles from MDCK cells to microtubules *in vitro*. *J. Cell Sci.* 95: 545-553.

van Zeijl, M.J., A.H. and K.S. Matlin. 1990. Microtubule perturbation inhibits intracellular transport of an apical membrane glycoprotein in a substrate-dependent manner in polarized Madin- Darby canine kidney epithelial cells. *Cell Reg.* 1: 921-936.

Villasante, A., D. Wang, P. Dobner, P. Dolph, S.A. Lewis, and N.J. Cowan. 1986. Six mouse alpha tubulins mRNAs encode five distinct isotypes: testis specific expression of two sister genes. *Mol. Cell Biol.* 6: 2409-2419.

Vogl, A.W. 1988. Changes in the distribution of microtubules in rat Sertoli cells during spermatogenesis. *Anat. Rec.* 222: 34-41.

Vogl, A.W. 1989. Distribution and function of organized concentrations of actin filaments in mammalian spermatogenic cells and Sertoli cells. *Int. Rev. Cyt.* 119: 1-56.

Vogl, A.W., B.D. Grove, and G.J. Lew. 1986. Distribution of actin in Sertoli cell ectoplasmic specializations and associated spermatids in the ground squirrel testis. *Anat. Rec.* 215: 331-341.

Vogl, A.W., B.D. Grove, D.M. Redenbach, and D.C. Pfeiffer. 1992. Sertoli cell cytoskeleton. *In* The Sertoli Cell. L. D. Russell and M. D. Griswold, editors. Cache River Press. Clearwater, Florida. (invited) in press.

Vogl, A.W., Y.C. Lin, M. Dym and D.W. Fawcett. 1983a. Sertoli cells of the golden-mantled ground squirrel (*Spermophilus lateralis*): a model system for the study of shape change. *Am. J. Anat.* 168: 83-98.

Vogl, A.W., R.W. Linck and M. Dym. 1983b. Colchicine-induced changes in the cytoskeleton of the golden mantled ground squirrel (*Spermophilus lateralis*) Sertoli cells. *Am. J. Anat.* 168: 99-108.

Vogl, A.W., D.C. Pfeiffer and D.M. Redenbach. 1991a. Ectoplasmic ('junctional') specializations in mammalian Sertoli cells: influence on spermatogenic cells. *Ann. N. Y. Acad. Sci.* 637: 173-202.

Vogl, A.W., D.C. Pfeiffer, and D.M. Redenbach. 1991b. Sertoli cell cytoskeleton: influence on spermatogenic cells. *In* Proceedings of the VI International Congress on Spermatology. Comparative spermatology 20 Years After. Serno Symposia (in press).

Vogl, A.W., and L.J. Soucy. 1985. Arrangement and possible function of actin filament bundles in ectoplasmic specializations of ground squirrel Sertoli cells. *J. Cell Biol.* 100: 814-825.

Vogl, A.W., L.J. Soucy, and V. Foo. 1985a. Ultrastructure of Sertoli - cell penetrating processes found in germ cells of the golden-mantled ground squirrel (*Spermophilus lateralis*). *Am. J. Anat.* 172: 75-86.

Vogl, A.W., L.J. Soucy, and G.J. Lew. 1985b. Distribution of actin in isolated seminiferous epithelia and denuded tubule walls of the rat. *Anat. Rec.* 213: 63-71.

Wagner, M.C., K.K. Pfister, G.S. Bloom, and S.T. Brady. 1989. Copurification of kinesin polypeptides with microtubule-stimulated Mg-ATPase activity and kinetic analysis of enzymatic properties. *Cell Motil. Cytoskeleton.* 12: 195-215.

Walker, R.A., E.D. Salmon. and S.A. Endow. (1990) The *Drosophila* claret segregation protein is a minus-end directed motor molecule. *Nature.* 347(6295): 780-2.

Weber, J.E., L.D. Russell, V. Wong, and R.N. Peterson. (1983) Three-dimensional reconstruction of a rat stage V Sertoli cell: II. morphometry of Sertoli-Sertoli and Sertoli-Germ-cell relationships. *Am. J. Anat.* 167: 163-179.

Wiche, G. 1989. High - M_r microtubule-associated proteins: properties and functions. *Biochem. J.* 259: 1-12.

Williams, R.C., and H.W. Detrich III. 1979. Separation of tubulin from microtubule-associated protein on phosphocellulose. Accompanying alterations in concentrations of buffer components. *Biochem.*18: 2499-2503.

Williams R. C. Jr., and J. C. Lee. 1982. Preparation of tubulin from brain. *Methods Enzymol.* 85: 376-385.

Wilson, L., H. P. Miller, K. W. Farrell, K. B. Snyder, W. C. Thompson, and D. L. Purich. 1985. Taxol stabilization of microtubules *in vitro*: dynamics of tubulin and addition and loss at opposite microtubule ends. *Biochem.* 24: 5254-5262.

Wolosewick, J. and J. De Mey. 1982. Localization of tubulin and actin in polyethylene glycol embedded rat seminiferous epithelium. *Biol. Cell.* 44: 85-88.

Yang, J.T., R.A. Laymon, and L.S.B. Goldstein. 1989. A three-domain structure of kinesin heavy chain revealed by DNA sequence and microtubule binding analyses. *Cell.* 56: 879-889.

Zechmeister, A. 1979. A new selective ultrahistochemical method for the demonstration of calcium using N, N-naphthaloylhydroxylamine. *Histochemistry.* 61: 223-232.

Zheng, Y, M.K. Jung, and B.R. Oakely. 1991. Gamma-tubulin is present in *Drosophila* melanogaster and *Homo sapiens* and is associated with the centrosome. Cell 65: 817-823.